Generalized Functions Approach to the Derivation of the High-Frequency Radar Cross-Section of Ocean Surfaces with Electromagnetically-Large Waves

by

© Murilo Teixeira Silva, B.Eng., M.Eng.

A thesis submitted to the School of Graduate Studies

in partial fulfilment of the requirements for the

degree of Ph.D. in Engineering, Electrical Engineering

Faculty of Engineering and Applied Science

Memorial University of Newfoundland

May 2021

St. John's Newfoundland Canada

Abstract

The radar cross-section (RCS) of the ocean surface mathematically describes the interaction between electromagnetic fields and ocean waves, allowing for a better understanding of observations made by coastal high-frequency (HF) radars. However, theoretical limitations have restricted the calculation of the RCS of the ocean surface to electromagnetically-small waves. This thesis proposes an approach to study and evaluate the scattering of electric fields over ocean surfaces with electromagnetically-large waves, as well as an extension of the generalized functions approach to the one-body scattering problem to curvilinear coordinates with variable basis vectors. The present work enables the analysis of HF radar signals scattered by the ocean surface during storms and electromagnetically-high sea states, expanding the capabilities of HF radars in radio oceanography.

First, a system of equations for the electric field in curvilinear coordinates in the presence of a single scatter is proposed. It is shown that the derived equations can be applied to coordinate systems with variable basis vectors, being reduced to the form presented in the literature [1] when Cartesian coordinates are considered. As a proof of concept, the system of equations for curvilinear coordinates is applied to a perfectly-electrically conductive (PEC) sphere, yielding the Stratton-Chu integral

equation for the electric field, a general solution in classic electromagnetics.

Then, the electric field scattering over a time-varying conductive random surface is obtained for an ocean surface with electromagnetically-large waves. First, the electric field expressions are obtained by applying the proposed system of equations to a time-varying conductive random surface, removing the restrictions to the growth of the roughness scales presented in the literature. This allows for the study of ocean surfaces with electromagnetically-large waves. The derivation results in additional electric field expressions that correct the height-restricted expression accounting for the energy of electromagnetically-large waves. The resulting expression is reduced to the height-restricted formulation if the roughness scale is sufficiently small. From the expression of the electric field, the RCSs of the correction terms are derived. These derivations yield expressions that can be reduced to a general form, allowing the generation of correction terms to the radar cross-section at a given order by a product with the desired correction factor. In a morphological analysis of the correction factors, it is shown that at small roughness scales, the correction terms do not affect the total cross-section for the ocean surface; however, by increasing the roughness scale beyond the limits presented in the literature, the contribution of the correction terms to the total RCS become significant. Evidence of the presence of the proposed correction terms was approved in field measurements; however, definitive proof of the effects observed here can be the object of future research.

Acknowledgements

I want to thank my supervisors, Dr. Eric W. Gill and Dr. Weimin Huang, for their guidance and support throughout the development of the present thesis. Their insights and experience were invaluable to completing this research, pulling me back to the facts on the ground when the derivations seemed to go astray. I would also like to thank supervisory committee member, Dr. Sarah Power, for agreeing to critically revise and participate in the development of the current work.

I am also grateful to past and present members of the Ocean Remote Sensing group at the Faculty of Engineering and Applied Science, especially Dr. Reza Shahidi, for his patience and support, as well as past and present colleagues in the group, Dr. Yue Ma, Dr. Qingyun Yan, Dr. Xinlong Liu, Dr. Shuyuan Chen, Dr. Pradeep Bobby, Yali Wang, Xinwei Chen, Pedram Ghasemigoudarzi, Mohsen Eslami Nazari, Joe Craig, and many others, for having the patience to endure my group meeting presentations and ramblings about generalized functions and curvilinear coordinates in the office. I am honoured to be a part of this group.

This work was financially supported by Memorial University, by Natural Sciences and Engineering Research Council (NSERC) grants to Dr. Eric W. Gill and Dr. Weimin Huang, by awards such as the C. J. Reddy Educational Grant, given by the

IEEE Antennas and Propagation Society and the Kenneth Hickey Award in Ocean Sensing from the Faculty of Engineering and Applied Science, and by research and teaching assistantships. For that, I would also like to thank Dr. Glyn George, Lori Hogan, and Desmond Power for trusting in my work and allowing me to gather the experience I needed to advance in my career.

In conclusion, I would like to thank my family. Without their support, encouragement, and understanding, I would not be here, halfway across the globe, doing the things I love and being able to finish this work. Thank you for being by my side, even when you didn't understand why I was still in school for so long. I would like to thank my wife, Rafaela, for accompanying me on this journey, for her work and understanding in her support of the past years I was a full-time graduate student. I also want to thank my friends here in Newfoundland and Labrador, in Brazil and scattered across Canada and the United States, for listening and sharing my successes and failures as I was working throughout this thesis and in the next steps of this journey.

Contents

List of Abbreviations

DREA	Defense Research Establishment Atlantic
FMCW	frequency-modulated continuous-wave
HF	high-frequency
NSERC	Natural Sciences and Engineering Research Council
PEC	perfectly-electrically conducting
RCS	radar cross-section
RMS	root mean square
SMB	Sverdrup-Munk-Bretschneider
VHF	very high-frequency

List of Symbols

This list of symbols includes only the most important symbols to the understanding of the present thesis, indicating the page where the symbol was first used. Local variables used in the derivation of expressions or for the demonstration of definitions were not included.

Symbol	**Description**	**Page**
H_s	Significant wave height	1
$\phi_m(\varepsilon)$	Asymptotic sequence of order m	7
ε	Perturbation parameter	7
$o[\cdot]$	Landau's "little-oh" notation	7
$f(\mathbf{x})$	Function in $\mathbb{R}^n$, used in the definition of perturbation expansion	7
$f_m(\mathbf{x};\varepsilon)$	m-th order term for the asymptotic approximation of $f(\mathbf{x})$	7
$F_N(\mathbf{x},\varepsilon)$	N-th asymptotic approximation of $f(\mathbf{x})$	7
$a_m(\mathbf{x})$	Function of the m-th order term in a Poincaré-type expansion	7

Symbol	Description	Page
$\psi(\varepsilon)$	Function of ε in the asymptotic sequence for the power series form expansion	7
$O[\cdot]$	Landau's "big-oh" notation	8
Δ	Surface impedance	10
E_x	x-component of the electric field in Barrick's [2] notation	10
E_y	y-component of the electric field in Barrick's [2] notation	10
E_z	z-component of the electric field in Barrick's [2] notation	10
E_0	Amplitude coefficient of the electric field in Barrick's [2] notation	10
k_0	Wavenumber corresponding to the central frequency of the transmitter	10
L	Side of the square patch over the rough surface in Barrick's [2] notation	10
$\zeta(x, y)$	Fourier series representing the rough surface elevation in Barrick's [2] notation	10
$P(m, n)$	Coefficients of the Fourier series representing the rough surface in Barrick's [2] notation	10
A_{mn}	Coefficient for the perturbation in the x-component of the electric field in Barrick's [2] notation	11

Symbol	Description	Page
B_{mn}	Coefficient for the perturbation in the y-component of the electric field in Barrick's [2] notation	11
C_{mn}	Coefficient for the perturbation in the z-component of the electric field in Barrick's [2] notation	11
R_1	Region of the scattering object in the Walsh and Donnelly [1] notation	13
h_{R_1}	Distributional representation of the region of the scattering object R_1 in the Walsh and Donnelly [1] notation	13
ϵ	Permittivity	13
σ	Conductivity	13
ϵ_1	Permittivity of the scattering object R_1	13
ϵ_0	Permittivity of the vacuum ($\epsilon_0 \approx 8.8542 \times 10^{-12}\ \mathrm{F} \cdot \mathrm{m}^{-1}$)	13
σ_1	Conductivity of the scattering object R_1	13
σ_0	Conductivity of the vacuum ($\sigma_0 = 0\ \Omega \cdot \mathrm{m}$)	13
μ_0	Magnetic constant, or magnetic permeability of free space	14
$\mathbf{E}$	Total electric field	14
$\mathbf{J}_c$	Conduction current density	14
$\mathbf{H}$	Total magnetic field	14

Symbol	Description	Page
n_0	Refraction coefficient of the whole space in the Walsh and Donnelly [1] notation.	14
n_{01}	Refraction coefficient of the scattering body R_1 in the Walsh and Donnelly [1] notation.	14
$\mathbf{B}$	Total magnetic flux density	14
k	Transmitter wavenumber	15
$\mathbf{E}^+$	Electric field at the outer boundary of the scattering object R_1 in the Walsh and Donnelly [1] notation.	15
$\mathbf{E}^-$	Electric field at the inner boundary of the scattering object R_1 in the Walsh and Donnelly [1] notation.	15
T_{SE}	Source vector operator in the Walsh and Donnelly [1] notation.	16
K_0	Scalar Green's function for the field propagation in the vacuum in the Walsh and Donnelly [1] notation.	17
K_1	Scalar Green's function for the field propagation in R_1 in the Walsh and Donnelly [1] notation.	17
$\Theta(\cdot)$	Heaviside Function	18
$f(x, y)$	Vertical surface displacement	18
$\mathbf{E}_s^{z^-}$	Source electric field at $z = z^- < f(x, y),\ \forall(x, y)$.	19
z^-	Point in the z-axis below the surface displacement for all values of z	19

Symbol	Description	Page
$\mathbf{E}_n^+$	Outer normal electric field	19
E_n^+	Magnitude of the outer normal electric field	19
$\mathbf{n}$	Outer normal to the $f(x, y)$ surface	19
u	Square-root of the difference between the squares of the rough surface and radar wavenumbers	19
K	Magnitude of the wavenumber of a rough surface	19
K_x	Magnitude of the x-component of the wavenumber of a rough surface	19
K_y	Magnitude of the y-component of the wavenumber of a rough surface	19
$\mathcal{F}_{xy}(\cdot)$	Two-dimensional Fourier transform over the xy-plane.	19
$\mathcal{N}\{\cdot\}$	Normal component operator	20
$\mathcal{L}\{\cdot\}$	L operator	20
$\hat{\mathbf{n}}$	Outer unit vector normal to the $f(x, y)$ surface	20
$\mathcal{L}^{-1}\{\cdot\}$	L-inverse operator	20
E_{0n}^+	Magnitude of the height-restricted outer normal electric field	20
$\mathcal{T}_1(\cdot)$	T-1 operator, as defined in [3]	20
$\mathcal{T}_2(\cdot)$	T-2 operator, as defined in [3]	21
E^s	Source operator, as defined in [3]	21
$F(\rho)$	Sommerfeld attenuation function	21

Symbol	Description	Page
ω	Angular frequency of time-harmonic fields	29
γ	Propagation constant of the entire space	29
γ_1	Propagation constant of scattering body defined by the region R_1	29
γ_0	Propagation constant of the vacuum	29
$\delta(\cdot)$	Dirac delta distribution	33
$\mathbf{r}$	Generic position vector in $\mathbb{R}^3$	33
$\mathbf{r}'$	Position vector of the source in $\mathbb{R}^3$	33
$\mathbf{E}_s$	Source electric field.	34
$\tilde{f}(\mathbf{r})$	Function defining the surface of a general scattering body	40
$\delta'(\cdot)$	Unit dipole distribution	41
$\mathbf{R}^+$	Auxilliary vector field for the system of equations of electric field immediately above the surface of a general scattering body	41
$\mathbf{R}^-$	Auxilliary vector field for the system of equations of electric field immediately below the surface of a general scattering body	41
$E^+_{\mathbf{n}}$	Magnitude of the normal component of the electric field immediately above the surface of a general scattering body	42

Symbol	Description	Page
$\mathbf{E}_n^+$	Normal component of the electric field immediately above the surface of a general scattering body	42
E^s	Normal source field in the operator equation for the normal electric field	53
$\mathcal{T}$	T-operator in the operator equation for the normal electric field	53
ρ	Magnitude of the radial component in polar (and cyllindrical) coordinates	54
$I(\omega)$	Frequency domain distribution of the current at the source	57
$\Delta\ell$	Length of the vertical dipole	57
σ_g^2	Mean-square slope of surface gravity waves	58
$(E_{\mathbf{n}}^+)_2$	Second-order electric field scattered by an ocean surface with arbitrary roughness scales	63
$\left[\left(E_{0\mathbf{n}}^+\right)_1\right]_n$	n-th order correction to the first-order electric field	65
$\left[\left(E_{0\mathbf{n}}^+\right)_2\right]_n$	n-th order correction to the second-order electric field	66
$\mathrm{d}F(\mathbf{K},\omega_{\mathbf{K}})$	Fourier-Stieltjes coefficient of the ocean surface displacement	67
$\mathbf{K}$	Wave vector	67
$\omega_{\mathbf{K}}$	Angular frequency of the wave represented by the wave vector $\mathbf{K}$	67

Symbol	Description	Page
$g(\theta_1)$	Directivity function as defined in [3]	68
$\mathcal{F}_t^{-1}\{\cdot\}$	Inverse temporal Fourier transform	70
c	Speed of light	70
ω_0	Dominant or representative frequency of the transmitter	70
η_0	Intrinsic impedance of the vacuum	70
$i(t)$	Source current in the time domain	71
τ_0	Pulse width	71
ρ_0	Distance between receiver and the centre of the scattering patch in a monostatic configuration	72
$\Delta\rho$	Radar range resolution or patch width	72
Sa	Sampling function	73
$(E_{0\mathbf{n}}^{+})_{mn}$	n-th order hydrodynamic, m-th order electromagnetic electric field	77
$\left[(E_{0\mathbf{n}}^{+})_{mn}\right]_{pq}$	q-th order hydrodynamic, p-th order correction to the n-th order hydrodynamic, m-th order electromagnetic electric field	77
$\zeta_{0q}^{p}(\boldsymbol{\rho};t)$	q-th order hydrodynamic, p-th order arbitrary heights function	78
$(E_{0\mathbf{n}}^{+})_{2P}$	Second-order patch-scatter electric field	78
τ	Autocorrelation time delay	95
$\mathcal{R}_{E_{\mathbf{n}}^{+}}$	Second-order patch-scatter electric field	95

Symbol	Description	Page
$\mathcal{R}(\tau)$	Second-order patch-scatter electric field	95
A_r	Free-space aperture area of the receiver antenna	95
$\mathcal{R}_{mn}(\tau)$	Autocorrelation of the n-th order hydrodynamic, m-th order electromagnetic electric field	97
$[\mathcal{R}_{mn}]_{pq}(\tau)$	Autocorrelation of the q-th order hydrodynamic, p-th order correction to the n-th order hydrodynamic, m-th order electromagnetic electric field	97
$\mathcal{P}_{mn}(\omega_d)$	Power spectral density of the n-th order hydrodynamic, m-th order electromagnetic electric field	103
$[\mathcal{P}_{mn}]_{pq}(\omega_d)$	Power spectral density of the q-th order hydrodynamic, p-th order correction to the n-th order hydrodynamic, m-th order electromagnetic electric field	103
A_p	Area of the scattering patch over the ocean surface	106
$\sigma_{11}(\omega_d)$	First-order radar cross-section of a height-restricted ocean surface	106
$\sigma_{2P}(\omega_d)$	Patch scattering second-order radar cross-section of a height-restricted ocean surface	108
$\Xi_{11}(\omega_d)$	First-order hydrodynamic, first-order correction factor	109
$\Xi_{12}(\omega_d)$	Second-order hydrodynamic, first-order correction factor	109

Symbol	Description	Page
$\Xi_{21}(\omega_d)$	First-order hydrodynamic, second-order correction factor	113
$\mathrm{d}A_p$	Differential scattering area	114
$\mathcal{P}_r$	Receiver power	114
$\mathcal{P}_t$	Transmitter power	114
$\sigma(\omega_d)$	Radar cross-section of the scattering object	114
G_t	Transmitter gain	114
G_r	Receiver gain	114
λ_0	Wavelength of the transmitted signal	114
T_p	Peak wave period	126
ω_p	Peak angular frequency	126
γ	Peakedness parameter of the JONSWAP model	126
θ_W	Dominant wave direction of the ocean surface	127
s	Directional spreading parameter in a $\cos^{2s}$ directional model for the ocean surface	127
s_m	Maximum directional spreading in a $\cos^{2s}$ directional model for the ocean surface	127
s_p	Significant wave steepness of the ocean surface	128
U_{10}	Wind speed meaured at 10 m from the ocean surface	139
u^i, v^i	Contravariant components of the vectors $\mathbf{u}$ and $\mathbf{v}$	193
$\mathbf{b}_i$	Covariant basis vector	193

Symbol	Description	Page
$\mathbf{b}^i$	Contravariant basis vector	194
δ^i_j	Kronecker delta	194
Γ^k_{ji}	Christoffel symbols of the second kind	194

List of Figures

Chapter 1

Introduction

1.1 Research Rationale

During the past decades, climatologists have observed a statistically significant positive trend on average of the highest third of waves in the ocean, a metric known as significant wave height (H_s) [4]–[6]. An analysis of buoy and altimeter data for wind speeds and wave heights between 1985 and 2008 [7] has shown a statistically significant positive trend in waves within the 99^{th} percentile of the significant wave height distribution across the globe at a 95% confidence level, varying from a 2.41 cm increase per year in the Gulf of Mexico to a 5.20 cm increase per year in wave heights in the North Atlantic. This corroborates the results shown in several other studies, which have reported an increase in the frequency of extreme wave events [8]–[12]; this increase in significant wave heights can appreciably impact the operation and safety of offshore industries, coastal developments, and transportation of goods and people. However, as stated in [13], in-situ measurements of extreme wave events is a chal-

lenging task, as the sensors deployed are prone to failure under such circumstances. On the other hand, remote sensing technologies have been employed in the last few decades to perform measurements of extreme wave events [13].

Due to the effect that different sea states have on the scattered electromagnetic signal within the high-frequency (HF) band (3–30 MHz), HF radars have been largely employed in the remote sensing of ocean environments for both target detection and radio oceanography [14], [15]. Physical interpretations and mathematical models have been developed over the years to interpret data received by HF radar systems, including expressions of the radar cross-section (RCS) of the ocean surface, accounting for different electromagnetic and hydrodynamic interactions [16], [17], as well as different radar configurations [18]. In these works, the electric field is derived from physical and geometric interpretations of the model, and from that, the RCS can be obtained. The radar cross-section of the ocean surface is one of the most important expressions in the study of radio oceanography signals in the HF band, as it is required for the development of methods for the extraction of statistical and meteorological information from the ocean surface [19]–[23]. One of the methods employed to approximate the RCS of the ocean surface involves the application of perturbation theory [2].

Perturbation theory has been widely used to approximate the analytical solution of complex problems [24]–[26]. Perturbation methods are used to approximate the solution of a complex problem by incrementally modifying — i.e. perturbing — the solution to a simpler, but similar one, by introducing a series of approximations regulated by a small quantity known as the perturbation parameter. This perturbation parameter should be small for the problem at hand [27]. This imposes a limitation to the approximated solution, which should be observed at every step in the analysis.

To enable the use of perturbation expansions, two restrictions have been imposed to the scattering problem: the roughness scale, the product of significant wave height of the ocean surface and the radar transmitting wavenumber, must be much smaller than 1 — a limitation that is known as the *small-height approximation*; and the slope of the ocean surface should also be much smaller than 1, known as *small-slope approximation*. These are suitable restrictions if different radar frequencies are used to observe different sea states, such that the theoretical limits imposed by the perturbation theory are being respected. However, as the sea-state grows beyond the limits of the small-height approximation for a given radar frequency, the RCS expressions derived using these restrictions lose their validity, impacting the interpretation of signals obtained during extreme wave events [28].

As stated in [28], a completely new mathematical approach would be required to remove both restrictions, abandoning the use of perturbation theory altogether and ignoring the body of work on the analysis of HF radar returns developed over the last half century, which lies in the asymptotic approximation of the Fourier coefficients for the ocean surface [29]. Therefore, the derivation of a new approach that would remove one of the limitations while keeping the asymptotic analysis for the hydrodynamic interactions of the ocean surface is a valid research endeavour.

The primary goal of the present work is the development of a scattering theory for high-frequency signals propagating over a time-varying conductive random surface with arbitrary roughness scales, with a particular focus on ocean surfaces where the significant wave height becomes an appreciable fraction of the transmitter wavelength, a situation described here as electromagnetically-high sea state. The research presented here is intended to further improve the representation of the ocean surface

through its radar cross-section, serving as a basis for future research in the inversion of meteorological measurements at electromagnetically-high sea states, as well as to enhance the development of the scattering theory over conductive rough surfaces better described through curvilinear coordinates.

1.2 Literature Review

Although there was a vibrant debate in the field of electromagnetic propagation at the beginning of the twentieth century (e.g., [30]–[38]), most of the studies developed during this time were dedicated to the understanding and improvement of wireless telegraphic communications. The operational use of electromagnetic waves for probing and detection started just before World War II [39], and were largely developed due to the efforts to develop and advance early warning systems for aircraft and naval defence during the war [40], [41]. A vast body of academic and journalistic literature has been dedicated to report the efforts involving the study of radar in the microwave frequency during the war – e.g., [39]–[46].

For both radio telegraphy and target detection, electromagnetic scattering from the ocean surface was treated as interference known as "sea clutter" [14]. In 1946, Davies and Macfarlane [47] tried to give a theoretical treatment to the problem of sea clutter in radar measurements, deriving a scattering coefficient that could be used to calculate the echo from the sea surface. According to their experiments, this scattering coefficient would depend on the ocean wave height, transmitted wavelength, and angle of incidence. In 1950, Blake [48], posited that reflections from a rough sea would randomly fluctuate, generating what he called a "sea return" in microwave

amplitude-modulated communications. Even though Blake was not interested in using the scattered signal for oceanographic purposes, he derived the probability distribution of the sea return using the principles of harmonic analysis developed for ocean wave measurements proposed by Seiwell and Wadsworth [49]. At the same time, a report was being produced for the Naval Research Laboratory in the United States [50], detailing the measurement of sea surface reflectivity using a Doppler radar; however, this research was conducted with the sole purpose of testing the impact of the ocean surface on Doppler radar measurements.

One year after Blake's paper, Rice [27] developed a scattering theory for a slightly rough surface. In his analysis, Rice perturbed the solution of the electric field propagation over a perfectly smooth surface to obtain a solution to the electromagnetic field scattered by a rough surface. As a consequence of employing a perturbation approach to the solution of this problem, Rice's results were limited to slightly rough surfaces, as restrictions had to be imposed on both roughness height and slope. Even with this limitation, the theory proposed by Rice was a very important development in the theory of electromagnetic scattering over rough surfaces. Following its publication, Rice's work was first applied to ocean surfaces by Davies [51] in 1954, and would later be expanded by Wait [52]–[55], Peake and Barrick [56], and Barrick [2], [57].

A comprehensive analysis of the different scattering theories for rough surfaces can be found in the works of Fung [58], Barrick [59], Barabanenkov *et al.* [60], and Elfouhaily and Guérin [61]. Each of these works presents a different classification, but, in general, the approximate scattering theories for rough surfaces can be classified into three main groups: the small perturbation method (small roughness scales),

Kirchhoff approximation (large roughness scales), and unifying theories [61]. Using this classification, the generalized functions approach [17], [62] used in this thesis can be identified as a unifying theory as it can be used to bridge the gap between small and large roughness scales.

It was not until Crombie [63] that HF radars started being used to obtain meteorological measurements from the ocean surface, birthing the research field known as *radio oceanography*. Crombie conjectured that sharp peaks in the Doppler spectrum of the electric field scattered by the ocean surface occurred at frequency shifts that could be predicted by Bragg's law – in other words, the ocean surface acts as diffraction gratings to the electromagnetic waves. A similar phenomenon was observed by Dowden [64] and Haubert [65] in ionospheric measurements. The first theoretical treatment of this phenomenon was later given by Wait [66] in 1966. Even though Crombie's results are largely correct, Naylor and Robson [67] point to some inconsistencies in the analogy to Bragg scattering, stating that the phenomenon observed in ocean waves has a similar mathematical description to Bragg's law, but different underlying physical phenomenon.

In the theoretical analysis of HF radar signals in radio oceanography, the two most widely-used approaches are the small perturbation method [68], [69], based on the work of Rice [27], and the generalized functions approach [3], [17], based on the work of Walsh [62]. At different stages of their derivations, asymptotic expansions have been employed to obtain approximate solutions to the scattering problem at hand. To understand the restrictions imposed on the previously-devised approaches and the framework in which this research has been developed, the concept of asymptotic expansion needs to be examined first.

1.2.1 Generalized Asymptotic Expansion

An asymptotic sequence $\{\phi_m(\varepsilon)\}$ of a parameter ε can be defined as a sequence of functions defined on a set Ω such that, for every $m \in \mathbb{N}$,

$$\phi_m(\varepsilon) \in o[\phi_{m-1}(\varepsilon)] \text{ as } \varepsilon \to \varepsilon_0, \tag{1.1}$$

where ε_0 is a limit point of Ω, and $o[\cdot]$ is the Landau symbol known as "little Oh", a set defined such that, using the notation shown in (1.1) [70],

$$\lim_{\varepsilon \to \varepsilon_0} \left| \frac{\phi_m(\varepsilon)}{\phi_{m-1}(\varepsilon)} \right| = 0 \tag{1.2}$$

Some examples of asymptotic sequences are $\varepsilon^m,\ \varepsilon^{m/3},\ (\log \varepsilon)^{-m}$ [24].

A generalized asymptotic expansion of the function $f(\mathbf{x}) \in \Omega$ with respect to the asymptotic sequence $\{\phi_m(\varepsilon)\}$ can be written as [70], [71]

$$f(\mathbf{x};\varepsilon) = \sum_{m=0}^{N} f_m(\mathbf{x},\varepsilon) + o[\phi_N(\varepsilon)],\ \text{as } \varepsilon \to \varepsilon_0 \tag{1.3}$$

where $f_m(\mathbf{x};\varepsilon) \in \Omega,\ \forall m$ are the coefficients of the asymptotic expansion of $f(\mathbf{x})$. Therefore, the asymptotic series $F_N(\mathbf{x},\varepsilon) = \sum_{m=0}^{N} f_m(\mathbf{x},\varepsilon)$ is said to be an asymptotic expansion of $f(\mathbf{x})$ with respect to $\{\phi_m(\varepsilon)\}$ as $\varepsilon \to \varepsilon_0$ up to the Nth-order.

From the form presented in (1.3), a number of different types of asymptotic expansion can be defined [70]. One of the most common types of asymptotic expansion is the Poincaré-type expansion [24], [72]. An asymptotic expansion is said to be of Poincaré type when $f_m(\mathbf{x};\varepsilon) = a_m(\mathbf{x})\phi_m(\varepsilon)$, where $a_m(\mathbf{x}) \in \Omega$ is independent of the parameter ε. Also, a power series form of asymptotic expansion is a Poincaré-type expansion that has an asymptotic sequence defined as $\phi_m(\varepsilon) = (\psi(\varepsilon))^{\lambda_m}$, where $\psi(\varepsilon)$ is a function of ε independent of $\mathbf{x}$ and m, and λ_m is a constant number for each m.

An asymptotic expansion is said to be *uniformly valid* if within a given set, for all points within the set, each term of the asymptotic expansion is a small correction to its predecessor [24]. Mathematically, the asymptotic perturbation expansion $F_N(\mathbf{x}, \varepsilon)$ is uniformly valid for $\mathbf{x} \in \mathcal{I}$, $I \subset \Omega$, if [72]

$$f(\mathbf{x}; \varepsilon) - F_N(\mathbf{x}; \varepsilon) \in O[\phi_{N+1}(\varepsilon)], \text{ as } \varepsilon \to \varepsilon_0. \tag{1.4}$$

where $O[\cdot]$ is the Landau symbol known as "big Oh", a set defined such that, using the notation shown in (1.4), there exist constants $C \in \mathbb{R}$ and ε_1 such that [24]

$$|f(\mathbf{x}; \varepsilon) - F_N(\mathbf{x}; \varepsilon)| \leq C|\phi_{N+1}(\varepsilon)|, \text{ for } \varepsilon_0 < \varepsilon < \varepsilon_1,$$

or

$$\lim_{\varepsilon \to \varepsilon_0} \left| \frac{f(\mathbf{x}; \varepsilon) - F_N(\mathbf{x}; \varepsilon)}{\phi_{N+1}(\varepsilon)} \right| = L, \tag{1.5}$$

with $-\infty < L < \infty$ [72]. For the specific case of a power series form of asymptotic expansion where $\psi(\varepsilon) = \varepsilon$ and $\lambda_m = m$, the parameter ε should be smaller than 1 for the asymptotic expansion to be considered uniformly valid.

Asymptotic expansions have been largely applied to wave problems in physical oceanography [73]–[75], as well as in scattering problems in radio oceanography [17], [29], and are an important part of the analytical approximation method known as perturbation theory. In the following section, the use of asymptotic expansions to the solution of the rough surface scattering problem in radio oceanography, as well as the limitations imposed on the derivations, will be examined in more detail.

1.2.2 Limitations of Scattering Theories Applied to Radio Oceanography in the HF Band

Here, the scattering theories most widely used in the HF radar literature are examined, with a particular focus on the assumptions and restrictions imposed during their derivations. As the methods presented in the following sections are heavily dependent on the mathematical notation used in the derivations, the notation used in the following sections closely follows their presentation in the original works.

1.2.2.1 Perturbation Theory

Perturbation theory is a set of analytical mathematical methods for approximating the solution of a problem by using an asymptotic expansion of a parameter or coordinate involved or artificially introduced to the problem [24]. The main approach described in the present analysis is known as *parameter perturbation*, where a parameter is added to the solution of a similar problem to liken it to a known solution of a different problem.

One year after Wait's theoretical explanation of the Bragg scattering phenomenon observed by Crombie [63], Peake and Barrick [56] used the perturbation theory approach proposed by Rice [27] to analyze the electromagnetic scattering and radiative properties of lunar-like surfaces. Later, in 1970, Barrick [59], [76] incorporated the approach proposed in the works of Wait [52]–[54] to expand the lunar surface analysis to the HF and VHF scattering over the ocean surface. After Barrick's work, Wait [55] expanded the perturbation theory approach to a two-dimensional periodic ocean surface.

The perturbation theory approach to the scattering over the ocean surface proposed by Barrick [2], [57], [59], [76] starts with the closed-form solution for the scattering over a perfectly flat surface of a highly conductive material with impedance Δ. As presented in [2], the electric field in Cartesian coordinates (E_x, E_y, E_z) over such surface can be described as

$$E_x \approxeq E_0 \Delta \exp[jk_0(1-\Delta^2)^{1/2}x - j(k_0\Delta)z], \tag{1.6}$$

$$E_y = 0, \tag{1.7}$$

$$E_z \approxeq E_0 \exp[jk_0(1-\Delta^2)^{1/2}x - j(k_0\Delta)z], \tag{1.8}$$

where E_0 is the amplitude coefficient for the electric field and k_0 is the radar transmitter wavenumber. The time-dependent factor has been omitted in these expressions. As is commonly done in approximations using perturbation theory, the simpler solution is then perturbed to solve a marginally more complex problem. Now, considering a perturbation introduced by slightly rough surface, periodic within a square of side L and defined as a Fourier series as

$$\zeta(x,y) = \sum_{m,n=-\infty}^{\infty}\sum P(m,n)\exp[ja(mx+ny)],$$

with $P(m,n)$ being the Fourier coefficients, $a = \frac{2\pi}{L}$, and m and n defined such that am and an are wavenumbers in the x and y directions, the electric fields would take the form [2]

$$E_x = \Delta E(h,0,z) + \sum_{m,n=-\infty}^{\infty}\sum A_{mn}E(m+h,n,z), \tag{1.9}$$

$$E_y = \sum_{m,n=-\infty}^{\infty}\sum B_{mn}E(m+h,n,z), \tag{1.10}$$

$$E_z = E(h,0,z) + \sum_{m,n=-\infty}^{\infty}\sum C_{mn}E(m+h,n,z), \tag{1.11}$$

where

$$E(m+h,n,z) \equiv E_0 \exp[ja(m+h)x + jany + jb(m+h,n)z],$$

$$b(m+h,n) \equiv \left[{k_0}^2 - a^2(m+h)^2 - a^2n^2\right]^{1/2}.$$

At this point, it is necessary to derive the coefficients A_{mn}, B_{mn} and C_{mn} in terms of $P(m,n)$ and other defined parameters to obtain the electric field over a rough surface [56]. According to Peake and Barrick [56], this is done by using a power series form of asymptotic expansion in all possible quantities involved in these equations, with $\phi(\varepsilon) = \varepsilon^m$ and ε being chosen between $k_0\zeta$, $\partial\zeta/\partial x$, and $\partial\zeta/\partial y$. As a consequence of the use of perturbation theory and for the asymptotic expansion to be uniformly valid, both the roughness scale and the slopes of the surface must be sufficiently small [28]. This assumption inhibits the removal of any of the height and slope limitations imposed on the derivations from the electric fields derived using Barrick's expressions.

1.2.2.2 Generalized Functions Approach

Another approach to the problem of high-frequency electromagnetic scattering over the ocean surface is the generalized functions method. The first application of distributions to the solution of Maxwell's equations was done in 1969 by Cerutti-Maori *et al.* [77], where they were deriving a numerical approach to the problem of electromagnetic waves propagating through diffraction gratings. The results presented in this work were later applied and expanded by Petit and Maystre [78], Maystre and Vincent [79], and Petit [80], and more recently by Akarid and Polack [81].

Independent from the developments shown in [77]–[80], Walsh [82] first presented

his approach to the application of generalized functions to electromagnetic problems in 1976, where he used mathematical distributions to obtain the currents in an antenna; this method was later applied to the analysis of currents in thin linear antennas by Walsh and Srivastava in 1977 [83], [84]. In a report to the Defense Research Establishment Atlantic (DREA) in 1980 [62], Walsh expanded the generalized functions method to analyze the electric field scattered by a rough surface, which was later extended by Srivastava [85] to obtain the radar cross-section of the rough surface. Based on all their previous research, Walsh and his colleagues refined the method of generalized functions, proposing a more general approach to rough surface scattering [86], expanded its application to mixed path propagation [87], and developed a general theory for the two-body scattering problem Walsh and Donnelly [1]. In 1990, Walsh and his colleagues applied their theory to the scattering of electric fields over the ocean surface [17], deriving expressions for the monostatic radar cross-section of the ocean surface including hydrodynamic interactions up to the third-order — i.e. the combination of up to three monochromatic waves [17]; this theory was later revised by Walsh and Gill [3] in 2000, and expanded to radars in bistatic configuration by Gill and Walsh [18], based on the results derived by Walsh and Dawe [88] and Gill [89].

The method consists of using mathematical distributions, also known as generalized functions, to represent scattering objects in the derivations of electromagnetic scattering. Albeit this method admittedly involves "a great deal of notation" [1], the generalized functions method is a powerful scattering analysis technique derived directly from Maxwell's equations, with the advantage of the boundary conditions coming out naturally from their derivations.

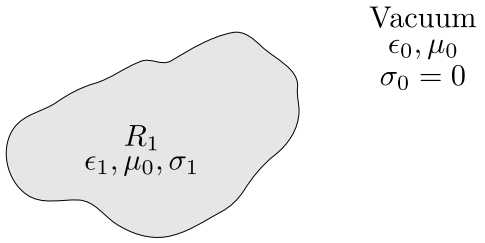

Figure 1.1: Geometric representation of a one-body scattering problem

For the sake of brevity, the generalized functions approach presented here will concern the scatter over a single body; for the two-body problem, please refer to [1].

Coordinate system restrictions imposed to the electric field scattered by a single body

Consider a single nonmagnetic isotropic physical body immersed in the vacuum, as shown in Figure 1.1. In a distributional sense, the region R_1 can be represented as

$$h_{R_1}(\mathbf{r}) = \begin{cases} 1, & \mathbf{r} \in R_1, \\ 0, & \text{otherwise.} \end{cases} \tag{1.12}$$

From (1.12), electromagnetic properties such as permittivity (ϵ) and conductivity (σ) can be derived for the entire space as

$$\epsilon = h_{R_1}\epsilon_1 + (1 - h_{R_1})\epsilon_0 \tag{1.13}$$

$$\sigma = h_{R_1}\sigma_1 + (1 - h_{R_1})\sigma_0 = h_{R_1}\sigma_1, \tag{1.14}$$

where ϵ_1 and ϵ_0 are respectively the permittivity of R_1 and of the vacuum ($\epsilon_0 \approx 8.8542 \times 10^{-12}\ \mathrm{F \cdot m^{-1}}$), and σ_1 and σ_0 are respectively the conductivity of R_1 and of the vacuum ($\sigma_0 = 0\ \Omega \cdot \mathrm{m}$). Since the body is considered to be nonmagnetic, the magnetic permeability of the scattering body is considered to equal to the magnetic

constant $\mu_0 = 4\pi \times 10^{-7}\ \mathrm{H} \cdot \mathrm{m}^{-1}$.

Applying (1.13) to the constitutive relation for the electric displacement field $\mathbf{D}$, and (1.14) to the Ohm's law for electromagnetic fields [90], the following expressions can be obtained:

$$\mathbf{D} = \epsilon\mathbf{E} = h_{R_1}\epsilon_1\mathbf{E} + (1 - h_{R_1})\epsilon_0\mathbf{E}, \tag{1.15}$$

$$\mathbf{J}_c = \sigma\mathbf{E} = h_{R_1}\sigma_1\mathbf{E}, \tag{1.16}$$

where $\mathbf{E}$ is the total electric field, and $\mathbf{J}_c$ is the conduction current density. Applying the definitions presented in (1.15) and (1.16) to the point form of the Maxwell's equations, the following system of equations can be obtained:

$$\nabla \times \mathbf{E} = -j\omega\mu_0\mathbf{H}, \tag{1.17}$$

$$\nabla \times \mathbf{H} = j\omega\epsilon_0 n_0^2\mathbf{E} + \mathbf{J}_s, \tag{1.18}$$

$$\nabla \cdot \mathbf{D} = \rho, \tag{1.19}$$

$$\nabla \cdot \mathbf{B} = \nabla \cdot \mathbf{H} = 0, \tag{1.20}$$

where $\mathbf{H}$ is the total magnetic field, n_0 is the refraction coefficient of the whole space, given as

$$n_0^2 = \left[\frac{\epsilon}{\epsilon_0} - \frac{\sigma}{j\omega\epsilon_0}\right] = n_{01}^2 h_{R_1} + (1 - h_{R_1}), \tag{1.21}$$

with n_{01} being the refraction coefficient of the scattering region R_1, defined as

$$n_{01}^2 \triangleq \frac{\epsilon_1}{\epsilon_0} + \frac{\sigma_1}{j\omega\epsilon_0},$$

$\mathbf{J}_s$ is the current density of the source, and $\mathbf{B}$ is the magnetic density, defined as [90] $\mathbf{B} = \mu_0\mathbf{H}$ for free space and nonmagnetic materials. Following the standard procedure

to obtain the Helmholtz equation for the electric field [90], the following expression can be obtained [1]:

$$\nabla^2\mathbf{E} + k^2 n_0^2 \mathbf{E} = \nabla\left(\nabla \cdot \mathbf{E}\right) + i\omega\mu_0 \mathbf{J}_s \tag{1.22}$$

where k is the transmitter wavenumber.

Now, applying the divergence operator on (1.18), knowing that the divergence of a curl is equal to zero, the following expression can be obtained [1]:

$$\nabla \cdot (n_0^2 \mathbf{E}) = -\frac{1}{j\omega\epsilon_0} \nabla \cdot \mathbf{J}_s. \tag{1.23}$$

From the definition in (1.21), and knowing that R_1 is an homogeneous and isotropic body, the divergence of $n_0^2\mathbf{E}$ can be written as

$$\begin{aligned} \nabla \cdot n_0^2 \mathbf{E} &= n_{01}^2 \nabla \cdot (h_{R_1}\mathbf{E}) + \nabla \cdot \left[(1 - h_{R_1})\mathbf{E}\right], \\ \therefore \nabla \cdot n_0^2 \mathbf{E} &= n_{01}^2 (h_{R_1} \nabla \cdot \mathbf{E} + \mathbf{E}^- \cdot \nabla h_{R_1}) + \left[(1 - h_{R_1})\nabla \cdot \mathbf{E} - \mathbf{E}^+ \cdot \nabla h_{R_1}\right]. \end{aligned} \tag{1.24}$$

The superscripts $+$ and $-$ in (1.24) indicate an operation at each side of the boundary of the scattering object: $\mathbf{E}^+$ is the electric field at the outer boundary of R_1, while $\mathbf{E}^-$ is the electric field at the inner boundary. This is due to the fact that, in generalized function terms, the gradient of h_{R_1} would only be valid at the boundary of the region defined by h_{R_1}. Here, ∇h_{R_1} is taken to be the inward-pointing normal, and therefore, quantities associated with it will be measured at the inner boundary of R_1; conversely, if a quantity is associated with $-\nabla h_{R_1}$, its measurements are taken at the outer boundary of R_1.

Substituting (1.24) into (1.23), and comparing terms with the same support, as-

suming a source outside R_1, the following expressions can be obtained:

$$h_{R_1}\nabla\cdot\mathbf{E}=0, \tag{1.25}$$

$$(1-h_{R_1})\nabla\cdot\mathbf{E}=-\frac{1}{j\omega\epsilon_0}\nabla\cdot\mathbf{J}_s, \tag{1.26}$$

$$(n_{01}^2\mathbf{E}^- - \mathbf{E}^+)\cdot\nabla h_{R_1}=0. \tag{1.27}$$

The expressions in (1.25) and (1.26) are mathematical representations of the initial condition that the source of the electric field is completely contained outside the region R_1. On the other hand, (1.27) reflects a boundary condition, quantifying the change in the electric field at the boundary of R_1. As noted in [1], this boundary condition naturally arises from the generalized function definition of the scattering body.

Using the generalized expression of the total electric field, it is possible to show that

$$\nabla\cdot\mathbf{E}=h_{R_1}(\nabla\cdot\mathbf{E})+(1-h_{R_1})(\nabla\cdot\mathbf{E})+(\mathbf{E}^- - \mathbf{E}^+)\cdot\nabla h_{R_1}. \tag{1.28}$$

Substituting the expressions in (1.25) to (1.27) into (1.28), the following expression can be obtained:

$$\nabla\cdot\mathbf{E}=-\frac{1}{j\omega\epsilon_0}\nabla\cdot\mathbf{J}_s-\frac{n_{01}^2-1}{n_{01}^2}\mathbf{E}^+ \tag{1.29}$$

Substituting (1.29) into (1.22), and defining the source vector operator T_{SE} as

$$T_{SE}(\mathbf{J}_s)\triangleq\frac{1}{j\omega\epsilon_0}\nabla\left(\nabla\cdot\mathbf{J}_s\right)-j\omega\mu_0\mathbf{J}_s, \tag{1.30}$$

the Helmholtz equation for the electric field in the presence of the scattering body R_1 can be written as

$$\nabla^2\mathbf{E}+k^2n_0^2\mathbf{E}=-T_{SE}(\mathbf{J}_s)-\frac{n_{01}^2-1}{n_{01}^2}\nabla\left(\mathbf{E}^+\cdot\nabla h_{R_1}\right), \tag{1.31}$$

with the Laplacian of E written in terms of generalized functions as

$$\nabla^2\mathbf{E} = \nabla^2(h_{R_1}\mathbf{E}) + \nabla^2\left[(1-h_{R_1})\mathbf{E}\right].$$

Up to this point, the expressions presented here can be applied to any coordinate system. However, when Walsh and Donnelly [1] interpreted the Laplacian as an operator applied to the scalar components of $\mathbf{E}$, they implicitly assumed that the basis of the coordinate system in question would be formed by constant vectors, that would be independent of the directional variables. While this assumption is true for the Cartesian coordinate system, its application render the results shown in [1] invalid for fields and objects represented in curvilinear coordinates that do not have constant basis vectors, such as is the case for spherical and cylindrical coordinates.

If Cartesian coordinates are considered, the electric field in the presence of a scattering object R_1 can be given as the solution of the following system of equations:

$$h_{R_1}\mathbf{E} = -\left\{\nabla\cdot[(\mathbf{E}^-)\nabla h_{R_1}] + (\nabla\mathbf{E})^-\cdot\nabla h_{R_1}\right\} * K_1, \tag{1.32}$$

$$(1-h_{R_1})\mathbf{E} = T_{SE}(\mathbf{J_s}) + \left\{\nabla\cdot[(\mathbf{E}^+)\nabla h_{R_1}] + (\nabla\mathbf{E})^+\cdot\nabla h_{R_1}\right\} * K_0, \tag{1.33}$$

$$(1-h_{R_1})\left\{\{\nabla\cdot[(\mathbf{E}^-)\nabla h_{R_1}] + (\nabla\mathbf{E})^-\cdot\nabla h_{R_1}\right\} * K_1\} = 0, \tag{1.34}$$

$$h_{R_1}\left\{\{T_{SE}(\mathbf{J_s}) + \nabla\cdot[(\mathbf{E}^+)\nabla h_{R_1}] + (\nabla\mathbf{E})^+\cdot\nabla h_{R_1}\right\} * K_0\} = 0, \tag{1.35}$$

with boundary condition

$$\left[(\nabla\mathbf{E})^- - (\nabla\mathbf{E})^+\right]\cdot\nabla h_{R_1} + \nabla\cdot\left[(\mathbf{E}^- - \mathbf{E}^+)(\nabla h_{R_1})\right] = -\left(\frac{{n_{01}}^2 - 1}{{n_{01}}^2}\right)\nabla(\mathbf{E}^+\cdot\nabla h_{R_1}), \tag{1.36}$$

where K_0 and K_1 are Green's functions of the form

$$K_m(x,y,z) = \frac{e^{-jA_m r}}{4\pi r}, \qquad m = 0 \text{ or } 1, \tag{1.37}$$

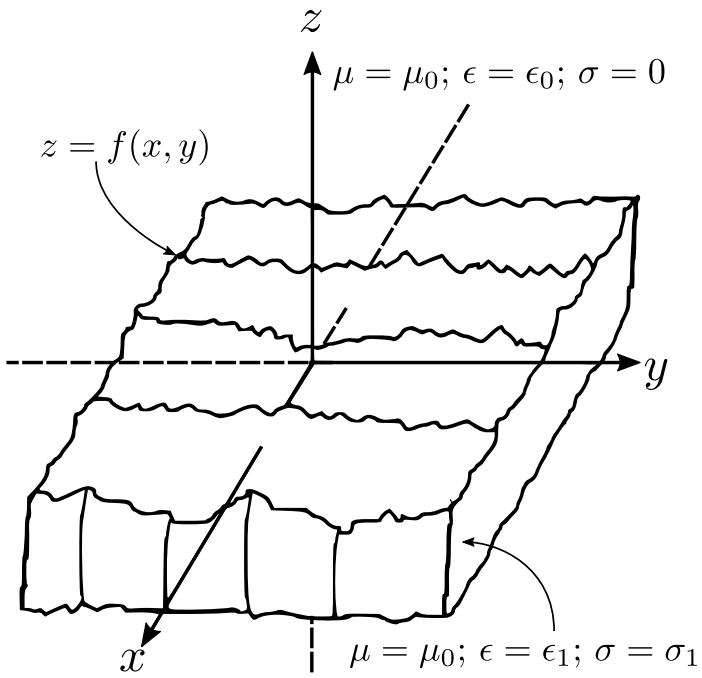

Figure 1.2: Geometric representation of a rough surface

with $r = \sqrt{x^2 + y^2 + z^2}$, $A_0 = k$, and $A_1 = kn_{01}$. From the system of equations presented in (1.32) to (1.36), the electric field scattered by any single nonmagnetic body can be derived. Based on this system of equations, Walsh and Gill [3] derived the expression for the electric field scattered by a time-varying periodic random rough surface.

Small-height and small-slope approximations in the generalized functions approach to the scattering over a conductive rough surface

Using the generalized functions approach, a rough surface with simplified geometrical representation shown in Figure 1.2 can be described as [3], [86]

$$h_{R_1}(x, y, z) = 1 - \Theta[z - f(x, y)], \tag{1.38}$$

where $\Theta(\cdot)$ is the Heaviside function, and $f(x, y)$ is the vertical surface displacement

with respect to $z = 0$.

Applying the generalized function representation of the rough surface presented in (1.38) to the system of equations for the electric field presented in (1.32) to (1.36) and following the derivation process presented in [3], the operator equation for the electric field scattering over rough surfaces can be obtained as

$$\mathcal{N}\mathcal{L}^{-1}\left[\frac{\mathcal{L}\mathcal{N}\mathcal{L}^{-1}\left[2u\mathcal{F}_{xy}(\mathbf{E}_s^{z^-})\right]}{u+jk\Delta}\right] = \mathbf{E}_n^+ + \mathcal{N}\mathcal{L}^{-1}\left[\frac{\mathcal{L}\mathcal{N}\left(\frac{\nabla_{xy}(|\mathbf{n}|E_n^+)}{|\mathbf{n}|^2}\right)}{u+jk\Delta}\right]. \tag{1.39}$$

Here the following definitions apply:

- $\mathbf{E}_s^{z^-}$ is the source electric field at the $z = z^- < f(x,y),\ \forall(x,y)$;
- $\mathbf{E}_n^+$ is the electric field normal to the ocean surface measured at a plane immediately above the surface with magnitude E_n^+;
- $\mathbf{n}$ is the outer normal vector to the surface $f(x,y)$, defined as

$$\mathbf{n} = \hat{\mathbf{z}} - \nabla f(x,y); \tag{1.40}$$

- k is the wavenumber of the electromagnetic signal;
- Δ is the surface impedance;
- $u = \sqrt{K^2 - k^2}$, with $K^2 = {K_x}^2 + {K_y}^2$ being the wavenumber of the ocean surface;
- $\mathcal{F}_{xy}(\cdot)$ is the spatial Fourier transform in the xy-plane, defined for a generic function $g(x,y)$ as

$$\mathcal{F}_{xy}(g(x,y)) = \iint g(x,y)e^{jK\sqrt{x^2+y^2}\cos(\theta-\theta_K)}\,\mathrm{d}x\,\mathrm{d}y,$$

where $\theta = \arctan\left(\frac{y}{x}\right)$ and $\theta_K = \arctan\left(\frac{K_y}{K_x}\right)$.

The operators $\mathcal{N}\{\cdot\}$ and $\mathcal{L}\{\cdot\}$ are respectively defined for a generic vector $\mathbf{A}$ as

$$\mathcal{N}\{\mathbf{A}\} \triangleq \hat{\mathbf{n}}\hat{\mathbf{n}} \cdot \mathbf{A} = \mathbf{A}_n \tag{1.41}$$

where $\hat{\mathbf{n}}$ is the unit vector in the direction of the outer normal vector $\mathbf{n}$, with $\mathbf{A}_n$ being the projection of $\mathbf{A}$ in the same direction of $\hat{\mathbf{n}}$, and

$$\mathcal{L}\{\mathbf{A}\} \triangleq \mathcal{F}_{xy}\left\{|\mathbf{n}|^2 \mathbf{A} e^{(z^- - f(x,y))u}\right\}, \tag{1.42}$$

with $\mathcal{L}^{-1}\{\cdot\}$ being the inverse of the $\mathcal{L}$-operator.

Now, in order to solve the operator equation in (1.39), the inverse $\mathcal{L}^{-1}$ must be derived. At this point, Walsh and Gill [3] took advantage of the often-imposed small-height approximation, making $|kf| << 1$ for all points in the xy-plane. Thus, the $\mathcal{L}$-operator could be redefined for a generic vector $\mathbf{A}$ as

$$\mathcal{L}\{\mathbf{A}\} \approx e^{z^- u}\mathcal{F}_{xy}\left\{|\mathbf{n}|^2 \mathbf{A}\right\}, \tag{1.43}$$

allowing $\mathcal{L}^{-1}$ to be approximated as

$$\mathcal{L}^{-1}\{\mathbf{A}\} \approx \frac{1}{|\mathbf{n}^2|}\mathcal{F}_{xy}^{-1}\left[e^{-z^- u}\mathbf{A}\right]. \tag{1.44}$$

From this point on, the results presented in [3] can only be applied to surfaces with $|kf| << 1$, but with unconstrained surface slope. Substituting these definitions into the operator equation, Walsh and Gill [3] arrive at the operator equation

$$E_{0n}^{+} - \mathcal{T}_1(E_{0n}^{+}) - \mathcal{T}_2(E_{0n}^{+}) = E^s, \tag{1.45}$$

where E_{0n}^{+} is the magnitude of the normal electric field measured immediately above the surface, including the small heights approximation, indicated by the 0 subscript,

$$\mathcal{T}_1(\cdot) = \frac{1}{|\mathbf{n}|^3} \cdot \left\{\frac{\nabla f}{|\mathbf{n}|^2} \cdot \nabla_{xy}[|\mathbf{n}|\,(\cdot)] \overset{xy}{*} F(\rho)\frac{e^{-jk\rho}}{2\pi\rho}\right\}, \tag{1.46}$$

$$\mathcal{T}_2(\cdot) = \frac{\nabla f}{|\mathbf{n}|^3} \cdot \left\{ \frac{\nabla f \nabla f}{|\mathbf{n}|^2} \cdot \nabla_{xy}[|\mathbf{n}|\,(\cdot)] \overset{xy}{*} F(\rho) \frac{e^{-jk\rho}}{2\pi\rho} \right\}, \tag{1.47}$$

and

$$E^s = \frac{\mathbf{n}}{|\mathbf{n}|^3} \cdot \left\{ \frac{\mathbf{nn}}{|\mathbf{n}|^2} \cdot \left[2u\mathcal{F}_{xy}(\mathbf{E}_s^{z^-}) e^{-z^- u} \right] \overset{xy}{*} F(\rho) \frac{e^{-jk\rho}}{2\pi\rho} \right\}, \tag{1.48}$$

with $F(\rho)$ being the Sommerfeld attenuation function [35], as defined in [91].

To simplify (1.45) Walsh and Gill imposed the small slopes approximation, making $|\nabla f|^2 << 1$, significantly reducing the complexity of the derivations. Moreover, disregarding any power of $|\nabla f|$ greater than one permits the complete removal of the $\mathcal{T}_2$ operator from (1.45), which greatly simplifies the use of the Neumann series to solve the operator equation.

At this point, it should be noted that no asymptotic expansion had been employed, and that the small-height and small-slope approximations have been included independently. The asymptotic expansion was only applied in [17] to represent the Fourier coefficients of the ocean surface during the derivation of the first-order electric field, as proposed by Weber and Barrick [29]. However, the asymptotic expansion in [29] was applied in the context of a perturbation expansion, and assumed the form suggested by Peake and Barrick [56] presented in Section 1.2.2.1, inheriting its small-height and small-slope restrictions embedded in their choice of perturbation parameter ε. As these conditions had already been applied to the expressions at that point, the asymptotic perturbation expansion of the Fourier coefficients for the ocean surface is considered valid. This resulted in radar cross-sections with a different formulation than the ones proposed by Barrick [16], with formulations converging for a sufficiently large patch width on the ocean surface [18], [92].

1.2.3 Choosing a Theoretical Framework for the EM Scattering Over Ocean Surfaces With Electromagnetically-Large Waves

As mentioned in Section 1.2, for HF radars applied to radio oceanography, the most widely-used approach to the scattering theory is the small perturbations method, based on the work of Rice [27], followed by the generalized functions approach introduced by Walsh [62].

Peake and Barrick [56] laid out the fundamentals for the analysis of electromagnetic scattering over rough surfaces that would later be used in the theory of HF and VHF scattering over the ocean surface [2]. Although this is apparently a straightforward method to obtain the electric field scattered by a slightly rough surface, constraints on surface height and slope are introduced directly to the electric field at the inception of the proposed problem, reinforced by the choice of a power series form of asymptotic perturbation expansion, as presented in Section 1.2.2.1. Both restrictions are fundamental to the small perturbations method, making it impossible to remove any one of the restrictions using the approach presented in [56].

On the other hand, from the theory of generalized functions presented in Section 1.2.2.2, the small height and small slope approximations are applied at different stages of the derivation, and their use is independent of the asymptotic expansion of the ocean surface, used here to obtain different hydrodynamic components of the electric field [17]. In short, while the perturbation expansion in [2] forbids any further relaxation on the surface constraints, the theory presented in [3] imposes these restrictions independently and then makes use of the constrained values independently

from each other. Therefore, the theoretical framework proposed by Walsh and Gill [3] and Walsh *et al.* [17] is better suited to the derivation of the scattered electric field from an ocean surface with arbitrary heights.

1.3 Scope of the Thesis

The primary goal of the present thesis is the development of a theoretical treatment to the scattering of electric fields over a time-varying, conductive random rough surface with arbitrary roughness scales, paying special attention to possible impacts of this theory on radio oceanography applications in the HF band. First, expressions for the electric field scattered by an ocean surface with electromagnetically large waves must be derived; then, having the corrected expressions for the scattered electric field, the radar cross-section must be obtained. However, to remove the small-height restriction from these expressions, a theoretical framework for the scattering analysis must be chosen.

As shown in Section 1.2.3, the generalized functions technique introduced by Walsh and Gill [3] and Walsh *et al.* [17] is the best suited to support the removal of the small-height restriction in the derivations. However, as noted in Section 1.2.2.2, the generalized functions method is limited to applications to problems with coordinate systems with constant vectors, such as Cartesian coordinates. Therefore, before proceeding with the derivations for the scattering over a rough surface, a new form for the system of equations for the electric field using the generalized functions method is proposed in Chapter 2, expanding the generalized functions method to any curvilinear coordinate system and allowing for the use of coordinate systems that better

describe some scattering objects, such as spherical and cylindrical coordinates.

From this new system of equations, the corrections to the electric field scattered by an ocean surface with electromagnetically-large waves are presented in Chapter 3 for different hydrodynamic and elecromagnetic orders. It is shown that, if the small-heights approximation is applied to these new expressions, they return to the height-restricted forms presented in [3]. The expressions derived for these new electromagnetic fields also employ the asymptotic expansion to the Fourier coefficients of the ocean surface, albeit with a different approach from the ones presented by Walsh *et al.* [17] and Peake and Barrick [56]. While previous works used both the roughness scale and surface slope as perturbation parameters in the asymptotic expansion, the present research work only uses the latter, as proposed by Hasselmann [75]. This approach permits the use of traditional analysis techniques based on different hydrodynamic and electromagnetic orders of scattering while allowing for the growth of the roughness parameter without invalidating the employed approximation.

Once the expressions for the scattered electric field for the ocean surface with electromagnetically-large waves are obtained, the radar cross-section of the ocean surface for each of the new expressions is shown in Chapter 4. The procedure followed here to obtain the new RCS terms combines the ones shown by Walsh *et al.* [17] and Gill and Walsh [18], in which the power spectral density of each term is derived from the normalized autocorrelation of the electric field and compared to the radar equation to identify the terms corresponding to the RCS. Observing the expressions for the resulting power spectral density of each correction term, it is evident that the resulting RCS can be obtained from the product between the height-restricted radar cross-section and a correction factor, unique to each correction order.

Using simulated RCSs, a morphological analysis of the correction terms is conducted in Chapter 5, observing their characteristics on the Doppler spectrum and its impact on total radar cross-section of the ocean surface. To validate the results presented in this thesis, an analysis of field data collected under electromagnetically-high sea states is also presented. From the characteristics observed in the morphological analysis, evidence of the presence of first-order correction terms can be identified in field data collected in Fedje, Norway, during the EuroROSE experiment [93]. While the evidence presented here is not conclusive, it provides a good indication that the terms derived here can be present in the total radar cross-section of the ocean surface, opening a new avenue for research in the future.

A summary of the findings presented in this thesis, as well as suggestions for future research are presented in Chapter 6.

1.4 Contributions to the Literature

An abridged form of the results presented here has been submitted and published in peer-reviewed journals and presented in international conferences. The content of these publications was organized in this thesis such that the reader can find a more coherent picture of the findings, and parts of the derivation were expanded based on the notes produced during this research.

The results on the curvilinear form of the system of equations for the electric field scattered by a single body presented in Chapter 2 can be found in [94], with some additional steps in the derivation included in this thesis to clarify the reasoning to the reader. Chapters 3 to 5 draw from the results published in [95]–[97] and

from an additional paper, currently in press at the IEEE Transactions on Antennas and Propagation [98], organized to present a clear picture of the research and the procedure followed in the derivation, and to reduce redundancy in the information presented to the reader.

Further abridged versions of the findings of this research were presented in international conferences. Some of the derivations of the first-order correction to the radar cross-section of the ocean surface for arbitrary heights were presented as a summary in [99] and expanded in [100], yielding an honourable mention in the Student Paper Competition in the latter conference. Preliminary derivations of the second-order correction term were presented in [101].

Chapter 2

Electric Field Scattering in Curvilinear Coordinates Using a Generalized Functions Method

2.1 Introduction

In a series of papers published in 1987 [1], [86], [87], Walsh and his colleagues presented a method for obtaining the mathematical expressions of scattered electromagnetic fields from different bodies using distributions, also known as generalized functions, to define the geometry of bodies with different physical properties in the scattering media. One of the main advantages of this method is that the boundary conditions appear naturally in the mathematical derivations, not being imposed from the start. This is a significant advantage when bodies with intricate geometries are considered. However, assumptions in the derivation of the system of equations for the electric

field have limited the analysis to spaces described in Cartesian coordinates.

The work presented in this chapter aims to extend the generalized functions method presented by Walsh and his colleagues to curvilinear coordinates. This allows for the derivation of electromagnetic field equations for scattering bodies with geometries that are better described by cylindrical, spherical, or any other curvilinear coordinate system. The derivations presented here are similar to the one shown by Walsh and Donnelly [1] for two-body scattering, and briefly introduced in Section 1.2.2.2 for a single body. Here, however, the system of equations is derived purely by using vector and dyadic calculus identities, independent of a coordinate system, allowing for a more general approach, in which no coordinate systems are imposed on the electric field until the definition of the scattering surface.

2.2 System of Equations for the Electric Field in Curvilinear Coordinates using Generalized Functions

For the present analysis, the generalized function representation of a single body immersed in the vacuum shown in Section 1.2.2.2 will be considered. The time-harmonic Maxwell's differential equations for the studied region can be written as

[90]

$$\nabla \times \mathbf{E} = -j\omega\mu_o\mathbf{H}, \tag{2.1}$$

$$\nabla \times \mathbf{H} = j\omega\mathbf{D} + \mathbf{J}_c + \mathbf{J}_s, \tag{2.2}$$

$$\nabla \cdot \mathbf{D} = \rho, \tag{2.3}$$

$$\nabla \cdot \mathbf{B} = 0, \tag{2.4}$$

with ω being the angular frequency of the time-harmonic fields, and remaining notation described in Section 1.2.2.2.

From (2.1) to (2.4), using the generalized function definitions of the electric displacement field $\mathbf{D}$ and conduction current density $\mathbf{J}_c$ in (1.15) and (1.16) respectively, a form of the Helmholtz vector differential equation for the electric field can be obtained as

$$\nabla \times \nabla \times \mathbf{E} + \gamma^2\mathbf{E} = -j\omega\mu_0\mathbf{J}_s, \tag{2.5}$$

where γ is the propagation constant for the entire space, which can be written with respect to h_{R_1} as

$$\begin{aligned} \gamma^2 &= h_{R_1}(j\omega\mu_0(\sigma_1 + j\omega\epsilon_1)) + (1 - h_{R_1})(j\omega\mu_0(j\omega\epsilon_0)), \\ \gamma^2 &\triangleq h_{R_1}{\gamma_1}^2 + (1 - h_{R_1}){\gamma_0}^2, \end{aligned} \tag{2.6}$$

with γ_1 and γ_0 defined respectively as the propagation constants for the region R_1 and the vacuum.

By applying the vector calculus identity for the double curl of a vector, (2.5) can be rewritten as

$$\nabla^2\mathbf{E} - \gamma^2\mathbf{E} = j\omega\mu_0\mathbf{J}_s + \nabla(\nabla \cdot \mathbf{E}). \tag{2.7}$$

Comparing the forms of the Helmholtz equation presented in (2.7) and that by Walsh and Donnelly [1] in (1.22), it is clear that $\gamma = -jkn_0$.

To obtain the system of equations for $\mathbf{E}$, the expressions for $\nabla^2\mathbf{E}$ and $\nabla \cdot \mathbf{E}$ must be defined. From (1.15), it can be inferred that

$$\mathbf{E} = h_{R_1}\mathbf{E} + (1 - h_{R_1})\mathbf{E}, \tag{2.8}$$

which indicates that the total electric field in space is the sum of the electric field inside and outside the region R_1. By applying the Laplacian on both sides of (2.8), the following expression can be obtained:

$$\nabla^2\mathbf{E} = \nabla^2(h_{R_1}\mathbf{E}) + \nabla^2[(1 - h_{R_1})\mathbf{E}] \tag{2.9}$$

As discussed in Section 1.2.2.2, at this point Walsh and Donnelly [1] implicitly assumed that a coordinate system with constant basis vectors had been used. This allowed them to apply the Laplacian operator only to the components of the electric field, disregarding any derivatives of the basis vectors. To avoid this assumption, vector and dyadic identities will be considered in this analysis.

Using the definition of the Laplacian operator, the first term of (2.9) can be expanded as

$$\nabla^2(h_{R_1}\mathbf{E}) = \nabla \cdot [\nabla(h_{R_1}\mathbf{E})].$$

Using dyadic identities to expand the inner gradient of the expression [102], the Laplacian can be written as

$$\nabla^2(h_{R_1}\mathbf{E}) = \nabla \cdot [(\nabla h_{R_1})\mathbf{E}^- + h_{R_1}\nabla\mathbf{E}].$$

where $\nabla\mathbf{E}$ is the dyadic representing the gradient of $\mathbf{E}$ and the negative superscript in $\mathbf{E}^-$ indicate that the electric field should be evaluated at the inner boundary of the

region R_1. This can be inferred from the physical interpretation of the gradient of the distribution h_{R_1}, where it would represent the boundary discontinuity approached from within the region in question.

Applying dyadic identities to expand the divergence operators, the first term of (2.9) can be written as

$$\nabla^2(h_{R_1}\mathbf{E}) = (\mathbf{E}^-)\nabla^2 h_{R_1} + 2[\nabla h_{R_1} \cdot (\nabla \mathbf{E})^-] + h_{R_1}\nabla^2\mathbf{E}, \tag{2.10}$$

It is important to note that, in the case of $(\nabla\mathbf{E})^- \cdot \nabla h_{R_1}$, the dot product is non-commutative [102]. Analogously, the second term in (2.9) can be expanded as

$$\nabla^2[(1-h_{R_1})\mathbf{E}] = -(\mathbf{E}^+)(\nabla^2 h_{R_1}) - 2[(\nabla h_{R_1}) \cdot (\nabla\mathbf{E})^+]\mathbf{E} + (1-h_{R_1})\nabla^2\mathbf{E} \tag{2.11}$$

where the positive superscript indicates the field or the evaluation of the Jacobian at the outer boundary of R_1. Substituting (2.10) and (2.11) into (2.9), gives

$$\nabla^2\mathbf{E} = (\mathbf{E}^- - \mathbf{E}^+)\nabla^2 h_{R_1} + 2\left\{\nabla h_{R_1} \cdot \left[(\nabla\mathbf{E})^- - (\nabla\mathbf{E})^+\right]\right\} + h_{R_1}\nabla^2\mathbf{E} + (1-h_{R_1})\nabla^2\mathbf{E} \tag{2.12}$$

Now, applying the divergence operator on both sides of (2.8), the following expression can be obtained:

$$\nabla \cdot \mathbf{E} = h_{R_1}\nabla \cdot \mathbf{E} + (1-h_{R_1})(\nabla \cdot \mathbf{E}) + \nabla h_{R_1} \cdot (\mathbf{E}^- - \mathbf{E}^+). \tag{2.13}$$

At this point in the derivations, an ancillary expression must be used to find the divergence terms on the left-hand side of (2.13). Following the procedure shown in [1] and taking the divergence on both sides of (2.2), knowing that $\nabla \cdot (\nabla \times \mathbf{A}) = 0,\ \forall\mathbf{A}$, gives

$$\nabla \cdot (j\omega\mathbf{D}) + \nabla \cdot \mathbf{J}_s = 0.$$

Knowing from the definition of the propagation constant [90] and electric induction in (1.15) that

$$j\omega\mathbf{D} = \frac{\gamma^2}{j\omega\mu_0}\mathbf{E},$$

there results

$$\nabla \cdot \left(\frac{\gamma^2}{j\omega\mu_0}\mathbf{E}\right) + \nabla \cdot \mathbf{J}_s = 0.$$

By expanding the propagation constant γ^2 using its generalized function definition in (2.6), assuming that both media are isotropic, the previous expression becomes

$$\gamma_1^2[\nabla \cdot (h_{R_1}\mathbf{E})] + \gamma_0^2[\nabla \cdot ((1 - h_{R_1})\mathbf{E})] = -j\omega\mu_0\nabla \cdot \mathbf{J}_s.$$

Expanding the divergence operators using vector calculus identities [102], gives

$$\gamma_1{}^2[h_{R_1}\nabla \cdot \mathbf{E} + \mathbf{E}^- \cdot \nabla h_{R_1}] + \gamma_0{}^2[(1 - h_{R_1})\nabla \cdot \mathbf{E} - \mathbf{E}^+ \cdot \nabla h_{R_1}] = -j\omega\mu_0\nabla \cdot \mathbf{J}_s. \quad (2.14)$$

Comparing terms with same support on both sides of (2.14), and situating the field source outside R_1, the term on the left-hand-side of (2.13) can be obtained:

$$h_{R_1}\nabla \cdot \mathbf{E} = 0, \quad (2.15)$$

$$(1 - h_{R_1})\nabla \cdot \mathbf{E} = -\frac{1}{j\omega\epsilon_0}\nabla \cdot \mathbf{J}_s, \quad (2.16)$$

$$(\gamma_1{}^2\mathbf{E}^- - \gamma_0{}^2\mathbf{E}^+) \cdot \nabla h_{R_1} = 0. \quad (2.17)$$

By substituting (2.15), (2.16), and (2.17) into (2.13), it is evident that there are two possible expressions for $\nabla \cdot \mathbf{E}$:

$$\nabla \cdot \mathbf{E} = -\frac{1}{j\omega\epsilon_0}\nabla \cdot \mathbf{J}_s + \left(1 - \frac{\gamma_1{}^2}{\gamma_0{}^2}\right)\mathbf{E}^- \cdot \nabla h_{R_1}, \quad (2.18)$$

$$\nabla \cdot \mathbf{E} = -\frac{1}{j\omega\epsilon_0}\nabla \cdot \mathbf{J}_s - \left(1 - \frac{\gamma_0{}^2}{\gamma_1{}^2}\right)\mathbf{E}^+ \cdot \nabla h_{R_1}. \quad (2.19)$$

In this case, either representation of $\nabla \cdot \mathbf{E}$ is considered valid. Taking, for example, (2.19) and (2.12) and substituting into (2.7), the expanded form of the Helmholtz equation using generalized functions can be written as

$$(\mathbf{E}^+ - \mathbf{E}^-)\nabla^2 h_{R_1} + 2\left\{\nabla h_{R_1} \cdot \left[(\nabla\mathbf{E})^+ - (\nabla\mathbf{E})^-\right]\right\} + h_{R_1}\nabla^2\mathbf{E} + (1-h_{R_1})\nabla^2\mathbf{E} - \left[h_{R_1}{\gamma_1}^2\mathbf{E} + (1-h_{R_1}){\gamma_0}^2\mathbf{E}\right] = -T_{SE}(\mathbf{J_s}) - \left(1 - \frac{{\gamma_0}^2}{{\gamma_1}^2}\right)\nabla(\mathbf{E}^+ \cdot \nabla h_{R_1}), \quad (2.20)$$

where $T_{SE}(\mathbf{J}_s)$ is defined as in (1.30). Comparing the terms with same support on both sides of (2.20), the following system of equations can be obtained:

$$h_{R_1}(\nabla^2\mathbf{E} - {\gamma_1}^2\mathbf{E}) = 0, \quad (2.21)$$

$$(1-h_{R_1})(\nabla^2\mathbf{E} - {\gamma_0}^2\mathbf{E}) = -T_{SE}(\mathbf{J}_s), \quad (2.22)$$

$$(\mathbf{E}^+ - \mathbf{E}^-)\nabla^2 h_{R_1} + 2\left\{\nabla h_{R_1} \cdot \left[(\nabla\mathbf{E})^+ - (\nabla\mathbf{E})^-\right]\right\} = \left(1 - \frac{{\gamma_0}^2}{{\gamma_1}^2}\right)\nabla(\mathbf{E}^+ \cdot \nabla h_{R_1}). \quad (2.23)$$

Here it is evident that (2.21) and (2.22) are electromagnetic wave equations for the electric fields in each region, while (2.23) functions as a boundary condition, relating terms in the immediate vicinity of the bounding surface of R_1. At this point, Green's functions can be used to solve for the electric field at each region.

2.2.1 Green's Function Solution to the Helmholtz Equations

With (2.21) to (2.23) in mind, consider the partial differential equation

$$\nabla^2 G_m(\mathbf{r},\mathbf{r}') - {\gamma_m}^2 G_m(\mathbf{r},\mathbf{r}') = -\delta(\mathbf{r}-\mathbf{r}'),\ m = 0, 1, \quad (2.24)$$

where $\delta(\cdot)$ is the Dirac delta distribution [103], [104], $\mathbf{r}$ represents a generic point in space and $\mathbf{r}'$ is the location of the source. The solution of (2.24) is the Green's

function [105]

$$G_m(\mathbf{r},\mathbf{r}') = \frac{e^{-\gamma_m|\mathbf{r}-\mathbf{r}'|}}{4\pi|\mathbf{r}-\mathbf{r}'|},\ m=0,1, \tag{2.25}$$

From this point forward, for compactness, the arguments of the Green's function G_m will be omitted.

One useful property of convolutions in a distributional sense is that derivatives can operate on either side of the convolution without affecting the result [103], [104]. For example, considering a convolution defined in V, with $(h_{R_1}\mathbf{E}), G_1 \in V$, the following equations hold:

$$\nabla^2 h_{R_1}\mathbf{E} \underset{V}{*} G_1 = h_{R_1}\mathbf{E} \underset{V}{*} \nabla^2 G_1 = \nabla^2(h_{R_1}\mathbf{E} \underset{V}{*} G_1). \tag{2.26}$$

Taking the first equality in (2.26) and substituting (2.10) and (2.24), we can find

$$h_{R_1}\nabla^2\mathbf{E} \underset{V}{*} G_1 + 2\left[\nabla h_{R_1}\cdot(\nabla\mathbf{E})^-\right] \underset{V}{*} G_1 + [(\mathbf{E}^-)\nabla^2 h_{R_1}] \underset{V}{*} G_1 = h_{R_1}\mathbf{E} \underset{V}{*} [-\delta(\mathbf{r}-\mathbf{r}') + {\gamma_1}^2 G_1].$$

Rearranging the terms, the following expression can be obtained:

$$h_{R_1}\mathbf{E} = -h_{R_1}(\nabla^2\mathbf{E} - {\gamma_1}^2\mathbf{E}) \underset{V}{*} G_1 - \left\{2\left[\nabla h_{R_1}\cdot(\nabla\mathbf{E})^-\right] + (\mathbf{E}^-)\nabla^2 h_{R_1}\right\} \underset{V}{*} G_1. \tag{2.27}$$

Now, knowing from (2.21) that the first term on the right-hand side of (2.27) is null, the expression for $h_{R_1}\mathbf{E}$ can be rewritten as

$$h_{R_1}\mathbf{E} = -\left\{2\left[\nabla h_{R_1}\cdot(\nabla\mathbf{E})^-\right] + (\mathbf{E}^-)\nabla^2 h_{R_1}\right\} \underset{V}{*} G_1. \tag{2.28}$$

Analogously, $(1-h_{R_1})\mathbf{E}$ can be written as

$$(1-h_{R_1})\mathbf{E} = \mathbf{E}_s + \left\{2\left[\nabla h_{R_1}\cdot(\nabla\mathbf{E})^+\right] + (\mathbf{E}^+)\nabla^2 h_{R_1}\right\} \underset{V}{*} G_0, \tag{2.29}$$

where

$$\mathbf{E}_s = T_{SE}(\mathbf{J_S}) \underset{V}{*} G_0.$$

As a consequence of the compact support of h_{R_1}, it is clear that

$$(1 - h_{R_1})\,(h_{R_1}\mathbf{E}) = 0, \tag{2.30}$$

$$h_{R_1}\,[(1 - h_{R_1})\mathbf{E}] = 0. \tag{2.31}$$

Substituting the definitions of $h_{R_1}\mathbf{E}$ and $(1 - h_{R_1})\mathbf{E}$ into (2.30) and (2.31), two other equations can be derived:

$$(1 - h_{R_1})\left\{\left\{2\left[\nabla h_{R_1} \cdot (\nabla \mathbf{E})^{-}\right] + (\mathbf{E}^{-})\nabla^2 h_{R_1}\right\} \underset{V}{*} G_1\right\} = 0, \tag{2.32}$$

$$h_{R_1}\left\{\mathbf{E}_s + 2\left\{\left[\nabla h_{R_1} \cdot (\nabla \mathbf{E})^{+}\right] + (\mathbf{E}^{+})\nabla^2 h_{R_1}\right\} \underset{V}{*} G_0\right\} = 0. \tag{2.33}$$

Therefore, based on the previously-derived equations, the electric field at any point in V can be defined as a solution of the following system of equations:

$$h_{R_1}\mathbf{E} = -\left\{2\left[\nabla h_{R_1} \cdot (\nabla \mathbf{E})^{-}\right] + (\mathbf{E}^{-})\nabla^2 h_{R_1}\right\} \underset{V}{*} G_1, \tag{2.34}$$

$$(1 - h_{R_1})\mathbf{E} = \mathbf{E}_s + 2\left\{\left[\nabla h_{R_1} \cdot (\nabla \mathbf{E})^{+}\right] + (\mathbf{E}^{+})\nabla^2 h_{R_1}\right\} \underset{V}{*} G_0, \tag{2.35}$$

$$(1 - h_{R_1})\left\{\left\{2\left[\nabla h_{R_1} \cdot (\nabla \mathbf{E})^{-}\right] + (\mathbf{E}^{-})\nabla^2 h_{R_1}\right\} \underset{V}{*} G_1\right\} = 0, \tag{2.36}$$

$$h_{R_1}\left\{\mathbf{E}_s + 2\left\{\left[\nabla h_{R_1} \cdot (\nabla \mathbf{E})^{+}\right] + (\mathbf{E}^{+})\nabla^2 h_{R_1}\right\} \underset{V}{*} G_0\right\} = 0, \tag{2.37}$$

$$(\mathbf{E}^{+} - \mathbf{E}^{-})\nabla^2 h_{R_1} + 2\left\{\nabla h_{R_1} \cdot \left[(\nabla \mathbf{E})^{+} - (\nabla \mathbf{E})^{-}\right]\right\} = \left(1 - \frac{{\gamma_0}^2}{{\gamma_1}^2}\right)\nabla(\mathbf{E}^{+} \cdot \nabla h_{R_1}). \tag{2.38}$$

Here, (2.34) and (2.35) can be used to represent the electric field in different regions of the space. These equations are subject to the boundary condition (2.38), and requires that (2.36) and (2.37) are also fulfilled.

At face value, the system of equations presented in [94] is different from the one in (2.34) to (2.38). This is due to a difference in the definition of the gradient of

a vector, as the former follows the form shown in [106], while the latter follows the notation shown, for example, in [102], [107]. Inconsistencies in the use of Gibbs' notation for vector calculus and dyadic identities are notorious in the literature, as discussed at length in [107]. Since the form of the gradient of a vector presented in [102], [107] is more natural to a reader familiar with vector calculus identities and is consistent with dyadic and tensor calculus without introducing a transpose operator, the system of equations presented here reverted to the notation for the vector gradient shown in [102], [107]. A proof of the equivalence between the two notations is shown in Appendix A.1, where the term in question is expanded in generalized curvilinear coordinates, and tensor calculus is applied to derive the final form of the expressions.

At this point, it is interesting to compare the current results with the one presented by Walsh and Donnelly [1]. Adapting the system of equations obtained in [1] for a single scattering body, the system of equations shown in (1.32) to (1.36) can be obtained. As discussed in Section 1.2.2.2, n_{01} is the refraction index of the medium, defined as

$$ {n_{01}}^2 = \frac{\epsilon_1}{\epsilon_0} + \frac{\sigma_1}{j\omega\epsilon_0}. $$

It is easy to prove, by using the definitions of each variable presented here and in [3], that

$$ \frac{{\gamma_1}^2}{{\gamma_0}^2} = \frac{1}{{n_{01}}^2}, \tag{2.39} $$

implying that the right-hand side of both boundary conditions are identical.

The other difference between the system of equations lies in the term $\nabla\cdot[(\mathbf{E}^{\pm})\nabla h_{R_1}]$. For the system of equations presented in [1] to be equal to the ones presented in (2.34)

to (2.38), the equality

$$\nabla \cdot [(\mathbf{E}^{\pm})\nabla h_{R_1}] \stackrel{?}{=} (\nabla \mathbf{E})^{\pm} \cdot \nabla h_{R_1} + \mathbf{E}^{\pm}\nabla^2 h_{R_1} \tag{2.40}$$

must hold without assuming any particular coordinate system. It should be noted that the argument of the divergence on the left-hand side of (2.40) is a dyadic product. Taking the divergence of the dyadic product in (2.40) leads to

$$\nabla \cdot [(\mathbf{E}^{\pm})\nabla h_{R_1}] = (\nabla \cdot \mathbf{E}^{\pm})\nabla h_{R_1} + \mathbf{E}^{\pm} \cdot \nabla(\nabla h_{R_1}). \tag{2.41}$$

Comparing the two expressions, it is clear that the equality in (2.40) would only hold, excluding a trivial solution, if and only if the dyadic product $(\mathbf{E}^{\pm})\nabla h_{R_1}$ is commutative, which would only be possible if the resulting dyadic was the identity dyadic [102]. Since that is evidently not the case for general definitions of $(\mathbf{E}^{\pm})$ and ∇h_{R_1}, the equality in (2.40) does not hold, invalidating the solution in [1] for general coordinates.

However, it should be noted that the system of equations presented in [1] is valid for the particular case in which the vectors in the basis functions are normalized and do not vary with the observed position in space. Without loss of generality, if it is assumed that V can be defined in a three-dimensional space, $\mathbf{E}^{\pm}$ and ∇h_{R_1} can be written as

$$\mathbf{E}^{\pm} = E_1^{\pm}\hat{\mathbf{e}}_1 + E_2^{\pm}\hat{\mathbf{e}}_2 + E_3^{\pm}\hat{\mathbf{e}}_3, \tag{2.42}$$

$$\nabla h_{R_1} = (\nabla h_{R_1})_1\hat{\mathbf{e}}_1 + (\nabla h_{R_1})_2\hat{\mathbf{e}}_2 + (\nabla h_{R_1})_3\hat{\mathbf{e}}_3. \tag{2.43}$$

Performing the dyadic product between $\mathbf{E}^{\pm}$ and ∇h_{R_1} gives

$$\begin{aligned}\mathbf{E}^{\pm}\nabla h_{R_1} =&[E_1^{\pm}(\nabla h_{R_1})_1]\hat{\mathbf{e}}_1\hat{\mathbf{e}}_1 + [E_1^{\pm}(\nabla h_{R_1})_2]\hat{\mathbf{e}}_1\hat{\mathbf{e}}_2 + [E_1^{\pm}(\nabla h_{R_1})_3]\hat{\mathbf{e}}_1\hat{\mathbf{e}}_3\\ &+ [E_2^{\pm}(\nabla h_{R_1})_1]\hat{\mathbf{e}}_2\hat{\mathbf{e}}_1 + [E_2^{\pm}(\nabla h_{R_1})_2]\hat{\mathbf{e}}_2\hat{\mathbf{e}}_2 + [E_2^{\pm}(\nabla h_{R_1})_3]\hat{\mathbf{e}}_2\hat{\mathbf{e}}_3\\ &+ [E_3^{\pm}(\nabla h_{R_1})_1]\hat{\mathbf{e}}_3\hat{\mathbf{e}}_1 + [E_3^{\pm}(\nabla h_{R_1})_2]\hat{\mathbf{e}}_3\hat{\mathbf{e}}_2 + [E_3^{\pm}(\nabla h_{R_1})_3]\hat{\mathbf{e}}_3\hat{\mathbf{e}}_3.\end{aligned}$$

From the definition of ∇h_{R_1}, the dyadic product can be rewritten as a sum of three dyadic products:

$$\mathbf{E}^{\pm}\nabla h_{R_1} = [E_1^{\pm}\nabla h_{R_1}]\hat{\mathbf{e}}_1 + [E_2^{\pm}\nabla h_{R_1}]\hat{\mathbf{e}}_2 + [E_3^{\pm}\nabla h_{R_1}]\hat{\mathbf{e}}_3. \tag{2.44}$$

Now applying the divergence operator to (2.44) and using dyadic identities [102], the expression $\nabla\cdot[(\mathbf{E}^{\pm})\nabla h_{R_1}]$ can be derived in a three-dimensional space as

$$\begin{aligned}\nabla\cdot[\mathbf{E}^{\pm}\nabla h_{R_1}] &= \nabla\cdot\left\{[E_1^{\pm}\nabla h_{R_1}]\hat{\mathbf{e}}_1 + [E_2^{\pm}\nabla h_{R_1}]\hat{\mathbf{e}}_2 + [E_3^{\pm}\nabla h_{R_1}]\hat{\mathbf{e}}_3\right\}\\ &= \left\{\nabla\cdot[E_1^{\pm}\nabla h_{R_1}]\right\}\hat{\mathbf{e}}_1 + [(E_1^{\pm}\nabla h_{R_1})\cdot\nabla\hat{\mathbf{e}}_1]\\ &+ \left\{\nabla\cdot[E_2^{\pm}\nabla h_{R_1}]\right\}\hat{\mathbf{e}}_2 + [(E_2^{\pm}\nabla h_{R_1})\cdot\nabla\hat{\mathbf{e}}_2]\\ &+ \left\{\nabla\cdot[E_3^{\pm}\nabla h_{R_1}]\right\}\hat{\mathbf{e}}_3 + [(E_3^{\pm}\nabla h_{R_1})\cdot\nabla\hat{\mathbf{e}}_3].\end{aligned} \tag{2.45}$$

For a coordinate system with constant basis vectors, such as the Cartesian coordinates, the terms involving the dyadic gradient of the unit vector can be interpreted as a null dyadic. Therefore, for Cartesian coordinates, (2.45) reduces to

$$\nabla\cdot[(\mathbf{E}^{\pm})\nabla h_{R_1}] = \nabla\cdot[(E_x^{\pm})\nabla h_{R_1}]\hat{\mathbf{i}} + \nabla\cdot[(E_y^{\pm})\nabla h_{R_1}]\hat{\mathbf{j}} + \nabla\cdot[(E_z^{\pm})\nabla h_{R_1}]\hat{\mathbf{k}}. \tag{2.46}$$

Taking, for example, the x-component in (2.46) and using vector calculus identities to expand it, the following expression can be obtained:

$$\nabla\cdot[(E_x^{\pm})\nabla h_{R_1}] = E_x^{\pm}\nabla^2 h_{R_1} + \nabla E_x^{\pm}\cdot\nabla h_{R_1}. \tag{2.47}$$

Replicating this expansion to the other coordinates, and rearranging the resulting terms terms, the following expression can be obtained:

$$\nabla \cdot [(\mathbf{E}^{-})\nabla h_{R_1}] = (\mathbf{E}^{-})\nabla^2 h_{R_1} + (\nabla \mathbf{E}^{-}) \cdot \nabla h_{R_1}. \tag{2.48}$$

Now, substituting (2.48) into, for example, (1.32), the expression for $h_{R_1}\mathbf{E}$ in Cartesian coordinates can be written as

$$h_{R_1}\mathbf{E} = -\left\{2[(\nabla \mathbf{E})^{-} \cdot \nabla h_{R_1}] + (\mathbf{E}^{-})\nabla^2 h_{R_1}\right\} \underset{V}{*} G_1.$$

It should be noted, however, that this still does not match the expression in (2.28), as dyadic products are only commutative for symmetric dyadics [102], [107]. From the Appendix in [1], it can be observed that the authors have interpreted the dyadic product $(\nabla \mathbf{E})^{-} \cdot \nabla h_{R_1}$ as

$$(\nabla \mathbf{E})^{-} \cdot \nabla h_{R_1} = (\partial_x h_{R_1})(\partial_x \mathbf{E})_x^{-} + (\partial_y h_{R_1})(\partial_y \mathbf{E})_y^{-} + (\partial_z h_{R_1})(\partial_z \mathbf{E})_z^{-}.$$

As such, the product would be commutative, as it follows the commutative property of the product between scalars and vectors. Therefore, the previous expression could be rewritten as $h_{R_1}\mathbf{E}$ in Cartesian coordinates can be written as

$$h_{R_1}\mathbf{E} = -\left\{2[\nabla h_{R_1} \cdot (\nabla \mathbf{E})^{-}] + (\mathbf{E}^{-})\nabla^2 h_{R_1}\right\} \underset{V}{*} G_1,$$

matching the result shown in (2.28). If this procedure is carried out for all expressions in the system of equations, it is clear that the system would match the one presented here. However, it should be noted that some mathematical liberty was taken in assuming the commutativity of the dyadic dot product, since the gradient of a vector field is symmetric if, and only if, the vector field in question is conservative [108], which is not the case for the electric field in the present analysis, as shown by (2.1).

Furthermore, the assumption of a Cartesian coordinate system is vital to the derivation shown in [1], since from both (2.45) and the definition of the dyadic product, it is necessary that a coordinate system with constant basis vectors is assumed. Otherwise, the expression in (2.46) does not hold, invalidating the expressions proposed by Walsh and Donnelly [1].

Therefore, since no coordinate system was assumed in the derivation of the system of equations shown in (2.34) to (2.38), the system presented here is the general form of the system of equations for the electric field scattered by a single body, with the results shown in [1] representing the particular case in which constant basis vectors are being considered.

2.3 Curvilinear System of Equations Applied to a General Scattering Body

From the system of equations presented here, it is clear that the electric field at any point in space is heavily dependent on the definition of h_{R_1}. If the surface of R_1 can be implicitly defined as the points such that $\tilde{f}(\mathbf{r}) = 0$, h_{R_1} can be written as

$$h_{R_1}(\mathbf{r}) = 1 - \Theta(\tilde{f}(\mathbf{r})), \tag{2.49}$$

where $\Theta(\cdot)$ is the Heaviside function [103], [104]. From this definition, the gradient and Laplacian of h_{R_1} can be written as

$$\nabla h_{R_1}(\mathbf{r}) = -\nabla \tilde{f}(\mathbf{r}) \delta(\tilde{f}(\mathbf{r})) \triangleq \mathbf{n} \delta(\tilde{f}(\mathbf{r})) \tag{2.50}$$

with $\mathbf{n} = \nabla\tilde{f}(\mathbf{r})$ being the normal to the surface of the scattering body, and

$$\nabla^2 h_{R_1}(\mathbf{r}) = -\left[(\nabla\cdot\mathbf{n})\delta(\tilde{f}(\mathbf{r})) + |\mathbf{n}|^2\delta'(\tilde{f}(\mathbf{r}))\right], \tag{2.51}$$

where $\delta'(\cdot)$ is the unit dipole distribution.

Substituting (2.49), (2.50) and (2.51) into (2.34) to (2.38), and defining the vector fields $\mathbf{R}^+$ and $\mathbf{R}^-$ as

$$\mathbf{R}^+ \triangleq -2\left[\mathbf{n}\cdot(\nabla\mathbf{E})^+\right] - \mathbf{E}^+(\nabla\cdot\mathbf{n}) = -\left\{\nabla\cdot(\mathbf{n}\mathbf{E}^+) + \mathbf{n}\cdot(\nabla\mathbf{E})^+\right\} \tag{2.52}$$

$$\mathbf{R}^- \triangleq -2\left[\mathbf{n}\cdot(\nabla\mathbf{E})^-\right] - \mathbf{E}^-(\nabla\cdot\mathbf{n}) = -\left\{\nabla\cdot(\mathbf{n}\mathbf{E}^-) + \mathbf{n}\cdot(\nabla\mathbf{E})^-\right\} \tag{2.53}$$

the system of equations for the electric field scattered by the body with surface $\tilde{f}(\mathbf{r})$ using general curvilinear coordinates can be written as

$$[1-\Theta(\tilde{f}(\mathbf{r}))]\mathbf{E} = \left\{|\mathbf{n}|^2\mathbf{E}^-\delta'(\tilde{f}(\mathbf{r})) - \mathbf{R}^-\delta(\tilde{f}(\mathbf{r}))\right\} \underset{V}{*} G_1, \tag{2.54}$$

$$\Theta(\tilde{f}(\mathbf{r}))\mathbf{E} = \mathbf{E}_s - \left\{|\mathbf{n}|^2\mathbf{E}^+\delta'(\tilde{f}(\mathbf{r})) - \mathbf{R}^+\delta(\tilde{f}(\mathbf{r}))\right\} \underset{V}{*} G_0, \tag{2.55}$$

$$\Theta(\tilde{f}(\mathbf{r}))\left\{\left\{|\mathbf{n}|^2\mathbf{E}^-\delta'(\tilde{f}(\mathbf{r})) - \mathbf{R}^-\delta(\tilde{f}(\mathbf{r}))\right\} \underset{V}{*} G_1\right\} = 0, \tag{2.56}$$

$$[1-\Theta(\tilde{f}(\mathbf{r}))]\left\{\mathbf{E}_s - \left\{|\mathbf{n}|^2\mathbf{E}^+\delta'(\tilde{f}(\mathbf{r})) - \mathbf{R}^+\delta(\tilde{f}(\mathbf{r}))\right\} \underset{V}{*} G_0\right\} = 0, \tag{2.57}$$

$$(\mathbf{E}^+ - \mathbf{E}^-)|\mathbf{n}|^2\delta'(\tilde{f}(\mathbf{r})) - (\mathbf{R}^+ - \mathbf{R}^-)\delta(\tilde{f}(\mathbf{r})) = \left(1 - \frac{{\gamma_0}^2}{{\gamma_1}^2}\right)\nabla\left[(\mathbf{E}^+\cdot\mathbf{n})\delta(\tilde{f}(\mathbf{r}))\right]. \tag{2.58}$$

Here it should be noted that, although the forms of the expressions in (2.54)–(2.58) are identical to the ones presented in [3], [17], the difference in the definition of $\mathbf{R}^+$ and $\mathbf{R}^-$ limits the application of the expressions presented in [3], [17] to a rough surface defined in Cartesian coordinates, while the definition shown in (2.52) and (2.53) can be applied to any general scattering body with a surface defined by a function $\tilde{f}(\mathbf{r})$.

At this point, as shown in [3], it is important to expand the gradient present on the right-hand side of (2.58). Since $\mathbf{E}^+ \cdot \mathbf{n} = E_n^+ |\mathbf{n}|$, where $E_{\mathbf{n}}^+$ is the magnitude of the outer normal electric field $\mathbf{E}_n^+$, the expression in question can be expanded

$$\nabla \left[(\mathbf{E}^+ \cdot \mathbf{n}) \delta(\tilde{f}(\mathbf{r})) \right] = \nabla \left[E_n |\mathbf{n}| \delta(\tilde{f}(\mathbf{r})) \right] = E_n^+ |\mathbf{n}| \nabla \delta(\tilde{f}(\mathbf{r})) + \delta(\tilde{f}(\mathbf{r})) \nabla (E_n^+ |\mathbf{n}|).$$

Since the $\nabla \delta(\tilde{f}(\mathbf{r})) = \nabla \tilde{f}(\mathbf{r}) \delta'(\tilde{f}(\mathbf{r})) = \mathbf{n} \delta'(\tilde{f}(\mathbf{r}))$,

$$\nabla \left[(\mathbf{E}^+ \cdot \mathbf{n}) \delta(\tilde{f}(\mathbf{r})) \right] = E_n^+ |\mathbf{n}| \hat{\mathbf{n}} \delta'(\tilde{f}(\mathbf{r})) + \delta(\tilde{f}(\mathbf{r})) \nabla (E_n^+ |\mathbf{n}|).$$

Since $E_n^+ |\mathbf{n}| \hat{\mathbf{n}} = \mathbf{E}_n^+ |\mathbf{n}|^2$,

$$\nabla \left[(\mathbf{E}^+ \cdot \mathbf{n}) \delta(\tilde{f}(\mathbf{r})) \right] = \mathbf{E}_n^+ |\mathbf{n}|^2 \delta'(\tilde{f}(\mathbf{r})) + \delta(\tilde{f}(\mathbf{r})) \nabla (E_n^+ |\mathbf{n}|). \tag{2.59}$$

Substituting these two expressions into (2.58) and comparing the terms with the same support, the boundary condition to the system of equations presented in (2.54)–(2.58) can be satisfied if

$$\mathbf{E}^- = \mathbf{E}^+ - \left(1 - \frac{{\gamma_0}^2}{{\gamma_1}^2} \right) \mathbf{E}_n^+ = \mathbf{E}_t^+ + \frac{{\gamma_0}^2}{{\gamma_1}^2} \mathbf{E}_n^+, \tag{2.60}$$

$$\mathbf{R}^- = \mathbf{R}^+ + \left(1 - \frac{{\gamma_0}^2}{{\gamma_1}^2} \right) \nabla (E_n^+ |\mathbf{n}|). \tag{2.61}$$

Again, the expression for the boundary condition presented here coincides with the one presented in [3], differing only in the definition of $\mathbf{R}^+$ and $\mathbf{R}^-$. Therefore, the general form of the system of equations for the electric field scattered by a general

scattering body can be derived as

$$[1-\Theta(\tilde{f}(\mathbf{r}))]\mathbf{E} = \left\{|\mathbf{n}|^2\mathbf{E}^-\delta'(\tilde{f}(\mathbf{r})) - \mathbf{R}^-\delta(\tilde{f}(\mathbf{r}))\right\} \underset{V}{*} G_1, \tag{2.62}$$

$$\Theta(\tilde{f}(\mathbf{r}))\mathbf{E} = \mathbf{E}_s - \left\{|\mathbf{n}|^2\mathbf{E}^+\delta'(\tilde{f}(\mathbf{r})) - \mathbf{R}^+\delta(\tilde{f}(\mathbf{r}))\right\} \underset{V}{*} G_0, \tag{2.63}$$

$$\Theta(\tilde{f}(\mathbf{r}))\left\{\left\{|\mathbf{n}|^2\mathbf{E}^-\delta'(\tilde{f}(\mathbf{r})) - \mathbf{R}^-\delta(\tilde{f}(\mathbf{r}))\right\} \underset{V}{*} G_1\right\} = 0, \tag{2.64}$$

$$[1-\Theta(\tilde{f}(\mathbf{r}))]\left\{\mathbf{E}_s - \left\{|\mathbf{n}|^2\mathbf{E}^+\delta'(\tilde{f}(\mathbf{r})) - \mathbf{R}^+\delta(\tilde{f}(\mathbf{r}))\right\} \underset{V}{*} G_0\right\} = 0, \tag{2.65}$$

$$\mathbf{E}^- = \mathbf{E}^+ - \left(1 - \frac{{\gamma_0}^2}{{\gamma_1}^2}\right)\mathbf{E}_n^+ = \mathbf{E}_t^+ + \frac{{\gamma_0}^2}{{\gamma_1}^2}\mathbf{E}_n^+, \tag{2.66}$$

$$\mathbf{R}^- = \mathbf{R}^+ + \left(1 - \frac{{\gamma_0}^2}{{\gamma_1}^2}\right)\nabla(E_n^+|\mathbf{n}|). \tag{2.67}$$

2.4 General Chapter Summary

In this chapter, a system of equations for the electric field has been proposed based on the one derived by Walsh and Donnelly [1]. The main advantage of the proposed system of equations is the fact that it has been derived without reference to a particular coordinate system, using only vector and dyadic identities to derive the expressions. Inconsistencies in notation between the presented results and the ones shown in [94] are reconciled by using vector, dyadic and tensor calculus fundamentals in Appendix A.

It is also shown that the system of equations proposed in [1] represents a particular case of the system of equations presented here, where a Cartesian coordinate system is assumed, and the gradient of the electric field at the surface of the scattering object can be assumed to be a symmetric dyadic. However, if the surface of the scattering body is implicitly defined as a function, and the terms proportional to the Dirac

delta are grouped in the auxiliary vector fields $\mathbf{R}^+$ and $\mathbf{R}^-$, the curvilinear system of equations for a general scattering body resembles the one presented in [3], with the main difference residing in the definition of the auxiliary vector fields.

Further results presented in [94] show that the system of equations in curvilinear coordinates using generalized functions can be reduced to the Stratton-Chu integral equation [109] for a perfectly-electrically conducting (PEC) sphere, indicating that the generalized functions approach can be reduced to the classical radiation theory result for the case of a PEC sphere. The inconsistency between the two notations does not affect the derivation of the Stratton-Chu integral equation in [94], as the term in question is removed from the analysis.

Chapter 3

Electric Field Expressions for the Scattering over Ocean Surfaces with Electromagnetically-Large Waves

3.1 Introduction

In Chapter 2, the system of equations for the electric field scattered by a body with surface implicitly defined by a function was presented. This derivation followed the steps presented by Walsh and Gill [3] and Walsh *et al.* [17], without assuming any particular coordinate system. Here, the results presented in the Chapter 2 will be applied to the scattering of electric fields over the ocean surface.

Two main differences can be found between the derivations presented here and

the ones shown in [3], [17]. First, the ocean surface is assumed to be random and time-varying from the start. The derivations in [3], [17] start with a static surface, with its time-varying nature only being introduced after the derivation of the first-order electric field is complete. While this does not affect the resulting first-order electric field, this only happens due to physical considerations, and not mathematical ones. The second and main difference between the two derivations is the removal of the small-heights restriction, which allows the measurement of waves in electromagnetically-large sea states.

The expression of the electric field presented here is a key part of the derivation of the radar cross-section of ocean surfaces with electromagnetically-large waves. In this Chapter, the corrections to the electric field will be presented up to the second-order of the correction power series expansion and up to the third overall order of the electric field.

3.2 Operator Equation for the Electric Field Over an Ocean Surface With Electromagnetically-Large Waves

As presented in Chapter 2, the electric field in the presence of a single, nonmagnetic, isotropic scatterer immersed in the vacuum as shown in Fig. 1.1 with surface implicitly defined as $f(\mathbf{r}) = 0$ can be derived from the system of equations from (2.62) to (2.66). For the ocean surface, f should be a time-varying random process, which can be considered ergodic for the observation time and area investigated here [75]. Thus, to

represent the ocean surface, the general surface of the scattering body $\tilde{f}(\mathbf{r})$ in (2.49) can be defined as the random, time-varying vertical displacement from sea level caused by the waves:

$$\tilde{f}(\mathbf{r}) = z - f(x, y; t) \tag{3.1}$$

where $f(x, y; t)$ is the vertical surface displacement, which can be defined as a zero-mean Gaussian random variable with standard deviation σ_f. Using this definition and the results presented in Section 2.3 and using the relation shown in (2.39) to return the expressions to the refraction index notation to define the scattering media as shown in [1], [3], the system of equations for the electric field scattered by a time-varying ocean surface can be written as

$$[1 - \Theta(z - f(x, y; t))]\mathbf{E} = \left\{|\mathbf{n}|^2\mathbf{E}^-\delta'(z - f(x, y; t)) - \mathbf{R}^-\delta(z - f(x, y; t))\right\} \underset{\mathbb{R}^3}{*} G_1, \tag{3.2}$$

$$\Theta(z - f(x, y; t))\mathbf{E} = \mathbf{E}_s - \left\{|\mathbf{n}|^2\mathbf{E}^+\delta'(z - f(x, y; t)) - \mathbf{R}^+\delta(z - f(x, y; t))\right\} \underset{\mathbb{R}^3}{*} G_0, \tag{3.3}$$

$$\Theta(z - f(x, y; t)) \left\{ \left\{|\mathbf{n}|^2\mathbf{E}^-\delta'(z - f(x, y; t)) - \mathbf{R}^-\delta(z - f(x, y; t))\right\} \underset{\mathbb{R}^3}{*} G_1 \right\} = 0, \tag{3.4}$$

$$[1 - \Theta(z - f(x, y; t))] \left\{ \mathbf{E}_s - \left\{|\mathbf{n}|^2\mathbf{E}^+\delta'(z - f(x, y; t)) - \mathbf{R}^+\delta(z - f(x, y; t))\right\} \underset{\mathbb{R}^3}{*} G_0 \right\} = 0, \tag{3.5}$$

$$\mathbf{E}^- = \mathbf{E}^+ - \left(1 - \frac{1}{{n_{01}}^2}\right)\mathbf{E}_n^+ = \mathbf{E}_t^+ + \frac{1}{{n_{01}}^2}\mathbf{E}_n^+, \tag{3.6}$$

$$\mathbf{R}^- = \mathbf{R}^+ + \left(1 - \frac{1}{{n_{01}}^2}\right)\nabla(E_{\mathbf{n}}^+|\mathbf{n}|), \tag{3.7}$$

where the domain of definition of the convolution is $\mathbb{R}^3$, and the outer normal to the ocean surface can be defined using an expansion to the gradient operator similar to the one presented in [110], [111] as

$$\mathbf{n} \triangleq \nabla \tilde{f}(x, y; t) = \hat{\mathbf{z}} - \nabla_{xy} f(x, y; t), \tag{3.8}$$

with being the unit vector in the z-direction, and ∇_{xy} being the gradient operator in the xy-plane.

It is interesting to observe that, apart from the definition of the auxiliary vector fields $\mathbf{R}^+$ and $\mathbf{R}^-$, the system of equations for the electric field scattered by a time-varying random rough surface is identical to the one presented in [3]. It should be noted, however, that the derivations presented in [3] do not require the expressions for the auxiliary fields, as only the expressions shown in (3.2) to (3.7) are used in the derivations. Therefore, following the derivations presented in [3], the operator equation for the electric field scattered by a rough surface can be written as

$$\mathcal{N}\mathcal{L}^{-1}\left[\frac{\mathcal{L}\mathcal{N}\mathcal{L}^{-1}\left[2u\mathcal{F}_{xy}(\mathbf{E}_s^{z^-})\right]}{u + jk\Delta}\right] = \mathbf{E}_n^+ + \mathcal{N}\mathcal{L}^{-1}\left[\frac{\mathcal{L}\mathcal{N}\left[\frac{\nabla_{xy}\left(|\mathbf{n}|E_{\mathbf{n}}^+\right)}{|\mathbf{n}|^2}\right]}{u + jk\Delta}\right], \tag{3.9}$$

where $\mathcal{F}_{xy}(\cdot)$ is the spatial Fourier transform in the xy-plane, $\mathbf{E}_s^{z^-}$ is the source electric field at the point $z = z^- < f(x, y; t)$, $\forall (x, y; t)$, $\mathbf{E}_n^+$ is normal electric field immediately above the ocean surface, k is the radar wavenumber, u is defined as

$$u \triangleq \sqrt{K^2 - k^2}, \tag{3.10}$$

with K being the surface wavenumber, Δ the surface impedance, defined as

$$\Delta \triangleq \frac{1}{{n_{01}}^2},$$

$\mathcal{N}\{\cdot\}$ the normal component operator defined in (1.41) and $\mathcal{L}\{\cdot\}$ the invertible operator defined in (1.42) [3]. One of the expressions required to derive (3.9) from the system of equations shown in (3.2) to (3.7) is the spatial Fourier transform of the Green's functions G_m, $m = 0, 1$ in the xy-plane. The Green's function solution for the Helmholtz equation, written in [1] as

$$G_m = \frac{e^{-jk\eta_m\sqrt{x^2+y^2+z^2}}}{4\pi\sqrt{x^2+y^2+z^2}}, \tag{3.11}$$

has, according to Walsh *et al.* [17], a two-dimensional Fourier transform equal to

$$\mathcal{F}_{xy}\{G_m\} = \frac{e^{-|z|\sqrt{k_x^2+k_y^2-k^2\eta_m^2}}}{2\sqrt{k_x^2+k_y^2-k^2\eta_m^2}}. \tag{3.12}$$

The earliest appearance of this form in Walsh's work is shown in his 1980's report [62], where the reader is asked to refer to an Appendix where the development of this formulation would be presented. However, the Appendix with this information has not been included in any physical or digital version of the report, and all subsequent work by Walsh and his colleagues include a reference to [62] as an explanation of how this result was obtained. To support the analysis presented in Walsh and Gill [3], the derivation of this expression of the Fourier transform of the Green's function solution to the Helmholtz equation is presented on Appendix B.1.

To solve (3.9) for the electric field normal to the ocean surface, the $\mathcal{L}^{-1}$ operator for arbitrary heights must be defined. As explained in Chapter 1, Walsh and Gill [3] applied the already widely-used small-height approximation at this point in the derivations to ease the process of obtaining the electric field normal to the ocean surface. Therefore, to obtain the normal electric field for an ocean surface with arbitrary heights, an arbitrary-height form to the $\mathcal{L}^{-1}$ operator must be derived.

3.2.1 $\mathcal{L}$- and $\mathcal{L}^{-1}$-Operators for Arbitrary Roughness Scales

After defining the operator equation show in (3.9), Walsh and Gill [3] applied the small-height approximation to the $\mathcal{L}$-operator, limiting the roughness scale of the ocean surface ($kf << 1$). Then, after imposing the small-height approximation, the $\mathcal{L}^{-1}$-operator was derived. Therefore, in order to properly remove the restriction on the roughness scales, the $\mathcal{L}$-operator should be applied in its original form written in (1.42), and $\mathcal{L}^{-1}$ must be derived without the small-height approximation.

The $\mathcal{L}$-operator, as defined in (1.42), is a bounded operator from the xy-space into the spatial frequency $k_x k_y$-space, which are defined as the Hilbert spaces X and K, respectively. Mathematically, $\mathcal{L} \in \mathscr{H}(\mathsf{X}, \mathsf{K})$, where $\mathscr{H}(\cdot)$ indicates that both arguments are Hilbert spaces. It can be logically inferred that, for $\mathcal{L}^{-1}$ to be considered an inverse operator, $\mathcal{L}^{-1} \in \mathscr{H}(\mathsf{K}, \mathsf{X})$, operating from the $k_x k_y$-space into the xy-space. Therefore, the relationship between $\mathcal{L}$ and $\mathcal{L}^{-1}$ can be characterized using the following equations [112]:

$$\mathcal{L}^{-1}\left\{\mathcal{L}\left\{\mathbf{A}\right\}\right\} = \mathbf{A}, \ \forall \mathbf{A} \in \mathsf{X}, \tag{3.13}$$

$$\mathcal{L}\left\{\mathcal{L}^{-1}\left\{\hat{\mathbf{A}}\right\}\right\} = \hat{\mathbf{A}} \in \mathsf{R}(\mathcal{L}), \tag{3.14}$$

where $\mathsf{R}(\mathcal{L})$ is the range space of the $\mathcal{L}$ operator [112].

Substituting (1.42) into (3.13),

$$\mathcal{L}^{-1}\left\{e^{z^- u}\mathcal{F}_{xy}\left\{|\mathbf{n}|^2 \mathbf{A} e^{-f(x,y;t)u}\right\}\right\} = \mathbf{A}.$$

Applying the $\mathcal{L}$-operator to both sides of the equation, and multiplying both sides by $e^{-z^- u}$, gives

$$\mathcal{F}_{xy}\left\{|\mathbf{n}|^2 \mathbf{A} e^{-f(x,y;t)u}\right\} = e^{-z^- u}\mathcal{L}\{\mathbf{A}\}.$$

Convolving the term $\mathcal{F}_{xy}\left\{e^{f(x,y;t)u}\right\}$ on both sides of the equation,

$$\mathcal{F}_{xy}\left\{|\mathbf{n}|^2\mathbf{A}\right\} = e^{-z^-u}\mathcal{L}\{\mathbf{A}\} * \mathcal{F}_{xy}\left\{e^{f(x,y;t)u}\right\}.$$

This results in

$$\mathbf{A} = \frac{1}{|\mathbf{n}|^2}\mathcal{F}_{xy}^{-1}\left\{e^{-z^-u}\mathcal{L}\{\mathbf{A}\}\right\}\mathcal{F}_{xy}^{-1}\left\{\mathcal{F}_{xy}\left\{e^{f(x,y;t)u}\right\}\right\}$$

after applying the inverse spatial Fourier transform in the xy-plane, $\mathcal{F}_{xy}^{-1}$. Comparing the previous result with (3.14), the $\mathcal{L}^{-1}$-operator can be defined as

$$\mathcal{L}^{-1}\{\mathbf{A}\} \triangleq \frac{1}{|\mathbf{n}|^2}\mathcal{F}_{xy}^{-1}\left\{e^{-z^-u}\mathbf{A}\right\}\mathcal{F}_{xy}^{-1}\left\{\mathcal{F}_{xy}\left\{e^{f(x,y;t)u}\right\}\right\}. \tag{3.15}$$

Here it should be observed that the forward and inverse Fourier transforms operating over $e^{f(x,y;t)u}$ cannot be cancelled out because the exponential has elements of both X and K spaces. This fact becomes evident if the exponential term is substituted by the integral

$$\mathcal{F}_{xy}^{-1}\left\{\mathcal{F}_{xy}\left\{e^{f(x,y;t)u}\right\}\right\} = \mathcal{F}_{xy}^{-1}\left\{\mathcal{F}_{xy}\left\{\int e^{zu}\delta(z - f(x,y;t))\,\mathrm{d}z\right\}\right\}.$$

Now, invoking Fubini's theorem over the Fourier transforms, the order of integration can be swapped, so that

$$\mathcal{F}_{xy}^{-1}\left\{\mathcal{F}_{xy}\left\{e^{f(x,y;t)u}\right\}\right\} = \int \mathcal{F}_{xy}^{-1}\left\{e^{zu}\mathcal{F}_{xy}\left\{\delta(z - f(x,y;t))\right\}\right\}\mathrm{d}z.$$

It is evident that whatever approach is taken to solve the previous equation, the resulting expression will be in the X-space, which shows that the Fourier transforms in (3.15) cannot be simply cancelled. However, the expression can be further simplified

by applying a power series expansion over $e^{f(x,y;t)u}$, resulting in

$$\begin{aligned}
\mathcal{F}_{xy}^{-1}\left\{\mathcal{F}_{xy}\left\{e^{f(x,y;t)u}\right\}\right\} &= \mathcal{F}_{xy}^{-1}\left\{\mathcal{F}_{xy}\left\{\sum_{n=0}^{\infty}\frac{(f(x,y;t)u)^n}{n!}\right\}\right\} \\
&= \mathcal{F}_{xy}^{-1}\left\{\sum_{n=0}^{\infty}\frac{1}{n!}\mathcal{F}_{xy}\left\{(f(x,y;t)u)^n\right\}\right\} \\
&= \sum_{n=0}^{\infty}\frac{1}{n!}\mathcal{F}_{xy}^{-1}\left\{\underset{m=0}{\overset{n}{*}}\left(\mathcal{F}_{xy}\left\{f(x,y;t)\right\}u\right)_m\right\} \\
&= \sum_{n=0}^{\infty}\frac{1}{n!}\left(\mathcal{F}_{xy}^{-1}\left\{\mathcal{F}_{xy}\left\{f(x,y;t)\right\}u\right\}\right)^n \\
\mathcal{F}_{xy}^{-1}\left\{\mathcal{F}_{xy}\left\{e^{f(x,y;t)u}\right\}\right\} &= e^{\zeta(x,y;t)}. \qquad (3.16)
\end{aligned}$$

Here, $e^{\zeta(x,y;t)}$ is defined as the *arbitrary heights factor*, where

$$\zeta(x,y;t) \triangleq \mathcal{F}_{xy}^{-1}\left\{\mathcal{F}_{xy}\left\{f(x,y;t)\right\}u\right\} = f(x,y;t) * \mathcal{F}_{xy}^{-1}\left\{u\right\} \qquad (3.17)$$

is a dimensionless quantity defined as *arbitrary heights function*. Therefore, the expression for the $\mathcal{L}^{-1}$ operator in (3.15) can be rewritten as

$$\mathcal{L}^{-1}\{\mathbf{A}\} = \frac{1}{|\mathbf{n}|^2}e^{\zeta(x,y;t)}\mathcal{F}_{xy}^{-1}\{e^{-z^-u}\mathbf{A}\}. \qquad (3.18)$$

One of the implications of the small-height approximation in [3] is that for a very small $kf(x,y;t)$, $f(x,y;t)u$ is approximately zero. Therefore, if the small-height approximation is applied to (3.18), the arbitrary heights factor $\zeta(x,y;t)$ would be approximately zero, and both operators would return to the form presented in [3].

Now that the $\mathcal{L}$ and $\mathcal{L}^{-1}$ have been derived, the operator equation for the electric field presented in (3.9) can be expanded.

3.2.2 Operator Equation for the Normal Electric Field Over an Ocean Surface with Arbitrary Heights

Here, the expansion of the operator equation for the normal electric field over an ocean surface shown in (3.9) follows a similar process to the one presented in [3], [17], but now considering an ocean surface without wave height limitations. From (3.9), it is clear that the variable of interest in the equation is the magnitude of the normal electric field, since its direction is already defined by the gradient of the ocean surface displacement. Therefore, taking the projection of the operator equation to the normal unit vector leads to

$$E^s = E_n^+ + \mathcal{T}(E_{\mathbf{n}}^+), \tag{3.19}$$

where

$$E^s = \hat{\mathbf{n}} \cdot \mathcal{N}\mathcal{L}^{-1}\left[\frac{\mathcal{L}\mathcal{N}\mathcal{L}^{-1}\left[2u\mathcal{F}_{xy}(\mathbf{E}_s^{z^-})\right]}{u + jk\Delta}\right] \tag{3.20}$$

$$\mathcal{T}(E_{\mathbf{n}}^+) = \hat{\mathbf{n}} \cdot \mathcal{N}\mathcal{L}^{-1}\left[\frac{\mathcal{L}\mathcal{N}\left[\frac{\nabla_{xy}\left(|\mathbf{n}|E_{\mathbf{n}}^+\right)}{|\mathbf{n}|^2}\right]}{u + jk\Delta}\right], \tag{3.21}$$

with $\hat{\mathbf{n}}$ being the outward normal to the ocean surface. Here, the $\mathcal{T}$ operator should not be confused with the transverse operator defined in [3], which results in the transverse component of its argument.

Taking the $\mathcal{T}$ operator in (3.21) and substituting the expressions for the $\mathcal{N}$ operator, and the arbitrary-height forms of $\mathcal{L}$ and $\mathcal{L}^{-1}$ defined in (1.42) and (3.18), the

expression can be rewritten as

$$\mathcal{T}(E^+_{\mathbf{n}}) = \hat{\mathbf{n}} \cdot \hat{\mathbf{n}}\hat{\mathbf{n}} \cdot \left\{ \frac{1}{|\mathbf{n}|^2} e^{\zeta} \mathcal{F}^{-1}_{xy} \left\{ \cancel{e^{-z^- u}} \left\{ \frac{1}{u + jk\Delta} \cancel{e^{z^- u}} \mathcal{F}_{xy} \left\{ \cancel{|\mathbf{n}|^2} e^{-fu} \left[\hat{\mathbf{n}}\hat{\mathbf{n}} \cdot \frac{\nabla(|\mathbf{n}|E^+_{\mathbf{n}})}{\cancel{|\mathbf{n}|^2}} \right] \right\} \right\} \right\} \right\}, \quad (3.22)$$

where the arguments of $\zeta(x, y; t)$ and $f(x, y; t)$ were suppressed. Using the convolution theorem [113] and the definition of the left dot product of a dyadic, the expression in (3.22) can be rewritten as

$$\mathcal{T}(E^+_{\mathbf{n}}) = e^{\zeta} \frac{(\hat{\mathbf{n}} \cdot \hat{\mathbf{n}})\hat{\mathbf{n}}}{|\mathbf{n}|^2} \cdot \left\{ \mathcal{F}^{-1}_{xy} \left\{ \frac{1}{u + jk\Delta} \right\} \underset{xy}{*} \left\{ \mathcal{F}^{-1}_{xy} \left\{ \mathcal{F}_{xy} \left\{ e^{-fu} \right\} \right\} \left[\hat{\mathbf{n}}\hat{\mathbf{n}} \cdot \nabla(|\mathbf{n}|E^+_{\mathbf{n}}) \right] \right\} \right\}. \quad (3.23)$$

Since $\hat{\mathbf{n}} \cdot \hat{\mathbf{n}} = 1$, and knowing that, for a conductive surface [91],

$$\mathcal{F}^{-1}_{xy} \left\{ \frac{1}{u + jk\Delta} \right\} \approx F(\rho) \frac{e^{jk\rho}}{2\pi\rho}, \quad (3.24)$$

where $\rho = \sqrt{x^2 + y^2}$ and $F(\rho)$ is the Sommerfeld attenuation function [35], and that, in an analogous derivation to the one shown in (3.16),

$$\mathcal{F}^{-1}_{xy} \left\{ \mathcal{F}_{xy} \left\{ e^{-f(x,y;t)u} \right\} \right\} = e^{-\zeta(x,y;t)u}, \quad (3.25)$$

with $\zeta(x, y; t)$ defined in (3.17), the expression in (3.23) can be rewritten as

$$\mathcal{T}(E^+_{\mathbf{n}}) = e^{\zeta} \frac{\hat{\mathbf{n}}}{|\mathbf{n}|^2} \cdot \left\{ F(\rho) \frac{e^{jk\rho}}{2\pi\rho} \underset{xy}{*} \left\{ e^{-\zeta} \left[\hat{\mathbf{n}}\hat{\mathbf{n}} \cdot \nabla(|\mathbf{n}|E^+_{\mathbf{n}}) \right] \right\} \right\}. \quad (3.26)$$

Now, substituting the expression for $\mathcal{N}$ and for the arbitrary-height forms of $\mathcal{L}$ and $\mathcal{L}^{-1}$ into the expression of E^s in (3.20) gives

$$E^s = \hat{\mathbf{n}} \cdot \hat{\mathbf{n}}\hat{\mathbf{n}} \cdot \left\{ \frac{1}{|\mathbf{n}|^2} e^{\zeta} \mathcal{F}^{-1}_{xy} \left\{ \cancel{e^{-z^- u}} \left\{ \frac{1}{u + jk\Delta} \cancel{e^{z^- u}} \mathcal{F}_{xy} \left\{ \cancel{|\mathbf{n}|^2} e^{-fu} \left(\hat{\mathbf{n}}\hat{\mathbf{n}} \cdot \frac{1}{\cancel{|\mathbf{n}|^2}} e^{\zeta} \mathcal{F}^{-1}_{xy} \left\{ e^{-z^- u} \left[2u \mathcal{F}_{xy} \left\{ \mathbf{E}^{z^-}_s \right\} \right] \right\} \right) \right\} \right\} \right\} \right\}. \quad (3.27)$$

Using the convolution theorem and the relationships shown in (3.24) and (3.25), knowing that $\hat{\mathbf{n}} \cdot \hat{\mathbf{n}} = 1$, the expression in (3.27) can be rewritten as

$$E^s = e^{\zeta} \frac{\hat{\mathbf{n}}}{|\mathbf{n}|^2} \cdot \left\{ F(\rho) \frac{e^{jk\rho}}{2\pi\rho} \underset{xy}{*} \cancel{e^{\zeta}} \left(\hat{\mathbf{n}}\hat{\mathbf{n}} \cdot \cancel{e^{\zeta}} \mathcal{F}_{xy}^{-1} \left\{ e^{-z^- u} \left[2u\mathcal{F}_{xy} \left\{ \mathbf{E}_s^{z^-} \right\} \right] \right\} \right) \right\}$$

$$\Rightarrow \; E^s = e^{\zeta} \frac{\hat{\mathbf{n}}}{|\mathbf{n}|^2} \cdot \left\{ F(\rho) \frac{e^{jk\rho}}{2\pi\rho} \underset{xy}{*} \left(\hat{\mathbf{n}}\hat{\mathbf{n}} \cdot \mathcal{F}_{xy}^{-1} \left\{ e^{-z^- u} \left[2u\mathcal{F}_{xy} \left\{ \mathbf{E}_s^{z^-} \right\} \right] \right\} \right) \right\}. \tag{3.28}$$

Comparing (3.26) and (3.28) to their small-height counterparts presented in [3], it is clear that the difference between them is the presence of the arbitrary heights factors $e^{\pm\zeta(x,y;t)}$. It is easy to show that in the small-height case,

$$\zeta(x,y;t) \triangleq \mathcal{F}_{xy}^{-1} \left\{ \mathcal{F}_{xy} \left\{ f(x,y;t) \right\} u \right\} = \mathcal{F}_{xy}^{-1} \left\{ \mathcal{F}_{xy} \left\{ f(x,y;t) u \right\} \right\} << 1,$$

and therefore it can be said that $\zeta(x,y;t) \approx 0$. In this case, the expressions in (3.26) and (3.28) reduce to the form shown in [3].

From the expression for the normal to the ocean surface defined in (3.8), the unit vector in the direction of the outward normal can be written as

$$\hat{\mathbf{n}} = \frac{\mathbf{n}}{|\mathbf{n}|} = \frac{\hat{\mathbf{z}} - \nabla_{xy} f(x,y;t)}{|\mathbf{n}|}. \tag{3.29}$$

Taking the first part of the relationship shown in (3.29) and substituting it into (3.28), the expression for E^s can be rewritten as

$$E^s = e^{\zeta} \frac{\mathbf{n}}{|\mathbf{n}|^3} \cdot \left\{ F(\rho) \frac{e^{jk\rho}}{2\pi\rho} \underset{xy}{*} \left(\frac{\mathbf{n}\mathbf{n}}{|\mathbf{n}|^2} \cdot \mathcal{F}_{xy}^{-1} \left\{ e^{-z^- u} \left[2u\mathcal{F}_{xy} \left\{ \mathbf{E}_s^{z^-} \right\} \right] \right\} \right) \right\}. \tag{3.30}$$

Now, from the second part of the equality in (3.29), it is clear that the dyadic product $\hat{\mathbf{n}}\hat{\mathbf{n}}$ can be written as

$$\hat{\mathbf{n}}\hat{\mathbf{n}} = \frac{1}{|\mathbf{n}|^2} \left\{ \hat{\mathbf{z}}\hat{\mathbf{z}} - \hat{\mathbf{z}}(\nabla f(x,y;t)) - (\nabla f(x,y;t))\hat{\mathbf{z}} + \nabla f(x,y;t) \nabla f(x,y;t) \right\}.$$

Therefore, by using the dyadic property for the right dot product, the product $\hat{\mathbf{n}}\hat{\mathbf{n}} \cdot \nabla(|\mathbf{n}|E_{\mathbf{n}}^{+})$ found in (3.26) can be written as

$$\hat{\mathbf{n}}\hat{\mathbf{n}} \cdot \nabla(|\mathbf{n}|E_{\mathbf{n}}^{+}) = \frac{1}{|\mathbf{n}|^2}\{\hat{\mathbf{z}}(\hat{\mathbf{z}} \cdot \nabla(|\mathbf{n}|E_{\mathbf{n}}^{+})) - \hat{\mathbf{z}}((\nabla f(x,y;t)) \cdot \nabla(|\mathbf{n}|E_{\mathbf{n}}^{+}))$$
$$- (\nabla f(x,y;t))(\hat{\mathbf{z}} \cdot \nabla(|\mathbf{n}|E_{\mathbf{n}}^{+})) + \nabla f(x,y;t)(\nabla f(x,y;t) \cdot \nabla(|\mathbf{n}|E_{\mathbf{n}}^{+}))\}. \quad (3.31)$$

From the definition of the normal vector in (3.8), the expression for $\nabla(|\mathbf{n}|E_{\mathbf{n}}^{+})$ can be written as

$$\nabla(|\mathbf{n}|E_{\mathbf{n}}^{+}) = (\nabla|\mathbf{n}|)E_{\mathbf{n}}^{+} + |\mathbf{n}|(\nabla E_{\mathbf{n}}^{+}). \quad (3.32)$$

Knowing from the definition of the normal vector in (3.8) that $|\mathbf{n}| = \sqrt{1^2 + |\nabla f(x,y)|^2}$, and that $E_{\mathbf{n}}^{+}$ is the magnitude of the electric field normal to the ocean surface calculated at $z = \lim_{\Delta z \to 0} f(x,y) + \Delta z \approx f(x,y)$, both terms in the sum in (3.32) are independent of z. Therefore, the resulting expression of $\nabla(|\mathbf{n}|E_{\mathbf{n}}^{+})$ will have a null component in the z-direction. Therefore, (3.31) reduces to

$$\hat{\mathbf{n}}\hat{\mathbf{n}} \cdot \nabla(|\mathbf{n}|E_{\mathbf{n}}^{+}) = \frac{1}{|\mathbf{n}|^2}\left\{-\hat{\mathbf{z}}[(\nabla f(x,y;t)) \cdot \nabla(|\mathbf{n}|E_{\mathbf{n}}^{+})] + \nabla f(x,y;t)\nabla f(x,y;t) \cdot \nabla(|\mathbf{n}|E_{\mathbf{n}}^{+})\right\}. \quad (3.33)$$

Now, substituting (3.33) into (3.26), and taking the dot product between $\hat{\mathbf{n}}$ and $\hat{\mathbf{n}}\hat{\mathbf{n}} \cdot \nabla(|\mathbf{n}|E_{\mathbf{n}}^{+})$, the $\mathcal{T}$ operator can be split into two parts:

$$\mathcal{T}(E_{\mathbf{n}}^{+}) = -\mathcal{T}_1(E_{\mathbf{n}}^{+}) - \mathcal{T}_2(E_{\mathbf{n}}^{+}),$$

where

$$\mathcal{T}_1(E_{\mathbf{n}}^{+}) = e^{\zeta}\frac{1}{|\mathbf{n}|^3} \cdot \left\{F(\rho)\frac{e^{jk\rho}}{2\pi\rho} \underset{xy}{*} \left\{e^{-\zeta}\left[\frac{\nabla f}{|\mathbf{n}|^2} \cdot \nabla(|\mathbf{n}|E_{\mathbf{n}}^{+})\right]\right\}\right\} \quad (3.34)$$

and

$$\mathcal{T}_2(E_{\mathbf{n}}^{+}) = e^{\zeta}\frac{\nabla f}{|\mathbf{n}|^3} \cdot \left\{F(\rho)\frac{e^{jk\rho}}{2\pi\rho} \underset{xy}{*} \left\{e^{-\zeta}\left[\frac{\nabla f \nabla f}{|\mathbf{n}|^2} \cdot \nabla(|\mathbf{n}|E_{\mathbf{n}}^{+})\right]\right\}\right\}. \quad (3.35)$$

Therefore, the operator equation for the magnitude of the electric field over the ocean surface can be written as

$$E^s = E^+_{\mathbf{n}} - \mathcal{T}_1(E^+_{\mathbf{n}}) - \mathcal{T}_2(E^+_{\mathbf{n}}), \tag{3.36}$$

with E^s defined in (3.30), and the expressions for $\mathcal{T}_1(E^+_{\mathbf{n}})$ and $\mathcal{T}_2(E^+_{\mathbf{n}})$ defined in (3.34) and (3.35) respectively. It should be noted that, as no restriction has been imposed on the expressions in (3.36) at this point, (3.36) is valid for any conductive rough surface at any frequency. This is due to the relaxation of the small-height constraint, which allows for an arbitrary roughness scale. However, it should be noted that the resulting expression for the scattered electric field is dependent on the choice of source, which is defined in the E^s operator. Therefore, to proceed with the derivation of the expression for the electric field scattered by an ocean surface with electromagnetically-large waves, an expression for the source of the electric field must be defined.

3.3 Electric Field for a Vertical Dipole Source

As described by Walsh and Gill [3], a vertical dipole source located at the origin and outside the scattering body can be mathematically described as

$$\mathbf{E}_s = \frac{I(\omega)\Delta\ell k^2}{j\omega\epsilon_0} G_0\hat{\mathbf{z}} \triangleq C_0 G_0\hat{\mathbf{z}}, \tag{3.37}$$

where $I(\omega)$ is the current distribution at the source and $\Delta\ell$ is the dipole length. Using the two-dimensional spatial Fourier transform of the Green's function solution to the Helmholtz equation presented in Appendix B.1, the Fourier transform of (3.37) at the plane $z = z^- < 0\ \forall z$ can be written as

$$\mathcal{F}_{xy}\left\{\mathbf{E}_s^{z^-}\right\} = C_0\frac{e^{z^- u}}{2u}\hat{\mathbf{z}}. \tag{3.38}$$

From this expression, it is easy to show that [3]

$$e^{-z^- u}\mathcal{F}_{xy}^{-1}\left\{2u\mathcal{F}_{xy}\left\{\mathbf{E}_s^{z^-}\right\}\right\} = C_0\delta(x)\delta(y)\hat{\mathbf{z}}, \tag{3.39}$$

where $\delta(\cdot)$ is the Dirac delta distribution. Substituting (3.39) into (3.30), the following expression can be obtained for the source field E^s:

$$E^s = C_0 e^{\zeta}\frac{\mathbf{n}}{|\mathbf{n}|^3}\cdot\left\{F(\rho)\frac{e^{jk\rho}}{2\pi\rho}\underset{xy}{*}\left(\frac{\mathbf{nn}}{|\mathbf{n}|^2}\cdot\delta(x)\delta(y)\hat{\mathbf{z}}\right)\right\}. \tag{3.40}$$

If it is assumed that the source is at sea level, the vertical displacement at the source position is null and $\mathbf{n} = \hat{\mathbf{z}}$. Therefore, (3.40) can be further reduced to

$$E^s = e^{\zeta(x,y;t)}\frac{C_0}{|\mathbf{n}|^3}F(\rho)\frac{e^{jk\rho}}{2\pi\rho}. \tag{3.41}$$

At this point in the analysis presented in [3], the small-slope approximation is invoked to simplify the expressions for the height-limited expressions for the electric field. The small-slope approximation presented in [3] can be defined as

$$|\mathbf{n}| = \sqrt{1+|\nabla f|^2} \approx 1, \tag{3.42}$$

which can be interpreted as $|\nabla f|^2 << 1$. From the results presented in the literature [114]–[117], it is clear that the mean-square slope of the ocean surface is indeed much smaller than one for surface gravity waves, which are the waves observed by a radar operating in the HF band [14]. For example, considering the formulation proposed in [114], the mean square slope for surface gravity waves considering a Phillips spectrum [118] and a high-frequency roll-off wavenumber of 6π can be calculated as

$$\sigma_g^2 = 0.0046(1+2\ln(U_{10})). \tag{3.43}$$

If the highest wind speed ever recorded on Earth is considered (135 m/s, measured during the Bridge Creek-Moore tornado [119]), the root mean square (RMS) slope

for surface gravity waves at this wind speed would only go up to 0.223. Therefore, considering a radar operating in the HF band, the small-slope approximation can be considered valid, and the E^s operator can be rewritten asked

$$E^s = e^{\zeta(x,y;t)} C_0 F(\rho) \frac{e^{jk\rho}}{2\pi\rho}. \tag{3.44}$$

Another consequence of the small-slope approximation is that if $|\nabla f|^2 << 1$, higher powers of the surface slope will be even smaller. Therefore, terms that are proportional to powers of the surface slope higher than one can be neglected through the small-slope approximation. So, by observing the expression for the $\mathcal{T}_2$ operator in (3.35), it is clear that under the small-slope approximation, the contribution of $\mathcal{T}_2(E^+_{\mathbf{n}})$ to the equation will be negligible. Applying the small-slope approximation to the $\mathcal{T}_1$ operator in (3.34), the following expression can be obtained:

$$\mathcal{T}_1(E^+_{\mathbf{n}}) = e^{\zeta} \left[F(\rho) \frac{e^{jk\rho}}{2\pi\rho} \underset{xy}{*} e^{-\zeta} \left(\nabla f \cdot \nabla(E^+_{\mathbf{n}}) \right) \right]. \tag{3.45}$$

Substituting (3.44) and (3.45) into (3.36), with $\mathcal{T}_2(E^+_{\mathbf{n}}) \approx 0$, the operator equation for the electric field scattered by an ocean surface with electromagnetically-large waves in the presence of a vertical dipole source can be written as:

$$E^+_{\mathbf{n}} - \left\{ e^{\zeta} \left[F(\rho) \frac{e^{-jk\rho}}{2\pi\rho} \underset{xy}{*} e^{-\zeta} \left(\nabla f \cdot \nabla(E^+_{\mathbf{n}}) \right) \right] \right\} = C_0 F(\rho) \frac{e^{-jk\rho}}{2\pi\rho} e^{\zeta}. \tag{3.46}$$

As proposed in [3] for the height-restricted case, the Neumann series solution [105] to the equation presented in (3.46) can be written as:

$$E^+_{\mathbf{n}} = E^s + T_1\{E^s\} + T_1^2\{E^s\} + \cdots \triangleq (E^+_{\mathbf{n}})_0 + (E^+_{\mathbf{n}})_1 + (E^+_{\mathbf{n}})_2 + \cdots, \tag{3.47}$$

where the subscripts in the bottom equation indicate the order of the *electromagnetic coupling* of the electric field and the ocean surface.

In high frequency radio oceanography, the scattered field can be characterized by two types of coupling, defined in terms of the interactions between ocean waves and the electromagnetic field. An electric field is said to have n^{th}-order *hydrodynamic coupling* if the received field was scattered by a wave that is a combination of n linear ocean waves, coupled as shown in [75]. Mathematically, the hydrodynamic components of the electric field can be obtained by applying an asymptotic perturbation expansion to the ocean surface displacement. If, however, the electric field "bounces" on n linear ocean waves before reaching the receiver, it is said that these ocean waves were electromagnetically coupled to the signal, and the field has an n^{th}-order *electromagnetic* coupling [57], [120]. From these definitions, it is easy to understand that the different powers in (3.47) represent the number of electromagnetic interactions the electric field had with the ocean surface before reaching the receiver. Here, the first- and second-order electric fields scattered by an ocean surface with electromagnetically-large waves will be derived.

3.3.1 First-Order Electric Field for an Ocean Surface With Electromagnetically-Large Waves

From (3.47), the expression for the first-order electric field can be written as

$$\left(E^{+}_{\mathbf{n}}\right)_1 = \mathcal{T}_1(E^s) = C_0 e^{\zeta}\left[F(\rho)\frac{e^{-jk\rho}}{2\pi\rho} \underset{xy}{*} e^{-\zeta}\left(\nabla f \cdot \nabla(E^s)\right)\right] \tag{3.48}$$

Substituting (3.41) into $\nabla(E^s)$,

$$\nabla(E^s) = \nabla\left(F(\rho)\frac{e^{-jk\rho}}{2\pi\rho}e^{\zeta}\right) = \nabla\left(F(\rho)\frac{e^{-jk\rho}}{2\pi\rho}\right)e^{\zeta} + F(\rho)\frac{e^{-jk\rho}}{2\pi\rho}\nabla e^{\zeta}. \tag{3.49}$$

From [3], the gradient in the first term of (3.49) can be written, in an asymptotic sense, as

$$\nabla\left(F(\rho)\frac{e^{-jk\rho}}{2\pi\rho}\right) \approx -jkF(\rho)\frac{e^{-jk\rho}}{2\pi\rho}\hat{\boldsymbol{\rho}}. \tag{3.50}$$

From the definition in (3.17), the arbitrary heights function on the gradient in the second term of (3.49) can be understood as the composition $\zeta(f(x,y;t))$, which results in

$$\nabla e^{\zeta(f)} = e^{\zeta(f)}\nabla\zeta(f) = \nabla f e^{\zeta(f)}\zeta'(f), \tag{3.51}$$

where $\zeta'(f)$ is the derivative of ζ with respect to f. Thus, substituting (3.50) and (3.51) into (3.49) gives

$$\nabla(E^s) \approx (-jk\hat{\boldsymbol{\rho}} + \nabla f\zeta'(f))e^{\zeta}F(\rho)\frac{e^{-jk\rho}}{2\pi\rho}. \tag{3.52}$$

Substituting (3.52) into (3.48), knowing that, by the small-slope approximation, $\nabla f \cdot \nabla f = |\nabla f|^2 \approx 0$, the first-order electric field can be written as

$$(E^+_{\mathbf{n}})_1 \approx -jkC_0e^{\zeta}\left[F(\rho)\frac{e^{-jk\rho}}{2\pi\rho} \underset{xy}{*} \cancel{e^{\zeta}}\cancel{e^{\zeta}}F(\rho)\frac{e^{-jk\rho}}{2\pi\rho}\left(\nabla f\cdot\hat{\boldsymbol{\rho}}\right)\right]. \tag{3.53}$$

Changing the coordinates of (3.53) to a cylindrical coordinate system yields

$$(E^+_{\mathbf{n}})_1 \approx -jkC_0e^{\zeta(\boldsymbol{\rho})}\left[F(\rho)\frac{e^{-jk\rho}}{2\pi\rho} \underset{\boldsymbol{\rho}}{*} F(\rho)\frac{e^{-jk\rho}}{2\pi\rho}\left(\nabla f(\boldsymbol{\rho})\cdot\hat{\boldsymbol{\rho}}\right)\right]. \tag{3.54}$$

Expressing (3.54) as a convolution integral, the electric field expression becomes

$$(E^+_{\mathbf{n}})_1 \approx \frac{-jkC_0}{(2\pi)^2}e^{\zeta(\boldsymbol{\rho})}\iint\limits_{\boldsymbol{\rho}_1}\left(\nabla f(\boldsymbol{\rho}_1)\cdot\hat{\boldsymbol{\rho}}_1\right)F(|\boldsymbol{\rho}_1|)\frac{e^{-jk|\boldsymbol{\rho}_1|}}{|\boldsymbol{\rho}_1|}F(|\boldsymbol{\rho}-\boldsymbol{\rho}_1|)\frac{e^{-jk|\boldsymbol{\rho}-\boldsymbol{\rho}_1|}}{|\boldsymbol{\rho}-\boldsymbol{\rho}_1|}\,\mathrm{d}A_1, \tag{3.55}$$

where

$$\mathrm{d}A_1 = \rho_1\,\mathrm{d}\rho_1\,\mathrm{d}\theta_1.$$

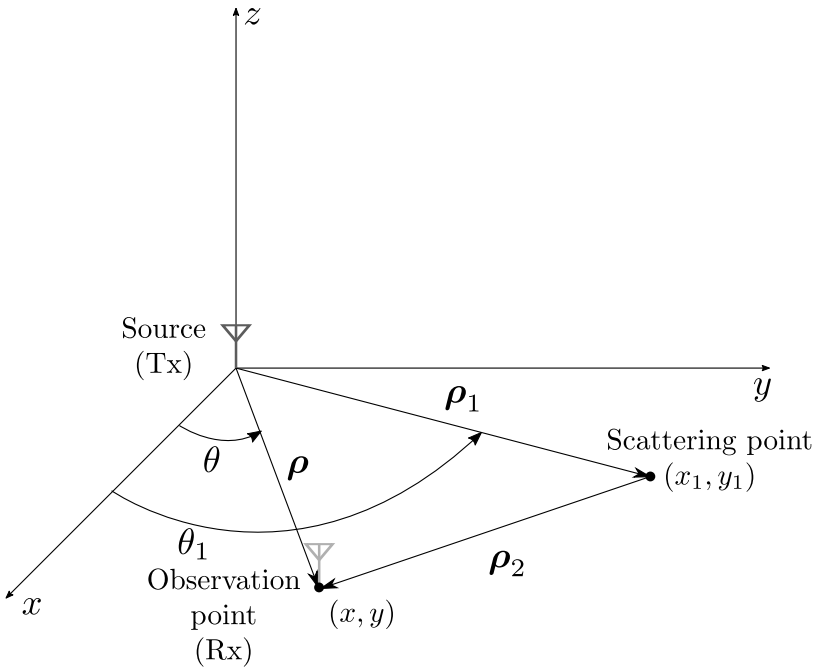

Figure 3.1: Scattering geometry for the first-order electric field

Making $\boldsymbol{\rho}_2 = \boldsymbol{\rho} - \boldsymbol{\rho}_1$, the expression for the first-order electric field scattered by an ocean surface with electromagnetically-large waves can be written as

$$\left(E_{\mathbf{n}}^{+}\right)_1 \approx \frac{-jkC_0}{(2\pi)^2} e^{\zeta(\boldsymbol{\rho};t)} \iint\limits_{\boldsymbol{\rho}_1} \left(\nabla f(\boldsymbol{\rho}_1;t)\cdot\hat{\boldsymbol{\rho}}_1\right) F(\rho_1)F(\rho_2)\frac{e^{-jk\rho_1+\rho_2}}{\rho_1\rho_2}\,\mathrm{d}A_1, \tag{3.56}$$

with the scattering geometry defined as shown in Figure 3.1. Again, it is evident that the expression in (3.56) will reduce to the form presented in [3] if the small-height approximation is applied. Comparing (3.56) with the form of the height-restricted first-order electric field presented in [3], (3.56) can be rewritten as

$$\left(E_{\mathbf{n}}^{+}\right)_1 = e^{\zeta(x,y;t)}\left(E_{0\mathbf{n}}^{+}\right)_1, \tag{3.57}$$

where $\left(E_{0\mathbf{n}}^{+}\right)_1$ is the height-restricted first-order electric field scattered by the ocean surface as proposed in [3].

Going back to the expression of the arbitrary heights function and following the same procedure shown for the convolution integral in (3.56), the convolution in (3.17) can be interpreted as

$$\zeta(x,y;t) = \zeta(\boldsymbol{\rho};t) = f(x,y;t) \underset{xy}{*} \mathcal{F}_{xy}^{-1}\{u\} = \iint\limits_{\boldsymbol{\rho}_1} f(\boldsymbol{\rho}_1;t)h(\boldsymbol{\rho}-\boldsymbol{\rho}_1)\,\mathrm{d}\boldsymbol{\rho}_1$$

$$\therefore\ \zeta(\boldsymbol{\rho};t) = \iint\limits_{\boldsymbol{\rho}_1} f(\boldsymbol{\rho}_1;t)h(\boldsymbol{\rho}_2)\,\mathrm{d}\boldsymbol{\rho}_1, \tag{3.58}$$

with

$$h(\boldsymbol{\rho}) = \mathcal{F}_{xy}^{-1}\{u\}(\boldsymbol{\rho})$$

and scattering geometry defined in Figure 3.1.

3.3.2 Second-Order Electric Field for an Ocean Surface With Electromagnetically-Large Waves

The second-order electric field as proposed in [3] represents the instances in which there is an interaction between the transmitted electric field and two first-order (monochromatic) waves on the ocean surface before the signal is observed by the receiver. Mathematically, in terms of the Neumann series, the second-order electric field can be understood as

$$(E_{\mathbf{n}}^{+})_2 = \mathcal{T}_1^2\{E^s\} = \mathcal{T}_1\{\mathcal{T}_1\{E^s\}\}, \tag{3.59}$$

From the definition of $\mathcal{T}_1$ in (3.45), (3.59) can be written as

$$(E_{\mathbf{n}}^{+})_2 \approx -jkC_0e^{\zeta}\left\{F(\rho)\frac{e^{jk\rho}}{2\pi\rho} \underset{xy}{*} e^{-\zeta}\left[\nabla f\cdot\nabla\left(\mathcal{T}_1(E^s)\right)\right]\right\}. \tag{3.60}$$

Knowing that $\mathcal{T}_1(E^s)$ is equal to the first-order electric field defined in Section 3.3.1, any of the expressions for $\mathcal{T}_1(E^s)$ in the derivation of $(E_{\mathbf{n}}^{+})_1$ can be used to derive the

gradient of $\mathcal{T}_1\{E^s\}$. Thus, from (3.54):

$$\nabla\left(\mathcal{T}_1\{E^s\}\right) = \nabla\left[e^{\zeta}\left(F(\rho)\frac{e^{-jk\rho}}{2\pi\rho} \underset{\boldsymbol{\rho}}{*} F(\rho)\frac{e^{-jk\rho}}{2\pi\rho}\left(\nabla f\cdot\hat{\boldsymbol{\rho}}\right)\right)\right]$$

$$\therefore\ \nabla\left(\mathcal{T}_1\{E^s\}\right) \triangleq I_1(x,y)\nabla e^{\zeta} + e^{\zeta}\nabla I_1(x,y), \tag{3.61}$$

where

$$I_1(x,y) = F(\rho)\frac{e^{-jk\rho}}{2\pi\rho}(\hat{\boldsymbol{\rho}}\cdot\nabla f(\boldsymbol{\rho};t)) \underset{xy}{*} F(\rho)\frac{e^{-jk\rho}}{2\pi\rho}.$$

Substituting the gradient of e^{ζ} derived in (3.51) into (3.61),

$$\nabla\left(\mathcal{T}_1\{E^s\}\right) = \nabla f e^{\zeta}\zeta'(f)I_1(x,y) + e^{\zeta}\nabla I_1(x,y). \tag{3.62}$$

Taking the dot product between (3.62) and ∇f, as shown in (3.60), it is clear that the first term in (3.62) will be approximately zero due to the small-slope approximation, making

$$\nabla f\cdot\nabla\left(\mathcal{T}_1\{E^s\}\right) = e^{\zeta}\nabla f\cdot\nabla I_1(x,y) = e^{\zeta}\nabla f\cdot\nabla\left(F(\rho)\frac{e^{-jk\rho}}{2\pi\rho}(\hat{\boldsymbol{\rho}}\cdot\nabla f(\boldsymbol{\rho};t)) \underset{xy}{*} F(\rho)\frac{e^{-jk\rho}}{2\pi\rho}\right) \tag{3.63}$$

Substituting (3.63) into (3.60) gives

$$(E^+_{\mathbf{n}})_2 \approx -jkC_0e^{\zeta}\left\{F(\rho)\frac{e^{jk\rho}}{2\pi\rho} \underset{xy}{*}\left[\nabla f\cdot\nabla\left(F(\rho)\frac{e^{-jk\rho}}{2\pi\rho}(\hat{\boldsymbol{\rho}}\cdot\nabla f(\boldsymbol{\rho};t)) \underset{xy}{*} F(\rho)\frac{e^{-jk\rho}}{2\pi\rho}\right)\right]\right\}. \tag{3.64}$$

Comparing (3.64) with the second-order electric field for a height-restricted ocean surface defined in [3], it is easy to show that

$$(E^+_{\mathbf{n}})_2 = e^{\zeta(\boldsymbol{\rho};t)}(E^+_{0\mathbf{n}})_2, \tag{3.65}$$

where $(E^+_{0\mathbf{n}})_2$ is the height-restricted second-order electric field [3]. As discussed in Section 3.3.1 for the first-order electric field, the expression shown in (3.65) reduces to the height-restricted second-order electric field as $\zeta(\rho;t) \to 0$, a consequence of the small-height approximation.

3.4 Power Series Expansion of the Arbitrary Heights Factor

From (3.57) and (3.65), it is clear that the first- and second-order scattered electric fields for an ocean surface with arbitrary roughness scales follow a pattern in which they are the result of the product between the exponential of the arbitrary heights function, here called the arbitrary heights factor, and the height-restricted electric field for their respective orders.

The arbitrary heights factor can be expanded in a power series, resulting in

$$e^{\zeta(\boldsymbol{\rho};t)} = \sum_{m=0}^{\infty} \frac{[\zeta(\boldsymbol{\rho};t)]^m}{m!} = 1 + \zeta(\boldsymbol{\rho};t) + \frac{1}{2}\zeta^2(\boldsymbol{\rho};t) + \cdots . \tag{3.66}$$

Substituting (3.66) into (3.57),

$$\left(E^+_{\mathbf{n}}\right)_1 = \left\{ \sum_{m=0}^{\infty} \frac{\zeta^m(\boldsymbol{\rho};t)}{m!} \right\} \left(E^+_{0\mathbf{n}}\right)_1 = \left(E^+_{0\mathbf{n}}\right)_1 + \zeta(\boldsymbol{\rho};t)\left(E^+_{0\mathbf{n}}\right)_1 + \frac{\zeta^2(\boldsymbol{\rho};t)}{2}\left(E^+_{0\mathbf{n}}\right)_1 + \cdots \tag{3.67}$$

From (3.67), it is clear that the first term shows the original height-restricted electric field, while subsequent terms consist of the height-restricted field multiplied by increasing powers of the arbitrary heights function. These terms represent different orders of the arbitrary heights correction to the electric field scattered by the ocean surface. Establishing the notation moving forward, (3.67) can be rewritten as

$$\left(E^+_{\mathbf{n}}\right)_1 \triangleq \left(E^+_{0\mathbf{n}}\right)_1 + \left[\left(E^+_{0\mathbf{n}}\right)_1\right]_1 + \left[\left(E^+_{0\mathbf{n}}\right)_1\right]_2 + \cdots \tag{3.68}$$

where the $\left[\left(E^+_{0\mathbf{n}}\right)_1\right]_n$ indicates the n-th order correction to the first-order electric field, defined as

$$\left[\left(E^+_{0\mathbf{n}}\right)_1\right]_n = \frac{\zeta^n(\boldsymbol{\rho};t)}{n!}\left(E^+_{0\mathbf{n}}\right)_1, \; n = 1, 2, \cdots . \tag{3.69}$$

Analogously, the arbitrary heights factor in (3.65) can be expanded in a power series, resulting in

$$\left(E^{+}_{\mathbf{n}}\right)_2 \triangleq \left(E^{+}_{0\mathbf{n}}\right)_2 + \left[\left(E^{+}_{0\mathbf{n}}\right)_2\right]_1 + \left[\left(E^{+}_{0\mathbf{n}}\right)_2\right]_2 + \cdots \tag{3.70}$$

where

$$\left[\left(E^{+}_{0\mathbf{n}}\right)_2\right]_n = \frac{\zeta^n(\boldsymbol{\rho};t)}{n!}\left(E^{+}_{0\mathbf{n}}\right)_2,\ n = 1, 2, \cdots\ . \tag{3.71}$$

Since both (3.68) and (3.70) are heavily dependent on the expressions for the height-restricted electric fields, special attention must be taken when dealing with these expressions. While most of the derivations of the height-restricted electric field have been presented in [3], [17] for a monostatic configuration and [18], [89], [121] for a bistatic configuration, in both cases the authors started from the assumption of a static random rough surface, introducing time variation later in the process. Since the corrections to the electric field depend on the height-restricted expressions, the derivation of the height-restricted electric fields must be revised before moving forward with the derivations of the correction term, as to introduce the time variation from the outset. Without loss of generality, the derivations of the height-restricted electric field for a time-varying conductive surface will be performed using the expression for the first-order electric field, knowing that the same patterns will be true in the case of a second-order electric field [3].

3.5 Electric Field Scattered by a Height-Restricted and Time-Varying Conductive Surface

Using the notation presented here, the expression for the height-restricted first-order electric field can be written as

$$(E_{0\mathbf{n}}^{+})_1 \approx \frac{-jkC_0}{(2\pi)^2} \iint\limits_{\boldsymbol{\rho}_1} \left(\nabla f(\boldsymbol{\rho}_1;t)\cdot\hat{\boldsymbol{\rho}}_1\right) F(\rho_1)F(\rho_2)\frac{e^{-jk\rho_1+\rho_2}}{\rho_1\rho_2}\,\mathrm{d}A_1. \tag{3.72}$$

As discussed in [3], some assumptions must be made about the ocean surface at this point in the derivations. It is trivial to assume that the ocean surface can be represented by a combination of random, independent and periodic ocean waves [122], [123]. Due to the sampling time and area of observation considered in the HF radar operation, this process can also be considered ergodic, meaning that the ensemble average of the ocean process is equal to its time average [122]. Therefore, it is possible to represent the ocean surface as Fourier-Stieltjes integral, or a Fourier-Stieltjes series.

3.5.1 Scattering From a Time-Varying Surface Represented by a Fourier Series

The displacement $f(\boldsymbol{\rho};t)$ can be represented by a Fourier-Stieltjes integral of the form [122]

$$f(\boldsymbol{\rho_1};t) = \int\limits_{\mathbf{K}'}\int\limits_{\omega_{\mathbf{K}'}} e^{-j\omega_{\mathbf{K}}t}e^{j\mathbf{K}\cdot\boldsymbol{\rho}_1}\,\mathrm{d}F(\mathbf{K},\omega_{\mathbf{K}}) \tag{3.73}$$

where $\mathrm{d}F(\mathbf{K},\omega_{\mathbf{K}})$ are random Fourier coefficients for an ocean surface with wave vector $\mathbf{K} = (K_x, K_y) = K\angle\theta_{\mathbf{K}}$ and angular frequency $\omega_{\mathbf{K}}$. Consequently, the Fourier

coefficient defined as [113]

$$\mathrm{d}F(\mathbf{K},\omega_{\mathbf{K}}) \triangleq f(\mathbf{K},\omega_{\mathbf{K}}) = \int_{\boldsymbol{\rho}_1}\int_{t} e^{j\omega_{\mathbf{K}}t}e^{-j\mathbf{K}\cdot\boldsymbol{\rho}_1}\,\mathrm{d}F(\boldsymbol{\rho_1};t), \tag{3.74}$$

with $\mathrm{d}F(\boldsymbol{\rho_1};t) \triangleq f(\boldsymbol{\rho_1};t)$. Since the surface displacement is a real function [27],

$$f(\mathbf{K},\omega_{\mathbf{K}}) = \overline{f(-\mathbf{K},-\omega_{\mathbf{K}})},$$

where the overline indicates the complex conjugate of the Fourier coefficient. For a more condensed presentation, (3.73) can be represented as a Fourier-Stieltjes series of the form [3], [29], [75]

$$f(\boldsymbol{\rho_1};t) = \sum_{\mathbf{K},\omega_{\mathbf{K}}} f(\mathbf{K},\omega_{\mathbf{K}})e^{-j\omega_{\mathbf{K}}t}e^{jK\rho_1\cos(\theta_{\mathbf{K}}-\theta_1)}. \tag{3.75}$$

Applying the gradient operator over (3.75) and taking the dot product with $\hat{\boldsymbol{\rho}}_1$ yields

$$\nabla f(\boldsymbol{\rho}_1;t)\cdot\hat{\boldsymbol{\rho}}_1 = \frac{\partial}{\partial\rho_1}f(\boldsymbol{\rho}_1;t) = j\sum_{\mathbf{K},\omega_{\mathbf{K}}} f(\mathbf{K},\omega_{\mathbf{K}})K\cos(\theta_{\mathbf{K}}-\theta_1)e^{-j\omega_{\mathbf{K}}t}e^{jK\rho_1\cos(\theta_{\mathbf{K}}-\theta_1)}. \tag{3.76}$$

Substituting (3.76) into (3.72), and introducing the directivity function $g(\theta_1)$ as done in [3] and considering the monostatic case, where $\rho_2 = \rho_1$, the first-order electric field can be approximated as

$$(E^{+}_{0\mathbf{n}})_1 \approx \frac{kC_0}{(2\pi)^2}\sum_{\mathbf{K},\omega_{\mathbf{K}}} f(\mathbf{K},\omega_{\mathbf{K}})Ke^{-j\omega_{\mathbf{K}}t}\int_{\boldsymbol{\rho}_1} F^2(\rho_1)\frac{e^{-2jk\rho_1}}{\rho_1} \cdot\int_{\theta_1} g(\theta_1)\cos(\theta_{\mathbf{K}}-\theta_1)e^{jK\rho\cos(\theta_{\mathbf{K}}-\theta)}\,\mathrm{d}\theta_1\,\mathrm{d}\rho_1. \tag{3.77}$$

It is easy to show that the product $\rho_1 K$ in the phase term of the integral over θ_1 in (3.78) is sufficiently large for the typical values involved in the remote sensing of the ocean surface. Therefore, defining the inner integral in (3.77) as

$$I_{\theta_1}(\rho_1) = \int_{\theta_1} g(\theta_1)\cos(\theta_{\mathbf{K}}-\theta_1)e^{jK\rho\cos(\theta_{\mathbf{K}}-\theta)}\,\mathrm{d}\theta_1, \tag{3.78}$$

(3.78) can be approximated using stationary phase integration [124]. The same procedure has been employed in [3], resulting in

$$I_{\theta_1}(\rho_1) \approx \sqrt{\frac{2\pi}{K\rho_1}} \left[g(\theta_{\mathbf{K}}) e^{-j\pi/4} e^{jK\rho_1} - g(\theta_{\mathbf{K}} + \pi) e^{j\pi/4} e^{-jK\rho_1} \right]. \tag{3.79}$$

Substituting (3.79) into (3.77) yields

$$(E^{+}_{0\mathbf{n}})_1 \approx \frac{kC_0}{(2\pi)^{3/2}} \sum_{\mathbf{K},\omega_{\mathbf{K}}} f(\mathbf{K},\omega_{\mathbf{K}}) \sqrt{K} e^{-j\omega_{\mathbf{K}} t} \int_{\boldsymbol{\rho}_1} F^2(\rho_1) \frac{e^{-j2k\rho_1}}{(\rho_1)^{3/2}} [g(\theta_{\mathbf{K}}) e^{-j\pi/4} e^{jK\rho_1} - g(\theta_{\mathbf{K}} + \pi) e^{j\pi/4} e^{-jK\rho_1}] \, \mathrm{d}\rho_1. \tag{3.80}$$

At this point, except for the time-dependent exponential term in (3.80), not much is different between the derivations presented here and the ones shown in [3]. However, this time-dependent term will play an important role in the analysis of the electric field in the time domain, especially considering a pulsed radar source.

3.5.2 Scattered Electric Field Considering a Pulsed Radar Source

At this point in the derivations, it is important to define the current distribution at the source. The two most common transmission modes for an HF radar are pulsed and frequency-modulated continuous-wave (FMCW) transmissions [125], which are better defined in the time domain. Therefore, to define the time-domain current distribution of the source in the expression for the scattered electric field, the expression in (3.80) must be transformed to time domain. As there are two different two frequencies involved in (3.80) — namely, the transmitter and ocean wave frequencies — it should be noted that the inverse Fourier transform to be applied here is performed with respect to the radar frequency.

Following the procedure described in [3], the Fourier transform of the first-order electric field presented in (3.80) results in

$$(E_{0\mathbf{n}}^{+})_1(t) \approx \frac{1}{(2\pi)^{3/2}} \cdot \left\{ \mathcal{F}_t^{-1}\{kC_0\} \underset{t}{\ast} \left\{ \sum_{\mathbf{K},\omega_{\mathbf{K}}} f_1(\mathbf{K},\omega_{\mathbf{K}}) e^{-j\omega_{\mathbf{K}}t} \sqrt{K} \int_{\rho_1} \frac{F^2(\rho_1,\omega_0)}{(\rho_1)^{3/2}} \right.\right.$$
$$\left.\left. \cdot\, \delta\left(t - 2\frac{\rho_1}{c}\right) \left\{ g(\theta_{\mathbf{K}}) e^{-j\pi/4} e^{jK\rho_1} - g(\theta_{\mathbf{K}}+\pi) e^{j\pi/4} e^{-jK\rho_1} \right\} \mathrm{d}\rho_1 \right\} \right\}, \quad (3.81)$$

where $\mathcal{F}_t^{-1}\{\cdot\}$ is the inverse temporal Fourier transform and c is the speed of light in the vacuum. Here, it should be noted that since the Sommerfeld attenuation function has only a slight variation within the frequency range of operations of an HF-radar [85],

$$\mathcal{F}_t^{-1}\left\{ F^2(\rho_1,\omega) e^{-2jk\rho_1} \right\} = F^2(\rho_1,\omega_0)\delta\left(t - 2\frac{\rho_1}{c}\right),$$

where ω_0 is the dominant (or representative) frequency of the transmitter [3].

Taking advantage of the sifting property of the Dirac delta [105], the integration over ρ_1 in (3.81) can be performed, resulting in

$$(E_{0\mathbf{n}}^{+})_1(t) \approx \frac{1}{(2\pi)^{3/2}} \cdot \left\{ \mathcal{F}_t^{-1}\{kC_0\} \underset{t}{\ast} \left\{ \sum_{\mathbf{K},\omega_{\mathbf{K}}} f_1(\mathbf{K},\omega_{\mathbf{K}}) e^{-j\omega_{\mathbf{K}}t} \sqrt{K} \left(\frac{c}{2}\right) \frac{F^2(ct/2,\omega_0)}{(ct/2)^{3/2}} \right.\right.$$
$$\left.\left. \cdot \left\{ g(\theta_{\mathbf{K}}) e^{-j\pi/4} e^{jKct/2} - g(\theta_{\mathbf{K}}+\pi) e^{j\pi/4} e^{-jKct/2} \right\} \right\} \right\}. \quad (3.82)$$

Now, using the definition of C_0 given in (3.37), kC_0 can be written as [3]

$$kC_0 = \frac{I(\omega)\Delta\ell k^2}{j\omega\epsilon_0} = -j\frac{\eta_0\Delta\ell}{c^2}\omega^2 I(\omega),$$

where η_0 is the intrinsic impedance of the vacuum. Therefore,

$$\mathcal{F}_t^{-1}\{kC_0\} = j\frac{\eta_0\Delta\ell}{c^2}\frac{\partial^2 i(t)}{\partial t^2}$$

To obtain the formulation for the electric field in (3.81), the current distribution at the transmitter, $I(\omega)$, needs to be determined. For a pulsed radar source, $i(t)$ can be defined in a distributional sense as

$$i(t) \triangleq I_0 e^{-j\omega_0 t}[\Theta(t) - \Theta(t-\tau_0)], \tag{3.83}$$

where τ_0 is the pulse width of the radar. Therefore,

$$\frac{\partial^2 i(t)}{\partial t^2} = -I_0\,{\omega_0}^2 e^{-j\omega_0\,t}\left[\Theta\left(t\right) - \Theta\left(t-\tau_0\right)\right] - 2jI_0\,\omega_0\,e^{-j\omega_0\,t}\left[\delta\left(t\right) - \delta\left(t-\tau_0\right)\right] + I_0\,e^{-j\omega_0\,t}\left[\delta'\left(t\right) - \delta'\left(t-\tau_0\right)\right] \tag{3.84}$$

Now, ignoring the edge terms in (3.84), the first term in the convolution in (3.82) can be written as [3],

$$\mathcal{F}_t^{-1}\{kC_0\} = -j\eta_0\Delta\ell I_0 k_0^2 e^{-j\omega_0\,t}\left[\Theta\left(t\right) - \Theta\left(t-\tau_0\right)\right]. \tag{3.85}$$

Substituting (3.85) back into (3.82), the expression for the first-order electric field in the time domain can be obtained as

$$(E_{0\mathbf{n}}^{+})_1(t) \approx -j\frac{\eta_0\Delta\ell I_0 k_0^2}{(2\pi)^{3/2}}\sum_{\mathbf{K},\omega_{\mathbf{K}}} f(\mathbf{K},\omega_{\mathbf{K}})\sqrt{K}\left(\frac{c}{2}\right)\Bigg\{\{e^{-j\omega_0\,t}\left[\Theta\left(t\right) - \Theta\left(t-\tau_0\right)\right]\} \underset{t}{*}\left\{e^{-j\omega_{\mathbf{K}}t}\frac{F^2(ct/2,\omega_0)}{(ct/2)^{3/2}}\Big\{g(\theta_{\mathbf{K}})e^{-j\pi/4}e^{jKct/2} - g(\theta_{\mathbf{K}}+\pi)e^{j\pi/4}e^{-jKct/2}\Big\}\right\}\Bigg\}. \tag{3.86}$$

In integral form, the convolution in (3.86) can be written as

$$I_t(t) = \int_{t'} e^{-j\omega_0\,(t-t')}\left[\Theta\left(t-t'\right) - \Theta\left(t-t'-\tau_0\right)\right]\frac{F^2(\frac{ct'}{2},\omega_0)}{(\frac{ct'}{2})^{3/2}}e^{-j\omega_{\mathbf{K}}t'}\Big\{g(\theta_{\mathbf{K}})e^{-j\frac{\pi}{4}}e^{jK\frac{ct'}{2}} - g(\theta_{\mathbf{K}}+\pi)e^{j\frac{\pi}{4}}e^{-jK\frac{ct'}{2}}\Big\}\,\mathrm{d}t'. \tag{3.87}$$

Using the integration property of the Heaviside function, (3.88) can be rewritten as

$$I_t(t) = e^{-j\omega_0 t} \int_{t-\tau_0}^{t} \frac{F^2(\frac{ct'}{2}, \omega_0)}{(\frac{ct'}{2})^{3/2}} \Big\{ g(\theta_{\mathbf{K}}) e^{(j\frac{c}{2}(K-2k_0)-\omega_{\mathbf{K}})t'} e^{-j\frac{\pi}{4}} - g(\theta_{\mathbf{K}}+\pi) e^{-(j\frac{c}{2}(K+2k_0)+\omega_{\mathbf{K}})t'} \cdot e^{j\frac{\pi}{4}} \Big\} \, \mathrm{d}t'. \quad (3.88)$$

As explained in [3], it can be assumed that $ct/2 \gg 1$ and $c\tau/2 \ll ct/2$ for pulse radar operation. Therefore, for $t' \in [t-\tau_0, t]$, $ct'/2 \gg 0$.

Now, defining the distance ρ_0 to the centre of the scattering patch as

$$\rho_0 \triangleq \frac{ct/2 + c(t-\tau_0)/2}{2} = \frac{c(t-\tau_0/2)}{2},$$

and knowing that the Sommerfeld attenuation function will slowly vary within a range bin examined by a single pulse [3], (3.88) can be further simplified as

$$I_t(t) = e^{-j\omega_0 t} \frac{F^2(\rho_0, \omega_0)}{(\rho_0)^{3/2}} \Bigg\{ g(\theta_{\mathbf{K}}) e^{-j\frac{\pi}{4}} \int_{t-\tau_0}^{t} e^{(j\frac{c}{2}(K-2k_0)-\omega_{\mathbf{K}})t'} \, \mathrm{d}t' - g(\theta_{\mathbf{K}}+\pi) e^{j\frac{\pi}{4}} \cdot \int_{t-\tau_0}^{t} e^{-(j\frac{c}{2}(K+2k_0)+\omega_{\mathbf{K}})t'} \, \mathrm{d}t' \Bigg\}$$

$$\therefore \; I_t(t) = \frac{2}{c} \Delta\rho e^{-jk_0\Delta\rho} \frac{F^2(\rho_0, \omega_0)}{(\rho_0)^{3/2}} e^{-j\omega_{\mathbf{K}}\left(t-\frac{\Delta\rho}{c}\right)} \Bigg\{ g(\theta_{\mathbf{K}}) e^{-j\frac{\pi}{4}} e^{j\rho_0 K} \cdot \mathrm{Sa}\left[\frac{\Delta\rho}{2} \left(\left(1 - 2\frac{c_p(K)}{c} \right) K - 2k_0 \right) \right] - g(\theta_{\mathbf{K}}+\pi) e^{j\frac{\pi}{4}} e^{-j\rho_0 K} \cdot \mathrm{Sa}\left\{ \frac{\Delta\rho}{2} \left[\left(1 + 2\frac{c_p(K)}{c} \right) K + 2k_0 \right] \right\} \Bigg\} \quad (3.89)$$

where $c_p(K)$ is the phase velocity of the ocean wave of wavenumber K, defined as [126]

$$c_p(K) \triangleq \frac{\omega_{\mathbf{K}}}{K},$$

$\Delta\rho$ is the range resolution (or patch width) of the radar, defined as [127]

$$\Delta\rho \triangleq \frac{c\tau_0}{2},$$

and Sa is the sampling function, defined as [128]

$$\mathrm{Sa}(x) = \frac{\sin(x)}{x},\ \forall x \neq 0.$$

Here it is important to point out that, for ocean waves, $c_p(K) \ll c,\ \forall K$, and for a pulse radar operation, $\tau_0/2 \ll t$, which allows us to further simplify the convolution expression in (3.88) to

$$I_t(t) = \frac{2}{c}\Delta\rho e^{-jk_0\Delta\rho}\frac{F^2(\rho_0,\omega_0)}{(\rho_0)^{3/2}}e^{-j\omega_{\mathbf{K}}t}\Bigg\{g(\theta_{\mathbf{K}})e^{-j\frac{\pi}{4}}e^{j\rho_0 K}\,\mathrm{Sa}\left[\frac{\Delta\rho}{2}\left(K-2k_0\right)\right] - g(\theta_{\mathbf{K}}+\pi)e^{j\frac{\pi}{4}}e^{-j\rho_0 K}\,\mathrm{Sa}\left[\frac{\Delta\rho}{2}\left(K+2k_0\right)\right]\Bigg\} \quad (3.90)$$

Inspecting the argument of both sampling functions in (3.90), it is evident that the maximum value of $\mathrm{Sa}\left[\frac{\Delta\rho}{2}\left(K-2k_0\right)\right]$ occurs at $2k_0$, while the maximum for $\mathrm{Sa}\left[\frac{\Delta\rho}{2}\left(K+2k_0\right)\right]$ occurs at $-2k_0$. Knowing that negative values of the wavenumber K are not defined, and considering the typical values of $\Delta\rho$ and k_0 for HF radar operations, it is clear that

$$\mathrm{Sa}\left[\frac{\Delta\rho}{2}\left(K-2k_0\right)\right] \gg \mathrm{Sa}\left[\frac{\Delta\rho}{2}\left(K+2k_0\right)\right],\ \forall K > 0.$$

Therefore,

$$I_t(t) \approx \frac{2}{c}\Delta\rho e^{-jk_0\Delta\rho}\frac{F^2(\rho_0,\omega_0)}{(\rho_0)^{3/2}}e^{-j\omega_{\mathbf{K}}t}g(\theta_{\mathbf{K}})e^{-j\frac{\pi}{4}}e^{j\rho_0 K}\,\mathrm{Sa}\left[\frac{\Delta\rho}{2}\left(K-2k_0\right)\right] \quad (3.91)$$

Now, substituting (3.91) into (3.86), the expression for the first-order electric field scattered by a height-restricted ocean surface can be approximated as

$$(E^{+}_{0\mathbf{n}})(t,t_0) \approx -2\pi j\eta_0\Delta\ell\Delta\rho I_0 k_0^2\Bigg\{\frac{F^2(\rho_0,\omega_0)}{(2\pi\rho_0)^{3/2}}e^{jk_0\Delta\rho}\sum_{\mathbf{K},\omega_{\mathbf{K}}} f(\mathbf{K},\omega_{\mathbf{K}})e^{-j\omega_{\mathbf{K}}t}\sqrt{K}g(\theta_{\mathbf{K}}) \cdot e^{-j\pi/4}e^{j\rho_0 K}\,\mathrm{Sa}\left[\frac{\Delta\rho}{2}(K-2k_0)\right]\Bigg\}. \quad (3.92)$$

Here, an important distinction must be made between the time events related to the ocean surface and the time events related to the radar. It is evident from the application of the time-inverse Fourier transform that there are two different time scales in this phenomenon, and that these events are not necessarily related. Logically, ocean surface events do not interfere in the time-related radar settings, such as pulse width and range resolution. Similar to the separation established in [3] between what they considered "observation time" and "experiment time", the two timescales are going to be defined in this work as the *radar time* t_0, which relates to radar parameters such as ρ_0, and *ocean time* t, which relates to ocean surface phenomena that are independent of the radar observation. This choice is reinforced by the mismatch between phase velocity and the speed of light that ultimately resulted in the simplification between (3.89) and (3.90); if the two velocities were not so disparate, there would be no justification for the two timescales, and both would be reduced to a single variable.

Comparing the expression shown in (3.92) and the one proposed in [3], it is clear that both equations are identical, but this is only due to the physical fact that the phase velocity of an ocean wave is much smaller than the speed of light. Such consideration is neither present in [3], nor in its corresponding report [17], as the time-dependence of the ocean surface is only included at the end of the electric field derivation, excluding it from the time convolution present in (3.86). The simplification due to the ratio between phase velocity and the speed of light is an important argument in this derivation, since it supports the decision of considering two different timescales for the radar and ocean times; in [3] and [17] the authors appeal to the common sense of the reader without showing the mathematical reasoning behind the use of two different timescales. However, the resulting expression is still mathematically correct,

and can be used in derivations for the scattering electric field over a height-restricted ocean surface.

Having defined the height-restricted first-order electric field, and knowing that the same reasoning can be applied to higher-order electric fields, the corrections to the electric field for ocean surfaces with arbitrary heights can be derived.

3.6 Corrections to the Electric Field for an Ocean Surface With Electromagnetically-Large Waves

Following the same procedure presented in Section 3.5 and in [3], the inverse temporal Fourier transform with respect to the radar frequency of the electric field must be taken to include the current formulations for the radar source. Taking, for example, the first-order electric field, applying the inverse temporal Fourier transform to (3.67), the first-order electric field over the ocean surface can be written as

$$\left(E_{\mathbf{n}}^{+}\right)_1(t) = \left(E_{0\mathbf{n}}^{+}\right)_1(t) + \mathcal{F}_t^{-1}\left\{\zeta(boldsymbol\rho; t)\right\} \underset{t}{*} \left(E_{0\mathbf{n}}^{+}\right)_1(t) + \frac{1}{2}\mathcal{F}_t^{-1}\left\{\zeta^2(\boldsymbol{\rho}; t)\right\} \underset{t}{*} \left(E_{0\mathbf{n}}^{+}\right)_1 + \cdots . \tag{3.93}$$

Using the definition of $\zeta(\boldsymbol{\rho}, t)$ in (3.58),

$$\mathcal{F}_t^{-1}\left\{\zeta(\boldsymbol{\rho}; t)\right\} = \mathcal{F}_t^{-1}\left\{\iint\limits_{\boldsymbol{\rho}_1} f(\boldsymbol{\rho}_1; t) h(\boldsymbol{\rho} - \boldsymbol{\rho}_1)\, \mathrm{d}\boldsymbol{\rho}_1\right\}.$$

Since the only term dependent on the frequency of the transmitter is $h(\boldsymbol{\rho} - \boldsymbol{\rho}_1)$, Fubini's theorem can be used to get

$$\mathcal{F}_t^{-1}\left\{\zeta(\boldsymbol{\rho}_1; t)\right\} = \iint\limits_{\boldsymbol{\rho}_1} f(\boldsymbol{\rho}_1; t) \mathcal{F}_t^{-1}\left\{h(\boldsymbol{\rho} - \boldsymbol{\rho}_1)\right\} \mathrm{d}\boldsymbol{\rho}_1.$$

Knowing that $h(\boldsymbol{\rho}-\boldsymbol{\rho}_1)=\mathcal{F}_{xy}^{-1}\left\{u\right\}(\boldsymbol{\rho}-\boldsymbol{\rho}_1)$, with u given by (3.10), and $k={}^{\omega}\!/_{c}$, the variation of u with respect to ω can be obtained:

$$\frac{du}{d\omega}=-\frac{\omega}{c^2\sqrt{K^2-\frac{\omega^2}{c^2}}}. \tag{3.94}$$

Using the typical orders of magnitude of the terms in (3.94) for the high-frequency remote sensing of the ocean surface, it can be observed that the variation of u with respect to ω is on the order of 10^{-10}. Therefore, in the HF-band, the radar frequency in u can be considered constant and equal to the transmitting frequency ω_0, resulting in a constant radar wavenumber k_0. Therefore, the time-domain inverse Fourier transform in the radar timescale of the arbitrary heights factor can be approximated as $\zeta_0(\boldsymbol{\rho};t)$, written as

$$\zeta_0(\boldsymbol{\rho};t)=\int_{x_1}\int_{y_1} f(\boldsymbol{\rho}_1;t)h_0(\boldsymbol{\rho}-\boldsymbol{\rho}_1)\,\mathrm{d}\boldsymbol{\rho}_1, \tag{3.95}$$

where

$$h_0(\boldsymbol{\rho}-\boldsymbol{\rho}_1)=\mathcal{F}_{xy}^{-1}\left\{\sqrt{K^2-k_0^2}\right\}(\boldsymbol{\rho}-\boldsymbol{\rho}_1)\triangleq\mathcal{F}_{xy}^{-1}\left\{u_0\right\}(\boldsymbol{\rho}-\boldsymbol{\rho}_1), \tag{3.96}$$

with $k_0=\omega_0/c$. Therefore, (3.93) can be written as

$$\left(E_{\mathbf{n}}^{+}\right)_1(t)=\left(E_{0\mathbf{n}}^{+}\right)_1(t)+\zeta_0(\boldsymbol{\rho};t)\underset{t}{*}\left(E_{0\mathbf{n}}^{+}\right)_1(t)+\frac{\zeta_0^2(\boldsymbol{\rho};t)}{2}\underset{t}{*}\left(E_{0\mathbf{n}}^{+}\right)_1+\cdots, \tag{3.97}$$

or, using the square bracket notation introduced in (3.68),

$$\left(E_{\mathbf{n}}^{+}\right)_1(t)=\left(E_{0\mathbf{n}}^{+}\right)_1(t)+\left[\left(E_{0\mathbf{n}}^{+}\right)_1\right]_1(t)+\left[\left(E_{0\mathbf{n}}^{+}\right)_1\right]_2(t)+\cdots, \tag{3.98}$$

where

$$\left[\left(E_{0\mathbf{n}}^{+}\right)_1\right]_n(t)=\frac{\zeta_0^n(\boldsymbol{\rho};t)}{n!}\underset{t}{*}\left(E_{0\mathbf{n}}^{+}\right)_1(t),\ n=1,2,\cdots. \tag{3.99}$$

Analogously, the second-order electric field in the time domain can be defined as

$$\left(E_{\mathbf{n}}^{+}\right)_2(t) = \left(E_{0\mathbf{n}}^{+}\right)_2(t) + \left[\left(E_{0\mathbf{n}}^{+}\right)_2\right]_1(t) + \left[\left(E_{0\mathbf{n}}^{+}\right)_2\right]_2(t) + \cdots, \tag{3.100}$$

where

$$\left[\left(E_{0\mathbf{n}}^{+}\right)_2\right]_n(t) = \frac{\zeta_0^n(\boldsymbol{\rho};t)}{n!} \underset{t}{*} \left(E_{0\mathbf{n}}^{+}\right)_2(t),\ n = 1, 2, \cdots. \tag{3.101}$$

Now, considering the Fourier-Stieltjes representation of the ocean surface presented in (3.75), the Fourier-Sieltjes coefficients of the series can be represented by an generalized asymptotic expansion introduced in Section 1.2.1:

$$f(\mathbf{K}, \omega_{\mathbf{K}}; \varepsilon) \approx f_1(\mathbf{K}, \omega_{\mathbf{K}}) + f_2(\mathbf{K}, \omega_{\mathbf{K}}) + \cdots \tag{3.102}$$

where the subscripts indicate the order of the perturbation expansion parameter and are implicitly included in the respective expansion terms [29], [75]. Here, the perturbation expansion parameter is taken to be the surface slope, as proposed in [75]. As discussed in Section 1.2.1, for the asymptotic expansion to be uniformly valid, the sequence of the asymptotic parameter must follow the definition shown in (1.1), and the higher orders terms of the asymptotic expansion of the Fourier coefficients should not be more singular than their lower-order counterparts, as defined in (1.4) [24]. Therefore, the expression for the m-th order electric field for arbitrary heights can be written as

$$(E_{0\mathbf{n}}^{+})_m = \sum_n (E_{0\mathbf{n}}^{+})_{mn} + \sum_n \sum_p \sum_q \left[(E_{0\mathbf{n}}^{+})_{mn}\right]_{pq} \tag{3.103}$$

where m indicates the order of the *electromagnetic* coupling, that is, the number of scatters that happen over the ocean surface before the field reaches the receiver, while n indicates the order of *hydrodynamic* coupling, that is, the number of monochromatic

ocean waves involved in each scatter [3], [17], [18]. The correction terms can be written as

$$\left[\left(E_{0\mathbf{n}}^{+}\right)_{mn}\right]_{pq}(t) = \frac{\zeta_{0q}^{p}(\boldsymbol{\rho};t)}{p!} \underset{t}{*} \left(E_{0\mathbf{n}}^{+}\right)_{mn}(t), \tag{3.104}$$

where p indicates the order of the power series expansion, and q indicates the order of the asymptotic expansion of the ocean surface within the arbitrary heights function. Therefore, the correction term in (3.104) is said to be the qth-order hydrodynamic, pth-order correction of $\left(E_{0\mathbf{n}}^{+}\right)_{mn}(t)$.

Observing the condition for uniformly validity of the perturbation expansion, higher-order perturbation terms cannot be greater (or more singular) than lower-order perturbation terms [24]. This fact has been noted from the resulting expressions in previous research when investigating the height-restricted radar cross-sections for each term of the electric field [17]. By examining (3.104), it is easy to show that the order of the correction term of the electric field is $p \times q + m \times n$. Therefore, when considering the order of the asymptotically-expanded terms in the corrected electric field, the order of the asymptotic expansion for the correction terms should be observed, e.g., the first-order hydrodynamic, first-order correction to the first-order electric field must be smaller than the height-restricted first-order electric field and at about the same order of magnitude of the second-order hydrodynamic electric field.

Also, as shown in [18], it is possible to combine the second-order hydrodynamic and second-order electromagnetic terms of the electric field occurring on the same patch of the ocean surface, resulting in

$$(E_{0\mathbf{n}}^{+})_{2P} = (E_{0\mathbf{n}}^{+})_{12} + (E_{0\mathbf{n}}^{+})_{21},$$

where $(E_{0\mathbf{n}}^{+})_{2P}$ is known as the second-order patch-scatter electric field. Therefore, by

using the asymptotic perturbation expansion on the first- and second-order electric fields, and considering correction terms up to the third-order, the corrections to the first- and second-order electric fields can be written as

$$\left[\left(E^{+}_{0\mathbf{n}}\right)_{11}\right]_{11}(t) = \zeta_{01}(\boldsymbol{\rho};t) \underset{t}{*} \left(E^{+}_{0\mathbf{n}}\right)_{11}(t), \tag{3.105}$$

$$\left[\left(E^{+}_{0\mathbf{n}}\right)_{11}\right]_{12}(t) = \zeta_{02}(\boldsymbol{\rho};t) \underset{t}{*} \left(E^{+}_{0\mathbf{n}}\right)_{11}(t), \tag{3.106}$$

$$\left[\left(E^{+}_{0\mathbf{n}}\right)_{11}\right]_{21}(t) = \frac{\zeta^{2}_{01}(\boldsymbol{\rho};t)}{2} \underset{t}{*} \left(E^{+}_{0\mathbf{n}}\right)_{11}(t), \tag{3.107}$$

$$\left[(E^{+}_{0\mathbf{n}})_{2P}\right]_{11}(t) = \zeta_{01}(\boldsymbol{\rho};t) \underset{t}{*} (E^{+}_{0\mathbf{n}})_{2P}(t), \tag{3.108}$$

$$\left[(E^{+}_{0\mathbf{n}})_{2P}\right]_{12}(t) = \zeta_{02}(\boldsymbol{\rho};t) \underset{t}{*} (E^{+}_{0\mathbf{n}})_{2P}(t), \tag{3.109}$$

$$\left[(E^{+}_{0\mathbf{n}})_{2P}\right]_{21}(t) = \frac{\zeta^{2}_{01}(\boldsymbol{\rho};t)}{2} \underset{t}{*} (E^{+}_{0\mathbf{n}})_{2P}(t), \tag{3.110}$$

Here, the correction terms derived from the first order of the power series expansion of the exponential of the arbitrary heights function, i.e. (3.105), (3.106), (3.108), and (3.109), will be referred as *first-order corrections* to the electric field, while the terms derived from the second-order term of the power series, i.e. (3.107) and (3.110), will be referred as *second-order corrections* to the electric field. In this section, the expressions for the correction terms for the electric field scattered by an ocean surface with arbitrary heights will be examined in more detail.

3.6.1 First-Order Corrections to the Electric Field

Observing the first-order correction terms in (3.105), (3.106), (3.108), and (3.109), it is clear that expressions for the first- and second-order hydrodynamic, first-order arbitrary heights functions, i.e. $\zeta_{01}(\boldsymbol{\rho};t)$ and $\zeta_{02}(\boldsymbol{\rho};t)$, must be derived. To differentiate between the terms coming from the arbitrary heights function and the ones

originally in the height-restricted expressions for the electric field, primes will be used in all variables related to the correction terms. Applying the asymptotic expansion of the ocean surface shown in (3.102) to (3.95), the first- and second-order terms of the generalized functions expansion of the arbitrary heights function can be respectively written as

$$\zeta_{01}(\boldsymbol{\rho};t) = \sum_{\mathbf{K}',\omega_{\mathbf{K}'}} f_1(\mathbf{K}',\omega_{\mathbf{K}'}) e^{-j\omega_{\mathbf{K}'}t} \iint\limits_{\boldsymbol{\rho}_1} e^{j\mathbf{K}'\cdot\boldsymbol{\rho}_1} h_0'(\boldsymbol{\rho}-\boldsymbol{\rho}_1)\,\mathrm{d}\boldsymbol{\rho}_1 \tag{3.111}$$

and

$$\zeta_{02}(\boldsymbol{\rho};t) = \sum_{\substack{\mathbf{K}_1',\omega_{\mathbf{K}_1'} \\ \mathbf{K}_1'+\mathbf{K}_2'=\mathbf{K}'}} \sum_{\mathbf{K}'_2,\omega_{\mathbf{K}_2'}} \Gamma'_H f_1(\mathbf{K}_1',\omega_{\mathbf{K}_1'}) f_1(\mathbf{K}_2',\omega_{\mathbf{K}_2'}) e^{-j(\omega_{\mathbf{K}_1'}+\omega_{\mathbf{K}_2'})t} \cdot \iint\limits_{\boldsymbol{\rho}_1} e^{j\mathbf{K}'\cdot\boldsymbol{\rho}_1} h_0'(\boldsymbol{\rho}-\boldsymbol{\rho}_1)\,\mathrm{d}\boldsymbol{\rho}_1, \tag{3.112}$$

where $f_1(\cdot)$ is the first-order term in the asymptotic expansion of the ocean surface as defined in (3.102), $\Gamma'_H = \Gamma_H(\mathbf{K}_1',\omega_{\mathbf{K}_1'},\mathbf{K}_2',\omega_{\mathbf{K}_2'})$, where Γ_H is the hydrodynamic coupling coefficient between two monochromatic waves, defined for $\mathbf{K}_m$ and $\mathbf{K}_n$ in deep-water as [74], [75]

$$\Gamma_H(\mathbf{K}_m,\omega_{\mathbf{K}_m},\mathbf{K}_n,\omega_{\mathbf{K}_n}) = \frac{1}{2}\Bigg[K_m + K_n + \frac{g}{\omega_{\mathbf{K}_m}\omega_{\mathbf{K}_n}}\left(K_mK_n - \mathbf{K}_m\cdot\mathbf{K}_n\right) \cdot \left(\frac{gK + (\omega_{\mathbf{K}_m}+\omega_{\mathbf{K}_n})^2}{gK - (\omega_{\mathbf{K}_m}+\omega_{\mathbf{K}_n})^2}\right)\Bigg], \tag{3.113}$$

with $\mathbf{K} = \mathbf{K}_m + \mathbf{K}_n$and $h_0'(x,y) = \mathcal{F}_{xy}^{-1}\{u_0'\}$, with u_0' defined as

$$u_0' = \sqrt{K'^2 - k_0^2}. \tag{3.114}$$

The integrals in (3.111) and (3.112) can be interpreted as the spatial Fourier transforms over $-\boldsymbol{\rho}_1$, with a $-\boldsymbol{\rho}$ shift [129]. Therefore, $\zeta_{01}(\boldsymbol{\rho};t)$ and $\zeta_{02}(\boldsymbol{\rho};t)$ can be

rewritten as

$$\zeta_{01}(\boldsymbol{\rho};t) = \sum_{\mathbf{K}',\omega_{\mathbf{K}'}} f_1(\mathbf{K}',\omega_{\mathbf{K}'})e^{-j\omega_{\mathbf{K}'}t}e^{j\mathbf{K}\cdot\boldsymbol{\rho}}\mathcal{F}_{x_1y_1}\left\{\mathcal{F}^{-1}_{x_1,y_1}\left\{u_0'\right\}\right\}$$

$$\Rightarrow\ \zeta_{01}(\boldsymbol{\rho};t) = \sum_{\mathbf{K}',\omega_{\mathbf{K}'}} f_1(\mathbf{K}',\omega_{\mathbf{K}'})u_0'e^{j\mathbf{K}'\cdot\rho}e^{-j\omega_{\mathbf{K}'}t} \tag{3.115}$$

and

$$\zeta_{02}(\boldsymbol{\rho};t) = \sum_{\substack{\mathbf{K}_1',\omega_{\mathbf{K}_1'}\\ \mathbf{K}_1'+\mathbf{K}_2'=\mathbf{K}'}} \sum_{\mathbf{K}'_2,\omega_{\mathbf{K}_2'}} \Gamma'_H f_1(\mathbf{K}_1',\omega_{\mathbf{K}_1'})f_1(\mathbf{K}_2',\omega_{\mathbf{K}_2'})u_0'e^{-j(\omega_{\mathbf{K}_1'}+\omega_{\mathbf{K}_2'})t}e^{j\mathbf{K}'\cdot\boldsymbol{\rho}}. \tag{3.116}$$

After applying the generalized asymptotic expansion over the first-order height-restricted electric field up to the second-order as presented in [3], [17], and combining the resulting second-order electric field with the first-order asymptotic expansion of the second-order electromagnetic electric field as done, for example, in [18], the first- and second-order patch scatter electric fields can be defined for a monostatic configuration as

$$(E^+_{0\mathbf{n}})_{11}(t,t_0) \approx -j\eta_0\Delta\ell\Delta\rho I_0k_0^2\frac{F^2(\rho_0,\omega_0)}{(2\pi\rho_0)^{3/2}}e^{jk_0\Delta\rho}\sum_{\mathbf{K},\omega_{\mathbf{K}}} f_1(\mathbf{K},\omega_{\mathbf{K}})e^{-j\omega_{\mathbf{K}}t}\sqrt{K}g(\theta_{\mathbf{K}})$$
$$\cdot\, e^{-j(\pi/4)}e^{j\rho_0K}\,\mathrm{Sa}\left[\frac{\Delta\rho}{2}(K-2k_0)\right] \tag{3.117}$$

and

$$(E^+_{0\mathbf{n}})_{2P}(t,t_0) \approx -j\eta_0\Delta\ell\Delta\rho I_0k_0^2\frac{F^2(\rho_0,\omega_0)}{(2\pi\rho_0)^{3/2}}e^{jk_0\Delta\rho}\sum_{\substack{\mathbf{K}_1,\omega_{\mathbf{K}_1}\\ \mathbf{K}_1+\mathbf{K}_2=\mathbf{K}}}\sum_{\mathbf{K}_2,\omega_{\mathbf{K}_2}} \Gamma_P f_1(\mathbf{K}_1,\omega_{\mathbf{K}_1})$$
$$\cdot\, f_1(\mathbf{K}_2,\omega_{\mathbf{K}_2})e^{-j(\omega_{\mathbf{K}_1}+\omega_{\mathbf{K}_2})t}\sqrt{K}g(\theta_{\mathbf{K}})e^{-j(\pi/4)}e^{j\rho_0K}\,\mathrm{Sa}\left[\frac{\Delta\rho}{2}(K-2k_0)\right], \tag{3.118}$$

where Γ_P is the patch scatter coupling coefficient, defined for $\mathbf{K}_m$ and $\mathbf{K}_n$ as [89],

$$\Gamma_P(\mathbf{K}_m,\omega_{\mathbf{K}_m},\mathbf{K}_n,\omega_{\mathbf{K}_n}) = \Gamma_H(\mathbf{K}_m,\omega_{\mathbf{K}_m},\mathbf{K}_n,\omega_{\mathbf{K}_n}) + {}_E\Gamma_P(\mathbf{K}_m,\mathbf{K}_n), \tag{3.119}$$

with ${}_E\Gamma_P(\mathbf{K}_m, \mathbf{K}_n)$ being the electromagnetic coupling coefficient between two monochromatic waves within the same scattering patch, defined as [89]

$$ {}_E\Gamma_P(\mathbf{K}_m, \mathbf{K}_n) = \left(\frac{j\sqrt{\mathbf{K}_m \cdot (\mathbf{K}_m - 2k_0\hat{\boldsymbol{\rho}}_1)} + k_0}{k_0^2 + \mathbf{K}_m \cdot (\mathbf{K}_m - 2k_0\hat{\boldsymbol{\rho}}_1)} \right) \left(\frac{(\mathbf{K}_n \cdot \hat{\boldsymbol{\rho}}_1)[\mathbf{K}_n \cdot (\mathbf{K}_m - 2k_0\hat{\boldsymbol{\rho}}_1)]}{\sqrt{\mathbf{K}_m \cdot (\mathbf{K}_m - 2k_0\hat{\boldsymbol{\rho}}_1)}} \right). \tag{3.120} $$

Observing expressions for the first-order corrections to the electric field in (3.105), (3.106), (3.108), and (3.109), the expressions for the arbitrary height functions in (3.115) and (3.116), and the height-restricted electric fields in (3.117) and (3.118), it is clear that the convolutions over the "ocean time" t shown in the correction terms have the form, for $\omega_a, \omega_b \in \mathbb{R}$ [113],

$$ e^{-j\omega_a t} \underset{t}{*} e^{-j\omega_b t} = \int_{-\infty}^{\infty} e^{-j\omega_b \tau} e^{-j\omega_a (t-\tau)} \, \mathrm{d}\tau \triangleq 2\pi e^{-j\omega_a t} \delta(\omega_a - \omega_b). $$

Substituting (3.115), (3.116), and the expressions for the height-restricted first- and second-order electric fields shown in [17] into (3.105), (3.106), (3.108), (3.109) and performing the convolutions over t, the first- and second-order hydrodynamic, first-order corrections to the first- and second-order electric fields can be obtained as

$$ \left[\left(E_{0\mathbf{n}}^{+} \right)_{11} \right]_{11} (t, t_0) = -2\pi j \eta_0 \Delta\ell \Delta\rho I_0 k_0^2 \frac{F^2(\rho_0, \omega_0)}{(2\pi\rho_0)^{3/2}} e^{jk_0\Delta\rho} \sum_{\mathbf{K}', \omega_{\mathbf{K}'}} \sum_{\mathbf{K}, \omega_{\mathbf{K}}} f_1(\mathbf{K}, \omega_{\mathbf{K}}) $$
$$ \cdot f_1(\mathbf{K}', \omega_{\mathbf{K}'}) u_0' \delta(\omega_{\mathbf{K}} - \omega_{\mathbf{K}'}) e^{-j\omega_{\mathbf{K}} t} \sqrt{K} g(\theta_{\mathbf{K}}) e^{-j(\pi/4)} e^{j\rho_0 K} e^{j\mathbf{K}' \cdot \boldsymbol{\rho}} \operatorname{Sa}\left[\frac{\Delta\rho}{2} (K - 2k_0) \right] \tag{3.121} $$

$$ \left[\left(E_{0\mathbf{n}}^{+} \right)_{2P} \right]_{11} (t, t_0) = -2\pi j \eta_0 \Delta\ell \Delta\rho I_0 k_0^2 \frac{F^2(\rho_0, \omega_0)}{(2\pi\rho_0)^{3/2}} e^{jk_0\Delta\rho} \sum_{\mathbf{K}', \omega_{\mathbf{K}'}} \sum_{\substack{\mathbf{K}_1, \omega_{\mathbf{K}_1} \\ \mathbf{K}_1 + \mathbf{K}_2 = \mathbf{K}}} \sum_{\mathbf{K}_2, \omega_{\mathbf{K}_2}} \Gamma_P $$
$$ \cdot f_1(\mathbf{K}_1, \omega_{\mathbf{K}_1}) f_1(\mathbf{K}_2, \omega_{\mathbf{K}_2}) f_1(\mathbf{K}', \omega_{\mathbf{K}'}) u_0' \delta((\omega_{\mathbf{K}_1} + \omega_{\mathbf{K}_2}) - \omega_{\mathbf{K}'}) e^{-j(\omega_{\mathbf{K}_1} + \omega_{\mathbf{K}_2})t} \sqrt{K} g(\theta_{\mathbf{K}}) $$
$$ \cdot e^{-j(\pi/4)} e^{j\rho_0 K} e^{j\mathbf{K}' \cdot \boldsymbol{\rho}} \operatorname{Sa}\left[\frac{\Delta\rho}{2} (K - 2k_0) \right], \tag{3.122} $$

$$\left[\left(E_{0\mathbf{n}}^{+}\right)_{11}\right]_{12}(t,t_0) = -2\pi j\eta_0\Delta\ell\Delta\rho I_0 k_0^2 \frac{F^2(\rho_0,\omega_0)}{(2\pi\rho_0)^{3/2}} e^{jk_0\Delta\rho} \sum_{\substack{\mathbf{K}_1',\omega_{\mathbf{K}_1'} \\ \mathbf{K}_1'+\mathbf{K}_2'=\mathbf{K}'}} \sum_{\mathbf{K}'_2,\omega_{\mathbf{K}_2'}} \sum_{\mathbf{K},\omega_{\mathbf{K}}} \Gamma'_H$$

$$\cdot f_1(\mathbf{K}_1',\omega_{\mathbf{K}_1'}) f_1(\mathbf{K}_2',\omega_{\mathbf{K}_2'}) f_1(\mathbf{K},\omega_{\mathbf{K}}) u_0' \delta\left(\omega_{\mathbf{K}} - (\omega_{\mathbf{K}_1'} + \omega_{\mathbf{K}_2'})\right) e^{-j\omega_{\mathbf{K}}t}\sqrt{K} g(\theta_{\mathbf{K}}) e^{-j(\pi/4)}$$

$$\cdot e^{j\rho_0 K} e^{j\mathbf{K}'\cdot\boldsymbol{\rho}} \operatorname{Sa}\left[\frac{\Delta\rho}{2}(K-2k_0)\right] \quad (3.123)$$

$$\left[\left(E_{0\mathbf{n}}^{+}\right)_{2P}\right]_{12}(t,t_0) = -2\pi j\eta_0\Delta\ell\Delta\rho I_0 k_0^2 \frac{F^2(\rho_0,\omega_0)}{(2\pi\rho_0)^{3/2}} e^{jk_0\Delta\rho} \sum_{\substack{\mathbf{K}_1',\omega_{\mathbf{K}_1'} \\ \mathbf{K}_1'+\mathbf{K}_2'=\mathbf{K}'}} \sum_{\mathbf{K}'_2,\omega_{\mathbf{K}_2'}} \sum_{\substack{\mathbf{K}_1,\omega_{\mathbf{K}_1} \\ \mathbf{K}_1+\mathbf{K}_2=\mathbf{K}}} \sum_{\mathbf{K}_2,\omega_{\mathbf{K}_2}} \Gamma_P$$

$$\cdot \Gamma'_H f_1(\mathbf{K}_1',\omega_{\mathbf{K}_1'}) f_1(\mathbf{K}_2',\omega_{\mathbf{K}_2'}) f_1(\mathbf{K}_1,\omega_{\mathbf{K}_1}) f_1(\mathbf{K}_2,\omega_{\mathbf{K}_2}) u_0' e^{-j(\omega_{\mathbf{K}_1}+\omega_{\mathbf{K}_2})t}\sqrt{K} g(\theta_{\mathbf{K}}) e^{-j(\pi/4)}$$

$$\cdot \delta\left((\omega_{\mathbf{K}_1} + \omega_{\mathbf{K}_2}) - (\omega_{\mathbf{K}_1'} + \omega_{\mathbf{K}_2'})\right) e^{j\rho_0 K} e^{j\mathbf{K}'\cdot\boldsymbol{\rho}} \operatorname{Sa}\left[\frac{\Delta\rho}{2}(K-2k_0)\right], \quad (3.124)$$

Here, the Dirac deltas in the expressions for the correction terms should be addressed. Taking, for example, the expression within the summation in the first-order hydrodynamic, first-order correction to the first-order electric field presented in (3.121), the Fourier-Stieltjes series can be written as Fourier-Stieltjes integrals of the form presented in (3.73):

$$\left[(I_{11})\right]_{11}(\boldsymbol{\rho},t,t_0) = \int_{\mathbf{K}} \int_{\omega_{\mathbf{K}}} \int_{\mathbf{K}'} \int_{\omega_{\mathbf{K}'}} [P_{11}]_{11}(\boldsymbol{\rho},\mathbf{K},\mathbf{K}',\omega_{\mathbf{K}},t,t_0)\delta(\omega_K' - \omega_K)\,\mathrm{d}F_1(\mathbf{K}',\omega_{\mathbf{K}'})$$

$$\cdot \mathrm{d}F_1(\mathbf{K},\omega_{\mathbf{K}}), \quad (3.125)$$

where

$$[P_{11}]_{11} \triangleq u_0' e^{-j\omega_{\mathbf{K}}t}\sqrt{K} g(\theta_{\mathbf{K}}) e^{j\rho_0 K} e^{j\mathbf{K}'\cdot\boldsymbol{\rho}} \operatorname{Sa}\left[\frac{\Delta\rho}{2}(K-2k_0)\right].$$

From, (3.125), the integration over $\omega_{\mathbf{K}'}$ can be written as

$$I_{\omega'_{\mathbf{K}}} = \int\limits_{\omega_{\mathbf{K}'}} \delta(\omega_{\mathbf{K}'} - \omega_{\omega_K})\, \mathrm{d}F_1(\mathbf{K}', \omega_{\mathbf{K}'}).$$

In a distributional sense, $I_{\omega_{\mathbf{K}'}}$ can be rewritten as

$$I_{\omega'_{\mathbf{K}}} = -\int\limits_{\omega_{\mathbf{K}'}} \Theta(\omega_{\mathbf{K}'} - \omega_{\omega_K}) \frac{\mathrm{d}\{\mathrm{d}F_1(\mathbf{K}', \omega_{\mathbf{K}'})\}}{\mathrm{d}\omega_{\mathbf{K}'}} = -\int\limits_{\omega_{\mathbf{K}}}^{+\infty} \frac{\mathrm{d}\{\mathrm{d}F_1(\mathbf{K}', \omega_{\mathbf{K}'})\}}{\mathrm{d}\omega_{\mathbf{K}'}},$$

Employing the fundamental theorem of calculus for Lebesgue-Stieltjes integrals [130] knowing that $\mathrm{d}F_1(\mathbf{K}'), \omega_{\mathbf{K}'}$ is differentiable at every point over $\omega_{\mathbf{K}'} \in \mathbb{R}$, and that according to the Riemann-Lebesgue lemma $dF(\mathbf{K}', \omega_{\mathbf{K}'}) \to 0$ as $\omega_{\mathbf{K}'} \to \infty$ [131], $I_{\omega_{\mathbf{K}'}}$ can be written as

$$I_{\omega'_{\mathbf{K}}} = \mathrm{d}F_1(\mathbf{K}', \omega_{\mathbf{K}'})|_{\omega_{\mathbf{K}'} = \omega_{\mathbf{K}}},$$

resulting in

$$[(I_{11})]_{11}(\boldsymbol{\rho}, t, t_0) = \int\limits_{\mathbf{K}} \int\limits_{\omega_{\mathbf{K}}} \int\limits_{\mathbf{K}'} [P_{11}]_{11}(\boldsymbol{\rho}, \mathbf{K}, \mathbf{K}', \omega_{\mathbf{K}}, t, t_0)\, \mathrm{d}F_1(\mathbf{K}', \omega_{\mathbf{K}'})|_{\omega_{\mathbf{K}'} = \omega_{\mathbf{K}}} \cdot \mathrm{d}F_1(\mathbf{K}, \omega_{\mathbf{K}}). \quad (3.126)$$

For a more complicated Dirac delta argument, i.e. the one presented in the Fourier-Stieltjes integral that can be observed in (3.124),

$$[(I_{2P})]_{12}(\boldsymbol{\rho}, t, t_0) = \int \cdots \int [P_{2P}]_{12}(\boldsymbol{\rho}, \mathbf{K}_1, \mathbf{K}_2, \mathbf{K}'_1, \mathbf{K}'_2, \mathbf{K}', \omega_{\mathbf{K}_1}, \omega_{\mathbf{K}_2}, \omega_{\mathbf{K}'_1}, \omega_{\mathbf{K}'_2}, t, t_0) \cdot \delta\left((\omega_{\mathbf{K}'_1} + \omega_{\mathbf{K}'_2}) - (\omega_{\mathbf{K}_1} + \omega_{\mathbf{K}_2})\right) \mathrm{d}F_1(\mathbf{K}'_1, \omega_{\mathbf{K}'_1})\, \mathrm{d}F_1(\mathbf{K}'_2, \omega_{\mathbf{K}'_2})\, \mathrm{d}F_1(\mathbf{K}_1, \omega_{\mathbf{K}_1}) \cdot \mathrm{d}F_1(\mathbf{K}_2, \omega_{\mathbf{K}_2}), \quad (3.127)$$

where

$$[P_{2P}]_{12} \triangleq \Gamma_P \Gamma'_H u'_0 e^{-j(\omega_{\mathbf{K}_1} + \omega_{\mathbf{K}_2})t} \sqrt{K} g(\theta_{\mathbf{K}}) e^{-j(\pi/4)} e^{j\rho_0 K} e^{j\mathbf{K}'\cdot\boldsymbol{\rho}} \operatorname{Sa}\left[\frac{\Delta\rho}{2}(K - 2k_0)\right],$$

the integration can be performed over one of the angular frequencies originating from the arbitrary heights function. Taking the integral over $\omega_{\mathbf{K}'_2}$ and rearranging the argument in the Dirac delta results in

$$I_{\omega_{\mathbf{K}'_2}} = \int\limits_{\omega_{\mathbf{K}'_2}} [P_{2P}]_{12}(\omega_{\mathbf{K}'_2})\delta\left(\omega_{\mathbf{K}'_2} - \left[(\omega_{\mathbf{K}_1} + \omega_{\mathbf{K}_2}) - \omega_{\mathbf{K}'_1}\right]\right) \mathrm{d}F_1(\mathbf{K}'_2, \omega_{\mathbf{K}'_2}).$$

Here, the term $[P_{2P}]_{12}$ has been retained as part of the integration because the hydrodynamic coupling coefficient Γ'_H depends on $\omega_{\mathbf{K}_2}$. By the same process employed for $I_{\omega_{\mathbf{K}'}}$, $I_{\omega_{\mathbf{K}'_2}}$ can be rewritten in a distributional sense as

$$I_{\omega_{\mathbf{K}'_2}} = -\int\limits_{(\omega_{\mathbf{K}'_2})_0}^{+\infty} \frac{\mathrm{d}}{\mathrm{d}\omega_{\mathbf{K}'_2}} \left\{[P_{2P}]_{12}(\omega_{\mathbf{K}'_2})\, \mathrm{d}F_1(\mathbf{K}'_2, \omega_{\mathbf{K}'_2})\right\}$$

$$\Rightarrow\ I_{\omega_{\mathbf{K}'_2}} = -\int\limits_{(\omega_{\mathbf{K}'_2})_0}^{+\infty} [P_{2P}]_{12}(\omega_{\mathbf{K}'_2}) \frac{\mathrm{d}}{\mathrm{d}\omega_{\mathbf{K}'_2}} \left\{\mathrm{d}F_1(\mathbf{K}'_2, \omega_{\mathbf{K}'_2})\right\} - \int\limits_{(\omega_{\mathbf{K}'_2})_0}^{+\infty} \frac{\mathrm{d}}{\mathrm{d}\omega_{\mathbf{K}'_2}} \left\{[P_{2P}]_{12}(\omega_{\mathbf{K}'_2})\right\}$$

$$\cdot\, \mathrm{d}F_1(\mathbf{K}'_2, \omega_{\mathbf{K}'_2})$$

where $(\omega_{\mathbf{K}'_2})_0 \triangleq (\omega_{\mathbf{K}_1} + \omega_{\mathbf{K}_2}) - \omega_{\mathbf{K}'_1}$. Applying integration by parts in one of the integrals, and again using the Riemann-Lebesgue lemma, $I_{\omega_{\mathbf{K}'_2}}$ reduces to

$$I_{\omega_{\mathbf{K}'_2}} = [P_{2P}]_{12}((\omega_{\mathbf{K}_1} + \omega_{\mathbf{K}_2}) - \omega_{\mathbf{K}'_1})\, \mathrm{d}F_1(\mathbf{K}'_2, \omega_{\mathbf{K}'_2})|_{\omega_{\mathbf{K}'_2} = (\omega_{\mathbf{K}_1} + \omega_{\mathbf{K}_2}) - \omega_{\mathbf{K}'_1}}.$$

Therefore, by applying the method presented here, the expressions in (3.121) to (3.124) can be written as

$$\left[\left(E^+_{0\mathbf{n}}\right)_{11}\right]_{11}(t, t_0) = -2\pi j \eta_0 \Delta\ell\Delta\rho I_0 k_0^2 \frac{F^2(\rho_0, \omega_0)}{(2\pi\rho_0)^{3/2}} e^{jk_0\Delta\rho} \sum_{\mathbf{K}'} \sum_{\mathbf{K}, \omega_{\mathbf{K}}} f_1(\mathbf{K}, \omega_{\mathbf{K}}) f_1(\mathbf{K}', \omega_{\mathbf{K}})$$

$$\cdot\, u'_0 e^{-j\omega_{\mathbf{K}}t} \sqrt{K} g(\theta_{\mathbf{K}}) e^{-j(\pi/4)} e^{j\rho_0 K} e^{j\mathbf{K}'\cdot\boldsymbol{\rho}}\, \mathrm{Sa}\left[\frac{\Delta\rho}{2}(K - 2k_0)\right] \quad (3.128)$$

$$\left[\left(E_{0\mathbf{n}}^{+}\right)_{2P}\right]_{11}(t,t_0) = -2\pi j\eta_0\Delta\ell\Delta\rho I_0 k_0^2 \frac{F^2(\rho_0,\omega_0)}{(2\pi\rho_0)^{3/2}} e^{jk_0\Delta\rho} \sum_{\mathbf{K}'} \sum_{\substack{\mathbf{K}_1,\omega_{\mathbf{K}_1} \\ \mathbf{K}_1+\mathbf{K}_2=\mathbf{K}}} \sum_{\mathbf{K}_2,\omega_{\mathbf{K}_2}} \Gamma_P$$

$$\cdot f_1(\mathbf{K}_1,\omega_{\mathbf{K}_1}) f_1(\mathbf{K}_2,\omega_{\mathbf{K}_2}) f_1(\mathbf{K}',\omega_{\mathbf{K}_1}+\omega_{\mathbf{K}_2}) u_0' e^{-j(\omega_{\mathbf{K}_1}+\omega_{\mathbf{K}_2})t} \sqrt{K} g(\theta_{\mathbf{K}}) e^{-j(\pi/4)} e^{j\rho_0 K}$$

$$\cdot e^{j\mathbf{K}'\cdot\boldsymbol{\rho}}\,\mathrm{Sa}\left[\frac{\Delta\rho}{2}(K-2k_0)\right], \quad (3.129)$$

$$\left[\left(E_{0\mathbf{n}}^{+}\right)_{11}\right]_{12}(t,t_0) = -2\pi j\eta_0\Delta\ell\Delta\rho I_0 k_0^2 \frac{F^2(\rho_0,\omega_0)}{(2\pi\rho_0)^{3/2}} e^{jk_0\Delta\rho} \sum_{\substack{\mathbf{K}_1',\omega_{\mathbf{K}_1'} \\ \mathbf{K}_1'+\mathbf{K}_2'=\mathbf{K}'}} \sum_{\mathbf{K}_2'} \sum_{\mathbf{K},\omega_{\mathbf{K}}} \Gamma_H'$$

$$\cdot f_1(\mathbf{K}_1',\omega_{\mathbf{K}_1'}) f_1(\mathbf{K}_2',\omega_{\mathbf{K}}-\omega_{\mathbf{K}_1'}) f_1(\mathbf{K},\omega_{\mathbf{K}}) u_0' e^{-j\omega_{\mathbf{K}}t} \sqrt{K} g(\theta_{\mathbf{K}}) e^{-j(\pi/4)} e^{j\rho_0 K} e^{j\mathbf{K}'\cdot\boldsymbol{\rho}}$$

$$\cdot \mathrm{Sa}\left[\frac{\Delta\rho}{2}(K-2k_0)\right], \quad (3.130)$$

$$\left[\left(E_{0\mathbf{n}}^{+}\right)_{2P}\right]_{12}(t,t_0) = -2\pi j\eta_0\Delta\ell\Delta\rho I_0 k_0^2 \frac{F^2(\rho_0,\omega_0)}{(2\pi\rho_0)^{3/2}} e^{jk_0\Delta\rho} \sum_{\substack{\mathbf{K}_1',\omega_{\mathbf{K}_1'} \\ \mathbf{K}_1'+\mathbf{K}_2'=\mathbf{K}'}} \sum_{\mathbf{K}_2'} \sum_{\substack{\mathbf{K}_1,\omega_{\mathbf{K}_1} \\ \mathbf{K}_1+\mathbf{K}_2=\mathbf{K}}} \sum_{\mathbf{K}_2,\omega_{\mathbf{K}_2}} \Gamma_P$$

$$\cdot \Gamma_H' f_1(\mathbf{K}_1',\omega_{\mathbf{K}_1'}) f_1(\mathbf{K}_2',(\omega_{\mathbf{K}_1}+\omega_{\mathbf{K}_2})-\omega_{\mathbf{K}_1'}) f_1(\mathbf{K}_1,\omega_{\mathbf{K}_1}) f_1(\mathbf{K}_2,\omega_{\mathbf{K}_2}) u_0' e^{-j(\omega_{\mathbf{K}_1}+\omega_{\mathbf{K}_2})t}$$

$$\cdot \sqrt{K} g(\theta_{\mathbf{K}}) e^{-j(\pi/4)} e^{j\rho_0 K} e^{j\mathbf{K}'\cdot\boldsymbol{\rho}}\,\mathrm{Sa}\left[\frac{\Delta\rho}{2}(K-2k_0)\right]. \quad (3.131)$$

From (3.129) to (3.131), it can be observed that the arbitrary heights function has been fully incorporated into the expressions for the first-order corrections to the electric field.

3.6.2 Second-Order Corrections to the Electric Field

Similar to the first-order case, the second-order correction terms are derived from the second-order of the power series expansion of the exponential of the arbitrary heights

function, e.g. (3.107) and (3.110). As higher-order corrections would result in a higher overall order for the electric field, and, consequently, a lower-energy radar cross-section [18], [132], the second-order correction will only be derived for the first-order hydrodynamic arbitrary heights function. From the definition of $\zeta_{01}(\boldsymbol{\rho};t)$ in (3.111), $\zeta_{01}^2(\boldsymbol{\rho};t)$ can be written as

$$\zeta_{01}^2(\boldsymbol{\rho};t) = \sum_{\mathbf{K}',\omega_{\mathbf{K}'}} \sum_{\mathbf{K}'',\omega_{\mathbf{K}''}} f_1(\mathbf{K}',\omega_{\mathbf{K}'}) f_1(\mathbf{K}'',\omega_{\mathbf{K}''}) u_0' u_0'' e^{-j(\omega_{\mathbf{K}'}+\omega_{\mathbf{K}''})t} e^{j(\mathbf{K}'+\mathbf{K}'')\cdot\boldsymbol{\rho}}, \quad (3.132)$$

where

$$u_0'' = \sqrt{K''^2 - {k_0}^2}.$$

Similar to the convolution presented for the first-order correction, considering $\omega_a, \omega_b, \omega_c \in \mathbb{R}$, the ocean time convolution present in the second-order correction terms can be interpreted as

$$e^{-j\omega_a t} \underset{t}{*} e^{-j(\omega_b+\omega_c)t} = \int_{-\infty}^{\infty} e^{-j(\omega_b+\omega_c)\tau} e^{-j\omega_a(t-\tau)}\,\mathrm{d}\tau = 2\pi e^{-j\omega_a t}\delta(\omega_a - (\omega_b+\omega_c)).$$

Therefore, by substituting (3.132) and the height-restricted first- and second-order electric fields into (3.107) and (3.110), the first-order hydrodynamic, second-order correction terms of the first- and second-order electric fields can be written as

$$\left[\left(E_{0\mathbf{n}}^{+}\right)_{11}\right]_{21}(t,t_0) = -\pi j\eta_0\Delta\ell\Delta\rho I_0 k_0^2 \frac{F^2(\rho_0,\omega_0)}{(2\pi\rho_0)^{3/2}} e^{jk_0\Delta\rho} \sum_{\mathbf{K}',\omega_{\mathbf{K}'}} \sum_{\mathbf{K}'',\omega_{\mathbf{K}''}} \sum_{\mathbf{K},\omega_{\mathbf{K}}} f_1(\mathbf{K},\omega_{\mathbf{K}})$$
$$\cdot f_1(\mathbf{K}',\omega_{\mathbf{K}'}) f_1(\mathbf{K}'',\omega_{\mathbf{K}''}) \delta(\omega_{\mathbf{K}} - (\omega_{\mathbf{K}'}+\omega_{\mathbf{K}''})) u_0' u_0'' e^{-j\omega_{\mathbf{K}}t} \sqrt{K}\, g(\theta_{\mathbf{K}}) e^{-j(\pi/4)} e^{j\rho_0 K}$$
$$\cdot e^{j(\mathbf{K}'+\mathbf{K}'')\cdot\boldsymbol{\rho}}\,\mathrm{Sa}\left[\frac{\Delta\rho}{2}(K-2k_0)\right] \quad (3.133)$$

and

$$\left[\left(E_{0\mathbf{n}}^{+}\right)_{2P}\right]_{21}(t,t_0) = -\pi j\eta_0\Delta\ell\Delta\rho I_0 k_0^2 \frac{F^2(\rho_0,\omega_0)}{(2\pi\rho_0)^{3/2}} e^{jk_0\Delta\rho} \sum_{\mathbf{K}',\omega_{\mathbf{K}'}} \sum_{\mathbf{K}'',\omega_{\mathbf{K}''}} \sum_{\substack{\mathbf{K}_1,\omega_{\mathbf{K}_1} \\ \mathbf{K}_1+\mathbf{K}_2=\mathbf{K}}} \sum_{\mathbf{K}_2,\omega_{\mathbf{K}_2}} \Gamma_P$$

$$\cdot f_1(\mathbf{K}_1,\omega_{\mathbf{K}_1}) f_1(\mathbf{K}_2,\omega_{\mathbf{K}_2}) f_1(\mathbf{K}',\omega_{\mathbf{K}'}) f_1(\mathbf{K}'',\omega_{\mathbf{K}''}) \delta(\omega_{\mathbf{K}_1}+\omega_{\mathbf{K}_2}-(\omega_{\mathbf{K}'}+\omega_{\mathbf{K}''})) u_0' u_0''$$

$$\cdot e^{-j(\omega_{\mathbf{K}_1}+\omega_{\mathbf{K}_2})t}\sqrt{K} g(\theta_{\mathbf{K}}) e^{-j(\pi/4)} e^{j\rho_0 K} e^{j(\mathbf{K}'+\mathbf{K}'')\cdot\boldsymbol{\rho}} \operatorname{Sa}\left[\frac{\Delta\rho}{2}(K-2k_0)\right]. \quad (3.134)$$

Here, as in (3.121) to (3.124), the Dirac deltas in the corrected electric fields should be addressed. As shown in Section 3.6.1, the Fourier-Stieltjes series in (3.133) to (3.134) can be interpreted as a Fourier-Stieltjes integral. Taking, for example, the Fourier-Stieltjes series in (3.133), the corresponding Fourier-Stieltjes integral can be written as

$$[(I_{11})]_{21}(\boldsymbol{\rho},t,t_0) = \int_{\mathbf{K}}\int_{\omega_{\mathbf{K}}}\int_{\mathbf{K}'}\int_{\omega_{\mathbf{K}'}}\int_{\mathbf{K}''}\int_{\omega_{\mathbf{K}''}} [P_{11}]_{21}(\boldsymbol{\rho},\mathbf{K},\mathbf{K}',\mathbf{K}'',\omega_{\mathbf{K}},t,t_0)\delta(\omega_{\mathbf{K}}-(\omega_{\mathbf{K}'}+\omega_{\mathbf{K}''}))$$

$$\cdot \mathrm{d}F_1(\mathbf{K}'',\omega_{\mathbf{K}''})\,\mathrm{d}F_1(\mathbf{K}',\omega_{\mathbf{K}'})\,\mathrm{d}F_1(\mathbf{K},\omega_{\mathbf{K}}), \quad (3.135)$$

where

$$[P_{11}]_{21} \triangleq u_0' e^{-j\omega_{\mathbf{K}}t}\sqrt{K} g(\theta_{\mathbf{K}}) e^{j\rho_0 K} e^{j(\mathbf{K}'+\mathbf{K}'')\cdot\boldsymbol{\rho}} \operatorname{Sa}\left[\frac{\Delta\rho}{2}(K-2k_0)\right].$$

Knowing that $\delta(x)=\delta(-x),\ \forall x$ [104], the integral in (3.135) can be rewritten as

$$[(I_{11})]_{21}(\boldsymbol{\rho},t,t_0) = \int_{\mathbf{K}}\int_{\omega_{\mathbf{K}}}\int_{\mathbf{K}'}\int_{\omega_{\mathbf{K}'}}\int_{\mathbf{K}''}\int_{\omega_{\mathbf{K}''}} [P_{11}]_{21}(\boldsymbol{\rho},\mathbf{K},\mathbf{K}',\mathbf{K}'',\omega_{\mathbf{K}},t,t_0)\delta(\omega_{\mathbf{K}''}-(\omega_{\mathbf{K}}-\omega_{\mathbf{K}'}))$$

$$\cdot \mathrm{d}F_1(\mathbf{K}'',\omega_{\mathbf{K}''})\,\mathrm{d}F_1(\mathbf{K}',\omega_{\mathbf{K}'})\,\mathrm{d}F_1(\mathbf{K},\omega_{\mathbf{K}}), \quad (3.136)$$

Following the same procedure presented in Section 3.6.1, $[(I_{11})]_{21}(\boldsymbol{\rho},t,t_0)$ can be

finally written as

$$[(I_{11})]_{21}(\boldsymbol{\rho},t,t_0)=\int\limits_{\mathbf{K}}\int\limits_{\omega_{\mathbf{K}}}\int\limits_{\mathbf{K}'}\int\limits_{\omega_{\mathbf{K}'}}[P_{11}]_{21}(\boldsymbol{\rho},\mathbf{K},\mathbf{K}',\mathbf{K}'',\omega_{\mathbf{K}},t,t_0)\,\mathrm{d}F_1(\mathbf{K}'',\omega_{\mathbf{K}''})|_{\omega_{\mathbf{K}''}=\omega_{\mathbf{K}}-\omega_{\mathbf{K}'}}$$
$$\cdot\,\mathrm{d}F_1(\mathbf{K}',\omega_{\mathbf{K}'})\,\mathrm{d}F_1(\mathbf{K},\omega_{\mathbf{K}}). \quad (3.137)$$

Analogously, the Fourier-Stieltjes integral form of the series presented in (3.134) can be written as $[(I_{11})]_{21}(\boldsymbol{\rho},t,t_0)$, which can be finally written as

$$[(I_{11})]_{21}(\boldsymbol{\rho},t,t_0)=\int\cdots\int[P_{2P}]_{21}(\boldsymbol{\rho},\mathbf{K}_1,\mathbf{K}_2,\mathbf{K}',\mathbf{K}'',\omega_{\mathbf{K}_1},\omega_{\mathbf{K}_2},t,t_0)$$
$$\cdot\,\mathrm{d}F_1(\mathbf{K}'',\omega_{\mathbf{K}''})|_{\omega_{\mathbf{K}''}=(\omega_{\mathbf{K}_1}+\omega_{\mathbf{K}_2})-\omega_{\mathbf{K}'}}\,\mathrm{d}F_1(\mathbf{K}',\omega_{\mathbf{K}'})\,\mathrm{d}F_1(\mathbf{K}_1,\omega_{\mathbf{K}_1})\,\mathrm{d}F_1(\mathbf{K}_2,\omega_{\mathbf{K}_2}), \quad (3.138)$$

where

$$[P_{2P}]_{21}\triangleq\Gamma_P u_0' u_0'' e^{-j(\omega_{\mathbf{K}_1}+\omega_{\mathbf{K}_2})t}\sqrt{K}g(\theta_{\mathbf{K}})e^{-j(\pi/4)}e^{j\rho_0 K}e^{j(\mathbf{K}'+\mathbf{K}'')\cdot\boldsymbol{\rho}}\,\mathrm{Sa}\left[\frac{\Delta\rho}{2}(K-2k_0)\right].$$

Substituting (3.137) and (3.138) respectively into (3.133) and (3.134), the expressions for the first-order hydrodynamic, second-order corrections to the electric field can be obtained as

$$\left[\left(E_{0\mathbf{n}}^{+}\right)_{11}\right]_{21}(t,t_0)=-\pi j\eta_0\Delta\ell\Delta\rho I_0 k_0^2\frac{F^2(\rho_0,\omega_0)}{(2\pi\rho_0)^{3/2}}e^{jk_0\Delta\rho}\sum_{\mathbf{K}',\omega_{\mathbf{K}'}}\sum_{\mathbf{K}''}\sum_{\mathbf{K},\omega_{\mathbf{K}}}f_1(\mathbf{K},\omega_{\mathbf{K}})$$
$$\cdot\,f_1(\mathbf{K}',\omega_{\mathbf{K}'})f_1(\mathbf{K}'',\omega_{\mathbf{K}'}-\omega_{\mathbf{K}})u_0' u_0'' e^{-j\omega_{\mathbf{K}}t}\sqrt{K}g(\theta_{\mathbf{K}})e^{-j(\pi/4)}e^{j\rho_0 K}e^{j(\mathbf{K}'+\mathbf{K}'')\cdot\boldsymbol{\rho}}$$
$$\cdot\,\mathrm{Sa}\left[\frac{\Delta\rho}{2}(K-2k_0)\right] \quad (3.139)$$

and

$$\left[\left(E_{0\mathbf{n}}^{+}\right)_{2P}\right]_{21}(t,t_0) = -\pi j\eta_0\Delta\ell\Delta\rho I_0 k_0^2 \frac{F^2(\rho_0,\omega_0)}{(2\pi\rho_0)^{3/2}} e^{jk_0\Delta\rho} \sum_{\mathbf{K}',\omega_{\mathbf{K}'}} \sum_{\mathbf{K}''} \sum_{\substack{\mathbf{K}_1,\omega_{\mathbf{K}_1} \\ \mathbf{K}_1+\mathbf{K}_2=\mathbf{K}}} \sum_{\mathbf{K}_2,\omega_{\mathbf{K}_2}} \Gamma_P$$

$$\cdot f_1(\mathbf{K}_1,\omega_{\mathbf{K}_1}) f_1(\mathbf{K}_2,\omega_{\mathbf{K}_2}) f_1(\mathbf{K}',\omega_{\mathbf{K}'}) f_1(\mathbf{K}'',(\omega_{\mathbf{K}_1}+\omega_{\mathbf{K}_2})-\omega_{\mathbf{K}'}) u_0' u_0'' e^{-j(\omega_{\mathbf{K}_1}+\omega_{\mathbf{K}_2})t}\sqrt{K}$$

$$\cdot g(\theta_{\mathbf{K}}) e^{-j(\pi/4)} e^{j\rho_0 K} e^{j(\mathbf{K}'+\mathbf{K}'')\cdot\boldsymbol{\rho}} \,\mathrm{Sa}\left[\frac{\Delta\rho}{2}(K-2k_0)\right]. \quad (3.140)$$

It should be noted that following the previously-defined convention to determine the order of the correction terms, (3.139) and (3.140) are respectively included in the third and fourth orders of the perturbation expansion of the electric field, and will likely have a very small influence on the total electric field.

3.7 General Chapter Summary

In this chapter, the equations for the first- and second-order electric fields for an ocean surface with electromagnetically-large waves have been derived. The system of equations for the electric field presented in Chapter 2 was considered for the case of scattering over a time-varying conductive random surface. It was shown that while most of the derivations are similar to the ones presented by Walsh and Gill [3] and Walsh *et al.* [17], the definition of the auxilliary vector fields $\mathbf{R}^+$ and $\mathbf{R}^-$ do not coincide with the ones presented in this chapter. Regardless, as the derivation of the operator equation for the electric field normal to the ocean surface does not depend on the definition of the auxiliary vectors, the results presented in [3] were used as a starting point.

Using the operator equation defined in [3], the electric field expression for the

first- and second-order electric fields for an ocean surface with arbitrary wave heights was derived. This derivation depended on the definition of the operator $\mathcal{L}^1$ for an ocean surface with arbitrary heights, since the expression presented in [3] was defined with the help of the small-height approximation. This resulted in the definition of the arbitrary heights factor, the exponential of the arbitrary heights function $\zeta(x, y; t)$, introducing new terms to the operators in the equation. This resulted in a general form for the first- and second-order electric field, where the height-restricted electric field expressions from [3] are multiplied by the arbitrary heights factor. While the derivations presented here are similar to the ones shown in [3], [17], the extra factor introduced by the redefinition of $\mathcal{L}^{-1}$ require that the whole process be followed including the arbitrary heights factor.

As both first- and second-order electric fields for an ocean surface with electromagnetically-large waves depend on their height-restricted expressions, the derivations for the height-restricted expressions for the electric field were revised. In [3], [17], the ocean surface is initially considered static, with the time variation being introduced once the electric field expressions have been derived. This could introduce some problems in the derivation, as a time convolution is required to obtain the electric field expressions in the time domain. Therefore, the expressions for the electric field were rederived considering a time-varying conductive random surface. For simplicity, since the derivation of the first- and second-order electric fields follow a similar pattern, the first-order electric field was used as an example. It was shown that while the final expressions for the electric field are identical, this is only due to the mismatch between the phase velocity of the ocean waves and the speed of light, which allows for the approximation to the expression presented in [3], [17].

Once the height-restricted expressions have been derived, the expressions for the first- and second-order electric field for an ocean surface with arbitrary heights could be obtained. From the power series expansion fo the arbitrary heights factor, it is clear that the first-order correction term has not been altered, and a series of correction terms have been included in the analysis. After the temporal inverse Fourier transform is applied to the electric field, the correction terms for the first- and second-order electric fields could be obtained by a convolution between the height-restricted electric field and the different terms in the power series expansion of the arbitrary heights factor. This resulted in the incorporation of the arbitrary heights function to the electric field expressions. It should also be noted that the results presented here can be extended to a bistatic configuration, as presented in [96]; the derivation of the first-order hydrodynamic, first-order correction to the first-order electric field is presented in Appendix B.2.

Considering the energy limitations of higher-order terms due to the uniform validity of the generalized asymptotic expansion of the ocean surface, the order of the correction terms have been restricted to the first-order hydrodynamic term of the second-order arbitrary heights function. The resulting expressions can now be used to calculate the different corrections to the radar cross-section of the ocean surface with electromagnetically-large waves.

Chapter 4

HF Radar Cross-Section of an Ocean Surface with Electromagnetically-Large Waves

As described in Chapter 1, the radar cross-section (RCS) of the ocean surface is one of the fundamental elements of radio oceanography in the HF band, as it allows for the extraction of multiple meteorological measurements, the ocean wave spectrum among them. The RCS of any scattering object can be obtained either by obtaining the far-field limit of the ratio between scattered and incident power densities [90], or by using the radar equation [120], [133], [134], which relates the power spectral density of the received field to the radar cross-section of the scattering object. In the derivation of the RCS of the ocean surface in the HF band, the latter method has been widely-used [17], [18], [120].

To obtain the radar cross-section through the radar equation method, the power

spectral density of the received electric field must be calculated and compared with the radar equation. First, a conveniently-normalized autocorrelation expression for the electric field is obtained, such that the zero-lag autocorrelation is equal to the average power in the receiver [18]. Then, by taking the Fourier transform of the autocorrelation with respect to the time delay, the power spectral density of the receiver electric field can be obtained. This power spectral density will be defined in terms of the Doppler frequency [17], [18], [120], being, therefore, the mathematical description of the part of the received Doppler spectrum obtained from the electric field scattered by the ocean surface. Finally, the radar cross-section of the ocean surface can be found by comparing the resulting power spectral density with the radar equation.

In this chapter, the radar cross-section for an ocean surface with arbitrary wave heights will be obtained by using the electric field equations derived in Chapter 3. As the height-restricted RCSs of the ocean surface have been previously derived in the literature [17], [18], [120], the chapter will focus on the RCS resulting from the correction terms introduced in Chapter 3.

4.1 Autocorrelation of the Electric Field over an Ocean Surface With Electromagnetically-Large Waves

According to [75], [123], [135], the ocean surface displacement $f(\boldsymbol{\rho}, t)$ can be understood as a zero-mean stationary Gaussian random process for a sufficiently large

observation time and scattering patch. Also, since the surface displacement is a continuous function for any interval in time and space [136], $f(\boldsymbol{\rho};t)$ is also Riemann integrable. Knowing that the surface displacement is a Gaussian random process, it is easy to see from the definition of the Fourier coefficients in (3.74) that $f(\mathbf{K},\omega_{\mathbf{K}})$ is also a Gaussian random variable through the central limit theorem [137]. Therefore, considering the electric field as being the result of a sum of stationary Gaussian processes [138], the autocorrelation of the electric field received from a patch of the ocean surface depends only upon the delay between observations $\tau = t_2 - t_1$ [139], and can be defined as

$$\mathcal{R}_{E^+_{\mathbf{n}}}(t_1,t_2) = \mathbb{E}\left\{E^+_{\mathbf{n}}(t_1,t_0)\overline{E^+_{\mathbf{n}}(t_2,t_0)}\right\} = \mathbb{E}\left\{E^+_{\mathbf{n}}(t)\overline{E^+_{\mathbf{n}}(t-\tau)}\right\} = \mathcal{R}_{E^+_{\mathbf{n}}}(\tau),$$

where the overline indicates the conjugate transpose and $\mathbb{E}\{\cdot\}$ is the expected value operator. It should be noted that the autocorrelation in this case is taken with respect to radar time. For convenience, the autocorrelation of the electric field can be normalized as in [18],

$$\mathcal{R}(\tau) = \frac{A_r}{2\eta_0}\mathcal{R}_{E^+_{\mathbf{n}}}(\tau) = \frac{A_r}{2\eta_0}\mathbb{E}\left\{E^+_{\mathbf{n}}(t,t_0)\overline{E^+_{\mathbf{n}}(t-\tau,t_0)}\right\}, \tag{4.1}$$

where A_r is effective free-space aperture of the receiving antenna. This normalization was chosen so that $\mathcal{R}(0)$ becomes the average power of the received electric field [140]

$$\mathcal{R}(0) = \frac{A_r}{2\eta_0}\mathbb{E}\left\{|E^+_{\mathbf{n}}(t,t_0)|^2\right\}.$$

Expanding the electric field expression in (4.1) using the general form of the electric field including the correction terms for an ocean surface with electromagnetically-large waves as shown in (3.103), the autocorrelation of the electric field can be

written as

$$\mathcal{R}(\tau) = \frac{A_r}{2\eta_0}\mathbb{E}\left\{\left(\sum_m\sum_n (E^+_{0\mathbf{n}})_{mn}(t,t_0) + \sum_m\sum_n\sum_p\sum_q \left[(E^+_{0\mathbf{n}})_{mn}\right]_{pq}(t,t_0)\right)\right.$$
$$\left.\cdot\left(\sum_m\sum_n \overline{(E^+_{0\mathbf{n}})_{mn}(t-\tau,t_0)} + \sum_m\sum_n\sum_p\sum_q \overline{\left[(E^+_{0\mathbf{n}})_{mn}\right]_{pq}(t-\tau,t_0)}\right)\right\}. \quad (4.2)$$

Since the coefficients of the Fourier-Stieltjes expansion of the ocean surface are defined such that, for any $\mathbf{K}_m, \omega_{\mathbf{K}_m}$ and $\mathbf{K}_n, \omega_{\mathbf{K}_n}$ [122], [135], [141]

$$\mathbb{E}\left\{\mathrm{d}F(\mathbf{K}_m,\omega_{\mathbf{K}_m})\overline{\mathrm{d}F(\mathbf{K}_n,\omega_{\mathbf{K}_n})}\right\} = \begin{cases} S(\mathbf{K}_m,\omega_{\mathbf{K}_m})\,\mathrm{d}\mathbf{K}_m\,\mathrm{d}\omega_{\mathbf{K}_m}, \text{ if } \mathbf{K}_m = \mathbf{K}_n,\ \omega_{\mathbf{K}_m} = \omega_{\mathbf{K}_n} \\ 0, \text{ otherwise,} \end{cases} \quad (4.3)$$

with $S(\mathbf{K}_m, \omega_{\mathbf{K}_m})$ being the ocean wave spectrum for $\mathbf{K}_m, \omega_{\mathbf{K}_m}$. Considering the autocorrelation of the Fourier coefficients in correction terms modified by the Dirac delta, the autocorrelation becomes

$$\mathbb{E}\left\{\mathrm{d}F(\mathbf{K}'_m,\omega_{\mathbf{K}'_m})\big|_{\omega_{\mathbf{K}'_m}=\omega_{\mathbf{K}_i}}\overline{\mathrm{d}F(\mathbf{K}'_n,\omega_{\mathbf{K}'_n})\big|_{\omega_{\mathbf{K}'_n}=\omega_{\mathbf{K}_j}}}\right\}$$
$$= \begin{cases} S(\mathbf{K}'_m,\omega_{\mathbf{K}_i})\,\mathrm{d}\mathbf{K}'_m, \text{ if } \mathbf{K}'_m = \mathbf{K}'_n,\ \omega_{\mathbf{K}_i} = \omega_{\mathbf{K}_j}, \\ 0, \text{ otherwise,} \end{cases} \quad (4.4)$$

with $\omega_{\mathbf{K}_i}, \omega_{\mathbf{K}_j}$ being angular frequencies resulting from the integration of the Dirac delta shown in Chapter 3. Therefore, following this principle, the Fourier coefficient terms affected by the Dirac delta are fundamentally different functions from their unaffected counterparts. Since the correlation of a Fourier coefficient of the ocean surface can only be defined between values of the same Fourier coefficient and the same wavenumber and frequencies [122], [141], all cross-correlations between electric field terms resulting from different orders of the asymptotic expansion of the ocean surface

will be null. In terms of the electric field, this means that only electric fields with the same hydrodynamic and electromagnetic orders will be able to interact without resulting in a null term. This was observed in [17], where the interaction between first- and second-order electric fields for a height-restricted conductive surface resulted in a negligible term. Consequently, the order of the correction terms in the correlation would need to be the same as well. Therefore, applying all aforementioned expansions to the normalized autocorrelation of the electric field results in

$$\mathcal{R}(\tau) = \sum_m \sum_n \mathcal{R}_{mn}(\tau) + \sum_m \sum_n \sum_p \sum_q [\mathcal{R}_{mn}]_{pq}(\tau) \tag{4.5}$$

with

$$\mathcal{R}_{mn}(\tau) = \frac{A_r}{2\eta_0} \mathbb{E}\left\{ (E^+_{0\mathbf{n}})_{mn}(t) \overline{(E^+_{0\mathbf{n}})_{mn}(t-\tau)} \right\} \tag{4.6}$$

being the autocorrelation of the small-heights electric fields, and

$$[\mathcal{R}_{mn}]_{pq}(\tau) = \frac{A_r}{2\eta_0} \mathbb{E}\left\{ [(E^+_{0\mathbf{n}})_{mn}]_{pq}(t) \overline{[(E^+_{0\mathbf{n}})_{mn}]_{pq}(t-\tau)} \right\} \tag{4.7}$$

being the autocorrelation of the correction terms. Since the autocorrelation of the height-restricted terms have been previously derived in [17] for the monostatic case, and in [89] for the bistatic case, the following sections will focus on the derivation of the autocorrelations of the electric field correction terms presented in Chapter 3.

4.1.1 Autocorrelation of the First-Order Corrections to the Electric Field

From (4.7), the autocorrelation of the first-order correction terms can be defined as

$$[\mathcal{R}_{11}]_{11}(\tau) \triangleq \frac{A_r}{2\eta_0}\mathbb{E}\left\{[(E^+_{0\mathbf{n}})_{11}]_{11}(t)\overline{[(E^+_{0\mathbf{n}})_{11}]_{11}(t-\tau)}\right\} \tag{4.8}$$

$$[\mathcal{R}_{2P}]_{11}(\tau) \triangleq \frac{A_r}{2\eta_0}\mathbb{E}\left\{[(E^+_{0\mathbf{n}})_{2P}]_{11}(t)\overline{[(E^+_{0\mathbf{n}})_{2P}]_{11}(t-\tau)}\right\} \tag{4.9}$$

$$[\mathcal{R}_{11}]_{12}(\tau) \triangleq \frac{A_r}{2\eta_0}\mathbb{E}\left\{[(E^+_{0\mathbf{n}})_{11}]_{12}(t)\overline{[(E^+_{0\mathbf{n}})_{11}]_{12}(t-\tau)}\right\} \tag{4.10}$$

$$[\mathcal{R}_{2P}]_{12}(\tau) \triangleq \frac{A_r}{2\eta_0}\mathbb{E}\left\{[(E^+_{0\mathbf{n}})_{2P}]_{12}(t)\overline{[(E^+_{0\mathbf{n}})_{2P}]_{12}(t-\tau)}\right\} \tag{4.11}$$

where the first-order electric fields are defined in (3.128) to (3.131). As most steps in the derivation are similar between the different terms in (4.8) to (4.11), for simplicity the derivations presented here will focus on the corrections to the first-order fields.

Considering first the autocorrelation for the first-order hydrodynamic, first-order electric field correction to the first-order electric field presented in (4.8) and substituting the electric field expression defined in (3.128) in its Fourier-Stieltjes integral form, $[\mathcal{R}_{11}]_{11}$ can be written as

$$\begin{aligned}[\mathcal{R}_{11}]_{11}(\tau) = \frac{A_r}{2\eta_0}\Bigg\{&(2\pi)^2{\eta_0}^2|I_0\Delta\ell|^2\Delta\rho^2k_0^4\frac{|F(\rho_0,\omega_0)|^4}{(2\pi)^3\rho_0^3}\int\cdots\int u_0'\overline{u_0'^*}e^{-j\omega_{\mathbf{K}}t}e^{j\omega_{\mathbf{K}^*}(t-\tau)}\\
\cdot\sqrt{K}\sqrt{K^*}g(\theta_{\mathbf{K}})\overline{g(\theta_{\mathbf{K}^*})}&e^{j\rho_0K}e^{-j\rho_0K^*}e^{-j\mathbf{K}'^*\cdot\boldsymbol{\rho}}e^{j\mathbf{K}'\cdot\boldsymbol{\rho}}\,\mathrm{Sa}\left[\frac{\Delta\rho}{2}(K-2k_0)\right]\mathrm{Sa}\left[\frac{\Delta\rho}{2}(K^*-2k_0)\right]\\
&\cdot\mathbb{E}\left\{\mathrm{d}F_1(\mathbf{K},\omega_{\mathbf{K}})\overline{\mathrm{d}F_1(\mathbf{K}^*,\omega_{\mathbf{K}^*})}\right\}\mathbb{E}\left\{\mathrm{d}F_1(\mathbf{K}',\omega_{\mathbf{K}})\overline{\mathrm{d}F_1(\mathbf{K}'^*,\omega_{\mathbf{K}^*})}\right\}\Bigg\},\end{aligned} \tag{4.12}$$

where the star superscripts indicate that the variables originate from the conjugate transpose functions. From the definitions of the expected values for the Fourier

coefficients in (4.3) and (4.4), the expression in (4.12) can be further expanded as

$$[\mathcal{R}_{11}]_{11}(\tau) = \frac{A_r}{2}\Bigg\{(2\pi)^2\eta_0|I_0\Delta\ell|^2\Delta\rho^2k_0^4\frac{|F(\rho_0,\omega_0)|^4}{(2\pi)^3\rho_0^3}\int\cdots\int S_1(\mathbf{K},\omega_{\mathbf{K}})S_1(\mathbf{K}',\omega_{\mathbf{K}})u_0'\overline{u_0'^*}$$
$$\cdot e^{-j\omega_{\mathbf{K}}t}e^{j\omega_{\mathbf{K}^*}(t-\tau)}\sqrt{K}\sqrt{K^*}g(\theta_{\mathbf{K}})\overline{g(\theta_{\mathbf{K}^*})}e^{j\rho_0K}e^{-j\rho_0K^*}e^{-j\mathbf{K}'^*\cdot\boldsymbol{\rho}}e^{j\mathbf{K}'\cdot\boldsymbol{\rho}}\,\mathrm{Sa}\left[\frac{\Delta\rho}{2}(K-2k_0)\right]$$
$$\cdot\mathrm{Sa}\left[\frac{\Delta\rho}{2}(K^*-2k_0)\right]\delta(\mathbf{K}^*-\mathbf{K})\delta(\omega_{\mathbf{K}^*}-\omega_{\mathbf{K}})\delta(\mathbf{K}'^*-\mathbf{K})\,\mathrm{d}\mathbf{K}^*\,\mathrm{d}\omega_{\mathbf{K}^*}\,\mathrm{d}\mathbf{K}'^*\,\mathrm{d}\mathbf{K}'\,\mathrm{d}\mathbf{K}\,\mathrm{d}\omega_{\mathbf{K}}\Bigg\}, \tag{4.13}$$

where $S_1(\mathbf{K},\omega_{\mathbf{K}})$ is the ocean wave spectrum for first-order waves [18]. Defining the wave vector space in polar coordinates, the Dirac deltas and differential wave vectors $\mathrm{d}\mathbf{K}^*$ and $\mathrm{d}\mathbf{K}'^*$ can be written as

$$\delta(\mathbf{K}^*-\mathbf{K}) = \frac{1}{K^*}\delta(K^*-K)\delta(\theta_{\mathbf{K}^*}-\theta_{\mathbf{K}}),$$

$$\delta(\mathbf{K}'^*-\mathbf{K}') = \frac{1}{K'^*}\delta(K'^*-K')\delta(\theta_{\mathbf{K}'^*}-\theta_{\mathbf{K}'}),$$

$$\mathrm{d}\mathbf{K}^* = K^*\,\mathrm{d}K^*\,\mathrm{d}\theta_{\mathbf{K}^*},$$

and

$$\mathrm{d}\mathbf{K}'^* = K'^*\,\mathrm{d}K'^*\,\mathrm{d}\theta_{\mathbf{K}'^*},$$

the Dirac delta in (4.13) can be integrated, using the sifting property [104] to obtain

$$[\mathcal{R}_{11}]_{11}(\tau) = \frac{A_r\eta_0k_0^4|I_0\Delta\ell|^2|F(\rho_0,\omega_0)|^4\Delta\rho^2}{2(2\pi)\rho_0^3}\int\cdots\int S_1(\mathbf{K},\omega_{\mathbf{K}})S_1(\mathbf{K}',\omega_{\mathbf{K}})|u_0'|^2$$
$$\cdot e^{-j\omega_{\mathbf{K}}\tau}K|g(\theta_{\mathbf{K}})|^2\,\mathrm{Sa}^2\left[\frac{\Delta\rho}{2}(K-2k_0)\right]\mathrm{d}\mathbf{K}'\,\mathrm{d}\mathbf{K}\,\mathrm{d}\omega_{\mathbf{K}}. \tag{4.14}$$

Following the same procedure for the second-order hydrodynamic, first-order correction to the first-order electric field in (4.10), $[\mathcal{R}_{11}]_{12}$ can be written as

$$[\mathcal{R}_{11}]_{12}(\tau) = \frac{A_r \eta_0 k_0^4 |I_0 \Delta\ell|^2 |F(\rho_0,\omega_0)|^4 \Delta\rho^2}{2(2\pi)\rho_0^3} \int\cdots\int |\Gamma'_H|^2 S_1(\mathbf{K},\omega_{\mathbf{K}}) S_1(\mathbf{K}'_1,\omega_{\mathbf{K}'_1})$$
$$\cdot S_1(\mathbf{K}'_2,\omega_{\mathbf{K}}-\omega_{\mathbf{K}'_1}) |u'_0|^2 e^{-j\omega_{\mathbf{K}}\tau} K |g(\theta_{\mathbf{K}})|^2 \,\mathrm{Sa}^2\left[\frac{\Delta\rho}{2}(K-2k_0)\right] \mathrm{d}\mathbf{K}\,\mathrm{d}\omega_{\mathbf{K}}\,\mathrm{d}\mathbf{K}'_1\,\mathrm{d}\omega_{\mathbf{K}'_1}\,\mathrm{d}\mathbf{K}'_2. \tag{4.15}$$

By definition, the directional ocean wave spectrum can be written in terms of the directional wavenumber spectrum using the dispersion relation of the ocean surface. ω as [122]

$$S_1(\mathbf{K},\omega_{\mathbf{K}}) = \frac{1}{2}\sum_{m=\pm1} S_1(m\mathbf{K})\delta(\omega_{\mathbf{K}} + m\omega).$$

For deep-water waves $\omega = \sqrt{gK}$ [142], where g is the acceleration due to gravity. Therefore, [18],

$$S_1(\mathbf{K},\omega_{\mathbf{K}}) = \frac{1}{2}\sum_{m=\pm1} S_1(m\mathbf{K})\delta(\omega_{\mathbf{K}} + m\sqrt{gK}), \tag{4.16}$$

where g is the acceleration due to gravity. Substituting (4.16) into (4.14) and (4.15), the first-order autocorrelations can be written as

$$[\mathcal{R}_{11}]_{11}(\tau) = \frac{A_r \eta_0 k_0^4 |I_0 \Delta\ell|^2 |F(\rho_0,\omega_0)|^4 \Delta\rho^2}{8(2\pi)\rho_0^3} \sum_{m=\pm1}\sum_{m'=\pm1} \int_{\mathbf{K}}\int_{\mathbf{K}'}\int_{\omega_{\mathbf{K}}} S_1(m\mathbf{K}) S_1(m'\mathbf{K}')$$
$$\cdot |u'_0|^2 e^{-j\omega_{\mathbf{K}}\tau} K \delta(\omega_{\mathbf{K}} + m\sqrt{gK})\delta(\omega_{\mathbf{K}} + m'\sqrt{gK'}) |g(\theta_{\mathbf{K}})|^2 \,\mathrm{Sa}^2\left[\frac{\Delta\rho}{2}(K-2k_0)\right]$$
$$\cdot \mathrm{d}\omega_{\mathbf{K}}\,\mathrm{d}\mathbf{K}'\,\mathrm{d}\mathbf{K}, \tag{4.17}$$

and

$$[\mathcal{R}_{11}]_{12}(\tau) = \frac{A_r \eta_0 k_0^4 |I_0 \Delta\ell|^2 |F(\rho_0,\omega_0)|^4 \Delta\rho^2}{16(2\pi)\rho_0^3} \sum_{m=\pm1}\sum_{m_1'=\pm1}\sum_{m_2'=\pm1} \int_{\mathbf{K}}\int_{\mathbf{K}_2'}\int_{\mathbf{K}_1'}\int_{\omega_{\mathbf{K}_1'}}\int_{\omega_{\mathbf{K}}} |\Gamma_H'|^2$$

$$\cdot S_1(m\mathbf{K}) S_1(m_1'\mathbf{K}_1') S_1(m_2'\mathbf{K}_2') |u_0'|^2 \delta(\omega_{\mathbf{K}} + m\sqrt{gK}) \delta(\omega_{\mathbf{K}_1'} + m_1'\sqrt{gK_1'})$$

$$\cdot\delta(\omega_{\mathbf{K}} - \omega_{\mathbf{K}_1'} + m_2'\sqrt{gK_2'}) e^{-j\omega_{\mathbf{K}}\tau} K |g(\theta_{\mathbf{K}})|^2 \,\mathrm{Sa}^2\left[\frac{\Delta\rho}{2}(K-2k_0)\right] \mathrm{d}\omega_{\mathbf{K}}\,\mathrm{d}\omega_{\mathbf{K}_1'}\,\mathrm{d}\mathbf{K}_1'\,\mathrm{d}\mathbf{K}_2'\,\mathrm{d}\mathbf{K} \tag{4.18}$$

Similarly, the first-order corrections to the second-order electric fields shown in (4.9) and (4.11) can be written as

$$[\mathcal{R}_{2P}]_{11}(\tau) = \frac{A_r \eta_0 k_0^4 |I_0 \Delta\ell|^2 |F(\rho_0,\omega_0)|^4 \Delta\rho^2}{16(2\pi)\rho_0^3} \sum_{m_1=\pm1}\sum_{m_2=\pm1}\sum_{m'=\pm1} \int_{\mathbf{K}_2}\int_{\mathbf{K}_1}\int_{\mathbf{K}'}\int_{\omega_{\mathbf{K}_2}}\int_{\omega_{\mathbf{K}_1}}$$

$$\cdot\, |{}_s\Gamma_P|^2 S_1(m_1\mathbf{K}_1) S_1(m_2\mathbf{K}_2) S_1(m'\mathbf{K}') |u_0'|^2 e^{-j(\omega_{\mathbf{K}_1}+\omega_{\mathbf{K}_2})\tau} K \delta(\omega_{\mathbf{K}_1} + \omega_{\mathbf{K}_2} + m'\sqrt{gK'})$$

$$\cdot\delta(\omega_{\mathbf{K}_1} + m_1\sqrt{gK_1}) \delta(\omega_{\mathbf{K}_2} + m_2\sqrt{gK_2}) |g(\theta_{\mathbf{K}})|^2 \,\mathrm{Sa}^2\left[\frac{\Delta\rho}{2}(K-2k_0)\right] \mathrm{d}\omega_{\mathbf{K}_1}\,\mathrm{d}\omega_{\mathbf{K}_2}\,\mathrm{d}\mathbf{K}'\,\mathrm{d}\mathbf{K}_1$$

$$\cdot\,\mathrm{d}\mathbf{K}_2, \tag{4.19}$$

and

$$[\mathcal{R}_{2P}]_{12}(\tau) = \frac{A_r \eta_0 k_0^4 |I_0 \Delta\ell|^2 |F(\rho_0,\omega_0)|^4 \Delta\rho^2}{32(2\pi)\rho_0^3} \sum_{m_1=\pm1}\sum_{m_2=\pm1}\sum_{m_1'=\pm1}\sum_{m_2'=\pm1}$$

$$\int_{\mathbf{K}_2}\int_{\mathbf{K}_1}\int_{\mathbf{K}_2'}\int_{\mathbf{K}_1'}\int_{\omega_{\mathbf{K}_2}}\int_{\omega_{\mathbf{K}_1}}\int_{\omega_{\mathbf{K}_1'}} |{}_s\Gamma_P|^2 |\Gamma_H'|^2 S_1(m_1'\mathbf{K}_1') S_1(m_2'\mathbf{K}_2') S_1(m_1\mathbf{K}_1) S_1(m_2\mathbf{K}_2) e^{-j(\omega_{\mathbf{K}_1}+\omega_{\mathbf{K}_2})\tau}$$

$$\cdot\delta(\omega_{\mathbf{K}_1} + m_1\sqrt{gK_1}) \delta(\omega_{\mathbf{K}_2} + m_2\sqrt{gK_2}) \delta(\omega_{\mathbf{K}_1'} + m_1'\sqrt{gK_1'}) \delta(\omega_{\mathbf{K}_1} + \omega_{\mathbf{K}_2} - \omega_{\mathbf{K}_1'} + m_2'\sqrt{gK_2'})$$

$$\cdot\, |u_0'|^2 K |g(\theta_{\mathbf{K}})|^2 \,\mathrm{Sa}^2\left[\frac{\Delta\rho}{2}(K-2k_0)\right] \mathrm{d}\omega_{\mathbf{K}_1'}\,\mathrm{d}\omega_{\mathbf{K}_1}\,\mathrm{d}\omega_{\mathbf{K}_2}\,\mathrm{d}\mathbf{K}_1'\,\mathrm{d}\mathbf{K}_2'\,\mathrm{d}\mathbf{K}_1\,\mathrm{d}\mathbf{K}_2, \tag{4.20}$$

where $\mathbf{K} = \mathbf{K}_1 + \mathbf{K}_2$, $\mathbf{K}' = \mathbf{K}_1' + \mathbf{K}_2'$ in (4.20), and ${}_s\Gamma_P$ is the symmetricized coupling

coefficient, defined as [89]

$$ {}_s\Gamma_P(\mathbf{K}_1,\omega_{\mathbf{K}_1},\mathbf{K}_2,\omega_{\mathbf{K}_2}) = \Gamma_H(\mathbf{K}_1,\omega_{\mathbf{K}_1},\mathbf{K}_2,\omega_{\mathbf{K}_2}) + \frac{1}{2}\left(\Gamma_E(\mathbf{K}_1,\mathbf{K}_2)+\Gamma_E(\mathbf{K}_2,\mathbf{K}_1)\right). \tag{4.21} $$

Although the Dirac deltas in (4.17), (4.19), (4.18), and (4.20) could be simplified though integration, they have been kept in the expressions to facilitate the derivation of the radar cross-section. Using the procedure presented here, it is possible to obtain the autocorrelation for the second-order terms.

4.1.2 Autocorrelation of the Second-Order Corrections to the Electric Field

From (4.7), the autocorrelation for the first-order hydrodynamic, second-order autocorrelation of the first- and second-order electric fields can be defined as

$$ [\mathcal{R}_{11}]_{21}(\tau) \triangleq \frac{A_r}{2\eta_0}\mathbb{E}\left\{[(E^+_{0\mathbf{n}})_{11}]_{21}(t)\overline{[(E^+_{0\mathbf{n}})_{11}]_{21}(t-\tau)}\right\} \tag{4.22} $$

$$ [\mathcal{R}_{2P}]_{21}(\tau) \triangleq \frac{A_r}{2\eta_0}\mathbb{E}\left\{[(E^+_{0\mathbf{n}})_{2P}]_{21}(t)\overline{[(E^+_{0\mathbf{n}})_{2P}]_{21}(t-\tau)}\right\} \tag{4.23} $$

Following the same procedure shown in Section 4.1.1, (4.22) and (4.23) can be expanded to obtain $[\mathcal{R}_{11}]_{21}$ and $[\mathcal{R}_{2P}]_{21}$ as

$$ \begin{aligned} [\mathcal{R}_{11}]_{21}(\tau) = {} & \frac{A_r\eta_0 k_0^4 |I_0\Delta\ell|^2 |F(\rho_0,\omega_0)|^4 \Delta\rho^2}{16(2\pi)\rho_0^3} \sum_{m=\pm1}\sum_{m'=\pm1}\sum_{m''=\pm1}\int\cdots\int S_1(m\mathbf{K}) \\ & \cdot S_1(m'\mathbf{K}')S_1(m''\mathbf{K}'')|u_0'|^2|u_0''|^2 K e^{-j\omega_{\mathbf{K}}\tau}\delta(\omega_{\mathbf{K}}+m\sqrt{gK})\delta(\omega_{\mathbf{K}'}+m'\sqrt{gK'}) \\ & \cdot \delta(\omega_{\mathbf{K}}-\omega_{\mathbf{K}'}+m''\sqrt{gK''})|g(\theta_{\mathbf{K}})|^2\,\mathrm{Sa}^2\left[\frac{\Delta\rho}{2}(K-2k_0)\right]\mathrm{d}\omega_{\mathbf{K}}\,\mathrm{d}\omega_{\mathbf{K}'}\,\mathrm{d}\mathbf{K}'\,\mathrm{d}\mathbf{K}''\,\mathrm{d}\mathbf{K}, \end{aligned} \tag{4.24} $$

$$[\mathcal{R}_{2P}]_{21}(\tau) = \frac{A_r \eta_0 k_0^4 |I_0 \Delta\ell|^2 |F(\rho_0, \omega_0)|^4 \Delta\rho^2}{32(2\pi)\rho_0^3} \sum_{m_1=\pm1} \sum_{m_2=\pm1} \sum_{m'=\pm1} \sum_{m''=\pm1} \int \cdots \int$$

$$\cdot \, |_s\Gamma_P|^2 S_1(m_1\mathbf{K}_1) S_1(m_2\mathbf{K}_2) S_1(m'\mathbf{K}') S_1(m''\mathbf{K}'') |u_0'|^2 |u_0''|^2 K e^{-j(\omega_{\mathbf{K}_1} + \omega_{\mathbf{K}_2})\tau}$$

$$\cdot \delta(\omega_{\mathbf{K}_1} + m_1\sqrt{gK_1}) \delta(\omega_{\mathbf{K}_2} + m_2\sqrt{gK_2}) \delta(\omega_{\mathbf{K}'} + m'\sqrt{gK'}) \delta(\omega_{\mathbf{K}_1} + \omega_{\mathbf{K}_2} - \omega_{\mathbf{K}'} + m''\sqrt{gK''})$$

$$\cdot \, |g(\theta_{\mathbf{K}})|^2 \, \mathrm{Sa}^2 \left[\frac{\Delta\rho}{2}(K - 2k_0) \right] \mathrm{d}\omega_{\mathbf{K}_1} \, \mathrm{d}\omega_{\mathbf{K}_2} \, \mathrm{d}\omega_{\mathbf{K}'} \, \mathrm{d}\mathbf{K}' \, \mathrm{d}\mathbf{K}'' \, \mathrm{d}\mathbf{K}_1 \, \mathrm{d}\mathbf{K}_2. \quad (4.25)$$

4.2 Power Spectral Density of the Electric Field Over an Ocean Surface With Electromagnetically-Large Waves

From the autocorrelation expressions derived in Section 4.1, the power spectral density of the scattered electric field can be obtained through a Fourier transform with respect to the time delay τ:

$$\mathcal{P}(\omega_d) = \mathcal{F}_\tau \{\mathcal{R}(\tau)\} = \sum_m \sum_n \mathcal{F}_\tau\{\mathcal{R}_{mn}(\tau)\} + \sum_m \sum_n \sum_p \sum_q \mathcal{F}_\tau\{[\mathcal{R}_{mn}]_{pq}(\tau)\}$$

$$\therefore \; \mathcal{P}(\omega_d) \equiv \sum_m \sum_n \mathcal{P}_{mn}(\omega_d) + \sum_m \sum_n \sum_p \sum_q [\mathcal{P}_{mn}]_{pq}(\omega_d), \quad (4.26)$$

where $\mathcal{P}_{mn}(\omega_d)$ are the power spectral densities of the height-restricted electric field terms and $[\mathcal{P}_{mn}]_{pq}(\omega_d)$ are the power spectral densities of the correction electric field terms defined in Chapter 3. This procedure will later allow the derivation of the radar cross-section terms by comparing the power spectral density obtained through the Fourier transform with that in the radar equation [18], [120].

4.2.1 Power Spectral Density of the First-Order Correction Terms

Taking first the correction terms related to the first-order electric field and applying the Fourier transform over τ, the power spectral density relative to (4.17) and (4.18) can be written as

$$[\mathcal{P}_{11}]_{11}(\omega_d) = 2\pi^3 k_0^2 \Delta\rho^2 \frac{A_r \eta_0 |I_0 \Delta\ell|^2 k_0^2 |F(\rho_0, \omega_0)|^4}{2(2\pi\rho_0)^3} \sum_{m=\pm 1} \sum_{m'=\pm 1} \int_{\mathbf{K}} \int_{\mathbf{K}'} \int_{\omega_{\mathbf{K}}} S_1(m\mathbf{K}) \cdot S_1(m'\mathbf{K}') |u_0'|^2 K \delta(\omega_d - \omega_{\mathbf{K}}) \delta(\omega_{\mathbf{K}} + m\sqrt{gK}) \delta(\omega_{\mathbf{K}} + m'\sqrt{gK'}) |g(\theta_{\mathbf{K}})|^2 \cdot \mathrm{Sa}^2 \left[\frac{\Delta\rho}{2}(K - 2k_0) \right] \mathrm{d}\omega_{\mathbf{K}} \, \mathrm{d}\mathbf{K}' \, \mathrm{d}\mathbf{K} \quad (4.27)$$

and

$$[\mathcal{P}_{11}]_{12}(\omega_d) = \pi^3 k_0^2 \Delta\rho^2 \frac{A_r \eta_0 |I_0 \Delta\ell|^2 k_0^2 |F(\rho_0, \omega_0)|^4}{2(2\pi\rho_0)^3} \sum_{m=\pm 1} \sum_{m_1'=\pm 1} \sum_{m_2'=\pm 1} \int_{\mathbf{K}} \int_{\mathbf{K}_2'} \int_{\omega_{\mathbf{K}_1'}} \int_{\mathbf{K}_1'} \int_{\omega_{\mathbf{K}}} \cdot |\Gamma_H'|^2 S_1(m\mathbf{K}) S_1(m'\mathbf{K}') |u_0'|^2 \delta(\omega_d - \omega_{\mathbf{K}}) \delta(\omega_{\mathbf{K}} + m\sqrt{gK}) \delta(\omega_{\mathbf{K}_1'} + m_1'\sqrt{gK_1'}) \cdot \delta(\omega_{\mathbf{K}} - \omega_{\mathbf{K}_1'} + m_2'\sqrt{gK_2'}) K |g(\theta_{\mathbf{K}})|^2 \, \mathrm{Sa}^2 \left[\frac{\Delta\rho}{2}(K - 2k_0) \right] \mathrm{d}\omega_{\mathbf{K}} \, \mathrm{d}\mathbf{K}_1' \, \mathrm{d}\omega_{\mathbf{K}_1'} \, \mathrm{d}\mathbf{K}_2' \, \mathrm{d}\mathbf{K}. \quad (4.28)$$

respectively. Using the reproducing property of the Dirac delta [104], the Dirac deltas in (4.27) and (4.28) can be written as

$$\delta(\omega_{\mathbf{K}} + m\sqrt{gK}) \delta(\omega_{\mathbf{K}} + m'\sqrt{gK'}) \delta(\omega_d - \omega_{\mathbf{K}}) = \delta(\omega_d + m\sqrt{gK}) \delta(\omega_d + m'\sqrt{gK'}) \cdot \delta(\omega_d - \omega_{\mathbf{K}})$$

and

$$\delta(\omega_{\mathbf{K}} + m\sqrt{gK})\delta(\omega_{\mathbf{K}'_1} + m'_1\sqrt{gK'_1})\delta(\omega_{\mathbf{K}} - \omega_{\mathbf{K}'_1} + m'_2\sqrt{gK'_2})\delta(\omega_d - \omega_{\mathbf{K}})$$
$$= \delta(\omega_d + m\sqrt{gK})\delta(\omega_{\mathbf{K}'_1} + m'_1\sqrt{gK'_1})\delta(\omega_d + m'_1\sqrt{gK'_1} + m'_2\sqrt{gK'_2})\delta(\omega_d - \omega_{\mathbf{K}}).$$

Then, performing the integral over $\omega_{\mathbf{K}}$ in (4.27) and $\omega_{\mathbf{K}}$ and $\omega_{\mathbf{K}'_1}$in (4.28), the power spectral densities can be further simplified to

$$[\mathcal{P}_{11}]_{11}(\omega_d) = 2\pi^3 k_0^2 \Delta\rho^2 \frac{A_r \eta_0 |I_0 \Delta\ell|^2 k_0^2 |F(\rho_0, \omega_0)|^4}{2(2\pi\rho_0)^3} \sum_{m=\pm1} \sum_{m'=\pm1} \int_{\mathbf{K}} \int_{\mathbf{K}'} S_1(m\mathbf{K}) S_1(m'\mathbf{K}')$$
$$\cdot |u'_0|^2 K \delta(\omega_d + m\sqrt{gK})\delta(\omega_d + m'\sqrt{gK'})|g(\theta_{\mathbf{K}})|^2 \,\mathrm{Sa}^2\left[\frac{\Delta\rho}{2}(K - 2k_0)\right] \mathrm{d}\mathbf{K}' \,\mathrm{d}\mathbf{K} \tag{4.29}$$

and

$$[\mathcal{P}_{11}]_{12}(\omega_d) = \pi^3 k_0^2 \Delta\rho^2 \frac{A_r \eta_0 |I_0 \Delta\ell|^2 k_0^2 |F(\rho_0, \omega_0)|^4}{2(2\pi\rho_0)^3} \sum_{m=\pm1} \sum_{m'_1=\pm1} \sum_{m'_2=\pm1} \int_{\mathbf{K}} \int_{\mathbf{K}'_2} \int_{\mathbf{K}'_1} |\Gamma'_H|^2$$
$$\cdot S_1(m\mathbf{K}) S_1(m'\mathbf{K}'_1) S_1(m'\mathbf{K}'_2) |u'_0|^2 \delta(\omega_d + m\sqrt{gK})\delta(\omega_d + m'_1\sqrt{gK'_1} + m'_2\sqrt{gK'_2}) K |g(\theta_{\mathbf{K}})|^2$$
$$\cdot \mathrm{Sa}^2\left[\frac{\Delta\rho}{2}(K - 2k_0)\right] \mathrm{d}\mathbf{K}'_1 \,\mathrm{d}\mathbf{K}'_2 \,\mathrm{d}\mathbf{K}. \tag{4.30}$$

Observing (4.29) and (4.30), it is clear that the integrals over $\mathbf{K}$ and $\mathbf{K}'$ in the former, and $\mathbf{K}$ and the double integral over $\mathbf{K}'_1$ and $\mathbf{K}'_2$ in the latter are iterable. After some algebraic manipulations, (4.29) and (4.30) can be written as a product between integrals:

$$[\mathcal{P}_{11}]_{11}(\omega_d) = \frac{A_r \eta_0 |I_0 \Delta\ell|^2 k_0^2 |F(\rho_0, \omega_0)|^4 A_p}{16(2\pi)^3 \rho_0^4} \left\{ 2^3 \pi k_0^2 \Delta\rho^2 \frac{\rho_0}{A_p} \sum_{m=\pm1} \iint S_1(m\mathbf{K}) \right.$$
$$\left. \cdot \delta(\omega_d + m\sqrt{gK}) K^2 |g(\theta_{\mathbf{K}})|^2 \,\mathrm{Sa}^2\left[\frac{\Delta\rho}{2}(K - 2k_0)\right] \mathrm{d}K \,\mathrm{d}\theta_{\mathbf{K}} \right\} \left\{ 2\pi^2 \sum_{m'=\pm1} \iint S_1(m'\mathbf{K}') \right.$$
$$\left. \cdot |u'_0|^2 K' \delta(\omega_d + m\sqrt{gK'}) \,\mathrm{d}K' \,\mathrm{d}\theta_{\mathbf{K}'} \right\}, \tag{4.31}$$

and

$$[\mathcal{P}_{11}]_{12}(\omega_d) = \frac{A_r \eta_0 |I_0 \Delta\ell|^2 k_0^2 |F(\rho_0,\omega_0)|^4 A_p}{16(2\pi)^3 \rho_0^4} \Bigg\{ 2^3 \pi k_0^2 \Delta\rho^2 \frac{\rho_0}{A_p} \sum_{m=\pm 1} \iint S_1(m\mathbf{K}) \cdot \delta(\omega_d + m\sqrt{gK}) K^2 |g(\theta_{\mathbf{K}})|^2 \,\mathrm{Sa}^2\left[\frac{\Delta\rho}{2}(K-2k_0)\right] \mathrm{d}K \,\mathrm{d}\theta_{\mathbf{K}} \Bigg\} \Bigg\{ \pi^2 \sum_{m_1'=\pm 1} \sum_{m_2'=\pm 1} \iiint\!\!\iint |\Gamma_H'|^2 \cdot S_1(m_1'\mathbf{K}_1') S_1(m_2'\mathbf{K}_2') |u_0'|^2 \delta(\omega_d + m_1'\sqrt{gK_1'} + m_2'\sqrt{gK_2'}) \,\mathrm{d}K_1' \,\mathrm{d}\theta_{\mathbf{K}_1'} \,\mathrm{d}K_2' \,\mathrm{d}\theta_{\mathbf{K}_2'} \Bigg\}, \tag{4.32}$$

where the area of the scattering patch A_p can be approximated by

$$A_p \approx \rho_0 \Delta\rho. \tag{4.33}$$

From intermediate results presented in [17], it is clear that the first integral in both (4.31) and (4.32) is the definition of the first-order HF Doppler radar cross-section $\sigma_{11}(\omega_d)$ over a height-restricted ocean surface. Therefore, making

$$\sigma_{11}(\omega_d) \equiv 2^3 \pi k_0^2 \Delta\rho^2 \frac{\rho_0}{A_p} \sum_{m=\pm 1} \iint S_1(m\mathbf{K}) \delta(\omega_d + m\sqrt{gK}) K^2 |g(\theta_{\mathbf{K}})|^2 \cdot \mathrm{Sa}^2\left[\frac{\Delta\rho}{2}(K-2k_0)\right] \mathrm{d}K \,\mathrm{d}\theta_{\mathbf{K}},$$

the power spectral density of the correction terms can be defined with respect to $\sigma_{11}(\omega_d)$ as

$$[\mathcal{P}_{11}]_{11}(\omega_d) = \frac{A_r \eta_0 |I_0 \Delta\ell|^2 k_0^2 |F(\rho_0,\omega_0)|^4 A_p}{16(2\pi\rho_0)^3} \sigma_{11}(\omega_d) \Bigg\{ 2\pi^2 \sum_{m'=\pm 1} \iint S_1(m'\mathbf{K}') |u_0'|^2 \cdot K' \delta(\omega_d + m\sqrt{gK'}) \,\mathrm{d}K' \,\mathrm{d}\theta_{\mathbf{K}'} \Bigg\}. \tag{4.34}$$

and

$$[\mathcal{P}_{11}]_{12}(\omega_d) = \frac{A_r\eta_0|I_0\Delta\ell|^2k_0^2|F(\rho_0,\omega_0)|^4A_p}{16(2\pi\rho_0)^3}\sigma_{11}(\omega_d)\Bigg\{\pi^2\sum_{m_1'=\pm1}\sum_{m_2'=\pm1}\iiiint|\Gamma_H'|^2$$
$$\cdot S_1(m_1'\mathbf{K}_1')S_1(m_2'\mathbf{K}_2')|u_0'|^2\delta(\omega_d+m_1'\sqrt{gK_1'}+m_2'\sqrt{gK_2'})\,\mathrm{d}K_1'\,\mathrm{d}\theta_{\mathbf{K}_1'}\,\mathrm{d}K_2'\,\mathrm{d}\theta_{\mathbf{K}_2'}\Bigg\}. \tag{4.35}$$

Following the same procedure, the power spectral densities for the corrections to the second-order electric field can be written as

$$[\mathcal{P}_{2P}]_{11}(\omega_d) = 2\pi\frac{A_r\eta_0k_0^4|I_0\Delta\ell|^2|F(\rho_0,\omega_0)|^4\Delta\rho^2}{16(2\pi)\rho_0^3}\sum_{m_1=\pm1}\sum_{m_2=\pm1}\sum_{m'=\pm1}\int_{\mathbf{K}_2}\int_{\mathbf{K}_1}\int_{\mathbf{K}'}|{}_s\Gamma_P|^2$$
$$\cdot S_1(m_1\mathbf{K}_1)S_1(m_2\mathbf{K}_2)S_1(m'\mathbf{K}')|u_0'|^2K\delta(\omega_d+m_1\sqrt{gK_1}+m_2\sqrt{gK_2})\delta(\omega_d+m'\sqrt{gK'})$$
$$\cdot|g(\theta_{\mathbf{K}})|^2\,\mathrm{Sa}^2\left[\frac{\Delta\rho}{2}(K-2k_0)\right]\mathrm{d}\mathbf{K}'\,\mathrm{d}\mathbf{K}_1\,\mathrm{d}\mathbf{K}_2, \tag{4.36}$$

and

$$[\mathcal{P}_{11}]_{12}(\omega_d) = 2\pi\frac{A_r\eta_0k_0^4|I_0\Delta\ell|^2|F(\rho_0,\omega_0)|^4\Delta\rho^2}{32(2\pi)\rho_0^3}\sum_{m_1=\pm1}\sum_{m_2=\pm1}\sum_{m_1'=\pm1}\sum_{m_2'=\pm1}$$
$$\int_{\mathbf{K}_2}\int_{\mathbf{K}_1}\int_{\mathbf{K}_2'}\int_{\mathbf{K}_1'}|{}_s\Gamma_P|^2|\Gamma_H'|^2S_1(m_1'\mathbf{K}_1')S_1(m_2'\mathbf{K}_2')S_1(m_1\mathbf{K}_1)S_1(m_2\mathbf{K}_2)|u_0'|^2K|g(\theta_{\mathbf{K}})|^2$$
$$\cdot\delta(\omega_d+m_1\sqrt{gK_1}+m_2\sqrt{gK_2})\delta(\omega_d+m_1'\sqrt{gK_1'}+m_2'\sqrt{gK_2'})\,\mathrm{Sa}^2\left[\frac{\Delta\rho}{2}(K-2k_0)\right]\mathrm{d}\mathbf{K}_1'\,\mathrm{d}\mathbf{K}_2'$$
$$\cdot\,\mathrm{d}\mathbf{K}_1\,\mathrm{d}\mathbf{K}_2, \tag{4.37}$$

Similar to the corrections to the first-order electric field, the expressions in (4.36) and (4.37) can be expressed as a product between integrals, one solely dependent on height-restricted (unprimed) variables, and the other only dependent on primed terms related to the arbitrary heights function. Therefore, after some algebraic ma-

nipulations, (4.36) and (4.37) can be rewritten as

$$[\mathcal{P}_{2P}]_{11}(\omega_d) = \frac{A_r \eta_0 |I_0 \Delta\ell|^2 k_0^2 |F(\rho_0,\omega_0)|^4 A_p}{16(2\pi\rho_0)^3} \Bigg\{ 2^3 \pi k_0^2 (\Delta\rho)^2 \rho_0 \sum_{m_1=\pm1} \sum_{m_2=\pm1} \int\limits_{\mathbf{K}_2} \int\limits_{\mathbf{K}_1} |{}_s\Gamma_P|^2$$
$$\cdot S_1(m_1\mathbf{K}_1) S_1(m_2\mathbf{K}_2) K \delta(\omega_d + m_1\sqrt{gK_1} + m_2\sqrt{gK_2}) |g(\theta_{\mathbf{K}})|^2 \,\mathrm{Sa}^2\left[\frac{\Delta\rho}{2}(K-2k_0)\right]$$
$$\cdot \,\mathrm{d}\mathbf{K}_1\,\mathrm{d}\mathbf{K}_2 \Bigg\} \Bigg\{ 2\pi^2 \sum_{m'=\pm1} \iint S_1(m'\mathbf{K}') |u_0'|^2 K' \delta(\omega_d + m\sqrt{gK'})\,\mathrm{d}K'\,\mathrm{d}\theta_{\mathbf{K}'} \Bigg\}. \quad (4.38)$$

$$[\mathcal{P}_{2P}]_{12}(\omega_d) = \frac{A_r \eta_0 |I_0 \Delta\ell|^2 k_0^2 |F(\rho_0,\omega_0)|^4 A_p}{16(2\pi\rho_0)^3} \Bigg\{ 2^3 \pi k_0^2 (\Delta\rho)^2 \rho_0 \sum_{m_1=\pm1} \sum_{m_2=\pm1} \int\limits_{\mathbf{K}_2} \int\limits_{\mathbf{K}_1} |{}_s\Gamma_P|^2$$
$$S_1(m_1\mathbf{K}_1) S_1(m_2\mathbf{K}_2) K \delta(\omega_d + m_1\sqrt{gK_1} + m_2\sqrt{gK_2}) |g(\theta_{\mathbf{K}})|^2 \,\mathrm{Sa}^2\left[\frac{\Delta\rho}{2}(K-2k_0)\right]$$
$$\cdot \,\mathrm{d}\mathbf{K}_1\,\mathrm{d}\mathbf{K}_2 \Bigg\} \Bigg\{ \pi^2 \sum_{m_1'=\pm1} \sum_{m_2'=\pm1} \iiiint |\Gamma_H'|^2 S_1(m_1'\mathbf{K}_1') S_1(m_2'\mathbf{K}_2') |u_0'|^2$$
$$\cdot \delta(\omega_d + m_1'\sqrt{gK_1'} + m_2'\sqrt{gK_2'})\,\mathrm{d}K_1'\,\mathrm{d}\theta_{\mathbf{K}_1'}\,\mathrm{d}K_2'\,\mathrm{d}\theta_{\mathbf{K}_2'} \Bigg\}. \quad (4.39)$$

Noting again that the first bracketed term is equivalent to an intermediate step in the derivation of the second-order radar cross-section for a height-restricted ocean surface $\sigma_{2P}(\omega_d)$ presented in [17], (4.38) and (4.39) can be further reduced to

$$[\mathcal{P}_{2P}]_{11}(\omega_d) = \frac{A_r \eta_0 |I_0 \Delta\ell|^2 k_0^2 |F(\rho_0,\omega_0)|^4 A_p}{16(2\pi\rho_0)^3} \sigma_{2P}(\omega_d) \Bigg\{ 2\pi^2 \sum_{m'=\pm1} \iint S_1(m'\mathbf{K}') |u_0'|^2$$
$$\cdot K' \delta(\omega_d + m\sqrt{gK'})\,\mathrm{d}K'\,\mathrm{d}\theta_{\mathbf{K}'} \Bigg\}. \quad (4.40)$$

and

$$[\mathcal{P}_{2P}]_{12}(\omega_d) = \frac{A_r \eta_0 |I_0 \Delta\ell|^2 k_0^2 |F(\rho_0,\omega_0)|^4 A_p}{16(2\pi\rho_0)^3} \sigma_{2P}(\omega_d) \Bigg\{ \pi^2 \sum_{m_1'=\pm1} \sum_{m_2'=\pm1} \iiiint |\Gamma_H'|^2$$
$$\cdot S_1(m_1'\mathbf{K}_1') S_1(m_2'\mathbf{K}_2') |u_0'|^2 \delta(\omega_d + m_1'\sqrt{gK_1'} + m_2'\sqrt{gK_2'})\,\mathrm{d}K_1'\,\mathrm{d}\theta_{\mathbf{K}_1'}\,\mathrm{d}K_2'\,\mathrm{d}\theta_{\mathbf{K}_2'} \Bigg\}, \quad (4.41)$$

where

$$\sigma_{2P}(\omega_d) = 2^3\pi k_0^2(\Delta\rho)^2\rho_0 \sum_{m_1=\pm1}\sum_{m_2=\pm1}\int_{\mathbf{K}_2}\int_{\mathbf{K}_1} |{}_s\Gamma_P|^2 S_1(m_1\mathbf{K}_1)S_1(m_2\mathbf{K}_2)K$$
$$\cdot\,\delta(\omega_d + m_1\sqrt{gK_1} + m_2\sqrt{gK_2})|g(\theta_{\mathbf{K}})|^2\,\mathrm{Sa}^2\left[\frac{\Delta\rho}{2}(K-2k_0)\right]\mathrm{d}\mathbf{K}_1\,\mathrm{d}\mathbf{K}_2. \quad (4.42)$$

Comparing the first- and second-order correction terms, it is clear that the bracketed terms in (4.34) and (4.40) are identical, as well as the ones presented in (4.35) and (4.41). This suggests a pattern for the first- and second-order hydrodynamic corrections, indicating that terms with the same correction order share a common factor. Therefore, defining the first-order hydrodynamic, first-order correction factor Ξ_{11} as

$$\Xi_{11}(\omega_d) = 2\pi^2\sum_{m'=\pm1}\iint S_1(m'\mathbf{K}')|K'^2 - {k_0}^2|\delta(\omega_d + m\sqrt{gK'})K'\,\mathrm{d}K'\,\mathrm{d}\theta_{\mathbf{K}'} \quad (4.43)$$

and the second-order hydrodynamic, first-order correction factor Ξ_{12} as

$$\Xi_{12}(\omega_d) = \pi^2\sum_{m_1'=\pm1}\sum_{m_2'=\pm1}\iiiint |\Gamma_H'|^2 S_1(m_1'\mathbf{K}_1')S_1(m_2'\mathbf{K}_2')\left||\mathbf{K}_1+\mathbf{K}_2|^2 - {k_0}^2\right|$$
$$\cdot\,\delta(\omega_d + m_1'\sqrt{gK_1'} + m_2'\sqrt{gK_2'})K_1'K_2'\,\mathrm{d}K_1'\,\mathrm{d}\theta_{\mathbf{K}_1'}\,\mathrm{d}K_2'\,\mathrm{d}\theta_{\mathbf{K}_2'}, \quad (4.44)$$

the power spectral densities for the first- and second-order corrections to the electric field can be further reduced to the following forms:

$$[\mathcal{P}_{11}]_{11}(\omega_d) = \frac{A_r\eta_0|I_0\Delta\ell|^2k_0^2|F(\rho_0,\omega_0)|^4A_p}{16(2\pi\rho_0)^3}\sigma_{11}(\omega_d)\Xi_{11}(\omega_d), \quad (4.45)$$

$$[\mathcal{P}_{11}]_{12}(\omega_d) = \frac{A_r\eta_0|I_0\Delta\ell|^2k_0^2|F(\rho_0,\omega_0)|^4A_p}{16(2\pi\rho_0)^3}\sigma_{11}(\omega_d)\Xi_{12}(\omega_d), \quad (4.46)$$

$$[\mathcal{P}_{2P}]_{11}(\omega_d) = \frac{A_r\eta_0|I_0\Delta\ell|^2k_0^2|F(\rho_0,\omega_0)|^4A_p}{16(2\pi\rho_0)^3}\sigma_{2P}(\omega_d)\Xi_{11}(\omega_d), \quad (4.47)$$

and

$$[\mathcal{P}_{2P}]_{12}(\omega_d) = \frac{A_r \eta_0 |I_0 \Delta\ell|^2 k_0^2 |F(\rho_0, \omega_0)|^4 A_p}{16(2\pi\rho_0)^3} \sigma_{2P}(\omega_d) \Xi_{12}(\omega_d). \tag{4.48}$$

Now that the power spectral density of the first-order correction terms have been defined, the expressions for the second-order correction terms must be derived.

4.2.2 Power Spectral Density of the Second-Order Correction Terms

Taking first the autocorrelation for the first-order hydrodynamic, second-order correction the the first-order electric field presented in (4.24) and applying the Fourier transform with respect to the time lag τ, the power spectral density $[\mathcal{P}_{11}]_{21}$ can be obtained as

$$\begin{aligned}[\mathcal{P}_{11}]_{21}(\omega_d) = \pi^3 k_0^2 \Delta\rho^2 \frac{A_r \eta_0 |I_0 \Delta\ell|^2 k_0^2 |F(\rho_0, \omega_0)|^4}{4(2\pi\rho_0)^3} \sum_{m=\pm1} \sum_{m'=\pm1} \sum_{m''=\pm1} \int \cdots \int S_1(m\mathbf{K}) \\ \cdot S_1(m'\mathbf{K}') S_1(m''\mathbf{K}'') |u_0'|^2 |u_0''|^2 K \delta(\omega_d - \omega_{\mathbf{K}}) \delta(\omega_{\mathbf{K}} + m\sqrt{gK}) \delta(\omega_{\mathbf{K}'} + m'\sqrt{gK'}) \\ \cdot \delta(\omega_{\mathbf{K}} + m'\sqrt{gK'} + m''\sqrt{gK''}) |g(\theta_{\mathbf{K}})|^2 \,\mathrm{Sa}^2 \left[\frac{\Delta\rho}{2}(K - 2k_0)\right] \mathrm{d}\omega_{\mathbf{K}} \,\mathrm{d}\omega_{\mathbf{K}'} \,\mathrm{d}\mathbf{K}' \,\mathrm{d}\mathbf{K}'' \,\mathrm{d}\mathbf{K}.\end{aligned} \tag{4.49}$$

Using the reproducing property of the Dirac delta

$$\begin{aligned}&\delta(\omega_d - \omega_{\mathbf{K}}) \delta(\omega_{\mathbf{K}} + m\sqrt{gK}) \delta(\omega_{\mathbf{K}'} + m'\sqrt{gK'}) \delta(\omega_{\mathbf{K}'} - \omega_{\mathbf{K}'} + m''\sqrt{gK''}) \\ &\quad = \delta(\omega_d - \omega_{\mathbf{K}}) \delta(\omega_{\mathbf{K}'} + m'\sqrt{gK'}) \delta(\omega_d + m\sqrt{gK}) \delta(\omega_d + m'\sqrt{gK'} + m''\sqrt{gK''})\end{aligned}$$

and performing the integration over $\omega_{\mathbf{K}}$ and $\omega_{\mathbf{K}'}$, (4.49) becomes:

$$[\mathcal{P}_{11}]_{21}(\omega_d) = \pi^3 k_0^2 \Delta\rho^2 \frac{A_r \eta_0 |I_0 \Delta\ell|^2 k_0^2 |F(\rho_0,\omega_0)|^4}{4(2\pi\rho_0)^3} \sum_{m=\pm1}\sum_{m'=\pm1}\sum_{m''=\pm1} \int\cdots\int S_1(m\mathbf{K})$$

$$\cdot S_1(m'\mathbf{K}') S_1(m''\mathbf{K}'') K^2 |g(\theta_{\mathbf{K}})|^2 \delta(\omega_d + m\sqrt{gK}) \delta(\omega_d + m'\sqrt{gK'} + m''\sqrt{gK''}) |u_0'|^2 |u_0''|^2 K'$$

$$\cdot K'' \,\mathrm{Sa}^2\left[\frac{\Delta\rho}{2}(K - 2k_0)\right] \mathrm{d}K \,\mathrm{d}\theta_{\mathbf{K}} \,\mathrm{d}K' \,\mathrm{d}\theta_{\mathbf{K}'} \,\mathrm{d}K'' \,\mathrm{d}\theta_{\mathbf{K}''}. \quad (4.50)$$

As observed in Section 4.2.1, the integrals in (4.50) can be represented as a product between two integrals:

$$[\mathcal{P}_{11}]_{21}(\omega_d) = \frac{A_r \eta_0 |I_0 \Delta\ell|^2 k_0^2 |F(\rho_0,\omega_0)|^4}{16(2\pi\rho_0)^3} \left\{ 2^3 \pi k_0^2 \Delta\rho^2 \rho_0 \sum_{m=\pm1} \iint S_1(m\mathbf{K}) K^2 |g(\theta_{\mathbf{K}})|^2 \right.$$

$$\left. \cdot\, \delta(\omega_d + m\sqrt{gK})\, \mathrm{Sa}^2\left[\frac{\Delta\rho}{2}(K - 2k_0)\right] \mathrm{d}K \,\mathrm{d}\theta_{\mathbf{K}} \right\} \left\{ \frac{\pi^2}{2} \sum_{m'=\pm1}\sum_{m''=\pm1} \iiint S_1(m'\mathbf{K}') \right.$$

$$\left. \cdot\, S_1(m''\mathbf{K}'') \delta(\omega_d + m'\sqrt{gK'} + m''\sqrt{gK''}) |u_0'|^2 |u_0''|^2 K' K'' \,\mathrm{d}K' \,\mathrm{d}\theta_{\mathbf{K}'} \,\mathrm{d}K'' \,\mathrm{d}\theta_{\mathbf{K}''} \right\}. \quad (4.51)$$

As in Section 4.2.1 the first bracketed term can be identified as the first-order radar cross-section $\sigma_{11}(\omega_d)$ for a height-restricted ocean surface. Therefore, (4.51) can be rewritten as

$$[\mathcal{P}_{11}]_{21}(\omega_d) = \frac{A_r \eta_0 |I_0 \Delta\ell|^2 k_0^2 |F(\rho_0,\omega_0)|^4}{16(2\pi\rho_0)^3} \sigma_{11}(\omega_d) \left\{ \frac{\pi^2}{2} \sum_{m'=\pm1}\sum_{m''=\pm1} \iiint S_1(m'\mathbf{K}') \right.$$

$$\left. \cdot\, S_1(m''\mathbf{K}'') |u_0'|^2 |u_0''|^2 \delta(\omega_d + m'\sqrt{gK'} + m''\sqrt{gK''}) K' K'' \,\mathrm{d}K' \,\mathrm{d}\theta_{\mathbf{K}'} \,\mathrm{d}K'' \,\mathrm{d}\theta_{\mathbf{K}''} \right\}. \quad (4.52)$$

Now, applying the Fourier transform to the autocorrelation of the first-order hydrodynamic, second-order correction to the second-order electric field presented in

(4.25) and following the steps presented for the correction to the first-order, the expression for $[\mathcal{P}_{2P}]_{21}$ can be written as

$$[\mathcal{P}_{2P}]_{21}(\omega_d) = \pi^3 k_0^2 \Delta\rho^2 \frac{A_r \eta_0 |I_0 \Delta\ell|^2 k_0^2 |F(\rho_0,\omega_0)|^4}{4(2\pi\rho_0)^3} \sum_{m_1=\pm1}\sum_{m_2=\pm1}\sum_{m'=\pm1}\sum_{m''=\pm1} \int\cdots\int$$
$$\cdot |{}_s\Gamma_P|^2 S_1(m_1\mathbf{K}_1) S_1(m_2\mathbf{K}_2) S_1(m'\mathbf{K}') S_1(m''\mathbf{K}'') |u_0'|^2 |u_0''|^2 K \delta(\omega_d + m_1\sqrt{gK} + m_2\sqrt{gK})$$
$$\cdot \delta(\omega_d + m'\sqrt{gK'} + m''\sqrt{gK''}) |g(\theta_{\mathbf{K}})|^2 \,\mathrm{Sa}^2\left[\frac{\Delta\rho}{2}(K-2k_0)\right] \mathrm{d}\omega_{\mathbf{K}_1}\,\mathrm{d}\omega_{\mathbf{K}_2}\,\mathrm{d}\omega_{\mathbf{K}'}\,\mathrm{d}\mathbf{K}'\,\mathrm{d}\mathbf{K}''\,\mathrm{d}\mathbf{K}_1$$
$$\cdot\,\mathrm{d}\mathbf{K}_2. \quad (4.53)$$

Similar to (4.50), it is easy to show that the integrals in (4.53) can be represented as a product between integrals. After some algebraic manipulation, (4.53) can be rewritten as

$$[\mathcal{P}_{2P}]_{21}(\omega_d) = \frac{A_r \eta_0 |I_0 \Delta\ell|^2 k_0^2 |F(\rho_0,\omega_0)|^4}{16(2\pi\rho_0)^3} \Bigg\{ 2^3 \pi k_0^2 (\Delta\rho)^2 \rho_0 \sum_{m_1=\pm1}\sum_{m_2=\pm1} \int_{\mathbf{K}_2}\int_{\mathbf{K}_1} |{}_s\Gamma_P|^2$$
$$\cdot S_1(m_1\mathbf{K}_1) S_1(m_2\mathbf{K}_2) K \delta(\omega_d + m_1\sqrt{gK_1} + m_2\sqrt{gK_2}) |g(\theta_{\mathbf{K}})|^2 \,\mathrm{Sa}^2\left[\frac{\Delta\rho}{2}(K-2k_0)\right] \mathrm{d}\mathbf{K}_1$$
$$\cdot\,\mathrm{d}\mathbf{K}_2. \Bigg\} \Bigg\{ \frac{\pi^2}{2} \sum_{m'=\pm1}\sum_{m''=\pm1} \iiiint S_1(m'\mathbf{K}') S_1(m''\mathbf{K}'') \delta(\omega_d + m'\sqrt{gK'} + m''\sqrt{gK''}) |u_0'|^2$$
$$\cdot |u_0''|^2 K' K'' \,\mathrm{d}K' \,\mathrm{d}\theta_{\mathbf{K}'} \,\mathrm{d}K'' \,\mathrm{d}\theta_{\mathbf{K}''} \Bigg\}. \quad (4.54)$$

As in Section 4.2.1, the first term in brackets can be identified as an intermediary step in the derivation of the second-order radar cross-section $\sigma_{2P}(\omega_d)$ of a height-restricted ocean surface [17]. Therefore, (4.54) can be rewritten as

$$[\mathcal{P}_{2P}]_{21}(\omega_d) = \frac{A_r \eta_0 |I_0 \Delta\ell|^2 k_0^2 |F(\rho_0,\omega_0)|^4}{16(2\pi\rho_0)^3} \sigma_{2P}(\omega_d) \Bigg\{ \frac{\pi^2}{2} \sum_{m'=\pm1}\sum_{m''=\pm1} \iint S_1(m'\mathbf{K}')$$
$$\cdot S_1(m''\mathbf{K}'') |u_0'|^2 |u_0''|^2 \delta(\omega_d + m'\sqrt{gK'} + m''\sqrt{gK''}) K' K'' \,\mathrm{d}K' \,\mathrm{d}\theta_{\mathbf{K}'} \,\mathrm{d}K'' \,\mathrm{d}\theta_{\mathbf{K}''} \Bigg\}. \quad (4.55)$$

From (4.52) and (4.55), it is clear that both expressions share identical bracketed terms. Similar to the observation made in Section 4.2.1, the expressions seem to follow a pattern, where terms of the same correction order share the same factor. Therefore, defining the first-order hydrodynamic, second-order correction factor Ξ_{21} as

$$\Xi_{21}(\omega_d) = \frac{\pi^2}{2} \sum_{m'=\pm 1} \sum_{m''=\pm 1} \iiint S_1(m'\mathbf{K}') S_1(m''\mathbf{K}'') |K'^2 - {k_0}^2||K''^2 - {k_0}^2| \\ \cdot \delta(\omega_d + m'\sqrt{gK'} + m''\sqrt{gK''}) K' K'' \, \mathrm{d}K' \, \mathrm{d}\theta_{\mathbf{K}'} \, \mathrm{d}K'' \, \mathrm{d}\theta_{\mathbf{K}''}. \quad (4.56)$$

the power spectral densities for the first-order hydrodynamic, second-order correction terms to the electric field can be written as

$$[\mathcal{P}_{11}]_{21}(\omega_d) = \frac{A_r \eta_0 |I_0 \Delta\ell|^2 k_0^2 |F(\rho_0, \omega_0)|^4 A_p}{16(2\pi\rho_0)^3} \sigma_{11}(\omega_d) \Xi_{21}(\omega_d), \quad (4.57)$$

and

$$[\mathcal{P}_{2P}]_{21}(\omega_d) = \frac{A_r \eta_0 |I_0 \Delta\ell|^2 k_0^2 |F(\rho_0, \omega_0)|^4 A_p}{16(2\pi\rho_0)^3} \sigma_{2P}(\omega_d) \Xi_{21}(\omega_d). \quad (4.58)$$

Comparing the power spectral densities for the height-restricted electric fields presented in [17] to the ones derived for the first-order corrections in (4.45) to (4.48), as well as the second-order corrections in (4.57) and (4.58), a general pattern seems to emerge: the correction to the power spectral density of a term can be obtained by merely multiplying the height-restricted power spectral density by the correction factor at the desired order. This pattern simplifies the derivation of the radar cross-section for the ocean surface with arbitrary wave heights, as shown in the next Section.

4.3 Radar Cross-Section of the Correction Terms for an Ocean Surface With Electromagnetically-Large Waves

According to Barrick [120], for a narrowband transmission, the radar equation can be defined with respect to the received Doppler spectrum for a differential scattering area $\mathrm{d}A_p$ as [120], [133], [134],

$$\mathrm{d}\mathcal{P}_r(\omega_d) = \frac{\mathcal{P}_t G_t G_r |F(\rho_1, \omega_0)|^2 |F(\rho_2, \omega_0)|^2 \lambda_0^2}{(4\pi)^3 {\rho_1}^2 {\rho_2}^2} \sigma(\omega_d)\, \mathrm{d}A_p \tag{4.59}$$

where $\mathcal{P}_r$ is the received power, $\mathcal{P}_t$ is the transmitted power, $\sigma(\omega_d)$ is the radar cross-section of the scattering body, ρ_1 and ρ_2 are respectively the distance between transmitter and scattering patch, and the distance between scattering body and receiver as defined in Figure 3.1, G_t and G_r are respectively the transmitter and receiver gains, $F(\rho_n, \omega_0)$ is the path attenuation function for each distance $\rho_n,\ n = 1, 2$ (e.g. [35], [143]), and λ_0 is the representative wavelength of the transmitted signal [120].

From [144], the effective aperture of the receiving antenna can be defined as

$$A_r = \frac{\lambda_0^2}{4\pi} G_r. \tag{4.60}$$

Also, the power radiated by a dipole of length $\Delta\ell$ is [140]

$$\mathcal{P}_{rad} = \frac{\eta_0}{12\pi} k_0^2 |I_0 \Delta\ell|^2. \tag{4.61}$$

Thus, knowing that the power pattern for a short dipole can be calculated as [140]

$$\mathcal{P}(r, \theta) = \frac{1}{2} \frac{k_0^2 \eta_2 |I_0 \Delta\ell|^2}{(4\pi r)^2} \sin^2\theta$$

and that the gain of an antenna can be defined as

$$G = \varepsilon_R \frac{\mathcal{P}(r,\theta)}{\frac{\mathcal{P}_{rad}}{4\pi r^2}},$$

where ε_R is the antenna efficiency and $\mathcal{P}_{rad}$ is the power radiated by the antenna, the gain of a lossless vertical dipole transmitter of length $\Delta\ell$ can be defined as

$$G_t = \frac{3}{4}\sin^2\theta. \tag{4.62}$$

Therefore, considering the maximum gain of the transmitter and substituting (4.60) to (4.62) into (4.59), the radar equation for a vertical dipole source can be written as

$$\mathrm{d}\mathcal{P}_r(\omega_d) = \frac{A_r \eta_0 |I_0 \Delta\ell|^2 k_0^2 |F(\rho_0,\omega_0)|^4}{16(2\pi\rho_0)^3}\sigma(\omega_d)\,\mathrm{d}A_p \tag{4.63}$$

Therefore, to obtain the radar cross-section of the ocean surface using the radar equation, the power spectral density of the received signal should be differentiated with respect to the area of the scattering patch and the resulting expression should be compared with the radar equation in (4.63). From (4.26), the expression for the derivative of the power spectral density of the received signal with respect to the area of the scattering patch can be written as

$$\frac{\mathrm{d}\mathcal{P}(\omega_d)}{\mathrm{d}A_p} = \sum_m \sum_n \frac{\mathrm{d}\mathcal{P}_{mn}(\omega_d)}{\mathrm{d}A_p} + \sum_m \sum_n \sum_p \sum_q \frac{\mathrm{d}[\mathcal{P}_{mn}]_{pq}(\omega_d)}{\mathrm{d}A_p}. \tag{4.64}$$

The first term in the summation shown in (4.64) shows the expressions used to obtain the radar cross-sections for a height-restricted ocean surface presented as in [18], [120]. To obtain the radar cross-section of the correction terms normalized to the scattering area, the power spectral densities of the correction terms should be differentiated with respect to the area of the scattering patch.

In Section 4.2, it was shown that, at least up to the first-order hydrodynamic, second-order correction to the electric field, the power spectral density of the correction terms fit the pattern

$$[\mathcal{P}_{mn}]_{pq}(\omega_d) = [\mathcal{P}_{mn}]_{pq}(\omega_d) = \frac{A_r \eta_0 |I_0 \Delta\ell|^2 k_0^2 |F(\rho_0, \omega_0)|^4 A_p}{16(2\pi\rho_0)^3} \sigma_{mn}(\omega_d) \Xi_{pq}(\omega_d), \quad (4.65)$$

where neither the height-restricted radar cross-section, nor the correction factors present any dependence on the area of the scattering patch. Therefore, the derivative of the power spectral density of the correction terms with respect to the area of the scattering patch can be written as

$$\frac{\mathrm{d}[\mathcal{P}_{mn}]_{pq}(\omega_d)}{\mathrm{d}A_p} = \frac{A_r \eta_0 |I_0 \Delta\ell|^2 k_0^2 |F(\rho_0, \omega_0)|^4}{16(2\pi\rho_0)^3} \sigma_{mn}(\omega_d) \Xi_{pq}(\omega_d). \quad (4.66)$$

Therefore, the correction terms of the radar cross-section of an ocean surface with electromagnetically-large waves can be defined for the first- and second-order hydrodynamic, first-order correction terms and for the first-order hydrodynamic, second-order correction term as

$$[\sigma_{mn}]_{pq}(\omega_d) = \sigma_{mn}(\omega_d) \Xi_{pq}(\omega_d). \quad (4.67)$$

From (4.67), it is clear that the radar cross-section terms resulting from the correction terms for the electric field scattered by an ocean surface with electromagnetically-large waves presented in Chapter 3 depend on the correction factors $\Xi_{pq}(\omega_d)$, which are common for terms of the same correction order. Therefore, an analysis of these correction terms is important to understand how they impact the total radar cross-section.

4.4 Correction Factors to the Radar Cross-Section of an Ocean Surface with Electromagnetically-Large Waves

As presented in Section 4.3, the correction terms of the radar cross-section are a product between their height-restricted terms and the correction factors $\Xi_{pq}(\omega_d)$. To analyze these correction terms, their expressions are repeated here:

$$\Xi_{11}(\omega_d) = 2\pi^2 \sum_{m'=\pm 1} \iint S_1(m'\mathbf{K}')|K'^2 - {k_0}^2|\delta(\omega_d + m\sqrt{gK'})K'\,\mathrm{d}K'\,\mathrm{d}\theta_{\mathbf{K}'} \quad (4.68)$$

$$\Xi_{12}(\omega_d) = \pi^2 \sum_{m_1'=\pm 1} \sum_{m_2'=\pm 1} \iiiint |\Gamma_H'|^2 S_1(m_1'\mathbf{K}_1')S_1(m_2'\mathbf{K}_2') \left||\mathbf{K}_1 + \mathbf{K}_2|^2 - {k_0}^2\right|$$
$$\cdot\, \delta(\omega_d + m_1'\sqrt{gK_1'} + m_2'\sqrt{gK_2'})K_1'K_2'\,\mathrm{d}K_1'\,\mathrm{d}\theta_{\mathbf{K}_1'}\,\mathrm{d}K_2'\,\mathrm{d}\theta_{\mathbf{K}_2'}, \quad (4.69)$$

$$\Xi_{21}(\omega_d) = \frac{\pi^2}{2} \sum_{m'=\pm 1} \sum_{m''=\pm 1} \iiiint S_1(m'\mathbf{K}')S_1(m''\mathbf{K}'')|K'^2 - {k_0}^2||K''^2 - {k_0}^2|$$
$$\cdot\, \delta(\omega_d + m'\sqrt{gK'} + m''\sqrt{gK''})K'K''\,\mathrm{d}K'\,\mathrm{d}\theta_{\mathbf{K}'}\,\mathrm{d}K''\,\mathrm{d}\theta_{\mathbf{K}''}. \quad (4.70)$$

These expressions are respectively the first- and second-order hydrodynamic, first-order correction factors, and the first-order hydrodynamic, second-order correction factor. These terms can be applied to any order of the radar cross-section of the ocean surface, but their effects are clearly different for each term. For instance, knowing that the nondirectional wavenumber spectrum of the ocean surface can be defined as

$$S(K) = \int_{\theta_{\mathbf{K}}} S(\mathbf{K}) d\theta_{\mathbf{K}}, \quad (4.71)$$

and observing (4.68) and (4.70), it is clear that both expressions can be rewritten solely in terms of the nondirectional spectrum:

$$\Xi_{11}(\omega_d) = 2\pi^2 \sum_{m'=\pm 1} \int S_1(m'K')|K'^2 - {k_0}^2|\delta(\omega_d + m\sqrt{gK'})K' \,\mathrm{d}K' \tag{4.72}$$

$$\Xi_{21}(\omega_d) = \frac{\pi^2}{2} \sum_{m'=\pm 1} \sum_{m''=\pm 1} \iint S_1(m'K')S_1(m''K'')|K'^2 - {k_0}^2||K''^2 - {k_0}^2| \cdot \delta(\omega_d + m'\sqrt{gK'} + m''\sqrt{gK''})K'K'' \,\mathrm{d}K' \,\mathrm{d}K''. \tag{4.73}$$

From (4.72) and (4.73), it can be observed that neither correction factor depends on the directional distribution of the ocean wave spectrum, retaining only the ocean wave spectrum terms related to the energy content of the ocean waves. This suggests that the first-order hydrodynamic terms presented here are compensating for the energy information missing due to the small-height approximation, independent of the direction the ocean waves are travelling. On the other hand, (4.69) retains the directional dependence in the argument of the integral, as the sum between $\mathbf{K}_1'$ and $\mathbf{K}_2'$ is present in the $|u_0|^2$ and would be included in the integrals with respect to $\theta_{\mathbf{K}_1}$ and $\theta_{\mathbf{K}_2}$.

Observing both (4.69) and (4.73), it is evident that both factors contain a Dirac delta function similar to the one present in the second-order radar cross-section, as shown in (4.42). However, unlike the second-order radar cross-section described in [17], the two wave vectors in each of these expressions do not add up to the Bragg wave vector, as this condition comes from the assumption of a sufficiently large patch width, which reduces the sampling function to a Dirac delta [17]. This restricts the ability to simplify the expressions in (4.69) and (4.73) to a more tractable form, since

both wave vectors can assume any magnitude or direction, as long as it fulfills the condition imposed by the Dirac delta argument. On the other hand, (4.72) can be reduced to the form

$$\Xi_{11}(\omega_d) = 2^2\pi^2 S_1(K)|K^2 - {k_0}^2|\frac{K^{3/2}}{\sqrt{g}}, \tag{4.74}$$

with $K' = \omega_d^2/g$. In this case, the value of K' is equal to the one found for K in the first-order height-restricted radar cross-section presented in [17], allowing, for example, the first-order hydrodynamic, first-order correction to the first-order radar cross section to be written as

$$[\sigma_{11}]_{11}(\omega_d) = 2^6\pi^3 k_0^2 \Delta\rho \sum_{m=\pm 1} S(m\mathbf{K})S(K)|K^2 - {k_0}^2|\frac{K^4}{g}\,\mathrm{Sa}^2\left[\frac{\Delta\rho}{2}(K - 2k_0)\right]. \tag{4.75}$$

In terms of the energy distribution of the correction terms with respect to the Doppler frequency, it is clear from the integrands in all three correction terms that the energy distribution depends on the interaction between the $|u_0|^2$ functions, Dirac delta conditions for the Doppler frequency, and ocean wave spectra. For instance, considering the first-order hydrodynamic, first order correction term $\Xi_{11}(\omega_d)$, the value of K' will be determined by the Dirac delta function in (4.72), such that $K' = \omega_d^2/g$. Substituting this relationship in $|u_0'|^2$ and considering a monostatic radar configuration, $|u_0'|^2$ in will be equal to zero when

$$\omega_d = \pm\frac{\omega_B}{\sqrt{2}}, \tag{4.76}$$

where ω_B is the Bragg frequency for deep-water waves, defined as $\omega_B = \sqrt{2gk_0}$ [17].

The dynamics between ocean wave spectra and u_0 is more complicated in the higher-order correction terms. In the second-order hydrodynamic, first-order correction factor, the balancing dynamic occurs between the two ocean wave spectra, the

hydrodynamic coupling coefficient, and $|u_0'|^2$. The relationship between these terms makes the analysis more complicated, as each of these terms includes their own maxima and minima with respect to the Doppler frequency, determined by the argument of the Dirac delta in (4.69), with some of them depending on the resulting wave direction. However, it is clear that the minima at $\pm\omega_B/\sqrt{2}$ introduced by $|u_0|^2$ still influences the resulting correction factor, limiting the growth of the function between these values. As for $\Xi_{21}(\omega_d)$, the competing mechanisms to increase the maxima are the ocean wave spectrum and $|u_0|^2$ for each different ocean wave number in (4.56). Since the Dirac delta in (4.56) imposes a condition that needs to be fulfilled in the integration, the zeros in the expression will depend on the solution of the nonlinear system involving the argument of the Dirac delta and the product between $|u_0'|^2$ and $|u_0''|^2$. From (4.73), the product between $|u_0'|^2$ and $|u_0''|^2$ can be written as

$$|u_0'|^2|u_0''|^2 = |K'^2 - {k_0}^2||K''^2 - {k_0}^2| = |k_0^4 - (K'^2 + K''^2)k_0^2 + K'^2K^2|. \tag{4.77}$$

To obtain the relationship between Doppler frequency and $|u_0'|^2|u_0''|^2$, the argument of the Dirac delta in (4.73) must be considered, as it determines the relationship between ω_d, K', and K''. Knowing that $m', m' = \pm 1$, it is possible to rewrite the argument of the Dirac delta in (4.73) as

$$K' + 2m'm''\sqrt{K'K''} + K'' = \frac{\omega_d^2}{g}.$$

After some algebraic manipulation, it can be verified that

$$K'^2K''^2 = \frac{1}{16}\left[\frac{\omega_d}{g} - (K' + K'')\right]^4. \tag{4.78}$$

Substituting (4.78) into (4.77), results in

$$|u_0'|^2|u_0''|^2 = \left|\frac{[\omega_d^2 - g(K' + K'')]^4}{16g^4} - k_0^2(K'^2 + K''^2) + k_0^4\right|.$$

By equating the product between $|u_0'|^2$ and $|u_0''|^2$ to zero and solving for ω_d, the following four possible pairs of Doppler frequencies where $|u_0'|^2|u_0''|^2$ is null can be obtained:

$$\omega_d = \pm\sqrt{-2(g^4k_0^2(K'^2 + K''^2 - k_0^2))^{1/4} + g(K' + K'')} \tag{4.79}$$

$$\omega_d = \pm\sqrt{-2j(g^4k_0^2(K'^2 + K''^2 - k_0^2))^{1/4} + g(K' + K'')} \tag{4.80}$$

$$\omega_d = \pm\sqrt{2j(g^4k_0^2(K'^2 + K''^2 - k_0^2))^{1/4} + g(K' + K'')} \tag{4.81}$$

$$\omega_d = \pm\sqrt{2(g^4k_0^2(K'^2 + K''^2 - k_0^2))^{1/4} + g(K' + K'')}. \tag{4.82}$$

As the Doppler frequencies in (4.79) to (4.82) depend on K' and K', null patterns in (4.73) will not be as straightforward as in the case of the first-order hydrodynamic, first-order correction shown in (4.76).

4.5 General Chapter Summary

In this chapter, the general form of the radar cross-section of an ocean surface with electromagnetically-large waves has been presented. The chosen approach to obtain the radar cross-section expressions was the comparison between the power spectral density of the electric field and the radar equation, as defined, for example, in [18], [120]. First, the autocorrelation of the electric field expressions presented in Chapter 3 was derived, assuming that the ocean surface displacement could be represented by stationary Gaussian process, as proposed in [75], [123], [135], such that the autocorrelation could be solely dependent on the time delay in the autocorrelation. It was shown that the cross-correlation terms between height-restricted and correction terms are null due to the definition of the Fourier coefficients. This shows the the total radar

cross-section to be a linear combination of the autocorrelation of the height-restricted and correction expressions for the electric field.

Once the autocorrelation expressions were derived, the power spectral density of the correction terms was obtained through a Fourier transform with respect to the autocorrelation lag. After applying the reproducing property of the Dirac delta, it was shown that the power spectral density of the correction terms could be represented by a product between two integrals, with one of them being an intermediary step in the height-restricted radar cross-section of the term being corrected, and the other term being shared among correction terms of the same order. The latter integrals were then identified as correction factors for each of the correction orders and the power spectral density was reduced to a common coefficient and the product between the radar cross-section of the corrected term and the correction factor relative to the correction order.

After the power spectral densities of the correction terms were obtained, their contributions to the radar cross-section were derived. Following the procedure as in [18], it was shown that the derivative of the power spectral densities of the correction terms with respect to the area of the scattering patch was identical to the one included in the radar equation for the power received by a differential element of the scattering patch, with a dipole source acting as the transmitter. This results in a radar cross-section for the correction terms found in (4.67), defined by the product between the radar cross-section term being corrected and the correction factor derived in the power spectral density calculations. This simple form was derived only for the first- and second-order hydrodynamic, first-order correction terms and for the first-order hydrodynamic, second order correction, but indicates a pattern for the subsequent

correction terms.

It is important to note that the expressions presented here were derived considering a monostatic radar configuration, and have been partly presented in [97], [100], [101], with the derivation of the general form of the correction terms included in [145], which is under review at the time of this writing. A bistatic expression for the first-order hydrodynamic, first-order radar cross-section has been presented in [96], without including the general form considerations; these derivations have been included in Appendix C.

It is clear that the effect of the correction terms on the total radar cross-section will be heavily dependent on the correction factors derived in this chapter. Therefore, it is important to conduct a morphological analysis of the correction terms presented here to better understand their form and behaviour under a variety of ocean conditions. Also, it is important to observe whether the behaviour of the resulting total radar cross-sections is similar to the one observed in the literature, as well as in field measurements where the small-height restriction has been violated.

Chapter 5

Analysis of the Correction Factors and Evidence of Their Presence in Field Data

As observed in Chapter 4, the power spectral density and, consequently, the radar cross-section corresponding to the electric field correction terms originating from the arbitrary heights factor presented in Chapter 3 can be obtained by a product between their height-restricted versions and functions that are defined according to the order of the correction terms. These functions were referred to as *correction factors* to the radar cross-section, and are defined by the symbol $\Xi_{pq}(\omega_d)$, where p indicates the order of the term in the power series expansion of the arbitrary heights factor, and q represents the order of the general asymptotic expansion, which represents the hydrodynamic coupling of the correction factor. In this chapter, the nature of the newly-derived correction factors, their impact on the total radar cross-section, and

evidence of their presence in field data will be discussed.

The shape, behaviour, and impact of the correction terms on the total radar cross-section of the ocean surface are discussed in Section 5.1. Then, in Section 5.2, evidence of the presence of the correction terms in HF Doppler spectra obtained from field data is presented.

5.1 Analysis of the Correction Factors

The analysis of the correction factors is presented in two parts: first, the morphology of the correction factors is analyzed at different ocean conditions and transmitter frequencies, independent of the height-restricted radar cross-sections, to provide a better understanding of the effects of each term on the total radar cross-section, as well as to relate the increase in energy caused by the correction terms at specific Doppler regions to the underlying physical phenomena; then, the impact of the correction terms on the total radar cross-section is evaluated by comparing the resulting corrected and uncorrected spectra, to demonstrate the practical effects of the proposed correction terms. To simulate different ocean conditions, a model for the directional ocean wave spectrum must be defined.

5.1.1 Model for the Directional Ocean Wave Spectrum

For the directional spreading factor, a $\cos^{2s}$ model [73] was employed. Here, the directional spreading function was considered frequency-dependent, following the distribution described in [146], with maximum directional spreading dependent on the significant wave steepness of the ocean surface. To simulate the different ocean con-

ditions, a directional ocean wave spectrum must be defined for different ocean conditions. Considering that the directional ocean wave spectrum can be defined such that

$$S(K) = S(K)D(\theta_{\mathbf{K}}, s(\omega)),$$

where $S(K)$ is the nondirectional spectrum, defined as [122]

$$S(K) = \int_{\theta_{\mathbf{K}}} S(\mathbf{K})\,\mathrm{d}\theta_{\mathbf{K}},$$

and $D(\theta_{\mathbf{K}}, s(\omega))$ is the directional spreading function, with $s(\omega)$ being the directional spreading factor, defined such that

$$\int_{\theta_{\mathbf{K}}} D(\theta_{\mathbf{K}}, s(\omega))\,\mathrm{d}\theta_{\mathbf{K}} = 1.$$

It is worth noting that, for deep-water waves, the ocean wavenumber spectrum $S(K)$ can be determined based on the ocean wave spectrum in the frequency domain $S(\omega)$ through the relationship

$$S(K) = \frac{g^2}{2\omega^3} S(\omega).$$

For the nondirectional spectrum, a modified JONSWAP model dependent solely on the significant wave height H_s and peak wave period T_p was used. The modified JONSWAP model is defined as [147]

$$S(\omega) = \frac{5}{16} {H_s}^2 \frac{\omega_p^4}{\omega^5} \exp\left[\frac{5}{4}\left(\frac{\omega_p}{\omega}\right)^4\right] \gamma^a (1 - 0.287 \ln\gamma) \tag{5.1}$$

where $\omega_p = 2\pi/T_p$ is the peak wave angular frequency, γ is the peakedness parameter,

which, following the recommendation in [148], is defined as

$$\gamma = \begin{cases} 5 & \text{for } \frac{T_p}{\sqrt{H_s}} \leq 3.6 \\ \exp\left(5.75 - 1.15\frac{T_p}{\sqrt{H_s}}\right) & \text{for } 3.6 < \frac{T_p}{\sqrt{H_s}} < 5 \\ 1 & \text{for } \frac{T_p}{\sqrt{H_s}} \geq 5, \end{cases} \tag{5.2}$$

and

$$a = \exp\left[-\frac{(\omega - \omega_p)^2}{2\sigma^2\omega_p^2}\right], \tag{5.3}$$

with $\sigma = 0.07$ if $\omega \leq \omega_p$ and $\sigma = 0.09$ otherwise.

For the directional spreading function, a $\cos^{2s}$ [73] was used. The $\cos^{2s}$ directional spreading model can be defined as [73], [122]

$$D(\theta_{\mathbf{K}}; s) = \frac{2^{2s-1}}{\pi}\frac{\Gamma^2(s+1)}{\Gamma(2s+1)}\cos^{2s}\left(\frac{\theta_{\mathbf{K}} - \theta_W}{2}\right), \tag{5.4}$$

where θ_W is the dominant wave direction and $\Gamma(\cdot)$ is the Gamma function [149], with both θ_W and θ_K measured with respect to the radar look direction. In the present work, the spreading parameter s is assumed to be frequency-dependent, following the relationship proposed in [146], where

$$s = \begin{cases} s_m\left(\frac{\omega}{\omega_p}\right)^5 & \text{for } \omega \leq \omega_p \\ s_m\left(\frac{\omega}{\omega_p}\right)^{-2.5} & \text{for } \omega \geq \omega_p. \end{cases} \tag{5.5}$$

A number of different definitions have been proposed for s_m depending of the application and available information to implement the model. Here, a definition of s_m that is dependent on the significant wave steepness is employed [150], where

$$s_m = 0.2{s_p}^{-1.28}, \tag{5.6}$$

where s_p is the significant wave steepness, defined as [148]

$$s_p = \frac{2\pi}{g}\frac{H_s}{{T_p}^2}. \tag{5.7}$$

Therefore, by choosing the described model to define the directional ocean spectrum, the ocean surface conditions can be determined solely by choosing a dominant wave direction, significant wave height and peak wave period.

To facilitate the subsequent analysis, most of the description of the ocean and radar conditions will be given in terms of dimensionless parameters such as roughness scale $k_0 H_s$ and significant wave steepness s_p. To contextualize these parameters, the upper limit of $k_0 H_s$ proposed in [28] for a valid height-restricted radar cross-section of the ocean surface is 0.7, while the significant wave steepness of a fully-developed sea is 0.025717, with the extremely steep seas defined by values of s_p greater than 0.048758 [151].

5.1.2 Morphology of the Correction Factors

Figure 5.1 shows the proposed correction factors for a fixed surface roughness condition ($k_0 H_s = 1.14$, $s_p = 0.027842$, and $\theta_W = 90°$) and changing transmitter frequencies ($f_0 = 6.91$ MHz, 13.385 MHz, and 27.65 MHz). Here the Doppler frequencies have been normalized to facilitate the comparison between different values of f_0. Observing the presented results, it is clear that, although the general shape of the correction factor is not affected, its magnitude depends on the radar transmitting frequency. This can be explained by the presence of $|u_0|^2$ in all correction expressions, as well as by the difference in total energy of the ocean surface that is necessary to reach the same roughness scale $k_0 H_s$.

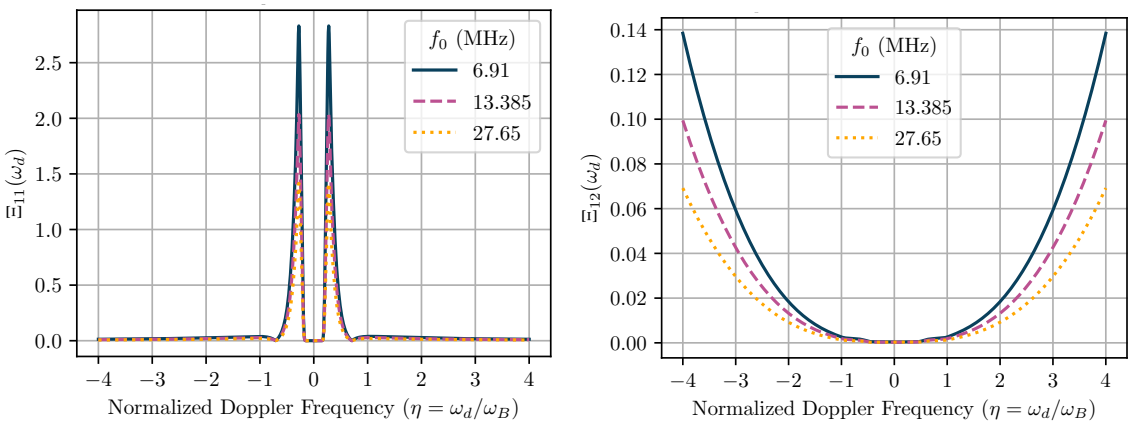

(a)

(b)

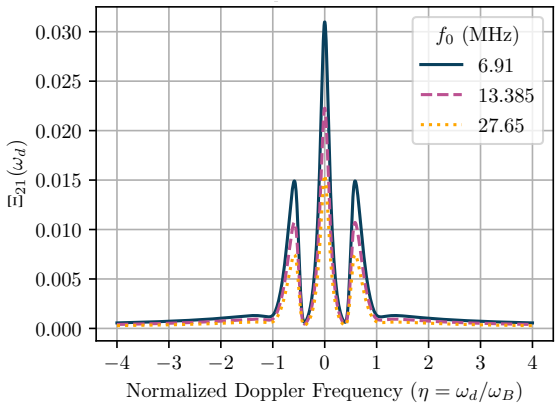

(c)

Figure 5.1: Correction factors for the ocean surface for electromagnetically large waves at a fixed ocean roughness condition ($k_0 H_s = 1.14$, $s_p = 0.027842$, $\theta_W = 90°$) and different transmitter frequencies; (a) is the first-order hydrodynamic, first-order correction $\Xi_{11}(\omega_d)$, (b) is the second-order hydrodynamic, first-order correction $\Xi_{12}(\omega_d)$, and (c) is the first-order hydrodynamic, second-order correction $\Xi_{21}(\omega_d)$.

Overall, the magnitude of consecutive orders of the correction term at the same frequency seems to decrease. This is a consequence of the uniform validity of the asymptotic expansion of the ocean surface, combined with convergence of the power series expansion of the exponential shown, for example, in (3.67). Evidence of the uniform validity of the proposed expressions can be seen in the comparison between terms with the same transmitter frequencies in Figs. 5.1a and 5.1b. Both correction terms considered here are first-order correction terms, but the latter is of a higher hydrodynamic order and, consequently, is less singular than the former. Now, the convergence of the power series expansion can be observed in the reduced magnitude between Figs. 5.1a and 5.1c, where both share the same hydrodynamic order, but the former is part of a higher-order term in the power series expansion of the exponential of the arbitrary heights function.

Observing the first-order hydrodynamic, first-order correction factor presented in Figure 5.1a, it can be observed that the effects of the correction factor are concentrated in the Doppler interval between the Bragg peaks, marked as 1 in the normalized Doppler frequency axis. This is consistent with the analysis of the first-order correction expression proposed in [97], further confirming the conclusion shown in Chapter 4 that the expression presented in [97] can be obtained by using the first-order hydrodynamic, first-order correction factor. This seems to indicate an increase in the energy of longer waves that are now allowed to grow beyond the small-height restriction imposed by the expressions derived in [3], [120]. The generalization of the correction form presented here seems to indicate that the increase in energy of large waves presented in [97] for the first-order radar cross-section can be extended to higher-order ocean surface interactions.

The second-order hydrodynamic, first-order correction factor presented in Fig. 5.1b indicates an increase in the energy of waves that are further away from zero-Doppler. By analyzing its energy distribution and the expression shown in (4.44), it can be concluded that this term stands for the contribution of second-order ocean waves resulting from the interaction between electromagnetically-large and small waves to the total radar cross-section, resulting in scatters that are represented by absolute Doppler frequencies outside the Bragg peaks. It is also important to note that, contrary to the expression for the height-restricted second-order radar cross-section, the combination of ocean wave vectors in the second-order hydrodynamic, first-order correction factor does not need to add up to the Bragg wave vector.

Even though the contribution of the first-order hydrodynamic, second-order correction factor presented in Fig. 5.1c seems very small compared to the other correction terms, its inclusion in the discussion serves to show that due to the convergence of the power series expansion of the exponential, the contributions of correction terms of orders higher than one tend to be very small. Therefore, radar cross-section terms obtained from the combination of height-restricted radar cross-section expressions and higher-order correction terms only affect the total radar cross-section of the ocean surface at extreme ocean conditions, and are comparatively much smaller than the first-order counterparts. It should also be noted that the main contribution of $\Xi_{21}(\omega_d)$ is the energy introduced at and near zero-Doppler, which seems to indicate that part of the energy added by this goes to waves which have a null resulting Doppler frequency in hydrodynamic couplings.

Comparing the morphology of each term presented in Fig. 5.1, both first-order hydrodynamic terms in Fig. 5.1a and Fig. 5.1c introduce energy to the total radar cross-

section around zero-Doppler, while the second-order hydrodynamic term introduces small amounts of energy across the second-order regions of the Doppler spectrum. Thus, even though the effects of the second-order hydrodynamic correction factor are harder to detect by visually inspecting the received radar signal than the effects of the first-order hydrodynamic corrections, its inclusion in the total radar cross-section can impact inversion methods such as those used in significant wave height estimation from the received HF radar data [152], that rely on the integration of terms in the second-order region.

As noted in (4.44), the second-order hydrodynamic, first-order correction factor retains its directional dependence due to the fact that direction-dependent terms other than the directional ocean wave spectra are present in the expression, inhibiting its simplification through integration. To understand the effects of wave direction on the correction factor, $\Xi_{12}(\omega_d)$ was simulated for the same ocean conditions presented in Fig. 5.1, but with different dominant wave directions θ_W, with results shown in Fig. 5.2.

From Fig. 5.2, it is clear that the distribution of energy is not equal for all dominant wave directions. In Fig. 5.2a, waves of the same frequency moving away from the radar have received more energy in the correction than the ones moving towards the radar, while in Fig. 5.2c more energy is given to waves moving towards the radar. This is expected, since at $\theta_W = 0°$ and $\theta_W = 180°$, all waves are moving respectively away and towards the receiver. However, at intermediate angles such as $\theta_W = 30°$, presented in Fig. 5.2b, the energy is more evenly distributed, similar to the one shown in Fig. 5.1b for $\theta_W = 90°$. Therefore, the directional dependence of the second-order hydrodynamic, first-order correction factor seems to affect the energy distribution of

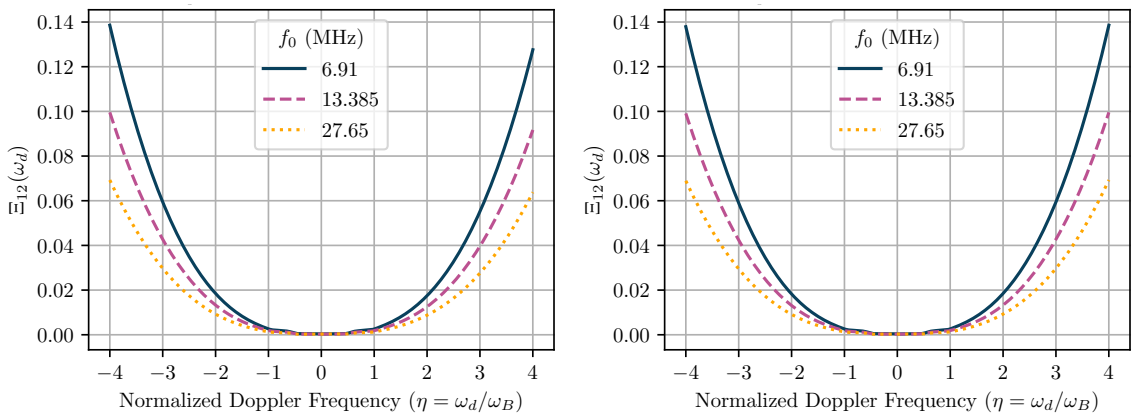

(a) (b)

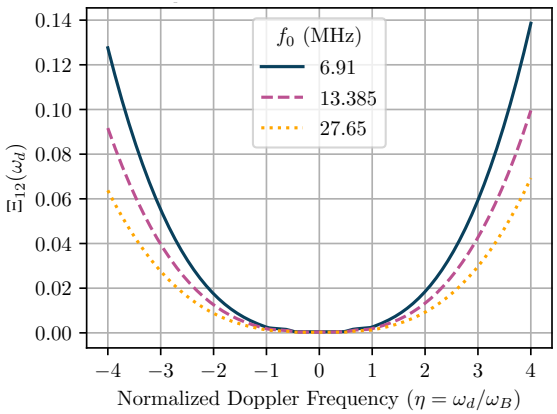

(c)

Figure 5.2: Second-order hydrodynamic, first-order correction factor for the ocean surface for electromagnetically large waves at a fixed ocean roughness condition ($k_0 H_s = 1.14$, $s_p = 0.027842$) and different transmitter frequencies and dominant wave directions: (a) $\theta_W = 0°$, (b) $\theta_W = 30°$, and (c) $\theta_W = 180°$ from broadside.

the total radar cross-section when there is a clear movement of waves towards or away from the radar, being more or less similar at intermediate angles.

Now, keeping a fixed radar configuration and changing the roughness conditions of the ocean surface, the general behaviour of the correction factor can be analyzed for different ocean conditions. Figure 5.3 shows the resulting correction factors, with the first column showing $\Xi_{11}(\omega_d)$, the second, $\Xi_{12}(\omega_d)$, and the third, $\Xi_{21}(\omega_d)$; each figure shows different significant wave steepness conditions, with the first line in Fig. 5.3 showing the correction terms for $k_0 H_s = 0.44$, the second, $k_0 H_s = 1.14$, and the third, $k_0 H_s = 2.70$; in all cases, the radar transmitter frequency is set to 13.385 MHz. For simplicity, only the correction terms for $\theta_W = 90^\circ$ are shown.

Observing Figs. 5.3a, 5.3d and 5.3g, it is interesting to see that the significant wave steepness will determine the position of the maximum in the first-order hydrodynamic, first-order correction factor, while it determines the energy distribution for the other proposed correction factors. For the same roughness scale, changes in significant wave steepness will only depend on the peak wave period of the ocean wave spectrum, indicating that the distance between zero-Doppler and the peaks in $\Xi_{11}(\omega_d)$ is determined by the peak wave period and Bragg frequency. Upon examination, it is understood that the peak of the first-order hydrodynamic, first-order correction factor occurs at exactly the Doppler frequency corresponding to the peak wave period.

Another important observation that can be made from the results for $\Xi_{11}(\omega_d)$ is that the dependence between s_p and the peak value of $\Xi_{11}(\omega_d)$ is not linear. This can be evidenced by the smaller maximum value found for $s_p = 0.0278$ compared to smaller and larger steepness values in Figs. 5.3d and 5.3g. As discussed in Chapter 4, the magnitude of the correction terms is determined by the equilibrium between the

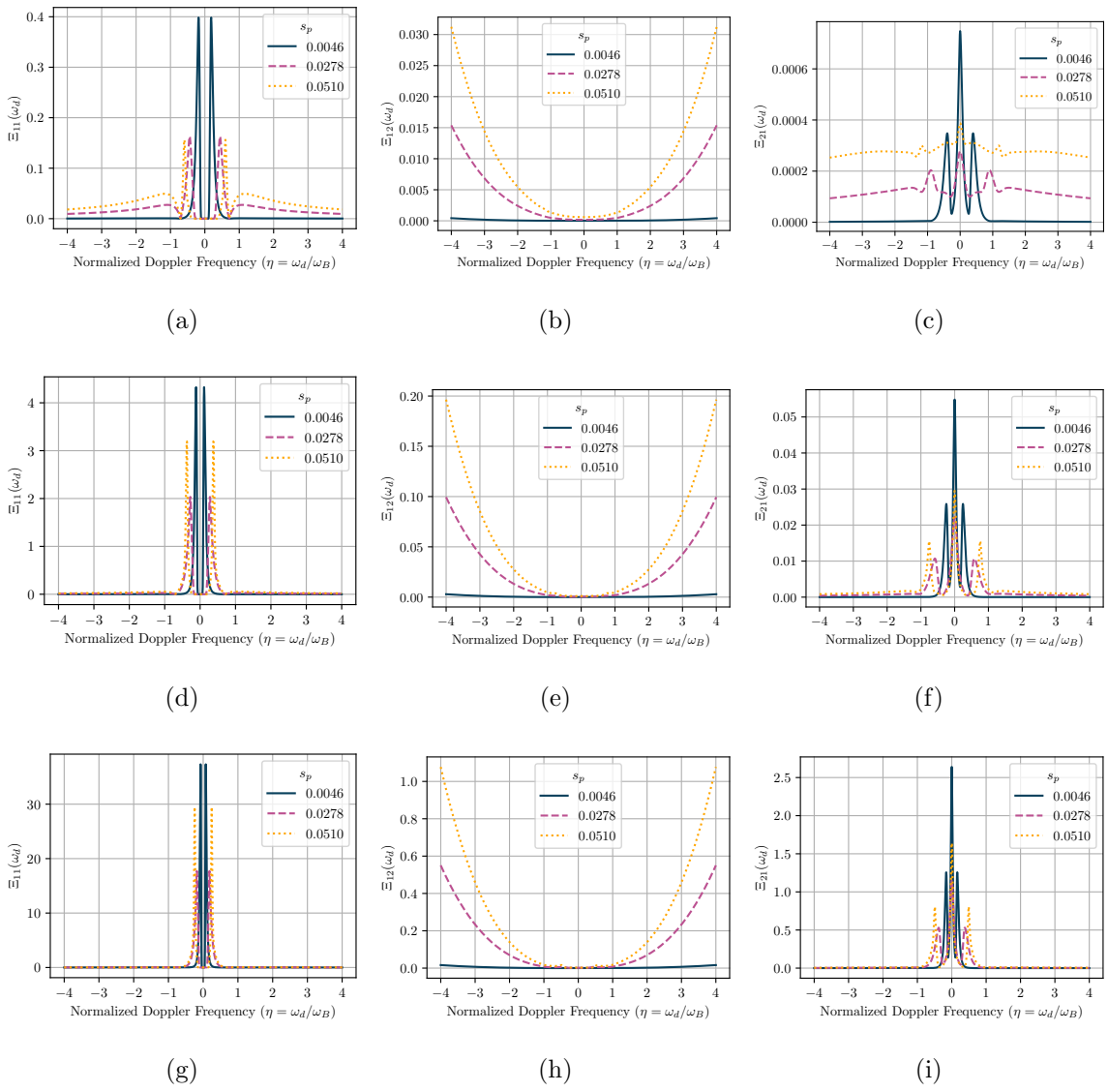

Figure 5.3: Correction factors factor for the ocean surface for electromagnetically large waves at a fixed radar configuration and different ocean roughness conditions: $k_0 H_s = 0.44$ for (a), (b), and (c), $k_0 H_s = 1.14$ for (d), (e), and (f), and $k_0 H_s = 2.70$ for (g), (h) and (i). The first column shows the first-order hydrodynamic, first-order correction factor, the second is the second-order hydrodynamic, first-order correction factor, and the third is the first-order hydrodynamic, second-order correction factor.

ocean wave spectral energy and $|u_0|^2$. It was also pointed out in Chapter 4 that for the first-order hydrodynamic, first-order correction factor in deep-water waves, $|u_0|^2$ will reach a minimum when $\omega_d = \pm\omega_B/\sqrt{2}$, where ω_B is the Bragg frequency for deep-water waves; this is precisely the frequency of the minima found in Fig. 5.3a. Knowing that the peaks in $\Xi_{11}(\omega_d)$ occur at the peak frequency of the ocean wave spectrum, and that $|u_0|^2$ increases monotonically at Doppler frequencies further from $\omega_d = -\omega_B/\sqrt{2}$ for $\omega_d < 0$ and $\omega_d = -\omega_B/\sqrt{2}$ for $\omega_d < 0$, the only remaining factor in the analysis is an increase in the peak value of the ocean wave spectrum due to JONSWAP's peakedness parameter γ at steeper seas [148]. Thus, the energy peak will increase the further the peak frequency is from $\pm\omega_B/\sqrt{2}$, but it will also depend on the peakedness parameter of the ocean wave spectrum; the larger maximum at $s_p = 0.0046$ is therefore due to the contribution of $|u_0|^2$ to the magnitude of the correction factor, and the larger peak for $s_p = 0.0510$ is due to the contribution of JONSWAP's γ to the ocean wave spectrum, with both factors contributing to the peak value at $s_p = 0.0278$.

From the considerations in Chapter 4, it was observed that distribution of the peaks and zeros for $\Xi_{21}(\omega_d)$ is much more intricate than observed in the first-order case due to the interaction between the two $|u_0|^2$ functions. This is evidenced by the figures in the third column of Fig. 5.3, where a less predictable pattern for peaks and zeros is observed.

For the electromagnetically-small sea surface heights shown in Figs. 5.3a to 5.3c, it is clear that the radar cross-section terms obtained from these correction factors will not be noticeable by observing the total radar cross-section. This is due to the fact that in all cases, the maximum value for each correction factor is smaller than

one, which will result in RCS terms that are much smaller than their height-restricted counterparts.

In Figs. 5.3d to 5.3f, the roughness condition of the ocean surface has violated the small-height restriction. With a roughness scale slightly greater than 1, the terms resulting from a product with $\Xi_{11}(\omega_d)$ start to introduce a significant amount of energy to the total radar cross-section, being greater than their height-restricted counterparts at the correction peaks. The higher-order terms still have values significantly below unity, but some energy has been added to the second-order regions due to $\Xi_{12}(\omega_d)$.

When the roughness scale is significantly larger than 1, as shown Figs. 5.3g to 5.3i, all first-order hydrodynamic terms start to introduce energy to the total radar cross-section. As expected most of the effect on the total radar cross-section comes from $\Xi_{11}(\omega_d)$, with $\Xi_{12}(\omega_d)$ introducing energy to the second-order region that could interfere in processes that rely on integration of the second-order regions. Again, most of the energy introduced by $\Xi_{21}(\omega_d)$ is situated at zero-Doppler, which would make it hard to distinguish its contributions in real measurements, as the direct path peak would bury the signal produced by the correction factor.

5.1.3 Impact of the Correction Terms on the Total Radar Cross-Section

Now that the general morphology of the correction factors has been presented, the impact of these terms on the total radar cross-section of the ocean surface can be evaluated. As detailed in Section 5.1.2, the correction terms can affect the total radar cross-section in two ways: first, by introducing energy peaks around zero-

Doppler through the first-order hydrodynamic terms; second, by introducing energy over the second-order region of the spectrum with the inclusion of the second-order hydrodynamic correction factor. The analysis will be divided in two parts. First, the maxima introduced by the first-order hydrodynamic terms will be studied by measuring the maximum difference between corrected and uncorrected spectra for a variety of ocean conditions. Then, the influence of the second-order term will be analyzed, by comparing the area under the second-order regions outside of the Bragg peaks. As previously mentioned, these are important regions of the radar cross-section of the ocean surface, as they are used in multiple estimation methods of meteorological measurements, such as significant wave height and peak wave period [152], and in the estimation of the directional spectrum of the ocean surface [19], [20], [23], [153]. The correction of these methods is not within the scope of the present work, but some insights on the effect of the correction term in these estimation methods can be taken from the present analysis.

5.1.3.1 Comparison Between Corrected and Uncorrected Spectra

Considering the ocean surface model presented in Section 5.1.1, the radar cross-section of the ocean surface was simulated for different ocean conditions, and the corrected and uncorrected Doppler spectra were compared. Figure 5.4 and Figure 5.5 respectively present a comparison between corrected and uncorrected spectra at electromagnetically-low and high sea states. In both cases, a monostatic radar with pulsed dipole source and narrow-beam receiver was considered, with transmitter frequency $f_0 = 13.385$ MHz. For the case presented in Figure 5.4, the significant wave height H_s was equal to 1.58 m, the peak wave period T_p was 9.1 s, which results in an es-

timated wind speed considering a Sverdrup-Munk-Bretschneider (SMB) [154], [155] estimation of the wind speed U_{10} measured at 10 m from the ocean surface equal to 7.7 m/s. On the other hand, the case presented in Figure 5.5 has $H_s = 7.86$ m, $T_p = 12.9$ s, which results in $U_{10} = 19.2$ m/s using the SMB method. To avoid fringe values in the analysis, the steepness of the ocean surface in both cases was chosen to be below the extreme steepness defined by Buckley [151].

From the results presented in Figure 5.4, it is clear that the correction terms do not present a significant impact on the total radar cross-section at electromagnetically-low sea states. This is expected, since the maximum values of the correction terms are below 1, indicating that the correction factors would not surpass the values for the height-restricted radar cross-section at any Doppler frequency, as noted in the morphological analysis presented in Section 5.1.2. In contrast, it is clear that the RCS correction terms presented in Figure 5.5 have an impact on the total radar cross-section of the ocean surface, as they represent the RCS of an electromagnetically-high sea state. This impact is concentrated on the region around zero-Doppler, as expected in the morphological analysis conducted in Section 5.1.2.

It is clear that the terms resulting from $\Xi_{11}(\omega_d)$ are responsible for most of the impact on the total radar cross-section, which is evident from the analysis presented in Section 5.1.2 and by the simulation results presented in Figure 5.5. It was also noted that the impact of the second-order hydrodynamic, first-order correction $\Xi_{12}(\omega_d)$ will only be visible in extreme cases, and would be mostly noticeable when comparing the area of the second-order regions outside the Bragg peaks. To understand how $\Xi_{12}(\omega_d)$ impacts the second-order region outside the Bragg peak, Figure 5.6 presents the outer second-order region on the side of the highest Bragg peak for $\theta_W = 30°$

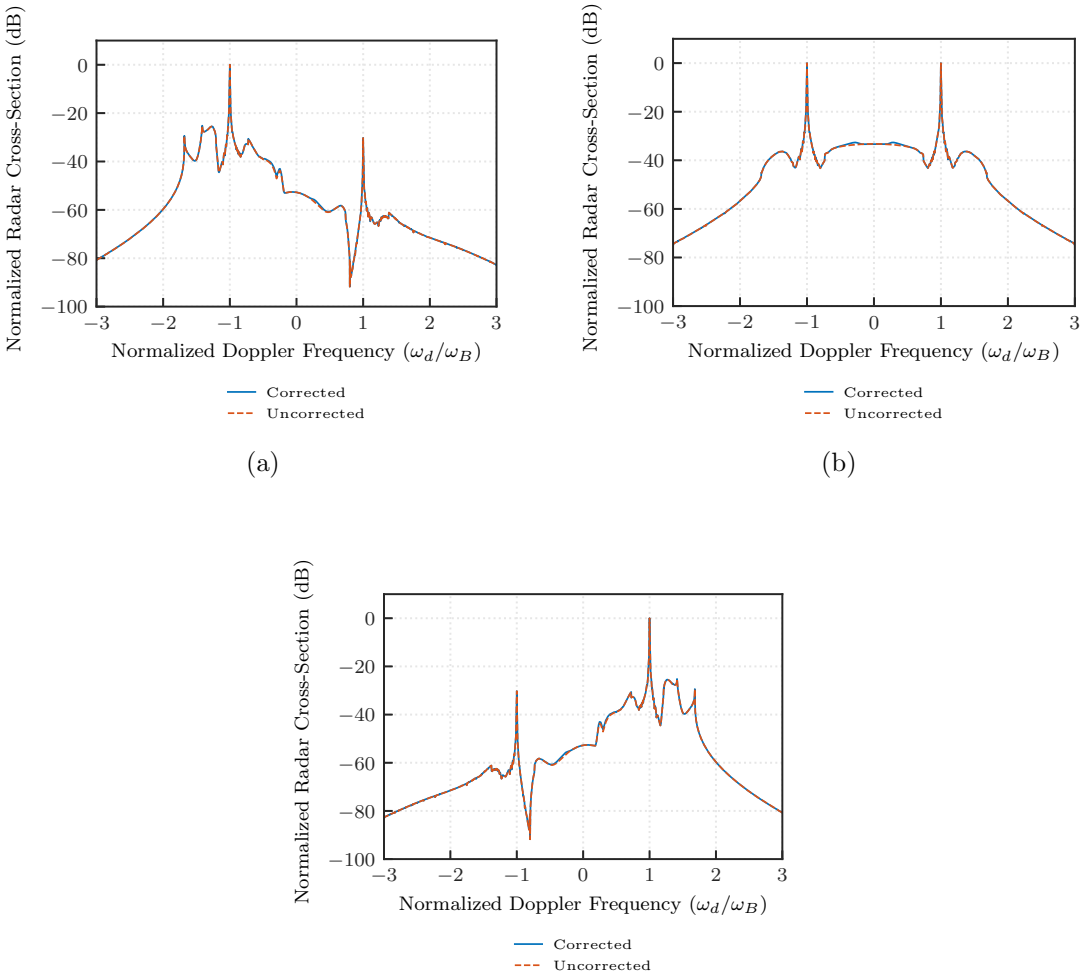

Figure 5.4: Comparison between corrected and uncorrected spectra at electromagnetically-low sea states with $k_0 H_s = 0.4429$, $s_p = 0.01224$, $f_0 = 13.385$ MHz and different dominant wave directions: (a) $\theta_W = 30°$, (b) $\theta_W = 90°$, and (c) $\theta_W = 150°$ from broadside.

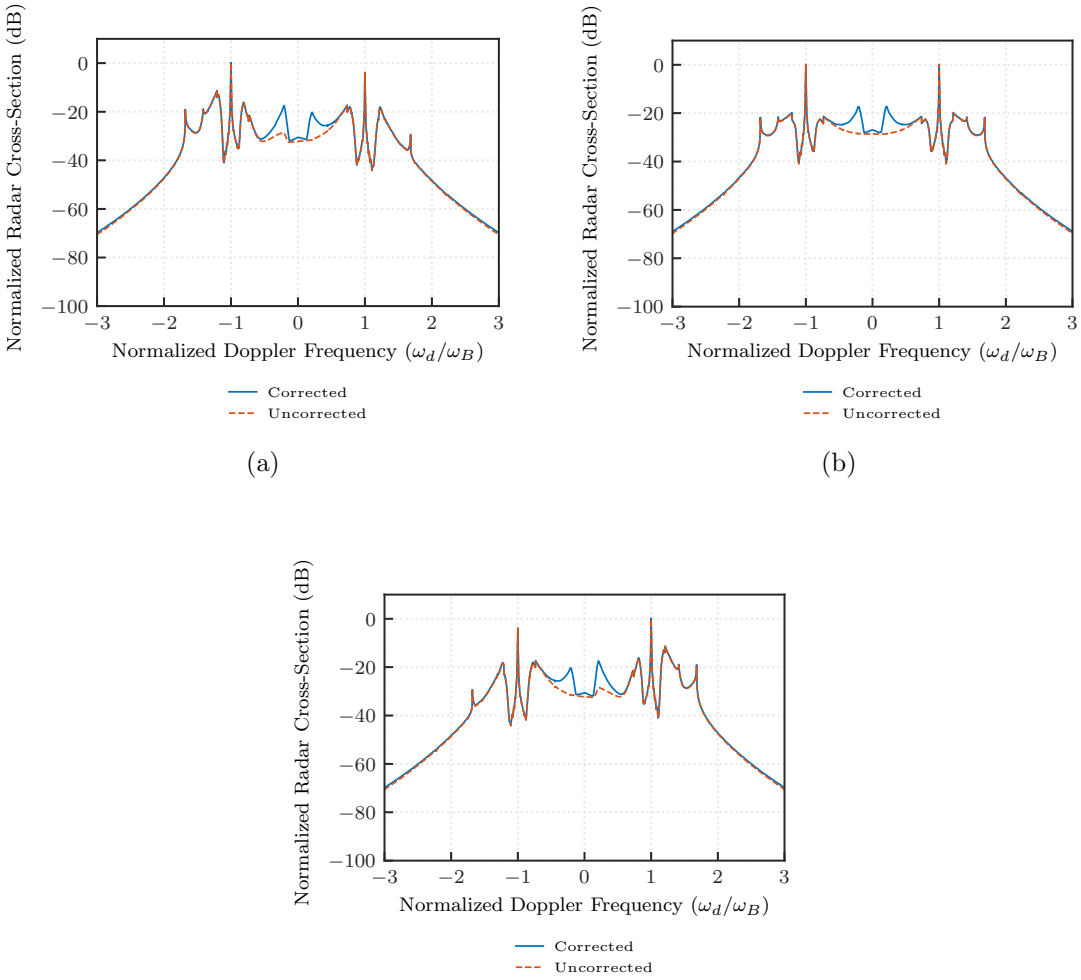

Figure 5.5: Comparison between corrected and uncorrected spectra at electromagnetically-high sea states with $k_0 H_s = 2.2036$, $s_p = 0.030233$, $f_0 = 13.385$ MHz and different dominant wave directions: (a) $\theta_W = 30°$, (b) $\theta_W = 90°$, and (c) $\theta_W = 150°$ from broadside.

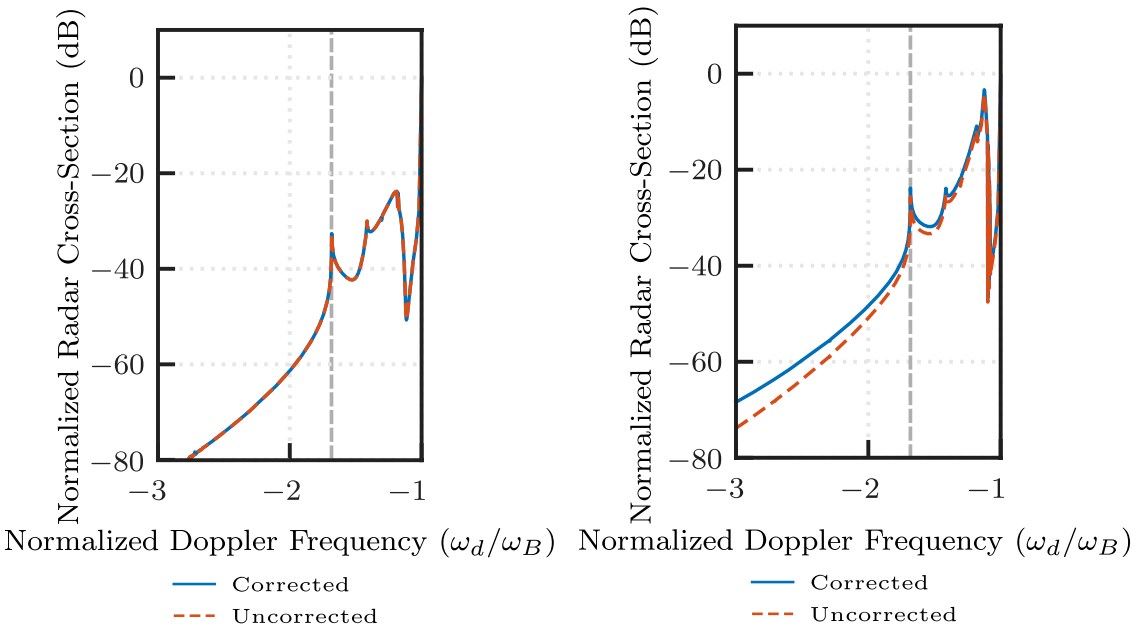

Figure 5.6: Comparison between the outer second-order regions of corrected and uncorrected spectra at electromagnetically-low and high sea states for $f_0 = 27.65$ MHz, $\theta_W = 30°$ from broadside, and different ocean conditions: (a) $k_0 H_s = 0.92$, $s_p = 4.93 \times 10^{-4}$ and (b) $k_0 H_s = 8.19$, $s_p = 1.55 \times 10^{-2}$

and a transmitter frequency of $f_0 = 27.65$ MHz. Figure 5.6a presents the RCS for an electromagnetically-low sea state with $k_0 H_s = 0.915032$, while Figure 5.6b shows the RCS for an electromagnetically-high sea state with $k_0 H_s = 8.188931$.

Comparing Figure 5.6a and Figure 5.6b, it is clear that the second-order hydrodynamic, first-order correction terms in the RCS have added energy to the tails of the spectrum, with a slight elevation between the $-\sqrt{2}\omega_B$ hydrodynamic singularity, marked as a vertical dashed line in Figure 5.6a and Figure 5.6b, and the negative Bragg peak. However, this difference can only be observed in an electromagnetically-very-high sea state, where $k_0 H_s$ is much greater than 1. Furthermore, the energy

in the regions beyond the hydrodynamic singularity, except possibly at the electromagnetic singularity, will likely be buried by the noise floor in field data. Again, while the impact of terms derived from $\Xi_{12}(\omega_d)$ is not likely to be visible in all electromagnetically-high sea states, its presence will cause an increase in the area of the second-order region between the hydrodynamic singularity and the Bragg peak. This increase in the area of the second-order region could affect inversion methods that rely on the intergration of these regions, such as the one presented in [152] to obtain the significant wave height of the ocean surface from the Doppler spectrum.

At this point, it should be noted that the correction terms are considered to be non-orthogonal to the height-restricted radar cross-sections of the same order, which allows, for example, a second-order hydrodynamic correction to the first-order radar cross-section. While this condition would be an intuitive one to impose, a clear mathematical motivation was not found in the present analysis, as it would require that different orders of the generalized asymptotic expansion of the Fourier-Stieltjes coefficients of the ocean surface to be orthogonal. As this orthogonality was not proven in this analysis, the subsequent sections will consider the least restrictive case, where the terms of different orders in the generalized asymptotic expansion of the Fourier-Stieltjes coefficients are not orthogonal.

Now that the form and location of the impact of correction terms on the total radar cross-section have been introduced, these factors should be explored under a variety of ocean conditions. This analysis will cover the magnitude and location of the maximum impact of the correction term on the total RCS, as well as quantify the changes in the area of the second-order region between the highest Bragg peak and the closest hydrodynamic singularity.

5.1.3.2 Maximum Impact on the Total RCS

Figure 5.7 shows the maximum difference between corrected and height-restricted spectra for a variety of ocean conditions, indicated by significant wave steepness s_p, roughness scale $k_0 H_s$, and dominant wave direction θ_W. The trend lines indicate a third-order polynomial fit.

As expected from the results observed in Section 5.1.2, the maximum difference between corrected and uncorrected RCSs increases with roughness scale and significant wave steepness, with the effect of competing terms in (4.43) shown in intermediate steepness values between the maximum and minimum differences for the same roughness scale, with the minimum steepness usually resulting in larger differences than intermediate steepness values, as shown in Fig. 5.3.

From Figure 5.7, it is clear that the maximum difference between corrected and uncorrected spectra does not depend on the dominant wave direction of the ocean surface. As observed in Section 5.1.2, the maximum impact of the correction terms on the total radar cross-section can be mainly attributed to the first-order hydrodynamic, first-order correction to the radar cross-section. While it is clear that $\Xi_{11}(\omega_d)$ in (4.43) does not depend on the directional distribution of the waves in the ocean surface, as discussed in Chapter 4, a directional dependence was detected when considering only the first-order hydrodynamic, first-order correction to the first order radar cross-section [97]. This directional dependence of the maximum difference between corrected and uncorrected spectra could be a result of the interaction of the correction term with the height-restricted first-order radar cross-section, however, due to the presence of the first-order hydrodynamic, first-order correction to the

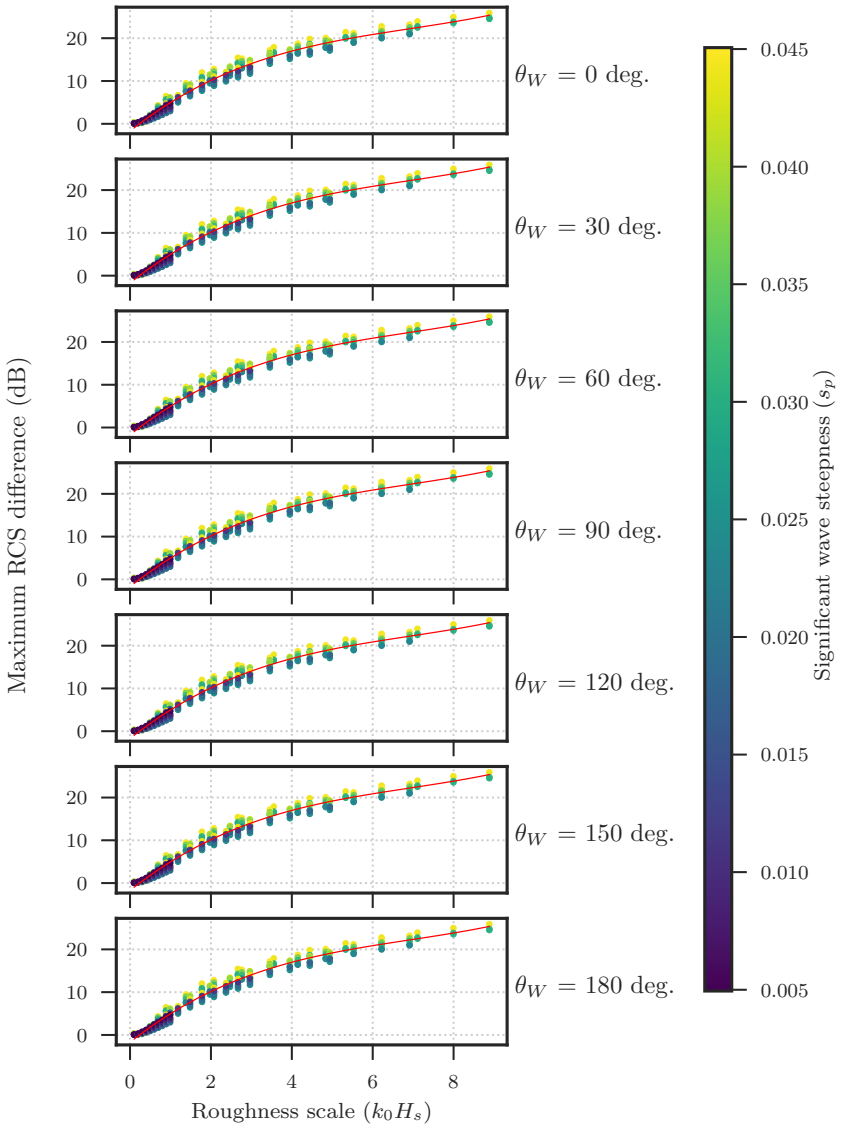

Figure 5.7: Maximum impact of the correction terms on the total radar cross-section of the ocean surface with respect to dominant wave direction θ_W and significant wave steepness s_p at different roughness scales $k_0 H_s$.

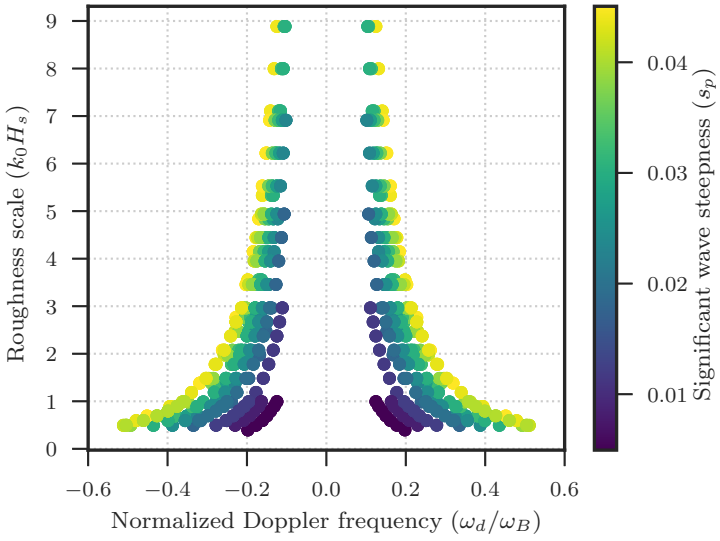

Figure 5.8: Normalized Doppler frequency distribution of the maximum impact of the correction terms on the total radar cross-section of the ocean surface with respect to significant wave steepness s_p and roughness scale k_0H_s.

second-order, the directional dependence was compensated with the saturation of the second-order radar cross-section.

Figure 5.8 shows the frequency of maximum difference between corrected and uncorrected spectra. As expected, the maximum difference occurs between the Bragg peaks, as it is mostly a consequence of terms derived from the first-order hydrodynamic, first order correction factor. Furthermore, as noted in Section 5.1.2, the frequency of maximum difference follows the increase in steepness of the ocean surface, since it determines the position of the peak wave frequency of the ocean wave spectrum. The exact symmetry of the differences shown here confirms the directional independence of $\Xi_{11}(\omega_d)$.

5.1.3.3 Impact of the Correction Terms on the Second-Order Region

Figure 5.9 shows the percentage increase in the area of the second-order region between the Bragg peak and the $\sqrt{2}\omega_B$ singularity of the dominant side of the Doppler spectrum for different dominant wave directions. Integration over the second-order region can be found in significant wave height estimation methods (e.g. [152]). To ensure the removal of swell influences from the simulation, the integration was performed between $1.21\omega_B$ and $\sqrt{2}\omega_B$ of the linear Doppler spectrum [156]. As noted in Section 5.1.2, these area increases in the second-order region outside the Bragg peaks are due to the second-order hydrodynamic, first-order correction factor, as the influence of the other proposed correction terms are mostly restricted to the region between the Bragg peaks.

The results presented in Figure 5.9 show an increase in the area of the second-order region of up to 30% at extreme sea states, with increases between 5% and 15% not being uncommon for roughness scales greater than 1. As discussed in Section 5.1.2, area increases of this magnitude can be almost negligible if observed point by point in a Doppler spectrum plot, and would be difficult to confirm by visual inspection of field data, except at extreme ocean conditions, which would also be hindered by noise levels in real data observations and windowing effects in the data processing. However, area increases of this magnitude could result in the overestimation of significant wave heights obtained using methods that have been derived based on height-restricted radar cross-sections, such as previously observed in [28], [157], [158]. Increases following the same pattern have also been observed at the dominant Bragg peaks, but the magnitude of the increase would not be noticeable in real data, as shown in Fig. 5.10.

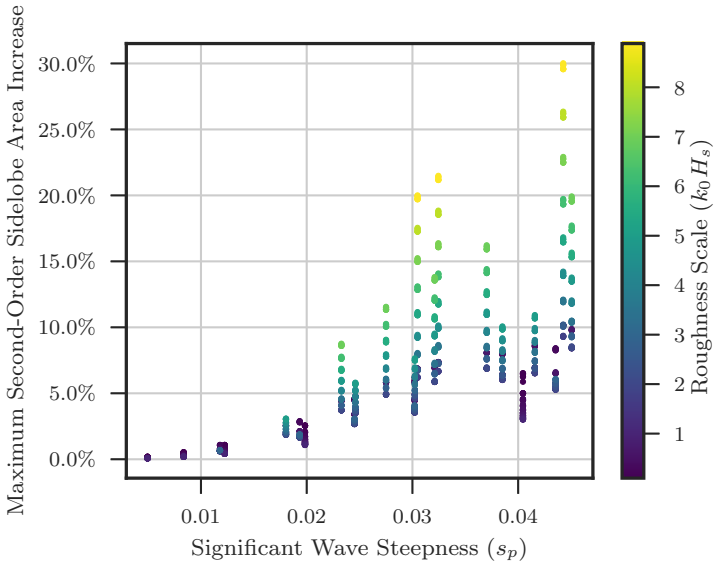

Figure 5.9: Impact of the correction terms on the area under the maximum outer second-order sidelobe of the total radar cross-section of the ocean surface with respect significant wave steepness s_p and roughness scale $k_0 H_s$.

One of the suggested solutions to the overestimation of significant wave heights at electromagnetically-high sea states is based on the canonical transformation in the Hamiltonian theory of water waves [157], [159]. In practice, based on the results shown in [159], the proposed solution is a wave-height-dependent rescaling of the second-order regions of the Doppler spectrum with respect to the first-order [157]. This rescaling of the second-order is similar to results presented in Figure 5.9, as the increase in the area of the second-order is proportional to the significant wave height of the ocean surface. However, the effects of the proposed correction term on the inversion of significant wave heights are outside of the scope of the present work, and further research should be done in order to confirm the relationship between the

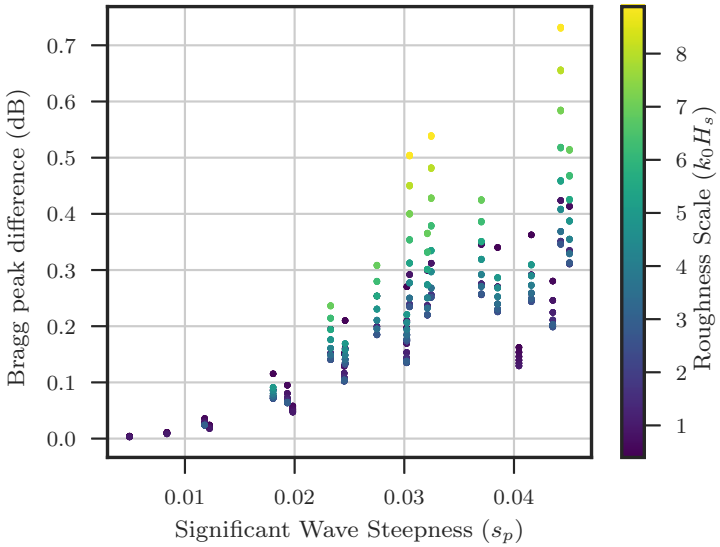

Figure 5.10: Impact of the correction terms on the magnitude of the maximum Bragg peak with respect significant wave steepness s_p and roughness scale $k_0 H_s$.

proposed correction term and the rescaling of the second-order mentioned in [157].

5.2 Evidence of the Presence of Correction Terms in Field Data

To observe the effects of the proposed correction terms in the real world, field data collected from electromagnetically-high sea states were analyzed. As noted in Section 5.1.2, the analysis of the field data will be concentrated on the effects of the first-order correction terms, since the second-order correction factor mostly affects the area under the spectral regions outside the Bragg peaks. Using the morphological analysis presented in Section 5.1.2 and the expected effects of the first-order correction terms the total radar cross-section shown in Sections 5.1.3 and 5.1.3.2, the field data

were examined to identify instances in which the correction terms would be visible.

The field data presented here were collected by the EuroROSE experiment [93] during a storm near Fedje, Norway, between March 6 and 7, 2000. A validation of the presented field data has been presented in [160]. Two WERA [161] HF radars systems were positioned in the Norwegian islands of Fedje and Lyngøy, observing the passage located in the south of the island of Fedje. Both radars were designed in a monostatic configuration, using a 16-antenna linear array of quarter-wavelength monopoles with half-wavelength spacing between each element as a receiver; a transmitter in FMCW mode was used at each site, with central transmitting frequency of 27.65 MHz and 125 kHz bandwidth, which enabled the observation of electromagnetically-large waves during the storm. The received signal was beamformed by the WERA radar system, with a $\cos^4$ window applied to raw antenna measurements [162]. Unfortunately, the data from the Lyngøy site had to be discarded from the current analysis, as the data quality was not sufficient to observe the effects of the ocean surface in the received signal.

For the ground truth, hourly data from the ERA5 Global Reanalysis [163] were used. As simulating the received Doppler spectrum for the exact ocean conditions presented at the location in question would require the estimation of a number of different variables that would greatly impact the simulated spectrum, a morphological analysis of the received radar signal was conducted. As noted in Section 5.1.2, the first-order correction peak should appear at the peak wave period of the ocean spectrum, with magnitude determined by the roughness scale and significant wave steepness of the ocean surface.

Figure 5.11 presents radar-received data for Fedje for two different ocean condi-

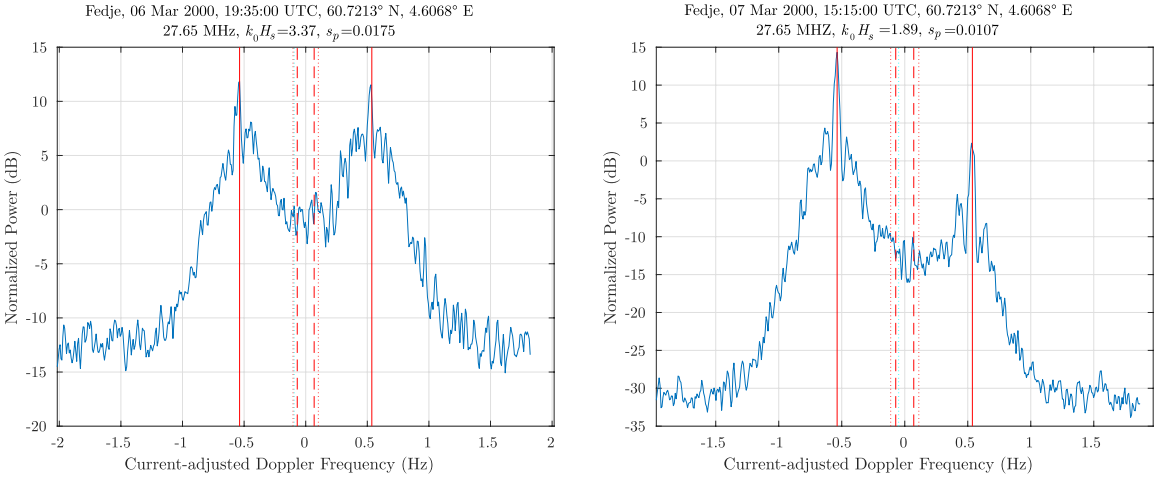

(a) (b)

Figure 5.11: Field data measured near Fedje, Norway, between March 06 and 07, 2000: (a) measured at 19:35 UTC on Mar. 06, 2000; (b) measured at 15:15 UTC on Mar. 07, 2000. The solid lines indicate the Bragg frequencies, while the dashed and dotted lines respectively indicate the peak wave frequency and the frequency of the largest wave.

tions: Fig. 5.11a was measured on Mar. 06, 2000 at 19:35 UTC, with a wind speed (U_{10}) of 15.5 m/s, measured at 10 m from the ocean surface, significant wave height (H_s) of 5.19 m and peak wave period (T_p) of 14.58 s., while Fig. 5.11b shows the data from Mar. 07, 2000, 15:15 UTC, with U_{10} of 8.40 m/s, H_s of 3.25 m, and T_p of 13.99 s. In terms of the adimensional parameters used in Section 5.1, Fig. 5.11a has a roughness scale k_0H_s of 3.37 and significant wave steepness s_p of 0.0175, while Fig. 5.11b has k_0H_s equal to 1.89, and s_p of 0.0107. Here, the Doppler frequencies were corrected to remove the effects of currents, as they are not part of the analysis presented here. The peak frequency f_p and frequency of maximum wave height f_m are respectively noted in Figs. 5.11a and 5.11b as dashed and dotted vertical lines.

The presented results show an increase in energy around the peak frequency on both sides of the spectra, which decreases in intensity with the roughness scale and steepness. This behaviour agrees with the morphology of the first-order correction term presented in Section 5.1.2, which might indicate the presence of the first-order correction to the first-order electric field. The exact magnitude of the increase in energy due to the correction term can be distorted by the $\cos^4$ window applied to the field data, but it generally agrees with the results presented in Section 5.1.3.2. Also, an energy peak has been detected at the frequency of the maximum wave height, however, such a peak was not observed in the analysis presented in Section 5.1.2. This may be due to the inability of single-peak ocean spectrum models to account for the presence of, for example, multiple swell systems and wind waves, as well as natural variations on the measured Doppler spectrum due to the presence of noise. It should be noted that the results presented here do not affect the previously-mentioned inversion algorithms, for example, in [19], [20], [152], as the effects observed here affect neither the first-, nor the dominant second-order regions of the spectrum.

Even though the energy increase in the region predicted in Section 5.1.2 can be observed in the field data, these observations are not sufficient to prove the presence of the correction terms in the Doppler spectrum. Variations in the measurements due to noise, combined with the resolution of the Doppler spectrum, can produce a false continuity between regions of the spectrum, as seen between the first-order peaks and the second-order regions in some of the spectra obtained in the Fedje experiment. The same effect could mask the effects of the correction terms, as both correction peaks can be close to the direct path peak, creating either a false continuity between them, or a "false bottom" in the second-order region that is higher than the pre-

dicted second order. However, due to quality concerns raised during the inversion of the meteorological measurements from radar data [160], and the difficulty of simulating the exact spectral distribution of the ocean surface from the meteorological information obtained by the buoy, this line of questioning was not pursued in this analysis. Therefore, the evidence presented here, while encouraging, is not conclusive.

5.3 General Chapter Summary

In this chapter, the correction factors presented in Chapter 4 were analyzed in more detail, with a morphological analysis of the correction term under a variety of ocean surface conditions, as well as a study on the impact of the correction terms on the total radar cross-section of the ocean surface. It was observed that the correction terms will only have significant impact on the total radar cross-section for roughness scale values that violate the small-height restriction. This confirms the observation made on Chapter 3, that the expression of the first- and second-order electric fields over an ocean surface with arbitrary wave heights returns to their height-restricted forms when the arbitrary function is sufficiently small. It also shows a seamless transition between the small and large wave heights in the radar cross-section.

From the analysis of the correction terms, it was observed that a large part of the energy added to the radar cross-section of the ocean surface is given to waves that are sufficiently long to become electromagnetically-large. The first-order hydrodynamic, first-order correction factor represents most of the localized energy increase in the spectrum, while the second-order hydrodynamic, first-order correction corrects for the energy in large waves under hydrodynamic coupling; the first-order hydrody-

namic, second-order correction term has been observed to be too small to influence the total radar cross-section, with the highest energy peak located at zero-Doppler. The energy increase due to the first-order hydrodynamic, first order correction factor is usually located at the peak wave period of the ocean wave spectrum, with its height modulated by the $|u_0|^2$ function, as discussed in Chapter 4. The second-order hydrodynamic, first-order correction term added energy to the second-order regions of the radar cross-section situated outside the Bragg peaks; while this energy increase is not sufficient to be noticeable by inspecting the resulting radar cross-section in most cases, the added energy has the potential to affect inversion methods that rely on the integration of the second-order region and can account for the discrepancy observed in inversion methods using radar returns obtained at electromagnetically-high sea-states. Some energy growth was also observed in the Bragg peaks, but with negligible amount to affect the analysis. It should be noted that since the correction terms do not include any theoretical restrictions with regard to the feasibility of wave growth, special attention must be taken to the conditions used in the simulation of the ocean wave spectrum.

After analyzing the proposed correction terms, the evidence of their presence in field data was examined. Using data collected during a storm observed by the EuroROSE Fedje experiment in March, 2000, an energy increase similar to the one generated by the first-order hydrodynamic, first-order correction terms was detected. These peaks were observed at Doppler frequencies corresponding to the peak wave period and at the frequency of the highest wave of the ocean surface, as measured by a buoy located at the scattering patch. However, due to windowing effects and distortions due to noise, the observed evidence is not conclusive. Further studies

using raw data are necessary to confirm the presence of the correction factors in real data, but the the observations made in this Chapter are encouraging and might indicate that the proposed correction terms can contribute to the representation of ocean surfaces with electromagnetically-large waves.

Chapter 6

Concluding Remarks

6.1 General Synopsis and Significant Results

The goal of developing a theoretical treatment for the scattering of electric fields over an ocean surface, represented by a time-varying random rough surface, with arbitrary roughness scales has been accomplished. After analyzing the different scattering frameworks used for radio oceanography in the HF band, it was observed that the pertubation theory in Barrick's approach to the problem [2] could not be lead to the removal of the small-height and slope restrictions, since the propose method requires these approximations to be valid. On the other hand, Walsh's generalized functions approach [17] does not require the use of height and slope constraints, although applying these constraints as in the past (e.g. [3], [17], [62]) simplifies the derivations. Therefore, the generalized functions approach was chosen as the theoretical framework of the present thesis.

While reviewing the generalized functions approach, it was observed that Walsh

and his colleagues have implicitly assumed the use of Cartesian coordinates to represent the scattering object. This assumption has implications in the use of the generalized functions method in curvilinear coordinates without constant basis vectors, such as spherical and elliptic coordinates. To address this problem, the generalized functions approach proposed in [1], [17], [85] was revised in Chapter 2 to allow its use in curvilinear coordinates, obtaining a revised system of equations for the electric field in the presence of a single scattering body which is valid for any curvilinear coordinate system. This was achieved by relying on vector and dyadic calculus to derive the system of equations defining the electric field in the generalized functions method without assuming any coordinate system. It was shown that the expressions presented in [1] could be obtained from the proposed system of equations by assuming a Cartesian coordinate system, but the opposite could not be achieved without taking some mathematical liberties. Finally, the resulting system of equations was employed for a general scattering body with surface implicitly defined by a function; this resulted in a system of equations similar to the one presented in [3], [17], but with different definitions for the auxiliary vector functions $\mathbf{R}^+$ and $\mathbf{R}^-$. This allowed a seamless progression between the proposed system of equations and the derivation of the electric field scattered by the ocean surface.

In Chapter 3, the electric field scattered by an ocean surface with electromagnetically-large waves was presented. This electric field relied on the system of equations proposed in Chapter 2, but since the derivation of the operator equation for the electric field scattered over a conductive surface does not rely on the definition of the auxiliary vector functions, the derivation starts with the operator equation shown in (3.9).

It should be noted that the derivation of the operator equation shown in [3], [17] rely on the Fourier transform of the Green's function solution to the Helmholtz equation, and the reader is referred to an Appendix in [62]; however, such an Appendix is not present in any of the available copies of [62]. In view of this, a solution to the Fourier transform of the Green's function solution to the Helmholtz equation is presented in Appendix B.1 of this thesis.

To simplify the solution of the operator equation, Walsh and his colleagues [3], [17] relied on the small-height approximation, as it was already commonly used in radio oceanography due to the works of Barrick [2]. The approximation was applied to the $\mathcal{L}$ and $\mathcal{L}^{-1}$ operators, considering that the ratio between surface displacement, or wave height, and wavelength is sufficiently small, i.e., the wavelength is sufficiently larger than wave height. To remove this approximation, the original, non-approximated, $\mathcal{L}$ operator was used, with an $\mathcal{L}^{-1}$ derived without applying the small-height restriction. The resulting operator contained a new factor, the *arbitrary heights factor* $e^{\zeta(\boldsymbol{\rho},t)}$, which is the exponential of a nondimensional function defined as the *arbitrary heights function* $\zeta(\boldsymbol{\rho}, t)$.

By following the derivation steps proposed in [3], [17] using the new inverse operator, the first- and second-order expressions for the electric field scattered by an ocean surface with arbitrary wave heights were derived. In this derivation, the source is assumed to be a pulsed vertical dipole whose radiation is at grazing incidence to the ocean surface. Furthermore, the slopes of the ocean surface were considered small enough to apply the small-slope approximation, as the root mean square (RMS) slope of surface gravity waves of dekametric wavelength — the types of waves observed by HF radars — is sufficiently small. It was found that the arbitrary heights version of

these expressions can be obtained by multiplying the arbitrary heights factor to the small-height version of the electric field expression.

At this point, since the height-restricted electric field is a key component of the arbitrary-height electric field, the small-height electric field was rederived, now assuming a time-varying ocean surface at the outset of the derivation. It was found that the expressions only arrive at the form presented in [3], [17] due to the physical fact that the phase velocity of ocean waves is much smaller than the speed of light. This fact supports the decision of including two different timescales in the derivation of the electric field expression, one regarding the processes related to the radar operation, and the other on the ocean surface processes. Even though the two timescales were included in [3], [17], the authors relied on the intuition of the reader instead of the phase velocity consideration that reduces the expression to the form known in the literature.

Once the height-restricted electric field expression was revised, the arbitrary heights factor in the electric field expression was expanded in a power series, considering a surface that could be represented by a Fourier-Stieltjes series with the Fourier coefficients expanded using a generalized asymptotic expansion. It became clear from this process that the total electric field is a linear combination between the height-restricted electric field and the series of corrections, classified by the order of the hydrodynamic coupling used in the asymptotic expansion of the Fourier coefficient and the order of the power series expansion of the arbitrary heights factor. This helped define the first- and second-order expressions for the electric field scattered by an ocean surface with electromagnetically-large waves with a pulsed vertical dipole as a source. The convolution between the arbitrary heights function and the electric

field introduced by the inverse Fourier transform with respect to the radar frequency introduced a Dirac delta to the Fourier-Stieltjes integral present in the electric field expressions, which needed to be treated with caution to be mathematically consistent. This resulted in the first- and second-order hydrodynamic, first-order corrections to the electric field, as well as the first-order hydrodynamic, second-order correction to the electric field, which can be used to obtain the radar cross-section of the correction terms.

The process used to obtain the radar cross-section of the correction terms was presented in Chapter 4. From the electric field expressions for the correction terms defined in Chapter 3, the autocorrelation expressions were calculated. First, the autocorrelation of the total electric field needs to be obtained, and due to the autocorrelation characteristics of the Fourier coefficients of the ocean surface, the cross-correlation terms between different scattering orders and correction terms are negligible, leaving only a linear combination between the height-restricted electric field and the correction terms. At this point, it is important to note that while the orthogonality between different Fourier coefficients is clear in their definition, this condition is too restrictive to impose on the asymptotic expansion coefficients, which results in the maintenance of terms such as the first-order hydrodynamic correction to the second-order electric field, and second-order hydrodynamic corrections to the electric field.

From the autocorrelation expressions of the correction terms, their radar cross-sections can be obtained by comparing the power spectral density for a differential area of the ocean surface with the radar equation proposed in [120]. By using the reproducing property of Dirac deltas, it was observed that the integrals in the power

spectral density of the correction terms could be represented by the product of two integrals, one representing an intermediate step in the derivation of the radar cross-sections of the height-restricted electric field being corrected, and another factor common among correction terms of the same order, identified as *correction factors*. It was easily shown that these new correction terms were present in the radar cross-section of the correction terms, defining the correction order of the radar cross-section term. After analyzing these correction factors, it was observed that the first-order hydrodynamic correction terms did not depend on the direction distribution of the ocean wave spectrum, while the second-order correction terms are dependent on the direction of each wave considered in the analysis. Furthermore, the $|u_0|^2$ functions present in the correction factors controlled the energy distribution with respect to the Doppler frequency, modulating the magnitude of energy peaks introduced by the first-order hydrodynamic terms.

Since the main difference between the height-restricted and the arbitrary-height spectra is the introduction of correction terms dependent on the correction factors derived in Chapter 4, the shape and behaviour of the correction factors was analyzed for a variety of ocean conditions in Chapter 5. The ocean surface was modelled such that the directional ocean wave spectrum would only depend on the choice of significant wave height, peak wave period, and dominant wave direction, with a frequency-dependent directional spreading factor. It was observed that most of the energy introduced by the correction factors comes from the first-order hydrodynamic, first-order correction factor, which adds energy to longer waves close to zero-Doppler and around the peak wave period of the ocean surface. The second-order hydrodynamic term adds energy across the spectrum, and can influence the inversion of mete-

orological variables from radar data obtained at electromagnetically-high sea states. The second-order correction terms mainly introduced energy at zero-Doppler, and its magnitude, in general, does not affect the total radar cross-section. It was observed that the correction terms affect the total radar cross-section at electromagnetically-high sea states, where the roughness scale $k_0 H_s$ is greater than 1, with some effect detected before this threshold is reached. The maximum impact does not depend on the dominant wave direction, and the RCS terms obtained from the first-order hydrodynamic, first-order correction factor were responsible for this discrepancy between corrected and uncorrected terms. It was also shown that the second-order hydrodynamic correction term increases the area under the second-order region outside the highest Bragg peak up to 30%, which can cause an overestimation of meteorological measurements obtained through inversion methods that rely on the integration of the outer second-order regions.

Once the behaviour and impact of the correction terms on the total radar cross-section was analyzed, evidence of the presence of these correction terms in field data measured under electromagnetically-high sea states was observed. The data used in this analysis was measured in Fedje, Norway, during a storm in March 2000 and was collected by the EuroROSE project. As the influence of the first-order hydrodynamic, first order correction can be detected by inspection, the analysis focused on increases in energy around the peak wave period of the ocean surface. Using the information obtained by a buoy located at the scattering patch, as well as ERA5 reanalysis data as reference, the Doppler spectrum at different points of the storm showed an increase of the energy at and around the peak wave period, and the frequency of the largest wave height. However, due to data quality concerns and noise and windowing effects

in the spectral data, the evidence of the presence of the correction terms derived in this thesis is not conclusive. However, signs of their presence indicate that future dedicated experimentation to confirm the results would be justified.

6.2 Suggestions for Future Work

From the outcomes of the research presented in this thesis, the interpretation of HF radar data obtained at electromagnetically-high sea states should now be possible. The derivations and results presented here can be taken into different areas of research in radio oceanography, and potentially enhance the utility of HF radars a tool for ocean remote sensing.

With respect to applications in radio oceanography, the present work can be applied to extend the capabilites of HF radars in electromagnetically-high sea states. When applied to measurements taken during storms or in electromagnetically-high sea states, inversion methods developed to obtain meteorological measurements from Doppler spectra have shown a tendency to overestimate the significant wave height of the ocean surface [28], [158]. Considering the corrections to the radar cross-section of the ocean surface presented in this thesis, this overestimation is expected; since the correction terms add energy to the second-order regions of the ocean wave spectrum, the inversion method tries to compensate for this extra energy by returning a higher significant wave height. From the present research, inversion methods can be developed considering the second-order hydrodynamic correction terms presented in this thesis.

It should be noted that the current thesis was developed with a particular radar

system in mind, in particular a monostatic configuration, pulsed dipole source in the HF band, and a narrow-beam receiver. Regarding the radar configuration, the results presented in this thesis could be extended to a bistatic configuration; the initial analysis has been presented for the first-order hydrodynamic, first-order correction in Appendices B.2 and C.1, which could guide the next steps of the derivation. After expanding to a bistatic configuration, the results presented here could be further expanded to different transmission modes, such as sky [164] or hybrid [165] wave modes, or to consider a transmitter on a floating platform [166], [167]. The radar transmitter could be modified in different ways, by changing the antenna type (e.g., dipole arrays, log-periodic antennas), current configuration (e.g., FMCW, FMICW), or a combination of both. The radar receiver can be also changed, for example, to consider a wide-beam receiver, commonly employed in CODAR radars [168].

In terms of the radar frequency, while a large part of the derivations rely on the fact that an HF radar is being used to observe the ocean surface, the results presented here can be also expanded to higher frequencies. The derivations found in Section 3.2.2 are valid for the electric field normal to a time-varying conductive surface at any transmitter frequency. However, it is possible for radars operating at higher frequencies to interact with scattering objects with RMS slopes larger than one. In this case, the small-slope assumption cannot be used, requiring the re-derivation of the electric field expressions with the reintroduction of higher powers of the slope term, as well as the $\mathcal{T}_2$ operator.

Another assumption made in the derivations presented in this thesis is that observed waves in the ocean surface are deep-water waves, i.e., the wavelengths of the ocean waves are much shorter than the ocean depth [142]. While this consideration is

crucial to the derivation of the second-order hydrodynamic radar cross-section (e.g., see [17]), the correction terms presented here have used this assumption sporadically, mostly when considering the dispersion relation of the ocean surface, and in the hydrodynamic coupling coefficient used in the second-order hydrodynamic correction terms. Therefore, the present work can be expanded both to shallow-water waves, or, more generally, to waves of intermediate depth; by doing so, the new correction terms can be applied to the analysis to develop inversion methods for nearshore environments.

While the present work was dedicated to ocean remote sensing applications, the concepts presented here could be expanded to different areas of research. Physically, the ocean surface can be interpreted as a time-varying random conductive surface. Therefore, the results presented here can be easily repurposed for the scattering over a time-invariant surface such as soil or other rough structures. In some cases, this would require the removal of the conductivity constraint, enabling the use of the concepts presented here to the scattering of electromagnetic waves at the boundary of media with intermediate contrast with their exterior. Also, the system of equations for the electric field in the presence of a scattering body proposed in Chapter 2 can be used in a variety of electromagnetic scattering problems, such as the derivation of the radar cross-section of a rough sphere [169], or of objects with more intricate geometries. If the derivation procedure proposed in [17] is chosen, the Fourier transform of the Greens's function solution to the Helmholtz equation in the chosen coordinate system will need to be defined.

Within the confines of the present research, more work can be done to solidify and advance the results obtained in the present thesis. From the system of equations for the electric field in curvilinear coordinates proposed in Chapter 2, a proof that

the generalized functions approach can be reduced to the Stratton-Chu integral equation in the case of a general scattering body can be determined, as, in principle, both methods should yield the same results. From the derivation shown in Chapter 4, more work can be done on the possible orthogonality between correction factors and the height-restricted terms. Non-orthogonality of these terms could result in the presence of cross-spectrum terms between height-restricted electric fields and correction terms. This could result in the nullification of some corrections, such as second-order corrections to first-order electric fields, and, consequently, in the reduction of the observed effect of the correction terms on the total radar cross-section, explaining in some part the magnitude of the supposed correction terms observed in field data.

Collection of field data under electromagnetically-high sea states is an important step to validate the results shown in the present thesis. This data can be used to understand the behaviour of the Doppler spectrum under these conditions, as well as to indicate the presence of the correction terms in field data with more certainty. To avoid problems in the data analysis, the field data should be processed from raw antenna measurements without the use of windowing methods, as they can distort the magnitude of some spectral features present in the field data. If ocean spectral data can be obtained from *in-situ* instruments, this information can be used as ground truth, allowing the simulation of Doppler spectra without relying on explicit ocean spectrum models; these models have a number of underlying assumptions and restrictions [146], [170]–[173], which can make the simulation of the Doppler spectrum difficult when only meteorological measurements are available.

In summary, the research results presented in this thesis can be the basis to interpret electromagnetic signals obtained from ocean surfaces with electromagneti-

cally-large waves, advancing the field of ocean remote sensing in the HF band. As discussed in this section, there are many opportunities to further the current research to more operational applications, as well as to expand these results to other radar configurations. Since these are the first steps in the field of the remote sensing of electromangetically-large waves using HF radars, the current thesis represents an attempt to advance the understanding of the interactions between ocean and electromagnetic waves in critical conditions, and has the potential to give an insight into unanswered questions in ocean remote sensing in the HF band.

Bibliography

[1] J. Walsh and R. Donnelly, "Consolidated approach to two-body electromagnetic scattering," *Physical Review A*, vol. 36, no. 9, pp. 4474–4485, Nov. 1987.

[2] D. E. Barrick, "Theory of HF and VHF propagation across the rough sea, 1, the effective surface impedance for a slightly rough highly conducting medium at grazing incidence," *Radio Science*, vol. 6, no. 5, pp. 517–526, 1971.

[3] J. Walsh and E. W. Gill, "An analysis of the scattering of high-frequency electromagnetic radiation from rough surfaces with application to pulse radar operating in backscatter mode," *Radio Science*, vol. 35, no. 6, pp. 1337–1359, Nov. 2000.

[4] S. Seneviratne, N. Nicholls, D. Easterling, *et al.*, "Changes in climate extremes and their impacts on the natural physical environment," in *Managing the Risks of Extreme Events and Disasters to Advance Climate Change Adaptation: A Special Report of Working Groups I and II of the Intergovernmental Panel on Climate Change (IPCC)*, C. B. Field, V. Barros, T. F. Stocker, *et al.*, Eds., Cambridge, UK, and New York, NY, USA: Cambridge University Press, 2012, ch. 3, pp. 109–230.

[5] M. Rhein, S. Rintoul, S. Aoki, *et al.*, "Observations: Ocean," in *Climate Change 2013: The Physical Science Basis. Contribution of Working Group I to the Fifth Assessment Report of the Intergovernmental Panel on Climate Change*, T. F. Stocker, D. Qin, G.-K. Plattner, *et al.*, Eds., Cambridge, United Kingdom; New York, NY, USA: Cambridge University Press, 2013, ch. 3, pp. 255–315.

[6] M. Collins, M. Sutherland, L. Bouwer, *et al.*, "Extremes, abrupt changes and managing risk," in *IPCC Special Report on the Ocean and Cryosphere in a Changing Climate*, H.-O. Pörtner, D. C. Roberts, V. Masson-Delmotte, *et al.*, Eds., In press, 2019, ch. 6, pp. 589–655.

[7] I. R. Young, S. Zieger, and A. V. Babanin, "Global trends in wind speed and wave height," *Science*, vol. 332, no. 6028, pp. 451–455, Mar. 2011.

[8] X. L. Wang, V. R. Swail, X. L. Wang, and V. R. Swail, "Changes of extreme wave heights in northern hemisphere oceans and related atmospheric circulation regimes," *Journal of Climate*, vol. 14, no. 10, pp. 2204–2221, May 2001.

[9] N. Mori, T. Yasuda, H. Mase, T. Tom, and Y. Oku, "Projection of extreme wave climate change under global warming," *Hydrological Research Letters*, vol. 4, no. 0, pp. 15–19, 2010.

[10] S. Caires, V. R. Swail, X. L. Wang, S. Caires, V. R. Swail, and X. L. Wang, "Projection and analysis of extreme wave climate," *Journal of Climate*, vol. 19, no. 21, pp. 5581–5605, Nov. 2006.

[11] I. Grabemann and R. Weisse, "Climate change impact on extreme wave conditions in the North Sea: An ensemble study," *Ocean Dynamics*, vol. 58, no. 3-4, pp. 199–212, Nov. 2008.

[12] P. Ruggiero, P. D. Komar, and J. C. Allan, "Increasing wave heights and extreme value projections: The wave climate of the U.S. Pacific Northwest," *Coastal Engineering*, vol. 57, no. 5, pp. 539–552, May 2010.

[13] R. S. Vose, S. Applequist, M. A. Bourassa, *et al.*, "Monitoring and understanding changes in extremes: Extratropical storms, winds, and waves," *Bulletin of the American Meteorological Society*, vol. 95, no. 3, pp. 377–386, Mar. 2014.

[14] E. D. R. Shearman, "Radio science and oceanography," *Radio Science*, vol. 18, no. 3, pp. 299–320, 1983.

[15] D. E. Barrick, "HF radio oceanography — a review," *Boundary-Layer Meteorology*, vol. 13, no. 1-4, pp. 23–43, Jan. 1978.

[16] D. E. Barrick, "Remote sensing of sea state by radar," in *Ocean 72 - IEEE International Conference on Engineering in the Ocean Environment*, 1972, pp. 186–192.

[17] J. Walsh, R. K. Howell, and B. J. Dawe, "Model development for evaluation studies of ground wave radar," Department of National Defence, Government of Canada, Tech. Rep., 1990.

[18] E. W. Gill and J. Walsh, "High-frequency bistatic cross sections of the ocean surface," *Radio Science*, vol. 36, no. 6, pp. 1459–1475, Nov. 2001.

[19] B. J. Lipa, "Derivation of directional ocean-wave spectra by integral inversion of second-order radar echoes," *Radio Science*, vol. 12, no. 3, pp. 425–434, May 1977.

[20] L. R. Wyatt, "A relaxation method for integral inversion applied to HF radar measurement of the ocean wave directional spectrum," *International Journal of Remote Sensing*, vol. 11, no. 8, pp. 1481–1494, Aug. 1990.

[21] R. K. Howell and M. L. Khandekar, "Measuring ocean surface waves using HF ground wave radar: Validation against a wave model," *Canadian Journal of Remote Sensing*, vol. 19, no. 1, pp. 102–109, 1993.

[22] W. Huang, E. W. Gill, X. Wu, and L. Li, "Measurement of sea surface wind direction using bistatic high-frequency radar," *IEEE Transactions on Geoscience and Remote Sensing*, vol. 50, no. 10, pp. 4117–4122, Oct. 2012.

[23] M. T. Silva, R. Shahidi, E. W. Gill, and W. Huang, "Nonlinear extraction of directional ocean wave spectrum from synthetic bistatic high-frequency surface wave radar data," *IEEE Journal of Oceanic Engineering*, vol. 45, no. 3, pp. 1004–1021, Jul. 2020.

[24] A. H. Nayfeh, *Perturbation Methods*. Weinheim, Germany: Wiley-VCH, 2004, p. 425.

[25] E. J. Hinch, *Perturbation Methods*. Cambridge University Press, 1991, p. 160.

[26] J. C. Luke, "A perturbation method for nonlinear dispersive wave problems," *Proceedings of the Royal Society of London. Series A. Mathematical and Physical Sciences*, vol. 292, no. 1430, pp. 403–412, May 1966.

[27] S. O. Rice, "Reflection of electromagnetic waves from slightly rough surfaces," *Communications on Pure and Applied Mathematics*, vol. 4, no. 2-3, pp. 351–378, Aug. 1951.

[28] L. R. Wyatt, "High order nonlinearities in HF radar backscatter from the ocean surface," *IEE Proceedings - Radar, Sonar and Navigation*, vol. 142, no. 6, p. 293, 1995.

[29] B. L. Weber and D. E. Barrick, "On the nonlinear theory for gravity waves on the ocean's surface. Part I: Derivations," *Journal of Physical Oceanography*, vol. 7, no. 1, pp. 3–10, Jan. 1977.

[30] J. W. Strutt, *The Theory of Sound*. London, United Kingdom: Macmillan and Co., 1877, vol. 1.

[31] J. W. Strutt, *The Theory of Sound*. London, United Kingdom: MacMillan and Co., 1878, vol. 2.

[32] J. W. Strutt, "On the dynamical theory of gratings," *Proceedings of the Royal Society A: Mathematical, Physical and Engineering Sciences*, vol. 79, no. 532, pp. 399–416, Aug. 1907.

[33] R. W. Wood, "On a remarkable case of uneven distribution of light in a diffraction grating spectrum," *Proceedings of the Physical Society of London*, vol. 18, no. 1, pp. 269–275, Jun. 1902.

[34] U. Fano, "The theory of anomalous diffraction gratings and of quasi-stationary waves on metallic surfaces (Sommerfeld's waves)," *Journal of the Optical Society of America*, vol. 31, no. 3, p. 213, Mar. 1941.

[35] A. Sommerfeld, "Über die Ausbreitung der Wellen in der drahtlosen Telegraphie," *Annalen der Physik*, vol. 333, no. 4, pp. 665–736, Jan. 1909.

[36] K. A. Norton, "The propagation of radio waves over the surface of the Earth and in the upper atmosphere, part I," *Proceedings of the IRE*, vol. 24, no. 10, pp. 1367–1387, Oct. 1936.

[37] K. A. Norton, "The propagation of radio waves over the surface of the earth and in the upper atmosphere, part II," *Proceedings of the IRE*, vol. 25, no. 9, pp. 1203–1236, Sep. 1937.

[38] K. A. Norton, "The physical reality of space and surface waves in the radiation field of radio antennas," *Proceedings of the IRE*, vol. 25, no. 9, pp. 1192–1202, Sep. 1937.

[39] M. Guarnieri, "The early history of radar [historical," *IEEE Industrial Electronics Magazine*, vol. 4, no. 3, pp. 36–42, Sep. 2010.

[40] M. Skolnik, "Fifty years of radar," *Proceedings of the IEEE*, vol. 73, no. 2, pp. 182–197, 1985.

[41] M. Skolnik, "Role of radar in microwaves," *IEEE Transactions on Microwave Theory and Techniques*, vol. 50, no. 3, pp. 625–632, Mar. 2002.

[42] R. H. Maynard, "Radar and weather," *Journal of Meteorology*, vol. 2, no. 4, pp. 214–226, Dec. 1945.

[43] G. C. Clark, "Deflating British radar myths of World War II," Air Command and Staff College, Maxwell Air Force Base, Alabama, USA, research rep. AU/ACSC/0609F/97-3, Mar. 1997.

[44] R. Buderi, *The Invention That Changed the World: How a Small Group of Radar Pioneers Won the Second World War and Launched a Technological Revolution*. Touchstone, 1998.

[45] R. Unwin, "The development of radar in new zealand in world war II," *IEEE Antennas and Propagation Magazine*, vol. 34, no. 3, pp. 31–39, Jun. 1992.

[46] S. Nakajima, "Japanese radar development prior to 1945," *IEEE Antennas and Propagation Magazine*, vol. 34, no. 6, pp. 17–22, Dec. 1992.

[47] H. Davies and G. G. Macfarlane, "Radar echoes from the sea surface at centimetre wave-lengths," *Proceedings of the Physical Society*, vol. 58, no. 6, pp. 717–729, Nov. 1946.

[48] L. V. Blake, "Reflection of radio waves from a rough sea," *PROCEEDINGS OF THE I.R.E.*, vol. 109, no. 2849, pp. 271–274, 1950.

[49] H. R. Seiwell and G. P. Wadsworth, "A new development in ocean wave research," *Science*, vol. 109, no. 2829, pp. 271–274, Mar. 1949.

[50] E. F. McClain and W. R. Ferris, "Reflectivity of sea surface for doppler radar," Naval Research Laboratory, Washington D.C., USA, Tech. Rep., 1949, p. 16.

[51] H. Davies, "The reflection of electromagnetic waves from a rough surface," *Proceedings of the IEE - Part IV: Institution Monographs*, vol. 101, no. 7, pp. 209–214, Aug. 1954.

[52] J. R. Wait, "Excitation of surface waves on conducting, stratified, dielectric-clad, and corrugated surfaces," *Journal of Research of the National Bureau of Standards*, vol. 59, no. 6, p. 365, Dec. 1957.

[53] J. R. Wait, "Guiding of electromagnetic waves by uniformly rough surfaces : Part i," *IRE Transactions on Antennas and Propagation*, vol. 7, no. 5, pp. 154–162, Dec. 1959.

[54] J. R. Wait, "Guiding of electromagnetic waves by uniformly rough surfaces: Part II," *IRE Transactions on Antennas and Propagation*, vol. 7, no. 5, pp. 163–168, Dec. 1959.

[55] J. R. Wait, "Perturbation analysis for reflection from two-dimensional periodic sea waves," *Radio Science*, vol. 6, no. 3, pp. 387–391, Mar. 1971.

[56] H. Peake and D. E. Barrick, "Scattering from surfaces with different roughness scales; analysis and interpretation," National Aeronautics and Space Administration, The Ohio State University ElectroScience Laboratory, Tech. Rep. 1388-26, Sep. 1967.

[57] D. E. Barrick, "Theory of HF and VHF propagation across the rough sea, 2, application to HF and VHF propagation above the sea," *Radio Science*, vol. 6, no. 5, pp. 527–533, May 1971.

[58] A. K. Fung, "Scattering theories and radar return," The University of Kansas, Center for Research Inc, Engineering Science Division, Lawrence, KS, USA, Tech. Rep. 48, 1965.

[59] D. E. Barrick, "Theory of ground-wave propagation across a rough sea at dekameter wavelengths," Tech. Rep. May, 1970.

[60] Y. N. Barabanenkov, Y. A. Kravtsov, S. M. Rytov, and V. I. Tamarskiĭ, "Status of the theory of propagation of waves in a randomly inhomogeneous medium," *Soviet Physics Uspekhi*, vol. 13, no. 5, pp. 551–575, May 1971.

[61] T. M. Elfouhaily and C.-A. Guérin, "A critical survey of approximate scattering wave theories from random rough surfaces," *Waves in Random Media*, vol. 14, no. 4, R1–R40, Oct. 2004.

[62] J. Walsh, "On the theory of electromagnetic propagation across a rough surface and calculations in the VHF region," Department of National Defence, Government of Canada, St. John's, Newfoundland and Labrador, Tech. Rep., 1980.

[63] D. D. Crombie, "Doppler spectrum of sea echo at 13.56 Mc./s.," *Nature*, vol. 175, no. 4459, pp. 681–682, Apr. 1955.

[64] R. L. Dowden, "Short-range echoes observed on ionospheric recorders," *Journal of Atmospheric and Terrestrial Physics*, vol. 11, no. 2, pp. 111–117, Jan. 1957.

[65] A. Haubert, "Échos radioélectriques observes sur la houle a la station de sondages ionosphériques de Casablanca," *Annales de Geophysique*, vol. 14, no. 3, pp. 368–373, 1958.

[66] J. R. Wait, "Theory of HF ground wave backscatter from sea waves," *Journal of Geophysical Research*, vol. 71, no. 20, pp. 4839–4842, 1966.

[67] G. R. S. Naylor and R. E. Robson, "Interpretation of backscattered HF radio waves from the sea," *Australian Journal of Physics*, vol. 39, no. 3, p. 395, 1986.

[68] D. E. Barrick and B. J. Lipa, "Analysis methods for narrow-beam high-frequency radar sea echo," National Oceanic and Atmospheric Administration, U.S. Department of Commerce, Boulder, Colorado, USA, research rep. ERL-420-WPL 56, Apr. 1982.

[69] B. J. Lipa and D. E. Barrick, "Extraction of sea state from HF radar sea echo: Mathematical theory and modeling," *Radio Science*, vol. 21, no. 1, pp. 81–100, Jan. 1986.

[70] R. Wong, *Asymptotic approximations of integrals*. Boston: Academic Press, 1989.

[71] A. Erdélyi and M. Wyman, "The asymptotic evaluation of certain integrals," *Archive for Rational Mechanics and Analysis*, vol. 14, no. 1, pp. 217–260, Jan. 1963.

[72] M. H. Holmes, *Introduction to Perturbation Methods*. Springer-Verlag GmbH, Jan. 1, 2013.

[73] M. S. Longuet-Higgins, D. E. Cartwright, and N. D. Smith, "Observations of the directional spectrum of sea waves using the motions of a floating buoy," in *Ocean Wave Spectra, Proc. Conf.*, Eaton, MD, USA: Prentice-Hall, 1963, pp. 111–132.

[74] J. N. Sharma, "Development and evaluation of a procedure for simulating a random directional second order sea surface and associated wave forces," Ph.D. dissertation, University of Delaware, Newark, Delaware, 1979, p. 139.

[75] K. Hasselmann, "On the non-linear energy transfer in a gravity-wave spectrum Part 1. General theory," *Journal of Fluid Mechanics*, vol. 12, no. 4, pp. 481–500, Apr. 1962.

[76] D. E. Barrick, "The interaction of HF/VHF radio waves with the sea surface and its implications," in *AGARD Conference proceedings No. 77 on Electro-*

magnetics of the Sea, A. G. for Aerospace Research & Development (AGARD), Ed., National Atlantic Threaty Organization (NATO), 1970, pp. 18-1 –18-25.

[77] G. Cerutti-Maori, R. Petit, and M. Cadilhac, "Etude numérique du champ diffracté par un réseau," *Comptes rendus hebdomadaires des séances de l'Académie des sciences*, vol. 268, pp. 1060–1063, Apr. 1969.

[78] R. Petit and D. Maystre, "Application des lois de l'électromagnétisme, à l'étude des réseaux," *Revue de Physique Appliquée*, vol. 7, no. 4, pp. 427–441, 1972.

[79] D. Maystre and P. Vincent, "Diffraction d'une onde electromagnetique plane par un objet cylindrique non infiniment conducteur de section arbitraire," *Optics Communications*, vol. 5, no. 5, pp. 327–330, Aug. 1972.

[80] R. Petit, "A tutorial introduction," in *Topics in Current Physics*, Springer Berlin Heidelberg, 1980, pp. 1–52.

[81] A. Akarid and F. Polack, "Computation of intensity and polarization state of diffracted fields from reflective gratings in conical geometry," *Review of Scientific Instruments*, vol. 90, no. 2, p. 021 709, 2019.

[82] J. Walsh, "On the solution of antenna currents," in *Antennas and Propagation Society International Symposium*, Institute of Electrical and Electronics Engineers, 1976.

[83] J. Walsh and S. Srivastava, "Method of analysis for thin, tubular, linear antennas," in *Antennas and Propagation Society International Symposium*, Institute of Electrical and Electronics Engineers, 1977.

[84] S. K. Srivastava, "Analysis of linear antenna systems: A different approach," M.S. thesis, Memorial University of Newfoundland, St. John's, Newfoundland and Labrador, Canada, Jul. 1977.

[85] S. K. Srivastava, "Scattering of high-frequency electromagnetic waves from an ocean surface : An alternative approach incorporating a dipole source," Ph.D. dissertation, Memorial University of Newfoundland. Faculty of Engineering and Applied Science, St. John's, Newfoundland and Labrador, Canada, 1984.

[86] J. Walsh and S. K. Srivastava, "Rough surface propagation and scatter: 1. general formulation and solution for periodic surfaces," *Radio Science*, vol. 22, no. 2, pp. 193–208, Mar. 1987.

[87] J. Walsh and R. Donnelly, "A new technique for studying propagation and scattering for mixed paths with discontinuities," *Proceedings of the Royal Society A: Mathematical, Physical and Engineering Sciences*, vol. 412, no. 1842, pp. 125–167, Jul. 1987.

[88] J. Walsh and B. J. Dawe, "Development of a model forthe first order bistatic ocean clutter radar cross section for ground wave radars," Department of National Defence, Government of Canada, Tech. Rep. DSS Contract Number W7714-1-9569/01-ST, 1994, Northern Radar Systems Limited con-tract report for the Defence Research Establishment Ottawa.

[89] E. W. Gill, "The scattering of high frequency electromagnetic radiation from the ocean surface : An analysis based on a bistatic ground wave radar configuration," Ph.D. dissertation, Memorial University of Newfoundland, St. John's, Newfoundland and Labrador, 1999.

[90] C. A. Balanis, *Advanced Engineering Electromagnetics*, 2nd. John Wiley & Sons, 2012, p. 1018.

[91] J. Walsh, "Asymptotic expansion of a Sommerfeld integral," *Electronics Letters*, vol. 20, no. 18, p. 746, 1984.

[92] E. W. Gill, W. Huang, and J. Walsh, "On the development of a second-order bistatic radar cross section of the ocean surface: A high-frequency result for a finite scattering patch," *IEEE Journal of Oceanic Engineering*, vol. 31, no. 4, pp. 740–750, Oct. 2006.

[93] H. Günther, K. W. Gurgel, G. Evensen, *et al.*, "EuroROSE—European radar ocean sensing," in *Proceedings of the COST conference provision and engineering/operational application of wave spectra. Paris, France*, 1998, pp. 21–25.

[94] M. T. Silva, E. W. Gill, and W. Huang, "Electromagnetic scattering in curvilinear coordinates using a generalized functions method," *Radio Science*, vol. 54, no. 11, pp. 1099–1111, Nov. 2019.

[95] M. T. Silva, E. W. Gill, and W. Huang, "First-order high-frequency scattering for ocean surfaces with large roughness scales," in *28th Annual Newfoundland Electrical and Computer Engineering Conference (NECEC 2019)*, IEEE Newfoundland and Labrador Section, St. John's, Newfoundland and Labrador, Canada, Nov. 2019.

[96] M. T. Silva, W. Huang, and E. W. Gill, "Bistatic high-frequency radar cross-section of the ocean surface with arbitrary wave heights," *Remote Sensing*, vol. 12, no. 4, p. 667, Feb. 2020.

[97] M. T. Silva, W. Huang, and E. W. Gill, "High-frequency radar cross-section of the ocean surface with arbitrary roughness scales: a generalized functions approach," *IEEE Transactions on Antennas and Propagation*, vol. 69, no. 3, pp. 1643–1657, Mar. 2021.

[98] M. T. Silva, W. Huang, and E. W. Gill, "High-frequency radar cross-section of the ocean surface with arbitrary roughness scales: higher-orders and generalized form," *IEEE Transactions on Antennas and Propagation*, vol. 69, Dec. 2021, In press.

[99] M. T. Silva, E. W. Gill, and W. Huang, "High-frequency radar cross-section for an ocean surface with arbitrary heights," in *Radiowave Oceanography Workshop 2019*, Ocean Networks Canada, Victoria, BC, Canada, Aug. 2019.

[100] M. T. Silva, E. W. Gill, and W. Huang, "HF radar cross-section of ocean surfaces with arbitrary wave heights," in *Proceedings of the 2020 IEEE International Symposium on Antennas and Propagation and North American Radio Science Meeting*, In press, IEEE, Jul. 2020.

[101] M. T. Silva, W. Huang, and E. W. Gill, "Second-order correction to the HF radar cross-section of the ocean surface at electromagnetically-high sea states," in *Global OCEANS2020*, IEEE, Oct. 2020.

[102] J. G. Van Bladel, *Electromagnetic Fields*, ser. IEEE Press Series on Electromagnetic Wave Theory. Hoboken, NJ, USA: Wiley-Interscience, May 2007, p. 1155.

[103] W. Rudin, *Functional Analysis*, 2nd, ser. International series in pure and applied mathematics. McGraw-Hill Science/Engineering/Math, 1991, p. 448.

[104] R. P. Kanwal, *Generalized Functions: Theory and Applications*, 3rd. Boston, MA: Birkhäuser Boston, 2004, p. 476.

[105] G. B. Arfken, H. J. Weber, and F. E. Harris, *Mathematical Methods for Physicists: A Comprehensive Guide*. Elsevier Science, 2013.

[106] P. A. Kelly, *Mechanics Lecture Notes, Part III: Foundations of Continuum Mechanics*. Auckland, NZ: University of Auckland, 2019.

[107] C.-T. Tai, *Generalized Vector and Dyadic Analysis: Applied Mathematics in Field Theory*, Second, ser. IEEE/OUP Series on Electromagnetic Wave Theory. IEEE Press, Apr. 1, 1997, 212 pp.

[108] M. L. Szwabowicz, "Pure strain deformations of surfaces," *Journal of Elasticity*, vol. 92, no. 3, pp. 255–275, May 2008.

[109] J. A. Stratton and L. J. Chu, "Diffraction theory of electromagnetic waves," *Physical Review*, vol. 56, no. 1, pp. 99–107, Jul. 1939.

[110] D. M. Milder, "An improved formalism for wave scattering from rough surfaces," *The Journal of the Acoustical Society of America*, vol. 89, no. 2, pp. 529–541, 1991.

[111] D. M. Milder, "An improved formalism for electromagnetic scattering from a perfectly conducting rough surface," *Radio Science*, vol. 31, no. 6, pp. 1369–1376, Nov. 1996.

[112] K. Jörgens, *Linear Integral Operators*. Boston, MA, USA: Pitman Advanced Pub. Program, 1982, p. 379.

[113] A. D. Poularikas, *Transforms and Applications Handbook*. CRC Press, 2010.

[114] Y. Liu, M.-Y. Su, X.-H. Yan, and W. T. Liu, "The mean-square slope of ocean surface waves and its effects on radar backscatter," *Journal of Atmospheric and Oceanic Technology*, vol. 17, no. 8, pp. 1092–1105, Aug. 2000.

[115] C. Cox and W. Munk, "Measurement of the roughness of the sea surface from photographs of the sun's glitter," *Journal of the Optical Society of America*, vol. 44, no. 11, p. 838, Nov. 1954.

[116] J. R. Apel, "An improved model of the ocean surface wave vector spectrum and its effects on radar backscatter," *Journal of Geophysical Research*, vol. 99, no. C8, p. 16 269, 1994.

[117] J. Wu, "Mean square slopes of the wind-disturbed water surface, their magnitude, directionality, and composition," *Radio Science*, vol. 25, no. 1, pp. 37–48, Jan. 1990.

[118] O. Phillips, *The Dynamics of the Upper Ocean*, Second, ser. Cambridge Monographs on Mechanics and Applied Mathematics. Cambridge University Press, 1977.

[119] J. Wurman, C. Alexander, P. Robinson, and Y. Richardson, "Low-level winds in tornadoes and potential catastrophic tornado impacts in urban areas," *Bulletin of the American Meteorological Society*, vol. 88, no. 1, pp. 31–46, Jan. 2007.

[120] D. E. Barrick, "Remote sensing of sea sate by radar," in *Remote Sensing of the Troposphere*, ser. Remote Sensing of the Troposphere, V. E. Derr, Ed., Boulder, Colorado, USA: National Oceanic and Atmospheric Administration, 1972, ch. 12, pp. 12–1–12–46.

[121] E. W. Gill and J. Walsh, "Bistatic form of the electric field equations for the scattering of vertically polarized high-frequency ground wave radiation from slightly rough, good conducting surfaces," *Radio Science*, vol. 35, no. 6, pp. 1323–1335, Nov. 2000.

[122] S. R. Massel, *Ocean Surface Waves: Their Physics and Prediction*, 3rd ed. World Scientific Publishing, 2017, p. 776.

[123] L. E. Borgman, "Statistical models for ocean waves and wave forces," in *Advances in Hydroscience*, V. T. Chow, Ed., vol. 8, New York City, NY, USA: Academic Press, Jan. 1972, pp. 139–181.

[124] A. Ishimaru, *Electromagnetic Wave Propagation, Radiation, and Scattering*. Hoboken, NJ, USA: John Wiley & Sons, Inc., May 2017.

[125] W. Huang and E. W. Gill, "HF surface wave radar," in *Wiley Encyclopedia of Electrical and Electronics Engineering*, J. G. Webster, Ed. American Cancer Society, 2019, pp. 1–11.

[126] F. Crawford, *Waves*, ser. Berkeley Physics Course. New York, USA: McGraw-Hill, 1968, vol. 3.

[127] E. F. Knott, J. F. Schaeffer, and M. T. Tulley, *Radar Cross Section*. SCITECH PUB, Nov. 2003, 626 pp.

[128] R. P. Singh, *Communication Systems: Analog & Digital*. New Delhi: Tata McGraw-Hill, 2007.

[129] N. Baddour, "Operational and convolution properties of three-dimensional Fourier transforms in spherical polar coordinates," *Journal of the Optical Society of America A*, vol. 27, no. 10, p. 2144, Oct. 2010.

[130] W. Rudin, *Principles of Mathematical Analysis*, Third. McGraw-Hill Education, Feb. 1, 1976, 352 pp.

[131] S. Lang, *Real and Functional Analysis*. Springer New York, 1993.

[132] K. Hasselmann, "Feynman diagrams and interaction rules of wave-wave scattering processes," *Reviews of Geophysics*, vol. 4, no. 1, p. 1, Feb. 1966.

[133] M. I. Skolnik, *Radar Handbook*, 3rd. McGraw-Hill, 2008.

[134] D. E. Barrick, "First-order theory and analysis of MF/HF/VHF scatter from the sea," *IEEE Transactions on Antennas and Propagation*, vol. 20, no. 1, pp. 2–10, Jan. 1972.

[135] W. J. Pierson, "A unified mathematical theory for the analysis, propagation, and refraction of storm generated ocean surface waves – Part I," U.S. Office of Naval Research, New York City, NY, USA, research rep. ONR-285, 1952.

[136] H. Royden and P. Fitzpatrick, *Real Analysis*. Prentice Hall, 2010.

[137] A. Leon-Garcia, *Probability, Statistics, and Random Processes for Electrical Engineering*. Upper Saddle River, NJ, USA: Pearson/Prentice Hall, 2008, p. 818.

[138] D. E. Barrick and J. B. Snider, "The statistics of HF sea-echo Doppler spectra," *IEEE Journal of Oceanic Engineering*, vol. 2, no. 1, pp. 19–28, Jan. 1977.

[139] K. I. Park, *Fundamentals of Probability and Stochastic Processes with Applications to Communications*. Holmdel, NJ: Springer International Publishing, 2018, 288 pp.

[140] R. S. Elliott, *Antenna Theory and Design*, ser. IEEE Press Series on Electromagnetic Wave Theory. John Wiley & Sons, 2003.

[141] A. M. Yaglom, *Correlation Theory of Stationary and Related Random Functions*. New York: Springer-Verlag, 1987.

[142] B. Kinsman, *Wind Waves: Their Generation and Propagation on the Ocean Surface*. Dover Publications, 1965, p. 676.

[143] B. J. Dawe, "Radio wave propagation over earth : Field calculations and an implementation of the roughness effect," M.S. thesis, Memorial University of Newfoundland. Faculty of Engineering and Applied Science, St. John's, Newfoundland and Labrador, Canada, 1988.

[144] E. C. Jordan and K. G. Balmain, *Electromagnetic Waves and Radiating Systems*, ser. Prentice-Hall Electrical Engineering. Prentice-Hall, 1968.

[145] M. T. Silva, E. W. Gill, and W. Huang, "Effects of electromagnetically-large waves on the second-order radar cross section of the ocean surface in the HF band," in *29th Annual Newfoundland Electrical and Computer Engineering Conference (NECEC 2020)*, IEEE Newfoundland and Labrador Section, St. John's, Newfoundland and Labrador, Canada, Nov. 2020.

[146] H. Mitsuyasu, F. Tasai, T. Suhara, *et al.*, "Observations of the directional spectrum of ocean waves using a cloverleaf buoy," *Journal of Physical Oceanography*, vol. 5, no. 4, pp. 750–760, Oct. 1975.

[147] American Bureau of Shipping, "Guidance notes on selecting design wave by long term stochastic method," American Bureau of Shipping, Tech. Rep., Oct. 2016.

[148] Det Norske Veritas, *Environmental Conditions and Environmental Loads (DNV-RP-C205)*, Det Norske Veritas, Oct. 2010.

[149] M. Abramowitz and I. A. Stegun, *Handbook of Mathematical Functions*. Dover Publications Inc., Jun. 1, 1965, p. 1046, 1046 pp.

[150] D. W.-C. Wang, "Estimation of wave directional spreading in severe seas," in *The Second International Offshore and Polar Engineering Conference*, International Society of Offshore and Polar Engineers, San Francisco, CA, USA, Jun. 1992.

[151] W. H. Buckley, "Extreme and climatic wave spectra for use in structural design of ships," *Naval Engineers Journal*, vol. 100, no. 5, pp. 36–58, Sep. 1988.

[152] D. E. Barrick, "Extraction of wave parameters from measured HF radar sea-echo Doppler spectra," *Radio Science*, vol. 12, no. 3, pp. 415–424, 1977.

[153] R. K. Howell and J. Walsh, "Measurement of ocean wave spectra using narrow-beam HF-radar," *IEEE Journal of Oceanic Engineering*, vol. 18, no. 3, pp. 296–305, Jul. 1993.

[154] C. L. Bretschneider, "Revisions in wave forecasting: Deep and shallow water," *Coastal Engineering Proceedings*, vol. 1, no. 6, p. 3, Jan. 1957.

[155] C. L. Bretschneider, "Significant waves and wave spectrum," *Ocean Industry*, vol. 3, no. 2, pp. 40–46, Feb. 1968.

[156] C. Shen, W. Huang, and E. W. Gill, "High-frequency radar cross-sections of swell-contaminated seas for a pulsed waveform," *IET Radar, Sonar & Navigation*, vol. 8, no. 4, pp. 382–395, Apr. 2014.

[157] L. R. Wyatt, J. J. Green, and A. Middleditch, "HF radar data quality requirements for wave measurement," *Coastal Engineering*, vol. 58, no. 4, pp. 327–336, Apr. 2011.

[158] M. Fernandes, C. Fernandes, T. Barroqueiro, P. Agostinho, N. Martins, and A. Alonso-Martirena, "Extreme wave height events in Algarve (Portugal): Comparison between HF radar systems and wave buoys," in *5.as Jornadas de Engenharia Hidrográfica*, Instituto Hidrográfico, Lisbon, Portugal, 2018, pp. 222–225.

[159] P. A. E. M. Janssen, "On some consequences of the canonical transformation in the Hamiltonian theory of water waves," *Journal of Fluid Mechanics*, vol. 637, pp. 1–44, 2009.

[160] L. R. Wyatt, J. J. Green, K. W. Gurgel, *et al.*, "Validation and intercomparisons of wave measurements and models during the EuroROSE experiments," *Coastal Engineering*, vol. 48, no. 1, pp. 1–28, 2003.

[161] K.-W. Gurgel, G. Antonischki, H.-H. Essen, and T. Schlick, "Wellen Radar (WERA): A new ground-wave HF radar for ocean remote sensing," *Coastal Engineering*, vol. 37, no. 3-4, pp. 219–234, Aug. 1999.

[162] K.-W. Gurgel and T. Schlick, "Remarks on signal processing in HF radars using FMCW modulation," in *Proc. Intl. Radar Symp. - IRS 2009*, Hamburg, Germany, Sep. 2009, pp. 1–5.

[163] H. Hersbach, B. Bell, P. Berrisford, *et al.*, "The ERA5 global reanalysis," *Quarterly Journal of the Royal Meteorological Society*, vol. 146, no. 730, pp. 1999–2049, Jun. 2020.

[164] J. M. Headrick and M. I. Skolnik, "Over-the-horizon radar in the HF band," *Proceedings of the IEEE*, vol. 62, no. 6, pp. 664–673, 1974.

[165] Y. Li, Z. Wang, Y. Zhu, Y. Wei, and R. Xu, "Cascaded method for ionospheric decontamination and sea clutter suppression for high-frequency hybrid sky-surface wave radar," *IET Signal Proc.*, vol. 9, no. 7, pp. 562–571, Sep. 2015.

[166] Y. Ma, E. W. Gill, and W. Huang, "First-order bistatic high-frequency radar ocean surface cross-section for an antenna on a floating platform," *IET Radar, Sonar and Navigation*, vol. 10, no. 6, pp. 1136–1144, Jul. 2016.

[167] Y. Ma, W. Huang, and E. W. Gill, "The second-order bistatic high-frequency radar cross section of ocean surface for an antenna on a floating platform," *Canadian Journal of Remote Sensing*, vol. 42, no. 4, pp. 332–343, Jul. 2016.

[168] E. W. Gill, "An algorithm for the extraction of ocean wave parameters from wide beam HF radar (CODAR) backscatter," M.S. thesis, Memorial University of Newfoundland. Faculty of Engineering and Applied Science, St. John's, Newfoundland and Labrador, Canada, 1990.

[169] E. Bahar, "Like and cross-polarized scatter cross sections for two-dimensional, multiscale rough surfaces based on a unified full wave variational technique," *Radio Science*, vol. 46, no. 4, n/a–n/a, Aug. 2011.

[170] S. A. Kitaigorodskii, "Applications of the theory of similarity to the analysis of wind-generated wave motion as a stochastic process," *Izvestiya Akademii Nauk SSR, Seriya Geofizicheskaya*, vol. 1, no. 1, pp. 105–117, 1962.

[171] K. Hasselmann, T. Barnett, E. Bouws, *et al.*, "Measurements of wind-wave growth and swell decay during the Joint North Sea Wave Project (JONSWAP)," Deutches Hydrographisches Institut, Tech. Rep., 1973.

[172] M. L. Heron, "Directional spreading of short wavelength fetch-limited wind waves," *Journal of Physical Oceanography*, vol. 17, no. 2, pp. 281–285, Feb. 1987.

[173] D. E. Hasselmann, M. Dunckel, and J. A. Ewing, "Directional wave spectra observed during JONSWAP 1973," *Journal of Physical Oceanography*, vol. 10, no. 8, pp. 1264–1280, Aug. 1980.

[174] J. L. Synge and A. Schild, *Tensor Calculus*. Guilford Publications, Apr. 2012, 336 pp.

[175] P. Grinfeld, *Introduction to Tensor Analysis and the Calculus of Moving Surfaces*. Springer-Verlag GmbH, Sep. 2013.

[176] E. de Souza Sánchez Filho, *Tensor Calculus for Engineers and Physicists*. Springer-Verlag GmbH, Jun. 2016.

[177] L. Hörmander, *The Analysis of Linear Partial Differential Operators I*, ser. Classics in Mathematics. Berlin, Heidelberg: Springer Berlin Heidelberg, 2003.

[178] J. A. Kong, *Electromagnetic Wave Theory*. John Wiley & Sons, 1986, p. 696.

[179] P. Török, P. R. Munro, and E. E. Kriezis, "Rigorous near- to far-field transformation for vectorial diffraction calculations and its numerical implementation," *Journal of the Optical Society of America A*, vol. 23, no. 3, p. 713, Mar. 2006.

[180] J. A. Stratton, *Electromagnetic Theory*. Hoboken, NJ, USA: John Wiley & Sons, Inc., 1941, p. 615.

[181] H. Bateman, *Tables of Integral Transforms*, A. Edrélyi, W. Magnus, F. Oberhettinger, and F. G. Tricomi, Eds., 6. New York City, NY, USA: McGraw-Hill Book Company, 1954, vol. 1 & 2, pp. 525–526.

[182] U. Graf, *Introduction to Hyperfunctions and Their Integral Transforms*. Basel: Birkhäuser Basel, 2010.

Appendix A

Derivations Pertinent to the System of Equations for the Electric Field in Curvilinear Coordinates

A.1 Proof of Equivalence Between the Notation in Chapter 2 and [94]

Comparing the system of equations shown in [94] and the one presented in Chapter 2, it is clear that the only difference between the two systems is the product between $(\nabla \mathbf{E})^{\pm}$ and ∇h_{R_1}. This difference comes from the application of the vector identity for the Laplacian of the product between a scalar function and a vector, as, for example

in $\nabla^2(h_{R_1}\mathbf{E})$. In this case, the expression can be expanded as [102]

$$\nabla^2(h_{R_1}\mathbf{E}) = h_{R_1}\nabla^2\mathbf{E} + 2[(\nabla h_{R_1}\cdot\nabla)\mathbf{E}] + \mathbf{E}^{-}\nabla^2 h_{R_1}. \tag{A.1}$$

More specifically, the difference between the two systems of equations can be found in the term $(\nabla h_{R_1}\cdot\nabla)\mathbf{E}$. In [94], the identity was directly applied and the directional derivative term was interpreted as $(\nabla\mathbf{E})^{\pm}\cdot\nabla h_{R_1}$, as it uses the notation for the gradient of the dyadic introduced in [106]. To avoid the direct use of identities, and to bring the expressions to a more common interpretation of the vector gradient [102], [107], the expression in (A.1) was not directly applied in Chapter 2, resulting in $\nabla h_{R_1}\cdot\nabla(\mathbf{E})^{\pm}$ in place of $(\nabla h_{R_1}\cdot\nabla)\mathbf{E}$ in (A.6). At face value, since the dyadic dot product is not commutative, the system of equations in [94] and the one presented in Chapter 2 are incompatible if the same notation is taken on both expressions at face value. However, to prove the compatibility between the two expressions, the directional derivative and the term in question will be expanded in general curvilinear coordinates using tensor calculus notation [174]–[176]. First, the equivalence between $(\nabla h_{R_1}\cdot\nabla)\mathbf{E}$ and $\nabla h_{R_1}\cdot\nabla\mathbf{E}$ must be shown.

In general curvilinear coordinates, the vectors $\mathbf{u}$ and $\mathbf{v}$ can be defined as

$$\mathbf{u} = u^i\mathbf{b}_i, \tag{A.2}$$

$$\mathbf{v} = v^i\mathbf{b}_i, \tag{A.3}$$

where u^i, v^i are respectively the contravariant components of the vectors $\mathbf{u}$ and $\mathbf{v}$, and $\mathbf{b}_i$ are the covariant basis vectors for every i [175]. The gradient operator can be written as [175]

$$\nabla = \mathbf{b}^i\partial_i \tag{A.4}$$

where $\mathbf{b}^i$ ∂_i are respecively the contravariant basis vectors and the partial derivatives to be taken with respect to the curvilinear coordinates for every i. From these definitions, the directional derivative operator in the direction of the vector $\mathbf{u}$ can be defined as

$$(\mathbf{u}\cdot\nabla) = u^i\mathbf{b}_i\cdot\mathbf{b}^j\partial_j = u^i\partial_j\delta^i_j = u^i\partial_i, \tag{A.5}$$

where δ^i_j is the Kronecker delta. Therefore, applying the directional derivative operator defined in (A.5) to the vector $\mathbf{v}$, the expression for the derivative of $\mathbf{v}$ in the direction of $\mathbf{u}$ can be written as

$$\begin{aligned}(\mathbf{u}\cdot\nabla)\mathbf{v} = u^i\partial_i(v^j\mathbf{b}_j) = u^i\left(\mathbf{b}_j(\partial_i v^j) + v^j(\partial_i\mathbf{b}_j)\right) = u^i\left(\mathbf{b}_j\partial_i v^j + v^j\Gamma^k_{ji}\mathbf{b}_k\right)\\ \therefore\ (\mathbf{u}\cdot\nabla)\mathbf{v} = u^i\left(\partial_i v^k + \Gamma^k_{li}v^l\right)\mathbf{b}_k,\end{aligned} \tag{A.6}$$

where Γ^k_{ji} are the Christoffel symbols of the second kind [175]. Now, to prove that $(\mathbf{u}\cdot\nabla)\mathbf{v}$ is equal to the left dyadic dot product between $\mathbf{u}$ and the gradient of $\mathbf{v}$, the latter expression must be expanded in the same manner.

From the definition of the gradient operator in (A.4), the gradient of the vector $\mathbf{v}$ can be written as

$$\nabla\mathbf{v} = \mathbf{b}^i\partial_i\left(v^j\mathbf{b}_j\right) = \mathbf{b}^i\left(\partial_i v^k + \Gamma^k_{ji}v^j\right)\mathbf{b}_k = \left(\partial_i v^k + \Gamma^k_{li}v^l\right)\mathbf{b}^i\otimes\mathbf{b}_k, \tag{A.7}$$

where $\mathbf{b}^i\otimes\mathbf{b}_k$ is the tensor (or direct) product between the vectors $\mathbf{b}^i$ and $\mathbf{b}_k$ [175]. In dyadic calculus, the direct product can be understood as the dyadic product between two vectors [107]. Now applying a left dot product with $\mathbf{u}$ in (A.7), knowing that the

tensor product is non-commutative, the following can be obtained.

$$\begin{aligned}
\mathbf{u}\cdot\nabla\mathbf{v} &= u^j\mathbf{b}_j\cdot\mathbf{b}^i\otimes\mathbf{b}_k\left(\partial_i v^k+\Gamma^k_{li}v^l\right)=u^j(\mathbf{b}_j\cdot\mathbf{b}^i)\mathbf{b}_k\left(\partial_i v^k+\Gamma^k_{li}v^l\right)\\
&\Rightarrow \mathbf{u}\cdot\nabla\mathbf{v}=u^j\delta^i_j\left(\partial_i v^k+\Gamma^k_{li}v^l\right)\mathbf{b}_k=u^i\left(\partial_i v^k+\Gamma^k_{li}v^l\right)\mathbf{b}_k \qquad \text{(A.8)}\\
&\therefore\ \mathbf{u}\cdot\nabla\mathbf{v}=(\mathbf{u}\cdot\nabla)\mathbf{v}\ \blacksquare
\end{aligned}$$

Now, using the notation introduced in [106], the gradient of a vector differs from the direct product between the nabla operator and a vector, and is defined such that $\operatorname{grad}\mathbf{v}=(\nabla\mathbf{v})^\top$, where $(\nabla\mathbf{v})^\top$ is the dyadic (or tensor) transpose of $\nabla\mathbf{v}$ [106]. Therefore,

$$\mathbf{u}\cdot\operatorname{grad}\mathbf{v}=\mathbf{u}\cdot(\nabla\mathbf{v})^\top=\nabla\mathbf{v}\cdot\mathbf{u},$$

as seen in the expressions shown in [94]. To avoid confusion between the two notations, the expressions were reverted to the notation presented, for example, in [107] and [102], as they are more natural to a reader familiar with vector, dyadic and tensor analysis, and its relationships can be derived without the use of transpose operators and the introduction of different notations for $\operatorname{grad}\mathbf{v}$ and $\nabla\mathbf{v}$.

A.2 Proof That the Curvilinear System of Equations for the Electric Field Reduces to the Stratton-Chu Equation for a PEC sphere

Based on the equations for a general scattering body defined in Section 2.3, the special case for a perfectly-electrically conducting (PEC) spherical scattering body is considered.

A.2.1 Electric Field Equation for a PEC Sphere

In the case of a PEC sphere, $\sigma_1 \to \infty$. In this case, considering the definition of ${\gamma_1}^2$ and ${\gamma_2}^2$ given in (2.6), their ratio can be written as

$$\frac{{\gamma_0}^2}{{\gamma_1}^2} = \frac{j\omega\mu_0(j\omega\epsilon_0)}{j\omega\mu_0(\cancelto{\infty}{\sigma_1} + j\omega\epsilon_1)} = 0. \tag{A.9}$$

From (A.9), the boundary condition for the electric field presented in (2.66) can be redefined for a PEC sphere:

$$\mathbf{E}^- - \mathbf{E}^+ = -\mathbf{E}_n^+.$$

Comparing terms with same support on both sides of the equation, the following equations can be obtained for the boundary conditions of the electric field:

$$\mathbf{E}^- = 0 \tag{A.10}$$

$$\mathbf{E}^+ = \mathbf{E}_n^+ \tag{A.11}$$

From (A.10), there is no electric field present at the inner boundary of the sphere. This can be confirmed by the fact that the skin depth δ for a PEC scattering body, given by [e.g., 144],

$$\delta = \left[\omega\sqrt{\frac{\mu_0\epsilon_1}{2}\left(\sqrt{1 + \frac{\cancelto{\infty}{\sigma_1^2}}{\omega^2{\epsilon_1}^2}} - 1\right)}\right]^{-1}. \tag{A.12}$$

is equal to zero for an infinite conductivity. Also, from (A.11), it can be seen that the tangential electric field at the external boundary of the sphere is null, and therefore, only the normal component is present. Thus,

$$[1 - h(r-a)]\mathbf{E} = 0,\ \mathbf{E}^- = 0,\ \mathbf{R}^- = 0. \tag{A.13}$$

Hence, the system of equations presented in (2.62) to (2.67) can be rewritten as,

$$\begin{aligned} &\mathbf{E} = h(r-a)\mathbf{E} \\ \Rightarrow &\mathbf{E} = \left\{T_{SE}(\mathbf{J_s}) - \mathbf{E}^{+}\delta'(r-a) + \mathbf{R}^{+}\delta(r-a)\right\} * G_0, \end{aligned} \tag{A.14}$$

with boundary conditions

$$\mathbf{E}_t^{+} = 0 \Rightarrow \mathbf{E}^{+} = \mathbf{E}_n^{+}, \tag{A.15}$$

$$\mathbf{R}^{+} = -\nabla(\mathbf{E}^{+} \cdot \hat{\mathbf{r}}). \tag{A.16}$$

Substituting (A.15) and (A.16) into (A.14), the expression for the total electric field in the presence of a PEC sphere can be obtained:

$$\mathbf{E} = \left\{T_{SE}(\mathbf{J_s}) - \mathbf{E}_n^{+}\delta'(r-a) - \nabla(\mathbf{E}^{+} \cdot \hat{\mathbf{r}})\delta(r-a)\right\} * G_0. \tag{A.17}$$

It is evident from (A.17) that the electric field can be divided in two parts: one that is generated by the source (incident field), and the other that is caused by the scattering of the electric field by the surface of the sphere (scattered field). Therefore, the total electric field can be redefined as [90]

$$\mathbf{E} = \mathbf{E}^{i} + \mathbf{E}^{s}, \tag{A.18}$$

where

$$\mathbf{E}^{i} = T_{SE}(\mathbf{J_s}) * G_0 \tag{A.19}$$

$$\mathbf{E}^{s} = -\left\{\mathbf{E}_n^{+}\delta'(r-a) + \nabla(\mathbf{E}^{+} \cdot \hat{\mathbf{r}})\delta(r-a)\right\} * G_0 \tag{A.20}$$

represent the incident and the scattered electric fields respectively.

A.2.1.1 Scattered Electric Field

Considering the scattered electric field $\mathbf{E}^s$ presented in (A.20), knowing that $\nabla\delta(\tilde{f}(\mathbf{r})) = \nabla\tilde{f}(\mathbf{r})\delta'(\tilde{f}(\mathbf{r})) = \mathbf{n}\delta'(\tilde{f}(\mathbf{r}))$ and $\hat{\mathbf{r}} = \hat{\mathbf{n}}$, the first term of $\mathbf{E}^s$ can be written as:

$$\mathbf{E}^s = -\left\{\mathbf{E}^+[\hat{\mathbf{n}}\cdot\nabla\delta(r-a)] + \nabla(\mathbf{E}^+\cdot\hat{\mathbf{n}})\delta(r-a)\right\} * G_0. \tag{A.21}$$

Using the vector triple product identity [e.g., 105], the following expression can be obtained:

$$\mathbf{E}^s = -\left\{(\mathbf{E}^+\cdot\hat{\mathbf{n}})\nabla\delta(r-a) + \hat{\mathbf{n}}\times(\mathbf{E}^+\times\nabla\delta(r-a)) + \nabla(\mathbf{E}^+\cdot\hat{\mathbf{n}})\delta(r-a)\right\} * G_0. \tag{A.22}$$

Now, using the Jacobi identity for the triple vector product [105],

$$\mathbf{E}^s = -\left\{(\mathbf{E}^+\cdot\hat{\mathbf{n}})\nabla\delta(r-a) + (\hat{\mathbf{n}}\times\mathbf{E}^+)\times\nabla\delta(r-a) + \mathbf{E}^+\times(\hat{\mathbf{n}}\times\nabla\delta(r-a)) + \nabla(\mathbf{E}^+\cdot\hat{\mathbf{n}})\delta(r-a)\right\} * G_0. \tag{A.23}$$

Since $\hat{\mathbf{n}}$ and $\nabla\delta(r-a)$ are colinear vectors, $\hat{\mathbf{n}}\times\nabla\delta(r-a) = 0$. Therefore,

$$\mathbf{E}^s = -\left\{(\mathbf{E}^+\cdot\hat{\mathbf{n}})\nabla\delta(r-a) + (\hat{\mathbf{n}}\times\mathbf{E}^+)\times\nabla\delta(r-a) + \nabla(\mathbf{E}^+\cdot\hat{\mathbf{n}})\delta(r-a)\right\} * G_0. \tag{A.24}$$

Considering that each one of the operators over the Dirac deltas in (A.24) is a linear differential operator, the convolution property of the Dirac delta allows $\mathbf{E}^s$ to be rewritten as

$$\mathbf{E}^s = -\left\{(\mathbf{E}^+\cdot\hat{\mathbf{n}})\nabla G_0 + (\hat{\mathbf{n}}\times\mathbf{E}^+)\times\nabla G_0 + \nabla(\mathbf{E}^+\cdot\hat{\mathbf{n}})G_0\right\} * \delta(r-a). \tag{A.25}$$

Taking the $\nabla(\mathbf{E}^+\cdot\hat{\mathbf{n}})$ term, and expanding it using the vector identity for the gradient of a dot product, the following expression can be obtained:

$$\nabla(\mathbf{E}^+\cdot\hat{\mathbf{n}}) = (\mathbf{E}^+\cdot\nabla)\hat{\mathbf{n}} + (\hat{\mathbf{n}}\cdot\nabla)\mathbf{E}^+ + \mathbf{E}^+\times(\nabla\times\hat{\mathbf{n}}) + \hat{\mathbf{n}}\times(\nabla\times\mathbf{E}^+). \tag{A.26}$$

Since $\hat{\mathbf{n}}$ is defined as the gradient of the function defining the surface of the scattering object, the curl of the normal unit vector will be zero. Also, since

$$\nabla\hat{\mathbf{n}} = \nabla\hat{\mathbf{r}} = \frac{\hat{\boldsymbol{\theta}}\hat{\boldsymbol{\theta}}}{r} + \frac{\hat{\boldsymbol{\phi}}\hat{\boldsymbol{\phi}}}{r},$$

$(\mathbf{E}^+ \cdot \nabla)\hat{\mathbf{n}}$ can be written as

$$(\mathbf{E}^+ \cdot \nabla)\hat{\mathbf{n}} = E_n^+ \hat{\mathbf{r}} \cdot \nabla\hat{\mathbf{r}} = \frac{E_n^+}{r}\left[(\hat{\mathbf{r}} \cdot \hat{\boldsymbol{\theta}})\hat{\boldsymbol{\theta}} + (\hat{\mathbf{r}} \cdot \hat{\boldsymbol{\phi}})\hat{\boldsymbol{\phi}}\right] = \mathbf{0} \tag{A.27}$$

Similarly,

$$(\hat{\mathbf{n}} \cdot \nabla)\mathbf{E}^+ = \hat{\mathbf{r}} \cdot \nabla(E_n^+\hat{\mathbf{r}}) = (\hat{\mathbf{r}} \cdot \nabla E_n^+)\hat{\mathbf{r}} + E_n^+\underbrace{(\hat{\mathbf{r}} \cdot \nabla\hat{\mathbf{r}})}_{\mathbf{0}}$$

$$\therefore\ (\hat{\mathbf{n}} \cdot \nabla)\mathbf{E}^+ = (\hat{\mathbf{r}} \cdot \nabla E_n^+)\hat{\mathbf{r}} \tag{A.28}$$

Since $\mathbf{E}^+$ is measured at the surface of the sphere, it can be inferred that

$$\mathbf{E}^+ = E_r^+(a^+, \theta, \phi)\hat{\mathbf{r}},$$

and therefore, E_n^+ does not contain any dependence on the radial component r, as it is taken as a fixed value for the sphere. Therefore,

$$(\hat{\mathbf{n}} \cdot \nabla)\mathbf{E}^+ = \left[\hat{\mathbf{r}} \cdot \left(\frac{1}{r}\frac{\partial E_n^+}{\partial\theta}\hat{\boldsymbol{\theta}} + \frac{1}{r\sin\theta}\frac{\partial E_n^+}{\partial\phi}\hat{\boldsymbol{\phi}}\right)\right]\hat{\mathbf{r}} = \mathbf{0}, \tag{A.29}$$

and, consequently, the derivative over $\mathbf{E}^+$ in the direction of $\hat{\mathbf{n}}$ can be written as

$$\nabla(\mathbf{E}^+ \cdot \hat{\mathbf{n}}) = \hat{\mathbf{n}} \times (\nabla \times \mathbf{E}^+). \tag{A.30}$$

Substituting (A.30) into (A.25), and knowing from (2.1) that

$$\nabla \times \mathbf{E}^+ = -j\omega\mu_0\mathbf{H}^+, \tag{A.31}$$

(A.25) can be written as

$$\mathbf{E}^s = -\left\{(\mathbf{E}^+ \cdot \hat{\mathbf{n}})\nabla G_0 + (\hat{\mathbf{n}} \times \mathbf{E}^+) \times \nabla G_0 - j\omega\mu_0(\hat{\mathbf{n}} \times \mathbf{H}^+)G_0\right\} * \delta(r-a). \tag{A.32}$$

Using the pull-back property of the Dirac delta [e.g., 177], defined for any $f(\mathbf{x})$ and $g(\mathbf{x})$ in $\mathbb{R}^n$,

$$\int_{\mathbb{R}^n} f(\mathbf{x})\delta(g(\mathbf{x}))d\mathbf{x} = \int\limits_{\substack{w:g(\mathbf{x})=0 \\ w\in\mathbb{R}^{n-1}}} f(\mathbf{x})\|\nabla g(\mathbf{x})\|^{-1}d\sigma(\mathbf{x}),$$

the integration over the whole volume of V can be reduced to a surface integral over ∂V, the surface that limits the volume V. Furthermore, knowing that [e.g., 178]

$$\nabla G_0(\mathbf{r}-\mathbf{r}') = -\nabla' G_0(\mathbf{r}-\mathbf{r}'),$$

where the primed operations indicate that they should be executed with respect to $\mathbf{r}'$, and that $\|\nabla(r-a)\| = 1$, the scattered electric field can be written as

$$\mathbf{E}^s(\mathbf{r}) = \int_{\partial V} \left\{(\hat{\mathbf{n}}\cdot\mathbf{E}^+)\nabla' G_0 + (\hat{\mathbf{n}}\times\mathbf{E}^+)\times\nabla' G_0 + j\omega\mu_0(\hat{\mathbf{n}}\times\mathbf{H}^+)G_0\right\} dS, \quad \text{(A.33)}$$

where $\partial V : r - a = 0$.

The expression in (A.33) is equivalent to the surface integral term of the Stratton-Chu integral equation, as presented by Török *et al.* [179]. This expression differs from the one presented by Stratton and Chu [109] because they intend to solve different problems: while the equation presented in (A.33) represents the electric field outside R_1, the form of the Stratton-Chu equation presented in Stratton and Chu [109] represents the electric field inside of a scattering body [179]. Also, the factor of 4π present in both cases is embedded the Green's function solution of the Helmholtz equation presented in (2.25). Also, it is evident that by nature of the boundary condition (A.15), the term $(\hat{\mathbf{n}}\times\mathbf{E}^+)\times\nabla G_0$ is null for a PEC sphere, since $\hat{\mathbf{n}}$ and $\mathbf{E}^+$ are colinear vectors.

A.2.1.2 Incident Electric Field and Total Electric Field

Now, taking the incident electric field expression in (A.19) and substituting $T_{SE}(\mathbf{J}_s)$ into the equation, the following expression for the incident electric field can be obtained:

$$\mathbf{E}^i = \left[\frac{1}{j\omega\epsilon_0}\nabla(\nabla\cdot\mathbf{J}_s) - j\omega\mu\mathbf{J}_s\right] * G_0 \tag{A.34}$$

Making

$$\nabla(\nabla\cdot\mathbf{J}_s) * G_0 = (\nabla\cdot\mathbf{J}_s) * \nabla G_0$$

for a Green's function in the distributional sense, according to (2.26), and changing ∇G_0 to $\nabla' G_0$ as in (A.33), (A.34) can be rewritten as

$$\mathbf{E}^i(\mathbf{r}) = \int_{V_s'}\left[-\frac{1}{j\omega\epsilon_0}(\nabla\cdot\mathbf{J}_s)\nabla' G_0 - j\omega\mu\mathbf{J}_s G_0\right] dV_s', \tag{A.35}$$

where V_s' indicates the volume that bounds the source.

Using the continuity equation [90], (A.35) can be further simplified as

$$\mathbf{E}^i(\mathbf{r}) = \int_{V_s'}\left[\frac{\rho_s}{\epsilon_0}\nabla' G_0 - j\omega\mu\mathbf{J}_s G_0\right] dV_s', \tag{A.36}$$

with ρ_s being the charge density at the source.

Here, the expression for the electric field is identical to the volume integral part of the Stratton-Chu equation, as presented by Elliott [140], with the 4π factor embedded in the Green's function.

Substituting both $\mathbf{E}^i$ and $\mathbf{E}^s$ into (A.18), the following expression can be obtained:

$$\mathbf{E}(\mathbf{r}) = \int_{V_s'}\left[\frac{\rho_s}{\epsilon_0}\nabla' G_0 - j\omega\mu\mathbf{J}_s G_0\right] dV_s' + \int_{\partial V}\Big\{(\hat{\mathbf{n}}\cdot\mathbf{E}^+)\nabla' G_0 + (\hat{\mathbf{n}}\times\mathbf{E}^+)\times\nabla' G_0 + j\omega\mu_0(\hat{\mathbf{n}}\times\mathbf{H}^+)G_0\Big\}\, dS. \tag{A.37}$$

Therefore, the electric field equation obtained through the generalized function method coincides with the solution of the Maxwell's equations in the presence of scattering bodies proposed, as described by the Stratton-Chu integral equation in [179].

Appendix B

Derivations Pertinent to the Electric Field Expression for an Ocean Surface With Electromagnetically-Large Waves

B.1 Fourier Transform of the Green's Function Solution to the Helmholtz Equation

The Green's function solution for the Helmholtz equation, defined in [1] as

$$G_m = \frac{e^{-jk\eta_m\sqrt{x^2+y^2+z^2}}}{4\pi\sqrt{x^2+y^2+z^2}},$$

has, according to [17], a two-dimensional Fourier transform equal to

$$\hat{G}_m = \frac{e^{-|z|\sqrt{k_x^2+k_y^2-k^2\eta_m^2}}}{2\sqrt{k_x^2+k_y^2-k^2\eta_m^2}}.$$

The earliest record of this expression in Walsh's work is shown in his 1980's report [62], where the reader is pointed to an Appendix, where the development of this formulation would be presented. However, the Appendix has not been included in any physical or digital version of the 1980's report. After some analysis, the derivation for this expression has been obtained.

The key to understanding how this expression was derived is knowing that the two-dimensional Fourier transform in the xy -plane is equivalent to the zeroth-order Hankel transform [180]. A complete derivation is shown in [113], but it can be summarized as

$$\mathcal{F}_{x,y}\{f(x,y)\} = \hat{f}(k_x,k_y) = \int f(\boldsymbol{\rho})e^{j(-\mathbf{k}\cdot\boldsymbol{\rho})}d\boldsymbol{\rho} = 2\pi\int f(\rho)J_0(K\rho)\rho\,\mathrm{d}\rho = \hat{f}(K), \tag{B.1}$$

where $x = \rho\cos\theta$, $y = \rho\sin\theta$, $k_x = K\cos\varphi$, $k_y = K\cos\varphi$. The 2π factor in the Hankel transform expression is only present due to the chosen form of the Fourier transform, presented in the previous section. This will be carried out in all following expressions.

It is important to know that there are different normalizations to the Hankel transform, and the choice of these normalizations has an impact in the solution. Besides the form presented in the previous expression, another common normalization presented in textbooks is the one shown in [181], written as

$$\mathcal{H}\{g(\rho)\} = \hat{g}(K) = 2\pi\int f(\rho)J_0\sqrt{\rho K}\,\mathrm{d}\rho. \tag{B.2}$$

In order to convert from this formulation to the previous one, $g(\rho)$ can be defined as $g(\rho) = \sqrt{\rho}f(\rho)$ and $\hat{g}(K) = \sqrt{K}\hat{f}(K)$ [182].

Now that the expressions for the Hankel transform have been defined, the Fourier

transform of the Green's function solution to the Helmholtz equation can be obtained. Converting the expression of the Green's function to cylindrical coordinates and using the notation proposed in [1], [3], the Green's function in (2.25) can be rewritten as

$$G_m = \frac{e^{-jkn_m\sqrt{\rho^2+z^2}}}{4\pi\sqrt{\rho^2+z^2}}, \tag{B.3}$$

where $\rho = x^2 + y^2$, and n_m is the refraction index defined in (1.21). Therefore, the two-dimensional Fourier transform of the Green's function can be written as

$$\hat{G}_m(k_x, k_y) = \hat{G}_m(K) = 2\pi \int G_m(\rho) J_0(K\rho)\rho \,\mathrm{d}\rho. \tag{B.4}$$

Now, converting to the form presented in [181], the Hankel transform can be written as

$$\sqrt{K}\hat{G}_m(K) = 2\pi \int \sqrt{\rho} G_m(\rho) J_0(K\rho)\sqrt{\rho K} d\rho. \tag{B.5}$$

Substituting the Green's function into the previous expression, the following expression can be obtained:

$$\sqrt{K}\hat{G}_m(K) = 2\pi \int \left(\sqrt{\rho}\frac{e^{-jkn_m\sqrt{\rho^2+z^2}}}{4\pi\sqrt{\rho^2+z^2}}\right) J_0(K\rho)\sqrt{\rho K}\,\mathrm{d}\rho. \tag{B.6}$$

The expression within the parenthesis in the previous expression has a definite zeroth-order Hankel transform. Using the Hankel transform presented by Bateman [181], the following expression can be obtained for $k\eta_m < K < \infty$ and $z > 0$:

$$\sqrt{K}\hat{G}_m(K) = 2\pi\sqrt{K}\frac{e^{-|z|\sqrt{K^2-k^2n_m^2}}}{4\pi\sqrt{K^2-k^2n_m^2}}. \tag{B.7}$$

In order to guarantee the condition $z > 0$, the value of z was substituted by its magnitude. Also, the first condition is safely met for conductive scattering bodies. Simplifying both sides of the expression, the expression for the Fourier transform of

the Green's function solution for the Helmholtz equation can be written as

$$\hat{G}_m = \frac{e^{-|z|\sqrt{K^2-k^2n_m^2}}}{2\sqrt{K^2-k^2n_m^2}} = \frac{e^{-|z|\sqrt{k_x^2+k_y^2-k^2n_m^2}}}{2\sqrt{k_x^2+k_y^2-k^2n_m^2}}, \tag{B.8}$$

as defined by [62].

B.2 Bistatic Equation for the First-Order Hydrodynamic, First-Order Correction to the First-Order Electric Field

From the form of the correction to the first-order electric field presented in (3.69), the bistatic correction terms can be obtained by using the height-restricted form of the bistatic electric fields defined in [89]. Thus, the first-order hydrodynamic, first-order correction to the first-order electric field can be written as

$$\left[(E_{0\mathbf{n}}^{+})_{11}\right]_{11} \sim \frac{kC_0}{(2\pi)^2}\zeta_1(\boldsymbol{\rho}_1;t)\sum_{\mathbf{K},\omega_K} f_1(\mathbf{K},\omega_K)e^{-j\omega_K t}K \iint\limits_{x_1,y_1} \cos(\theta_{\mathbf{K}}-\theta_1)\frac{F(\rho_1)F(\rho_2)}{\rho_1\rho_2}$$
$$\cdot\, e^{-jk\rho_2}e^{j\rho_1[K\cos(\theta_{\mathbf{K}}-\theta_1)-k]}dx_1dy_1. \tag{B.9}$$

For the purposes of the derivation of the bistatic electric field and radar cross-section, scattering geometry for the first-order electric field is depicted in Figure B.1.

Comparing the double integrals in (B.9) with those in the first-order electric field expression in [3], [89], it is evident that they are identical. Therefore, following the same procedure detailed in [89] for the first-order bistatic electric field, the following

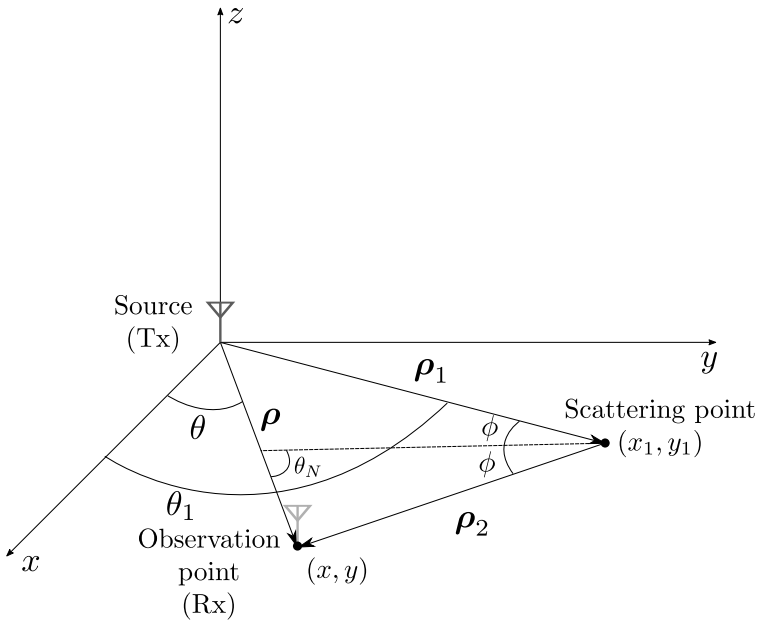

Figure B.1: Scattering geometry for the bistatic first-order electric field

expression is obtained as

$$\left[(E^{+}_{0\mathbf{n}})_{11}\right]_{11} \approx \frac{kC_0}{(2\pi)^{3/2}}\zeta_1(\boldsymbol{\rho}_1;t)\sum_{\mathbf{K},\omega_K} f_1(\mathbf{K},\omega_{\mathbf{K}})e^{-j\omega_{\mathbf{K}}t}\sqrt{K}e^{j\frac{\boldsymbol{\rho}}{2}\cdot\mathbf{K}} \cdot \int_{\rho_s} \frac{F(\rho_1)F(\rho_2)}{\sqrt{\rho_s\left[\rho_s^2-\left(\frac{\rho}{2}\right)^2\right]}} e^{\mp j\pi/4}\left(\pm\sqrt{\cos\phi}\right)e^{j\rho_s[\pm K\cos\phi-2k]}d\rho_s, \quad \text{(B.10)}$$

where ρ_s is defined as [89]

$$\rho_s = \frac{\rho_1+\rho_2}{2},$$

ϕ is the bistatic angle, defined as the bisection of the angle between $\boldsymbol{\rho}_1$ and $\boldsymbol{\rho}_2$, and $\boldsymbol{\rho}$ is the vector between transmitter and receiver shown in Figure B.1.

If, similar to [3], [18], an inverse Fourier transform with respect to the radar frequency is applied to (B.10), and using the associative property of the convolution,

the following expression can be obtained:

$$\left[(E^{+}_{0\mathbf{n}})_{11}\right]_{11}(t) \sim \frac{1}{(2\pi)^{3/2}}\Bigg\{\mathcal{F}_t^{-1}\left\{kC_0\right\} \underset{t}{*} \mathcal{F}_t^{-1}\Bigg\{\sum_{\mathbf{K},\omega_{\mathbf{K}}} f_1(\mathbf{K},\omega_{\mathbf{K}}) e^{-j\omega_K t}\sqrt{K} e^{j\frac{\boldsymbol{\rho}}{2}\cdot\mathbf{K}} \cdot \int\limits_{\rho_s} \frac{F(\rho_1)F(\rho_2)}{\sqrt{\rho_s\left[\rho_s^2 - \left(\frac{\rho}{2}\right)^2\right]}} e^{\mp j\pi/4}\left(\pm\sqrt{\cos\phi}\right) e^{j\rho_s[\pm K\cos\phi - 2k]} d\rho_s\Bigg\}\Bigg\} \underset{t}{*} \mathcal{F}_t^{-1}\left\{\zeta_1(\boldsymbol{\rho}_1;t)\right\}. \tag{B.11}$$

Again, it can be easily observed that the time convolution ($*_t$) inside the braces is similar to the one presented in Equation (5) of [18], with the exception of the time-dependent exponential term for the Fourier series expansion of the ocean surface; although this term will not affect the inverse Fourier transform, it might have an effect on the final convolution. It is easy to show that the additional time-dependent exponential term does not affect the resulting expression, since the added terms in the final expression are significantly smaller than the rest of the terms in the expression. Therefore, substituting the resulting expression for the first-order time-varying electric field in [18] for a pulsed radar source, the expression in (B.11) becomes

$$\left[(E^{+}_{0\mathbf{n}})_{11}\right]_{11}(t) \sim \Bigg\{\frac{-j\eta_0\Delta\ell I_0 k_0^2}{(2\pi)^{3/2}} \sum_{\mathbf{K},\omega_{\mathbf{K}}} f_1(\mathbf{K},\omega_{\mathbf{K}})\sqrt{K\cos\phi_0} e^{j\omega_{\mathbf{K}}t} e^{jk_0\Delta\rho_s} e^{j\rho_{0s}(K\cos\phi_0)} \cdot e^{j\frac{\boldsymbol{\rho}}{2}\cdot\mathbf{K}} \frac{F(\rho_{01},\omega_0)F(\rho_{02},\omega_0)}{\sqrt{\rho_{0s}\left[\rho_{0s}^2 - \left(\frac{\rho}{2}\right)^2\right]}} e^{j\pi/4}\Delta\rho_s\,\mathrm{Sa}\left[\frac{\Delta\rho_s}{2}\left(\frac{K}{\cos\phi_0} - 2k_0\right)\right]\Bigg\} \underset{t}{*} \mathcal{F}_t^{-1}\left\{\zeta_{01}(\boldsymbol{\rho};t)\right\}. \tag{B.12}$$

where $\zeta_{01}(\boldsymbol{\rho};t)$ is defined in (3.111). Here it should be noted that the zero-subscripts in ϕ_0, ρ_{01} and ρ_{02} indicate that the scattering patch is considered to be sufficiently small, allowing variable values at the centre of the scattering patch to be taken as representative of their values on the whole patch [89]. Consequently, ρ_{0s} is defined as

$$\rho_{0s} = \frac{c(t - \frac{\tau_0}{2})}{2} = \frac{\rho_{01} + \rho_{02}}{2}.$$

Substituting (3.111) into (B.12) performing the convolution over ocean time and dealing with the resulting Dirac delta as presented in Chapter 3, the time-varying bistatic electric field for arbitrary heights is obtained:

$$\left[(E^{+}_{0\mathbf{n}})_{11}\right]_{11}(t, t_0) \sim \frac{-j\eta_0 \Delta\ell I_0 k_0^2}{(2\pi)^{3/2}} \Delta\rho_s \sum_{\mathbf{K},\omega_{\mathbf{K}}} \sum_{\mathbf{K}'} f_1(\mathbf{K}, \omega_{\mathbf{K}}) f_1(\mathbf{K}', \omega_{\mathbf{K}}) u_0' \sqrt{K \cos\phi_0}$$
$$\cdot\, e^{-j\omega_{\mathbf{K}'} t} e^{j\boldsymbol{\rho}_1 \cdot \mathbf{K}'} e^{j\omega_{\mathbf{K}} t} e^{jk_0 \Delta\rho_s} e^{j\frac{\boldsymbol{\rho}}{2}\cdot\mathbf{K}} e^{j\rho_{0s}(K\cos\phi_0)} \frac{F(\rho_{01}, \omega_0) F(\rho_{02}, \omega_0)}{\sqrt{\rho_{0s}\left[\rho_{0s}^2 - \left(\frac{\rho}{2}\right)^2\right]}} e^{j\pi/4}$$
$$\cdot\, \mathrm{Sa}\left[\frac{\Delta\rho_s}{2}\left(\frac{K}{\cos\phi_0} - 2k_0\right)\right], \quad \text{(B.13)}$$

where ρ_{0s}, ρ_{01} and ρ_{02} are functions of t_0.

Appendix C

Derivations Pertinent to the Radar Cross-Section of an Ocean Surface With Electromagnetically-Large Waves

C.1 First-Order Hydrodynamic, First-Order Bistatic Radar Cross-Section of an Ocean Surface With Arbitrary Wave Heights

Taking the autocorrelation of (B.13) according to the expression presented in (4.7), and proceeding with the derivations, the following expression is obtained:

$$[\mathcal{R}_{11}]_{11}(\tau) = \frac{A_r \pi^2 \eta_0 |\Delta\ell I_0|^2 k_0^4 |F(\rho_{01},\omega_0)F(\rho_{02},\omega_0)|^2}{2(2\pi)^3 \rho_{0s}\left[\rho_{0s}^2 - \left(\frac{\rho}{2}\right)^2\right]} \sum_{m=\pm 1} \iint S(m\mathbf{K})S(mK)$$
$$\cdot\, |K^2 - {k_0}^2| e^{-j\omega_{\mathbf{K}}\tau} \frac{K^{\frac{7}{2}}}{\sqrt{g}} {\Delta\rho_s}^2 \,\mathrm{Sa}^2\left[\frac{\Delta\rho_s}{2}\left(\frac{K}{\cos\phi_0} - 2k_0\right)\right] dK d\theta_{\mathbf{K}}. \quad \text{(C.1)}$$

From [18], it is known that

$$\frac{d\mathcal{P}(\omega_d)}{dA} = \frac{A_r \eta_0 |\Delta\ell I_0|^2 k_0^2 |F(\rho_{01},\omega_0)F(\rho_{02},\omega_0)|^2}{16(2\pi)^3(\rho_{01}\rho_{02})^2}\sigma(\omega_d), \quad \text{(C.2)}$$

where $\mathcal{P}(\omega_d)$ is the power spectral density of the electric field, defined as the Fourier transform of the autocorrelation with respect to τ, and $\sigma(\omega_d)$ is the radar cross-section of the scattering object. After obtaining the power spectral density from the autocorrelation in (C.1), knowing from the bistatic scattering geometry that $\theta_{\mathbf{K}} = \theta_N$, where θ_N is the direction normal to the scattering ellipse at the scattering patch, and that [18]

$$\frac{\Delta\rho_s d\theta_N}{\rho_{0s}\left[\rho_{0s}^2 - \left(\frac{\rho}{2}\right)^2\right]} = \frac{dA}{(\rho_{01}\rho_{02})^2},$$

the second-order correction to the first-order bistatic radar cross-section for an ocean surface with arbitrary heights can be obtained by comparison with (C.2), as

$$[\sigma_{11}]_{11}(\omega_d) = 2^6\pi^3 {k_0}^2 \Delta\rho \sum_{m=\pm 1} S(m\mathbf{K})S(mK)\left|K^2 - {k_0}^2\right| \frac{K^4}{g}\cos\phi_0$$
$$\cdot\, \mathrm{Sa}^2\left[\frac{\Delta\rho_s}{2}\left(\frac{K}{\cos\phi_0} - 2k_0\right)\right]. \quad \text{(C.3)}$$

As expected, the form of the bistatic radar cross-section converges to the monostatic expression presented in [97] for $\cos\phi_0 = 1$. Also, considering the form of the correction

factor presented in Chapter 4, it is clear that the expression shown in (C.3) can be reduced to

$$[\sigma_{11}]_{11}(\omega_d) = \sigma_{11}(\omega_d)\Xi_{11}(\omega_d), \tag{C.4}$$

where $\sigma_{11}(\omega_d)$ is the bistatic first-order radar cross-section for a height restricted ocean surface, defined as [18],

$$\sigma_{11}(\omega_d) = 2^4\pi {k_0}^2 \Delta\rho \sum_{m=\pm 1} S(m\mathbf{K}) \frac{K^{5/2}}{\sqrt{g}} \cos\phi_0 \,\mathrm{Sa}^2 \left[\frac{\Delta\rho_s}{2}\left(\frac{K}{\cos\phi_0} - 2k_0\right)\right], \tag{C.5}$$

where $K = \omega_d^2/g$, and $\Xi_{11}(\omega_d)$ is defined by the integral-free expression of the first-order hydrodynamic, first-order correction factor shown in (4.74), knowing that$K' = \omega_d^2/g$. Substituting (4.74) and (C.5) into (C.4), noting that $K = K'$, first-order correction to the first-order radar cross-section becomes the expression presented in (C.3).